Atomic Energy Control Board
P.O. Box 1046
Ottawa, Canada
K1P 5S9

Commission de contrôle de l'énergie atomique
C.P. 1046
Ottawa, Canada
K1P 5S9

INFO-0291

INTERACTION BETWEEN WATER, SEDIMENTS AND RADIONUCLIDES

by

W.J. Snodgrass, P. McKee,
J. Garnett and L. Stieff
Beak Consultants Limited

A research report prepared for the
Atomic Energy Control Board
The National Uranium Tailings
Program (NUTP)
and
Environment Canada

August 1988

Canada

Research report

89-05137/

INTERACTION BETWEEN WATER, SEDIMENTS AND RADIONUCLIDES

A report presented to the Atomic Energy Control Board by W.J. Snodgrass, P. McKee, J. Cornett and L. Stieff, Beak Consultants Ltd.

ABSTRACT

A model-based measurements program was carried out to evaluate the primary mechanisms controlling transport of uranium 238 and thorium 232 decay chain radionuclides in Quirke Lake, a water body draining much of the uranium mining and milling district near Elliot Lake, Ontario. This program included studies of radionuclide accumulation in sediments, particle settling and lake mass-balance studies. Also, sediment studies were undertaken to evaluate chemical fractionation, mineralogical associations, and sediment-water adsorption and release. A limnocorral experiment was conducted in an isolated portion of a lake to measure radium 226 removal from the water column and diffusion from the sediments back to the water. Modelling studies were made to assess the data. Substantial agreement was obtained using the model originally developed for the AECB between model predictions and observations for Quirke Lake and for the limnocorrals. Further work is required to complete the studies undertaken in this project to assess the significance of the efflux of radionuclides from the sediments. These studies include a laboratory program to measure kinetics of adsorption, sediment-water modelling studies of the results and a field measurement program to develop a mass-balance analysis for thorium.

RÉSUMÉ

Un programme de mesures, basé sur des modèles, a été exécuté pour évaluer les mécanismes primaires du transport des radionucléides de la chaîne de désintégration de l'uranium 238 et du thoriom 232 au lac Quirke, un réservoir qui draine presque toute l'eau de la région d'extraction minière et de concentration d'uranium près d'Elliot Lake (Ontario). Le programme comprenait des études sur l'accumulation de radionucléides dans les sédiments, le dépôt de particules et le bilan-matières du lac. On a aussi entrepris des études de sédiments pour évaluer le fractionnement chimique, les associations minéralogiques, ainsi que l'adsorption et le rejet d'eau par les sédiments. On a installé une enceinte limnologique («limnocorral») dans une partie isolée d'un autre lac pour mesurer l'enlèvement de radium 226 de la colonne d'eau, puis de sa rediffusion dans l'eau à partir des sédiments. On a effectué des études de modélisation pour évaluer les données. On a obtenu des concordances importantes en utilisant le modèle d'abord mis au point par la CCEA entre les prévisions de modèles et les observations du lac Quirke, d'une part, et des enceintes limnologiques, d'autre part. D'autres travaux sont nécessaires pour compléter les études du projet afin d'évaluer l'importance de l'écoulement des radionucléides dans les sédiments. Ces études comprennent un programme de laboratoire pour mesurer les caractéristiques cinétiques de l'adsorption, l'examen des résultats à la lumière d'études de modélisation des sédiments et de l'eau, ainsi qu'un programme de mesure sur le terrain pour mettre au point une analyse de bilan-matières du thorium.

DISCLAIMER

The Atomic Energy Control Board is not responsible for the accuracy of the statements made or opinions expressed in this publication and neither the Board nor the author assume liability with respect to any damage or loss incurred as a result of the use made of the information contained in this publication.

TABLE OF CONTENTS

			Page
ABSTRACT			i
1.0	INTRODUCTION		1.1
	1.1	Background	1.1
	1.2	Objectives	1.2
2.0	STUDY AREA		2.1
3.0	SEDIMENTATION RATE MEASUREMENTS		3.1
	3.1	Introduction	3.1
	3.2	Methods	3.3
	3.3	Results and Discussion	3.6
4.0	PARTICLE FLUX MEASUREMENTS		4.1
	4.1	Introduction	4.1
	4.2	Methods	4.1
	4.3	Results and Discussion	4.2
5.0	MASS BALANCE ANALYSIS FOR QUIRKE LAKE AND THE SERPENT RIVER SYSTEM		5.1
	5.1	Mass Balance Program	5.1
	5.2	Results of Mass Balance Study	5.3
	5.3	Implications of Mass Balance Study	5.8
6.0	SEDIMENT STUDIES		6.1
	6.1	Fractionization of Radioisotopes According to a Sequential Extraction Operationally Defined Procedure	6.1
		6.1.1 Protocols for Chemical Characterization of Sediment	6.1
		6.1.2 Methods	6.3

	6.2	Mineralogical and Nuclear Emulsion Studies on Quirke Lake Sediments	6.5
		6.2.1 Introduction	6.5
		6.2.2 Results of Nuclear Emulsion and Mineralogy Studies	6.6
	6.3	Characterization of Adsorption Processes in Quirke Lake Sediments	6.8
		6.3.1 Description of Adsorption Experiment	6.8
		6.3.2 Results	6.9
7.0	EXPERIMENTAL FIELD MEASUREMENT OF RADIUM TRANSPORT BETWEEN SEDIMENT AND WATER		7.1
	7.1	Background	7.1
	7.2	Methods	7.1
	7.3	Results	7.4
	7.5	Relative Importance of Settling and Diffusion	7.7
	7.6	Other Sources of Error in the Limnocorral Experiments	7.7
8.0	MODELLING ANALYSES OF THE SEDIMENT AND WATER TRANSPORT OF U-238 AND Th-232 DECAY SERIES RADIONUCLIDES		8.1
	8.1	Structure of Model Used in Previous Studies	8.1
	8.2	Sediment Transport Dynamics	8.6
	8.3	Modelling of the Results of the Field Experiments Using a Kinetically-Controlled Sediment Adsorption, Sediment Settling and Diffusion Model	8.7
	8.4	Evaluation of the Limnocorral Data Using a Simple Model	8.8
	8.5	Model Validation Studies With Limnocorral and Quirke Lake Data	8.9
9.0	SUMMARY		9.1
10.0	REFERENCES		10.1

APPENDIX A.1 Method of Concentration of Radionuclides From Bulk Lake Samples

APPENDIX A.2 Chemical Methods of Analysis by Ministry of the Environment (Ministry of Labour)

APPENDIX A.3 Chemical Methods of Analysis by Momenco Laboratories Calgary, Alberta

APPENDIX A.4 Chemical Methods of Analysis by Becquerel Laboratories

LIST OF TABLES

Table 2.1: Uranium Mines, Mills and Tailings Management Facilities in the Serpent River Basin[a]

Table 3.1: Sedimentation Rates in Quirke Lake, Stations 1 to 5, 1984 and 1986

Table 3.2: Means and Variation in Radionuclide Levels in Surficial[1] Sediments of Quirke Lake, 1984.

Table 3.3: Mean Present-Day and Pre-Mining Radionuclide Accumulation Rates in Sediments at Water Depths of 20 to 40 m and at 100 m[1]. Units are $Bq \cdot m^{-2} \cdot yr^{-1}$ unless indicated otherwise

Table 4.1: Accumulated Masses of Solids and Radionuclide Concentrations (Bq/g unless indicated otherwise) in Quirke Lake Sediment Traps, 1986

Table 4.2: Annual Mass and Radionuclide Settling Rates* For U-238 and Th-232 Decay Chain Radionuclides in Quirke Lake. Values are based on solids from three sediment traps per depth. Expressed as rate measured in first experiment/rate measured in second experiment.

Table 4.3: Comparison of Particle Settling Fluxes With net Sediment Accumulation Rates Determined From Sediment Cores in Quirke Lake ($g \cdot m^{-2} \cdot yr^{-1}$)

Table 4.4: Comparison of Radionuclide Fluxes From Particle Settling With Net Radionuclide Accumulation Rates at 100 m and 20-40 m Lake Depths in Quirke Lake. Units are $mg \cdot^{-2} \cdot yr^{-1}$ for total U, $Bq \cdot m^{-2} \cdot yr^{-1}$ for others.

Table 5.1: Radionuclide Data For Quirke Inlet (Amplified MOE Monitoring Program)

Table 5.2: Radionuclide Data For Quirke Lake (Amplified MOE Monitoring Program)

Table 5.3: Radionuclide Data for Panel Discharge (Amplified MOE Monitoring Program)

Table 5.4: Mass Balance Analysis of Thorium Isotopes From Large Volume

Table 5.5: Mass Balance Analysis for Radium Data (Bq/L) For Large Volumes

Table 5.6: Mass Balance Analysis for Polonium Data (Bq/L) For Large Volumes

Table 5.7: Mass Balance Analysis for Uranium Data (ug/L) From Sample Obtained at Same Time as Large Volumes

Table 5.8: Summary of Mass Balance Results (concentration units in Bq/L, except Uranium ug/L; fluxes in mg $m^{-2}yr^{-1}$ for total U; Bq $m^{-2}yr^{-1}$ for others)

Table 6.1b: Concentration Extracted (ug/g)

Table 6.1a: Extracted Concentration (ug/g)

Table 6.2a: K_D Values (mL/g) From First Adsorption Experiment
Table 6.2b: K_D Values (mL/g) From Second Adsorption Experiment
Table 7.1: Loss Rates From Limnocorrals (Plus or Minus/Standard Deviation)
Table 7.2: Comparison of Loss Rates to Setting and Calculated Diffusion
Table 8.1: Model Equations
Table 8.2: Steady-State Form of Model Equations
Table 8.3: Net Accumulation of Settling Flux (%)
Table A3a: Operating Characteristics of Radionuclide Analysis For Water (Routine Procedure)

LIST OF FIGURES

Figure 2.1: Bathymetric Map of Quirke Lake, Showing Survey Stations 1 to 5

Figure 2.2: Schematic Representation of Serpent River System Hydrology Based on Mean Annual Discharges Measured by Environment Canada (1985)

Figure 3.1: Pollen Diagram For A Core From Station 3, 1984

Figure 3.2: Diatom-Inferred pH in Sediment Cores From Stations 1,2,3, 1984

Figure 3.3: Diatom-Inferred pH in Sediment Core From Station 5, 1985

Figure 3.4: Thorium Activity Profiles (Bq/g) in Sediment Cores From Stations 2, 4 and 5 (100, 40 and 20 m deep respectively)

Figure 3.5: Thorium Activity Profiles (Bq/g) in Sediment Cores From Stations 1,2 and 3, 1984. Dashed line corresponds to depth of diatom-inferred pH decline

Figure 3.6: Iron Concentration Profiles (%) in Sediment Cores From Stations 2,4 and 5 (100, 40 and 20 m deep respectively)

Figure 4.1: General Arrangement of Resuspended Sediment Sampler (RSS) and Sedimentation Tubes Specifications (adapted from Rosa et al, 1983)

Figure 6.1: Photomicrograph of Nuclear Emulsion Slide

Figure 6.2: Photomicrograph of Nuclear Emulsion Slide

Figure 6.3: Photomicrograph of Nuclear Emulsion Slide

Figure 6.4: Photomicrograph of Nuclear Emulsion Slide

Figure 6.5: Photomicrograph of Nuclear Emulsion Slide

Figure 6.6: Photomicrograph of Nuclear Emulsion Slide

Figure 6.7: Photomicrograph of Nuclear Emulsion Slide

Figure 6.8: Photomicrograph of Nuclear Emulsion Slide

Figure 6.9: Photomicrograph of Nuclear Emulsion Slide

Figure 7.1: Loss Rates of Radium-226 and Barium-133 in Limnocorrals

Figure 7.2: Comparison oRa-226 Fluxes Using Gamma Spectroscopy and Radon-222 Counting

Figure 7.3: Comparison of Loss Rates of Barium-133 in Two Control Bags

Figure 7.4: Ba-133 Desorption in C-2

Figure 7.5: Desorption Rate Data

Figure 7.6: Variation of Particulate Flux in Controls (1-2) and in Perch Lake

Figure 7.7a Settling Rate of Ra-226 in Control

Figure 7.7b Settling Rate of Ra-226 in Humic Acid Limnocorrals

Figure 7.7c Settling Rate of Ra-226 in Sediment-Spiked Limnocorrals
Figure 7.8a Behaviour of Non-Particulate Reactive Tracers (After Cornett and Chant, 1987)
Figure 7.8b Loss of Na-22 From a Limnocorral During a Storm Event
Figure 7.9: Accumulation of Various Radionuclides on Limnocorral Wells (After Cornett and Chant, 1986)
Figure 7.10 Flux of Na-22 in Sediment Traps (After Cornett and Chant, 1987)
Figure 8.1: Major Mechanisms in Lake Model
Figure 8.2a: Depth Penetration into Sediments for Kd=10 L/kg for Pore Water Concentration
Figure 8.2b: Depth Penetration into Sediments for Kd=50 L/kg for Pore Water Concentration
Figure 8.2c: Depth Penetration into Sediments for Kd=100 L/kg for Pore Water Concentration
Figure 8.2d: Depth Penetration into Sediments for Kd=500 L/kg for Pore Water Concentration
Figure 8.2e: Depth Penetration into Sediments for Kd=1000 L/kg for Pore Water Concentration
Figure 8.3: Representation of Sediment-Water Transport by Santschii et al (1985)
Figure 8.4: Validation of Santschii et al (1985) Model
Figure 8.5: Monte Carlo Simulation of Santschi Model ± Standard Deviations
Figure 8.6: Effective Removal Velocity (Eq. 8.2) as a Function of Percent Particulate

1.0 INTRODUCTION

1.1 Background

The uranium mining and milling industry is active in two regions of Canada - near Lake Athabasca, Saskatchewan, and near Elliot Lake, Ontario. These operations release natural radionuclides of the U-238 and Th-232 decay chains to aquatic and atmospheric environments, primarily from tailings disposal areas. Large amounts of acid, stable trace metals and milling reagents are also released to the environment by these operations. Once released, radionuclides are transported through environmental pathways and may impact radiologically on human receptors and natural biota.

In freshwater systems, transport of radionuclides is influenced to some degree by sorption onto particulate phases, precipitation reactions and uptake by biota. Settling of these particulate forms results in a loading to the sediments. As well, soluble forms of radionuclides may diffuse between lake water and bottom sediments. Sedimentation of radionuclides acts to reduce downstream export and thus moderates the impact of releases in downstream areas. Following the cessation of mining and milling and the associated termination of these point source aqueous releases, these contaminated sediments may act as a source of radionuclides to the water column, resulting in long-term impacts.

Some investigators have documented high concentrations of radionuclides in sediments of watersheds downstream of uranium mining and milling operations (Neame et al., 1982; McKee et al., 1987); however, very few studies have examined closely the mechanisms and rates at which radionuclides migrate between particulate and aqueous phases in the environment. A clearer understanding of these processes is required to evaluate their role in controlling radionuclide transport in aquatic environments, and to develop and apply predictive environmental transport and dosimetry models with confidence.

A mathematical model was developed by Beak Consultants Limited (BEAK) on behalf of the Atomic Energy Control Board to predict aqueous transport and consequence (dose commitment) due to releases of U-238 and Th-232 decay chain radionuclides from uranium mill tailings in the Quirke Lake basin, near Elliot Lake, Ontario (Lush et al., 1982; Snodgrass et al., 1983, 1986). This modelling effort provided the conceptual

framework for testing the sensitivity of outcome (dose) to environmental processes, and the required focus for defining the environmental measurements needed to calibrate and fine-tune the model. Initial modelling efforts using estimated environmental parameter values indicated that dose rates were most sensitive to radionuclide removal by sedimentation (Lush et al., 1982; Snodgrass et al., 1983), demonstrating the need for improved understanding of the behaviour of radionuclides in natural sediment-water systems. Initial measurements of radionuclide sedimentation rates in Quirke Lake by BEAK (McKee et al., 1987) confirmed that considerable quantities of U-238 and Th-232 decay chain radionuclides have accumulated in the sediments of Quirke Lake since the beginning of mining and milling in the basin.

1.2 Objectives

The overall objective of this study is to undertake a series of field and laboratory measurements as a means of developing a better understanding of watershed processes affecting radionuclide transport in the natural environment. This information is necessary to refine, calibrate and more meaningfully apply environmental models of radionuclide transport and consequence, including the model developed for the Quirke Lake system for the AECB (Lush et al., 1982; Snodgrass et al., 1983, 1986).

The specific objectives of this project are to:

- identify the critical mechanisms affecting sediment-water transport using the existing Quirke Lake model and preliminary field study results (McKee et al., 1987) as the framework for identification. Use of the modelling framework is critical because it ensures that key measurements required to develop a predictive model are made;
- make field measurements and to conduct laboratory experiments to determine the rate at which radionuclides will be returned to the water column of rivers and lakes by different sediment-water transport processes;
- make field measurements to determine the rate of settling of particulate radionuclides into the sediments, and the variability of this rate;
- make field measurements to develop a radionuclide mass budget for Quirke Lake;

- refine the existing modelling framework and apply the actual data to make some evaluation of long-term (post-mining) environmental transport; and
- estimate uncertainty associated with the model predictions.

In order to meet these objectives, BEAK undertook several field and laboratory studies:

- measurements of whole-lake average sedimentation rates using radiometric and palaeobiological methods;
- measurements of radionuclide fluxes to the sediments in settling particles in the water column;
- measurements of aqueous concentrations of radionuclides flowing into and out of Quirke Lake, and at the mouth of the watershed to construct mass balances;
- measurements of radionuclide movements in limnocorrals treated with experimental radionuclide additions;
- eludicidation of sediment-water exchange processes using a combination of field measurements and sequential extraction techniques; and
- solid phase studies to examine micro-scale association of radionuclides in sediment particles.

These studies are discussed in detail beginning in Section 3.0 of this report.

2.0 STUDY AREA

Quirke Lake is a relatively large, deep waterbody (Figures 2.1 and 2.2) in the headwaters of the Serpent River watershed draining into the North Channel of Lake Huron. The lake is situated on the Precambrian Shield, approximately 120 km west of Sudbury, Ontario, at 46°30'N, 42°35'W. It is the largest lake in the Serpent River system, with a surface area of 2,040 ha, mean and maximum depths of 39 and 102 m, respectively, and a hydraulic detention time of approximately 5 years (Snodgrass et al., 1983).

At water depths greater than 3 m, sediments in the lake consist of a dark, fine-grained gyttja with a surficial orange-brown flocculent deposit over about 50% of the lake bottom. Sediments in the deep basins ($\geq$ 98 m) are brown-black muds, overlain by approximately 10 cm of an orange-brown layer in the two western basins and by approximately 10 cm of a light brown deposit in the eastern basin. We found the orange-brown layer to be rich in iron (unpubl. data). Releases of iron from the mining and milling of pyritic ores are the probable source, although post-depositional diffusion of iron upward in reducing porewaters and precipitation at the oxidizing interface in the surficial sediments (e.g., Carignan and Flett, 1981; Cornwell, 1985) may contribute to this phenomenon.

The first uranium mine in the watershed began production in 1955. By 1957, there were 11 operating mines in the system. Uranium production decreased in the early 1960's and increased in the late 1960's in response to market demand. There are presently several active and inactive mining and milling operations and tailings disposal sites located within the Quirke watershed. Table 2.1 provides an historic summary of uranium mines, mills and tailings management facilities in the Serpent River basin.

Mill process waters are acidic due to the sulphuric acid leaching process used to dissolve uranium from the ore during milling. This acidity favours the release of radionuclides from the ores. Uranium is removed from the acidic solution, and other dissolved constituents are precipitated by neutralization and discharged with the tailings to the tailings management area. Acidic conditions develop in the tailings due to pyrite oxidation, resulting in the dissolution of radionuclides and subsequent release to surface waters. Acidic conditions (pH 4.5 to 5.7) consequently occurred in Quirke Lake in the 1960's and 1970's, with a gradual increase in pH to 5.5 to 6.4 observed in 1984 (Ontario

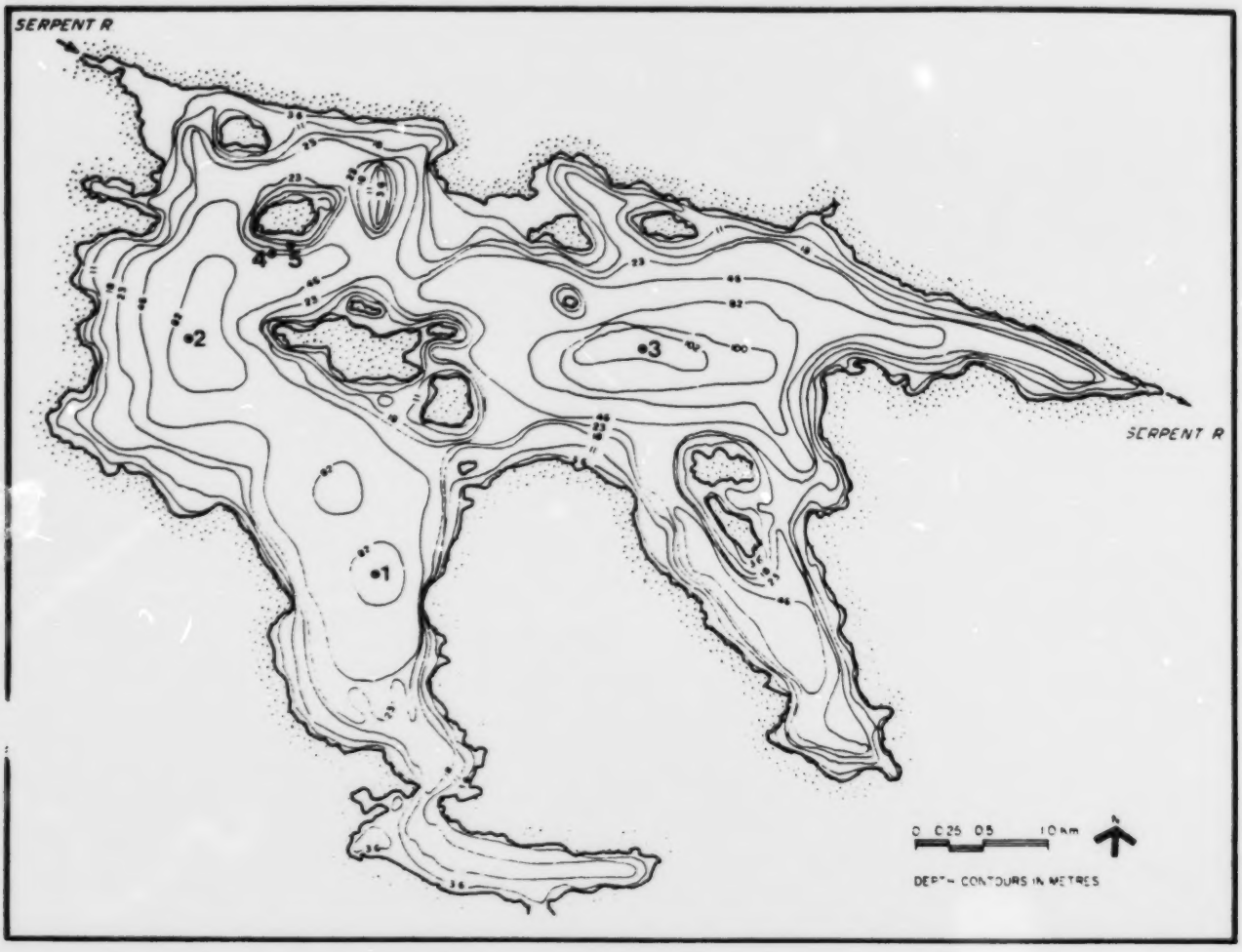

FIGURE 2.1: **BATHYMETRIC MAP OF QUIRKE LAKE, SHOWING SURVEY STATIONS 1 TO 5**

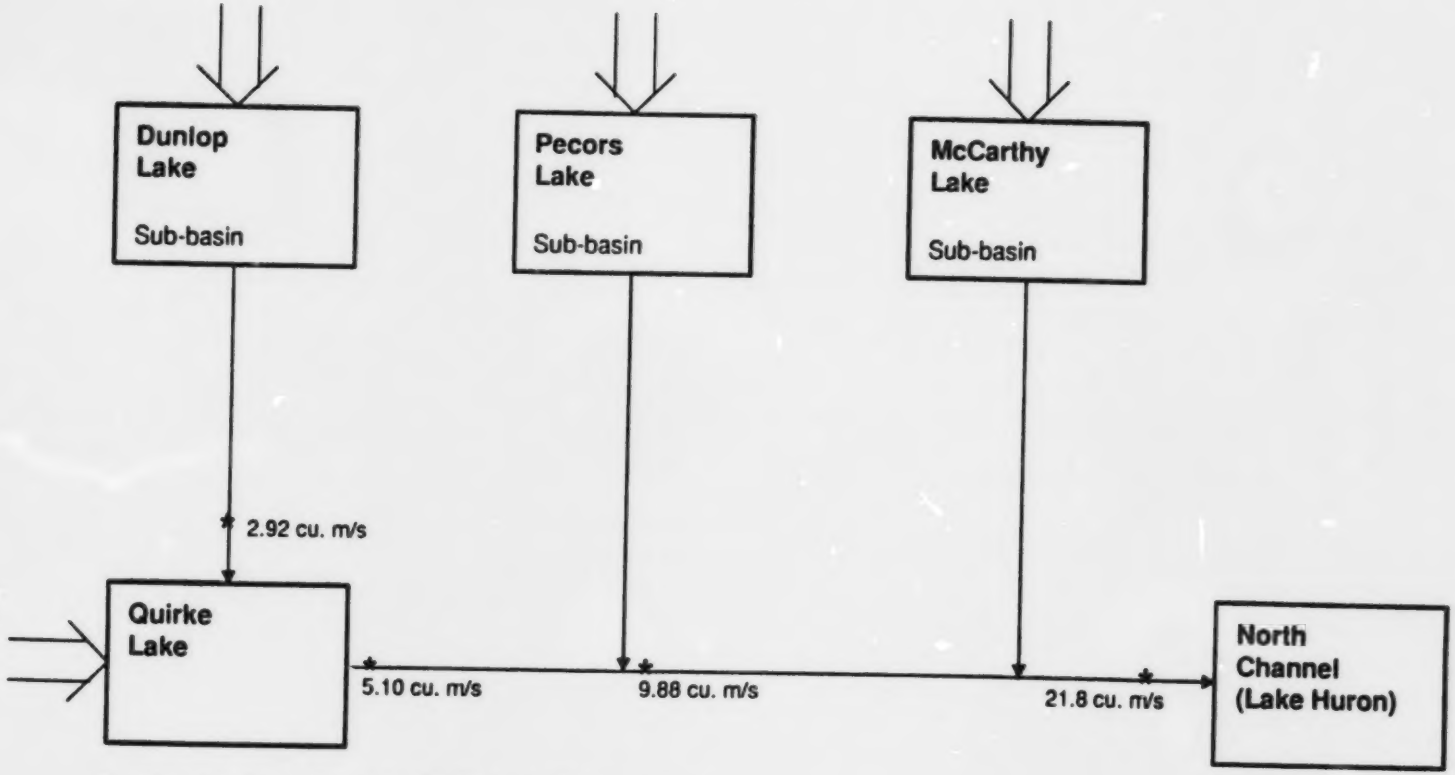

Large Arrows Denote Tailings Discharges

FIGURE 2.2
Schematic Representation of Serpent River System Hydrology Based on Mean Annual Discharges Measured by Environment Canada (1985)

Ministry of the Environment, unpubl. data) apparently due to improvements in effluent treatment, neutralization of tailings seepage, and improved containment of leachates in new tailings structures over the last 10 to 15 years.

Five stations (1 to 5) were sampled in Quirke Lake for sedimentation measurements (Figure 2.1). Stations 1 to 3 are located in the three deep basins of the lake, and have water depths of 98 to 102 m. Stations 4 (40 m deep) and 5 (20 m deep) correspond approximately to the mean depth of the lake and to the littoral zone-profundal zone boundary, as defined by the region of greatest change in densities of benthic invertebrates (McKee et al., 1985).

Water samples for radionuclide determination were collected at the inlet to Quirke Lake, in Quirke Lake approximately half-way between Station 3 and the north shore, and near the mouth of the Serpent River into the North Channel, at the Highway 17 crossing (Figure 2.2). Water quality at the Quirke Lake station was assumed to be comparable to water quality at the lake outlet.

TABLE 2.1: URANIUM MINES, MILLS AND TAILINGS MANAGEMENT FACILITIES IN THE SERPENT RIVER BASIN[a]

Facility	Dates of Operation	Tailings Tonnage[b] (10^6 tonnes)	Tailings Area[h] (ha)
Denison Mines Ltd., Elliot Lake[g]			
Mines and Mills:			
o Main Facility*	1957-Present		
o Stanrock	1958-1964, 1983-Present[c]		
Tailings Management Areas			
o Long Lake*	1959-Present	37.3	75
o Williams Lake	1957-1959		
o Stanrock	1958-1964[d]	7.7	52
Rio Algom Ltd., Elliot Lake[g]			
Mines, Mills and Tailings Management Facilities:			
o Panel*	1958-1961, 1979-Present	4.2	40
o Quirke*	1956-1961, 1968-Present	22.7	80
o Stanleigh*	1958-1960[e], 1983-Present	7.5	33
o Nordic	1957-1968[f]	10.4	107
o Pronto	1955-1966	2.1	47
o Lacnor	1957-1960[f]	2.7	24
o Spanish American	1958-1959[f]	0.5	6

[a] IJC (1983).
[b] Tonnage as of 1980.
[c] All ore is milled at the Denison Main Facility.
[d] Tailings area also used by CANMET during this period.
[e] Tailings area also used by Milliken Mine, 1958-1964.
[f] Receive no effluent treatment.
[g] Current owner.
[h] EMR (1981).
* Active sites.

3.0 SEDIMENTATION RATE MEASUREMENTS

3.1 Introduction

In aquatic environments, transport of radionuclides is influenced to some degree by sorption onto particulate phases, precipitation reactions, and uptake by biota. Settling of these forms results in a loading to the sediments. As well, soluble forms of radionuclides may diffuse between lake water and bottom sediments. Sedimentation of radionuclides acts to reduce downstream export and thus moderates the impact of releases in downstream areas. Following the cessation of mining and milling and the reduction or termination of aqueous releases, these contaminated sediments may act as a source of radionuclides to the water column, resulting in long-term impacts.

Pb-210 and Ra-226 of the U-238 decay chain have been widely measured in sediment cores to determine sediment accumulation rates in studies on nutrient cycling, trace element loading, particle reworking, and sediment diagenesis (Robbins and Callender, 1975; de March, 1978; Kipphut, 1978; Robbins, 1978; Evans and Rigler, 1980a, b; Carignan and Flett, 1981; Cornwell, 1985). Terrestrial and atmospheric loadings and particulate-solute partitioning of U-238 decay chain radionuclides were studied in Lake 239 (Experimental Lakes Area, northwestern Ontario; Brunskill and Wilkinson, 1987) and in four lakes in the eastern Keewatin District, Northwest Territories (G.J. Brunskill, Freshwater Institute, Winnipeg, Manitoba, pers. comm.), in investigations of radionuclide budgets in watersheds unaffected by the uranium industry.

This study was undertaken to determine accumulation rates and the degree of contamination by U-238 and Th-232 decay chain radionuclides in the sediments of Quirke Lake, based on analysis of sediment cores. Radionuclide flux measurements based on collection and analysis of water column particulates were also made, as described in Section 4.0 of this report. Sedimentation rates were measured to relate the time scale of sediment contamination with the history of mining and milling in the basin. Sedimentation rates are also of concern in light of recent interest in examining the feasibility of deep lake disposal of uranium mill tailings. The burial of emplaced tailings with "clean" sediment after the cessation of mining and milling would result in a barrier to diffusion that would increasingly inhibit remobilization of radionuclides from the sediments back to the water column over the long term.

Lush et al. (1982) modelled the downstream transport, migration through food chains, and effective dose commitments resulting from releases of radionuclides from a hypothetical tailings mass on the shore of Quirke Lake. This model was developed in part as a decision-making tool for regulatory agencies in the management of radioactive releases to surface waters from uranium mines and mills. Model parameters were assigned values based on a review of the literature, rather than on any specific measurements in Quirke Lake or downstream environments. In their sensitivity analysis, the authors found that model predictions (radiation doses) were sensitive to sedimentation parameters in downstream watersheds. The present study provides data on sedimentation rates and net radionuclide accumulation rates for Quirke Lake for use in the refinement and calibration of the model.

Sediment chronologies can be determined from Pb-210 profiles only in cases where the supply of Pb-210 to the sediment occurs at a constant rate, or if the Pb-210 supply is proportional to a varying sedimentation rate (Appleby and Oldfield, 1983). These assumptions are almost certainly violated in Quirke Lake, because uranium milling increases radionuclide loadings to the lake, and these loadings vary in quantity and relative proportions of radionuclides depending upon the intensity of mining and milling activity and the wastewater treatment technologies employed. In an attempt to apply Pb-210 dating in Quirke Lake, McKee et al. (1985) found Pb-210 activities in recent sediment layers that were about 50 times greater than expected natural Pb-210 activities, demonstrating that mining and milling sources were "swamping" natural sources, thereby preventing the application of Pb-210 dating techniques.

In a recent study, McKee et al. (1987) determined sedimentation rates at Stations 1 to 3 in Quirke Lake using fossil diatom and fossil pollen profiles in sediment cores. Diatom communities respond to acid loadings by shifting to more acidophilous (acid-loving) species assemblage (e.g., Battarbee, 1984; Charles, 1985). The sulphuric acid leaching process and the production of pyritic tailings in uranium milling led to the acidification of Quirke Lake beginning around 1957. More recent neutralization of aqueous discharge has permitted a recovery from pH 4.5 to 5.5 in the early 1960's to pH 5.5 to 6.4 observed during this study. Diatoms in the core samples were analyzed and lake pH-core depth relationships determined, using approaches similar to those described by Delorme et al. (1984) and Dickman et al. (1984). In Quirke Lake, the decline in diatom-inferred pH was used as a marker for the onset of acidification in 1957, and the mass of more recent

sediment accumulation to estimate modern sedimentation rates. Historic sedimentation rates representative of the century preceding the mid-1950's were estimated by analysis of the Ambrosia pollen rise in sediment cores (e.g., Huhn, 1974; Kemp and Harper, 1976; Kemp et al., 1978; Warwick, 1980; McAndrews and Boyko-Diakonow, 1987).

In this earlier study, depth profiles of U-238 and Th-232 decay chain radionuclides in sediments were also determined. A good correspondence was found between the diatom-inferred 1957 horizon, and the beginning of the rise in sediment thorium (Th-232), indicating that this element may provide a useful "marker" for sedimentation rate determination. Other radionuclides showed evidence for downcore migration, apparently due to post-depositional diffusion of these radionuclides or their decay parents.

Sedimentation rates often vary with water depth in lakes - a phenomenon termed sediment focussing. For example, Evans and Rigler (1980a, 1983) found that depth accounted for as much as 97% of the variation in sediment accumulation rates in three small Shield lakes in southern Ontario. In order to determine the importance of focussing in Quirke Lake, and thereby permit the determination of a lakewide average sediment accumulation rate for modelling purposes, sedimentation rates were measured at 40 m and 20 m depths (Stations 4 and 5, respectively) in this study. This was done by analysis of sediment Th profiles, with corroboration provided by fossil diatom and fossil pollen dating at Station 5.

3.2 Methods

All sediment cores were collected as described in McKee et al. (1985, 1987). Sediment cores were collected using a weighted KB corer outfitted with 4.7-cm (inside diameter) polycarbonate core tubes. Undisturbed cores about 30 cm long were collected with the aid of a CRT-type depth sounder to monitor core entry. Only cores exhibiting a flocculent layer at the sediment-water interface and a layer of overlying water were retained.

In the initial study (McKee et al., 1985, 1987), five cores were collected in October 1984 from each of Stations 1, 2 and 3 - two cores for radionuclide analysis and one core each for diatom analysis, pollen analysis and dry bulk density determination. In the present study, cores were collected in August 1986 from Stations 2, 4 and 5 - one core from

Station 2, three cores from Station 4 and two cores from Station 5 were collected for determination of elemental profiles (including Th), and two cores from Station 5 were collected for fossil diatom and fossil pollen determination. Dry bulk densities were determined from cores collected for elemental analysis.

Cores were sectioned fresh, usually within 24 h of collection. Cores for pollen analysis were sectioned into 1-cm intervals from top to bottom. Before sectioning, horizontal laminations observed in the pollen cores collected in 1984 were counted and measured. The core collected for pollen analysis in 1986 was sliced into 0.7-cm thicknesses from the surface to 10 cm, 1-cm thicknesses between 10 and 19 cm, and 2-cm thicknesses between 19 and 35 cm. Cores collected in 1984 for diatom analysis were sectioned into 0.2-cm intervals to a sediment depth of 2 cm, 0.5-cm intervals from 2 to 5 cm, and 1- to 3-cm intervals to a depth of 16 cm. The core collected in 1986 for diatom analysis was sectioned into 0.7-cm slices to a sediment depth of 7 cm, and 1-cm slices from 7 to 33 cm. Dry bulk densities were determined on core sections after oven-drying. Cores collected in 1986 for elemental analyses were sliced into measured thicknesses of about 0.5 cm to a sediment depth of 10 to 12 cm, and 1 cm between here and 15 to 26 cm below the sediment surface. Cores for elemental analysis were sub-cored during sample extrusion to remove a 1-mm thick smear zone around the outside of the cores.

Samples for pollen analysis were first spiked with a known number of Lycopodium clavatum spores to permit accurate pollen density estimates (Stockmarr, 1970). Fossil pollen was then concentrated from sediment samples with HCl, KOH and acetolysis solution. Pollen grains and spores were counted until approximately 200 tree and shrub pollen grains per sample were obtained. Pollen was identified following McAndrews et al. (1973). Chronologically significant pollen horizons were expected to occur in more recent sediments; thus, every core section from the surface to 11 to 15 cm of depth was examined. Only three intervals between 11 to 15 cm and the bottom of each core were analyzed. Once analyzed, percentage abundance of pollen was used to define pollen zones in the cores based on the rise in weed pollen (Ambrosia, Gramineae, Chenopodiineae, Rumex, Plantago) that can be related to the beginning of farming by European settlers in southern Ontario at about 1830-40 (McAndrews and Boyko-Diakonow, 1987).

Core sections for diatom analysis were freeze-dried and blended, and 0.05 g was then digested with a mixture of HNO_3 and H_2SO_4. Following washings with distilled water to remove acidity, diatom samples were quantitatively settled onto cover glasses in Battarbee chambers (Battarbee, 1973), and then mounted on glass slides using Napthrax, a synthetic resin of high refractive index. At least 500 diatoms per sample were counted.

Several techniques have been developed to assess trends in acidification based on sedimentary diatoms using equations for inferring lake water pH. Problems and uncertainties associated with this methodology are discussed in Davis and Anderson (1984) and Charles (1985). In this study, we assigned each diatom species into one of five categories defined by Hustedt (1939): acidobiontic, acidophilic, indifferent, alkaliphilic and alkalibiontic. Assignment of diatoms to these categories was based on the work of Merilainen (1967) and Taylor (1986). Changes in the percent categories in a sediment core were used to reconstruct trends in lake water pH, following the Renberg and Hellberg (1982) index B approach:

$$B = \frac{\%\ \text{indifferent} + 5\ (\%\ \text{acidophilic}) + 40\ (\%\ \text{acidobiontic})}{\%\ \text{indifferent} + 3.5\ (\%\ \text{alkaliphilic}) + 108\ (\%\ \text{alkalibiontic})}$$

The predicted pH-sediment depth profiles were examined, and the historic pH decline was assumed to correspond to the acidification of Quirke Lake caused by the beginning of uranium milling in 1957 in the watershed.

Prior to analysis of radionuclide concentrations or activities, sediments were dried at 50°C and ground to ensure sample homogeneity. Samples for Ra-226 and Th isotope analyses were dissolved by KF-pyrosulphate fusion. Samples for total U, Pb-210 and Po-210 analyses were digested in a hot, concentrated mixture of HNO_3, $HClO_4$ and HF, followed by a pyrosulphate fusion.

U, Th isotopes, Ra-226 and Pb-210 were then measured by the methods detailed by Chiu and Dean (1984) and Pb-210 by the method of Smithson (1979). Total U in the solution was determined fluorometrically as its fluoride complex following fusion with NaF-LiF. Th isotopes were determined using high-resolution alpha spectrometry (HRAS). Prior to analysis, Th-234 was added to the digested sample as a tracer. Th was coprecipitated

with $PbSO_4$, isolated by solvent extraction, and then coprecipitated with cerous hydroxide. The precipitate was beta-counted for Th-234 to measure the overall yield and then Th-230, Th-232 and Th-228 measured by HRAS. Ra-226 was determined by HRAS using Ba-133 as a tracer. Ra was coprecipitated with $BaSO_4$ and the chemical yield measured by gamma counting of Ba-133. Pb-210 was measured indirectly using Bi-210. The sample solution was held for 30 days prior to analysis to permit greater than 98% ingrowth of Bi-210. A carrier solution of stable Pb and Bi was added before digestion. Bi was then solvent-extracted, precipitated as BiOCl, and Bi-210 measured by beta-counting. Po-210 was measured by HRAS using Po-208 as a tracer. Po isotopes were deposited on a nickel disc and the yield measured by recovery of the tracer. Radiochemical determinations were also carried out on one or two UTS reference standards, developed for the National Uranium Tailings Program, Department of Energy, Mines and Resources Canada, for every 15 to 20 sediment samples analyzed.

Radionuclide counting errors (1σ) were generally $\leq 12\%$ of total activity for all activity concentrations of Pb-210 and Po-210, and for Ra-226 activities > 1 $Bq \cdot g^{-1}$. Errors were usually $\leq 25\%$ for Th isotopes at activities of > 1 $Bq \cdot g^{-1}$. At lower activities, counting errors for Ra-226 and for Th isotopes generally ranged from 10 to 50%.

Core samples collected for elemental determination in 1986 were analyzed for about 25 elements by neutron activation. Concentration profiles of total U and total Th are used in documenting enrichment by mining and milling. Profiles of Fe, Ba and Al are of interest in evaluation of the role of coprecipitation and adsorption processes in the deposition of radionuclides, and in estimating density corrections. Detailed data for the pollen and diatom analysis of sediment cores from Stations 1, 2 and 3 are provided in McKee et al. (1985). The additional analyses of Station 5 are incorporated in this work to provide estimates of sediment accumulation rate.

3.3 Results and Discussion

Sedimentation Rates

Two major pollen zones were found in each core (Figure 3.1); Zone 3 is characterized as having $< 2\%$ weed pollen, while Zone 4 has $> 4\%$ (pollen zonation as described by McAndrews, 1981). Two Zone 4 subzones were identified - 4a has less than 18% Betula,

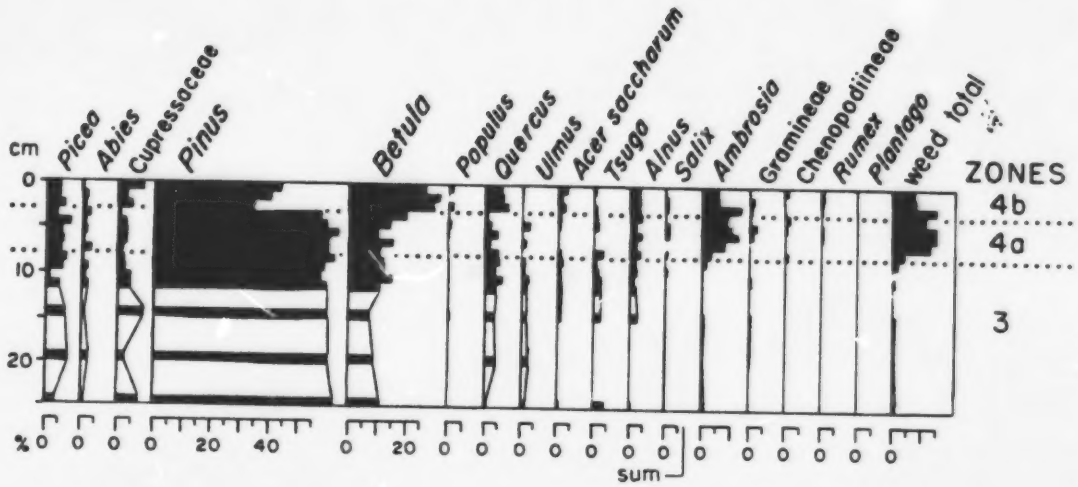

FIGURE 3.1: POLLEN DIAGRAM FOR A CORE FROM STATION 3, 1984

while 4b has 19% or more Betula. Since farming is not widespread in the North Channel region, it is assumed that southern Ontario is the major source of weed pollen in Quirke Lake sediments. Although ragweed (Ambrosia) is rare in the Quirke Lake area and northward, it is represented in the pollen record in lake sediments of the region (Huhn, 1974). As in southern Ontario, the Zone 3/Zone 4 pollen zone boundary is assumed to be dated at about 1830-40 (McAndrews and Boyko-Diakonow, 1987); thus, the overlying sediment represents 150 years of accumulation. The 3/4 boundary occurred at sediment depths of 12, 11, 8 and 5.68 cm in Cores 1, 2, 3 and 5, respectively. The 4a/4b boundary was estimated to correspond to a 50-year-old boundary based on regional forestry records and forest successional patterns (McKee et al., 1985). However, because the Th rise and the diatom-inferred pH decline in sediments provide similar estimates of sedimentation rate and can be directly attributed to mining history (McKee et al., 1987), and because the chronology of the 4a/4b horizon is less certain, only the diatom and Th profiles are used to determine post-mining sedimentation rates. Sediments between the 3/4 pollen zone boundary and the Th rise/diatom-inferred pH decline have accumulated between the beginning of southern Ontario farming and the beginning of uranium mining and milling in the watershed.

The diatom-inferred pH values derived from the surficial sediment (Figures 3.2 and 3.3) are within the present lake water pH range of 5.5 to 6.4. Furthermore, the inferred pH minima of approximately 5.2 to 5.5 for Stations 1, 2 and 5 correspond to reported minima of pH 4.5 to 5.5 for the early 1960's. However, the inferred pH minimum of 6.0 for Station 3 is at variance with this observation. Inspection of the diatom assemblages from Station 3 reveals a predominance of the pH-indifferent planktonic diatom Cyclotella stelligera in deeper sediments, which would tend to overestimate pH. The spatial variability of diatoms in sediments is mainly a function of basin morphometry and, according to the criteria of Earle et al. (1987), planktonic diatoms would tend to be overestimated and littoral diatoms underestimated at Station 3. Station 3 is located in the eastern portion of Quirke Lake, and is somewhat isolated from the western portion containing Stations 1 and 2 by a chain of islands. This segregation of the two basins may account for the development of different diatom assemblages in each.

Thorium profiles in sediment cores show concentration rises beginning at 6.0 cm at Station 2, 1.1 to 2.8 cm at Station 4, and 4.1 to 4.3 cm at Station 5 (Figure 3.4). The Th rise at Station 2 occurred at a slightly greater depth than the beginning diatom-inferred

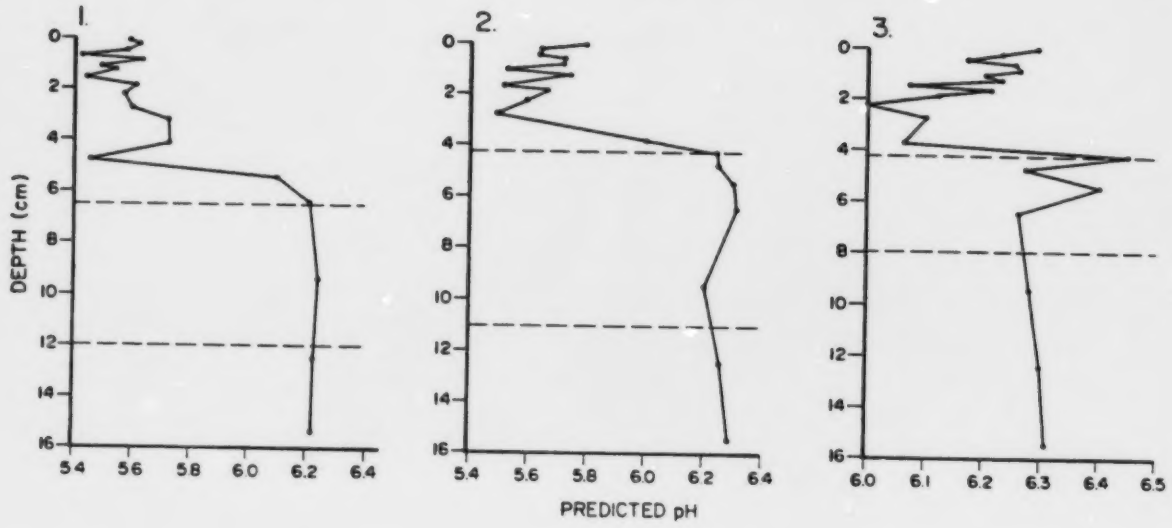

FIGURE 3.2: DIATOM-INFERRED pH IN SEDIMENT CORES FROM STATIONS 1, 2, 3, 1984.

Broken lines show the 3/4 pollen zone boundaries (lower), and the beginning of the decline in inferred pH (upper).

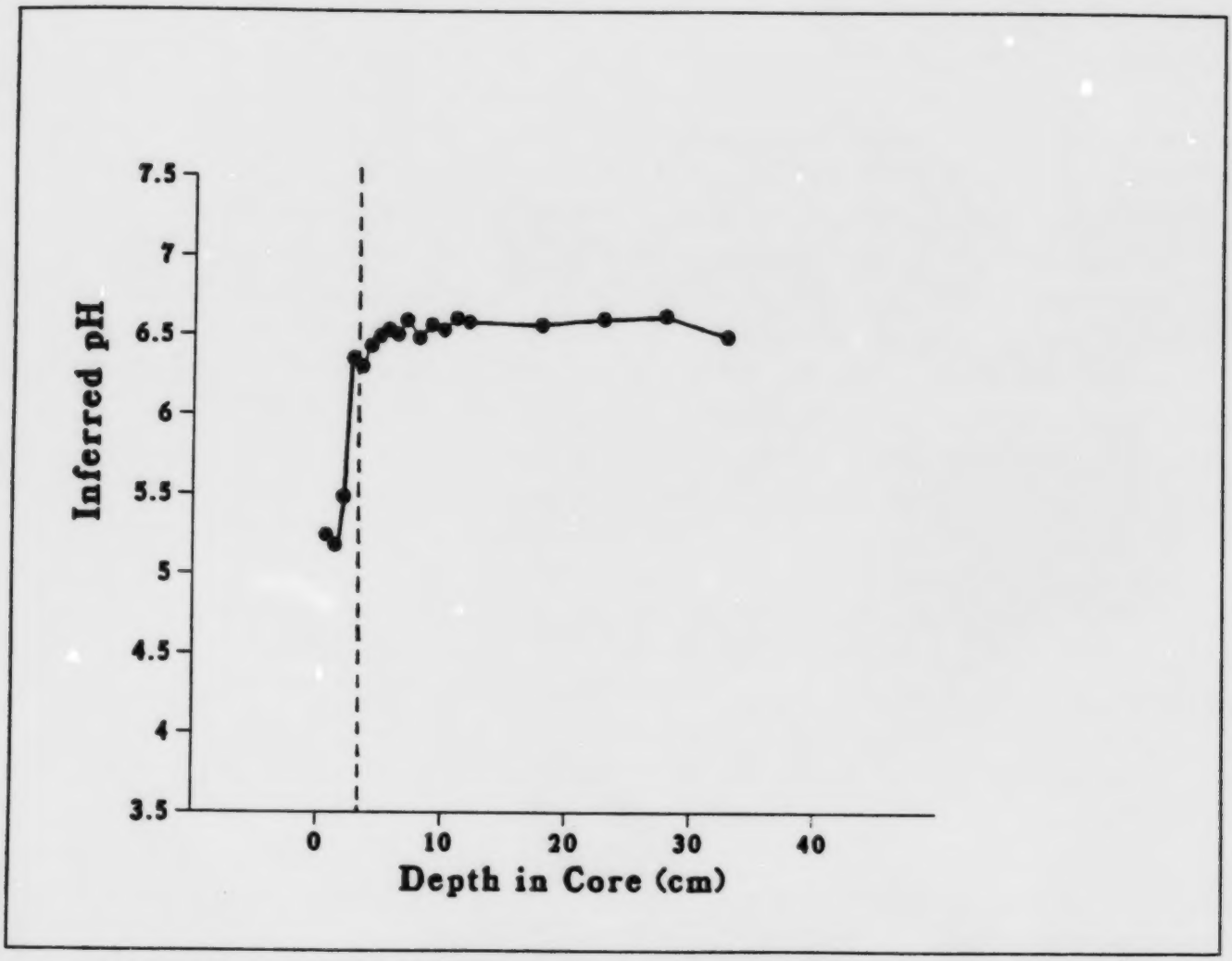

FIGURE 3.3: DIATOM-INFERRED pH IN SEDIMENT CORE FROM STATION 5, 1986.

Broken line shows the beginning of the decline in inferred pH.

pH decline measured in 1984 (Figure 3.2), probably reflecting variation between cores and small differences in sampling locations in the two surveys. The variation in the Th rise in cores from Station 4 (40 m water depth) is considerable, and is due to sampling effects or to local heterogeneity in surficial sediments. The two Th profiles from Station 5 (20 m water depth) were in closer agreement with each other, but concentration rises occurred about 1 cm deeper than did the diatom-inferred pH decline at the same station (Figure 3.3). The difference between the diatom and Th horizons at Station 5 is less than the difference between Th horizon depths at Station 4 (Figure 3.4), indicating that this degree of variation between sediment cores is probably due to sampling effects rather than to the difference in analytical approach. Excellent agreement between Th-232 and diatom horizons was found at two of three stations sampled in 1984 (Figure 3.5), further indicating that Th and fossil diatom dating methods provide comparable results.

Based on the analysis of Th profiles, fossil diatoms and fossil pollen, present sedimentation rates range from 0.4 to 2.4 $mm \cdot yr^{-1}$ (Table 3.1), with the average value being 1.4 $mm \cdot yr^{-1}$. Corresponding mass accumulation rates were found to range between 67 and 205 $g \cdot m^{-2} \cdot yr^{-1}$ (Table 3.1), with an average of 130 $g \cdot m^{-2} \cdot yr^{-1}$. In comparison, pre-mining sedimentation rates are estimated at 24 to 64 $g \cdot m^{-2} \cdot yr^{-1}$ (mean of 44 $g \cdot m^{-2} \cdot yr^{-1}$). The higher present-day sedimentation rates may be related to uranium mining and milling activities. Suspended solids levels may be high in runoff from disturbed areas, and precipitates formed from ferrous minerals dissolved by milling or later in tailings management areas may accumulate in Quirke Lake sediments. The occurrence of enhanced iron deposition is supported by iron concentrations of up to 20% and greater in Quirke Lake sediments (Figure 3.6), while typical iron concentrations in Shield lake sediments are in the order of 3% (estimated from data in Brunskill et al., 1971). Based on estimated sedimentation rates (Table 3.1), there is no evidence for sediment focussing in Quirke Lake under present conditions, although pre-mining sedimentation rates estimated from pollen analysis suggests some degree of focussing. Although focussing is typical in Shield lakes (Evans and Rigler, 1980a, 1983), it may not occur in some lakes (Cornwell, 1985). The variation in post-1957 sedimentation rates may in part be attributed to the variable but significant iron contents of surficial layers (typically 5 to 25%), which affects sediment density. This indicates that estimated mass sedimentation rates under present conditions are influenced by proximity to shore-based iron discharges and local redox conditions more than by focussing.

Figure 3.4 Thorium Activity Profiles (Bq/g) in Sediment Cores From Stations 2, 4 and 5 (100, 40 and 20 m deep respectively)

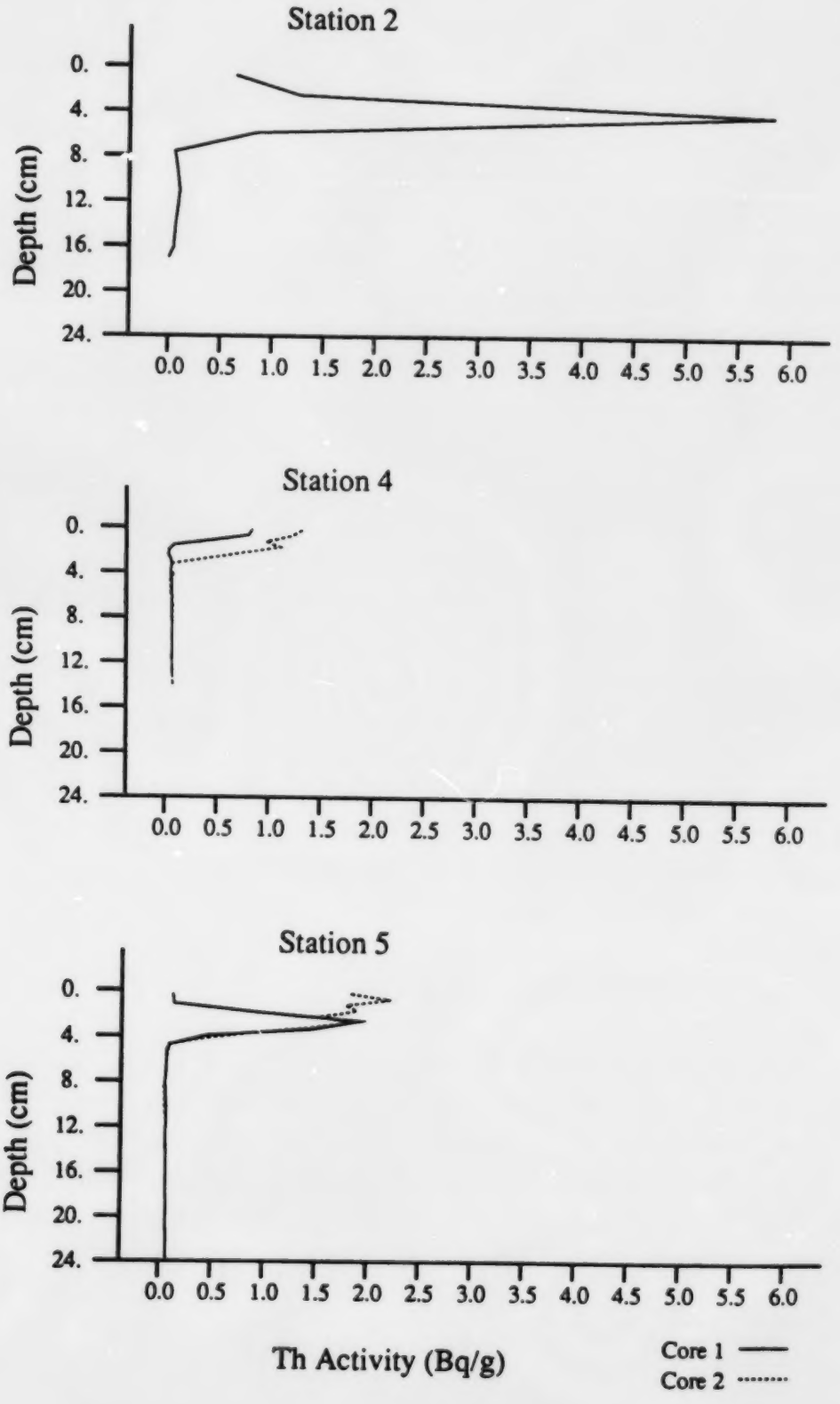

Radium vs. Time

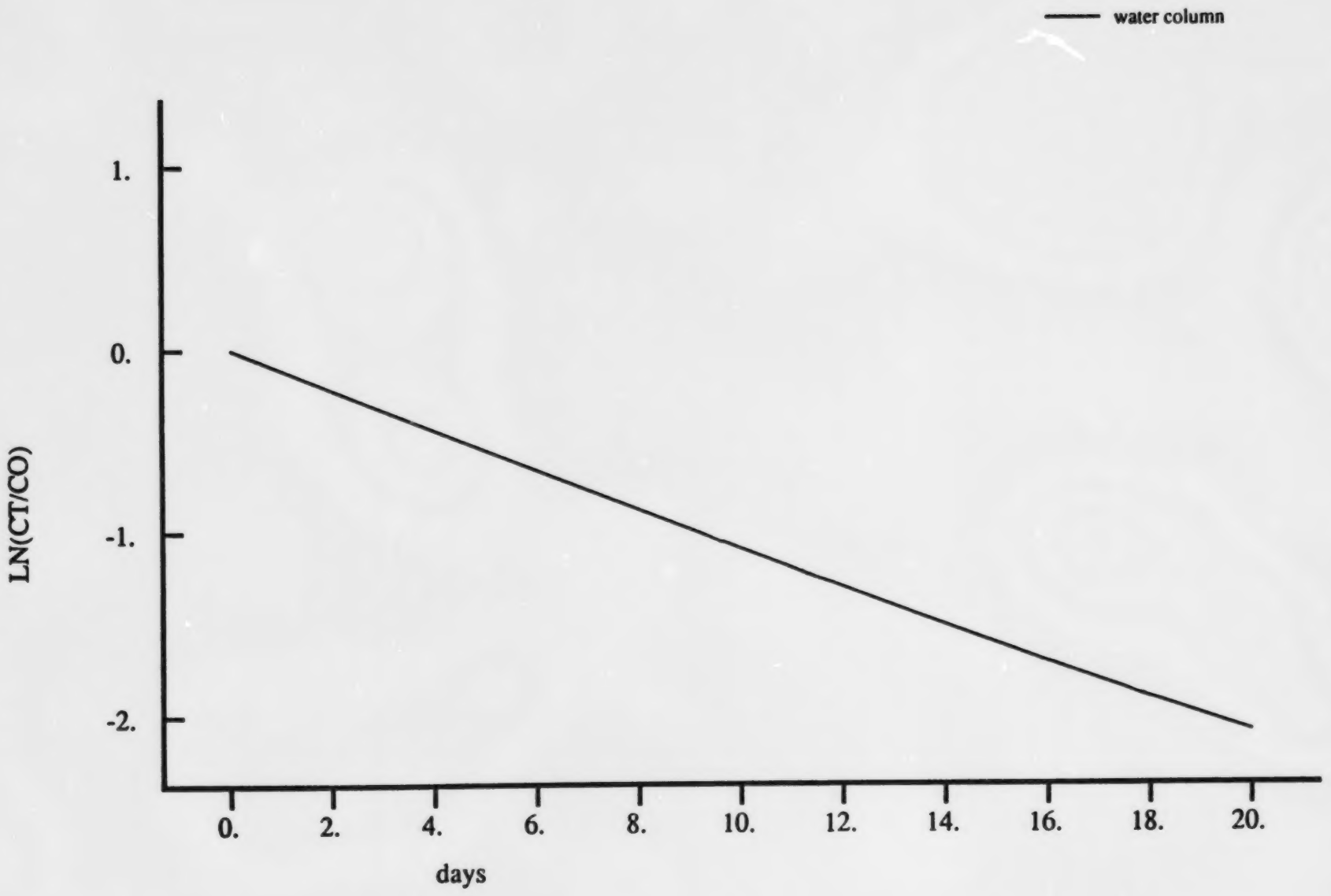

Flux vs. Time

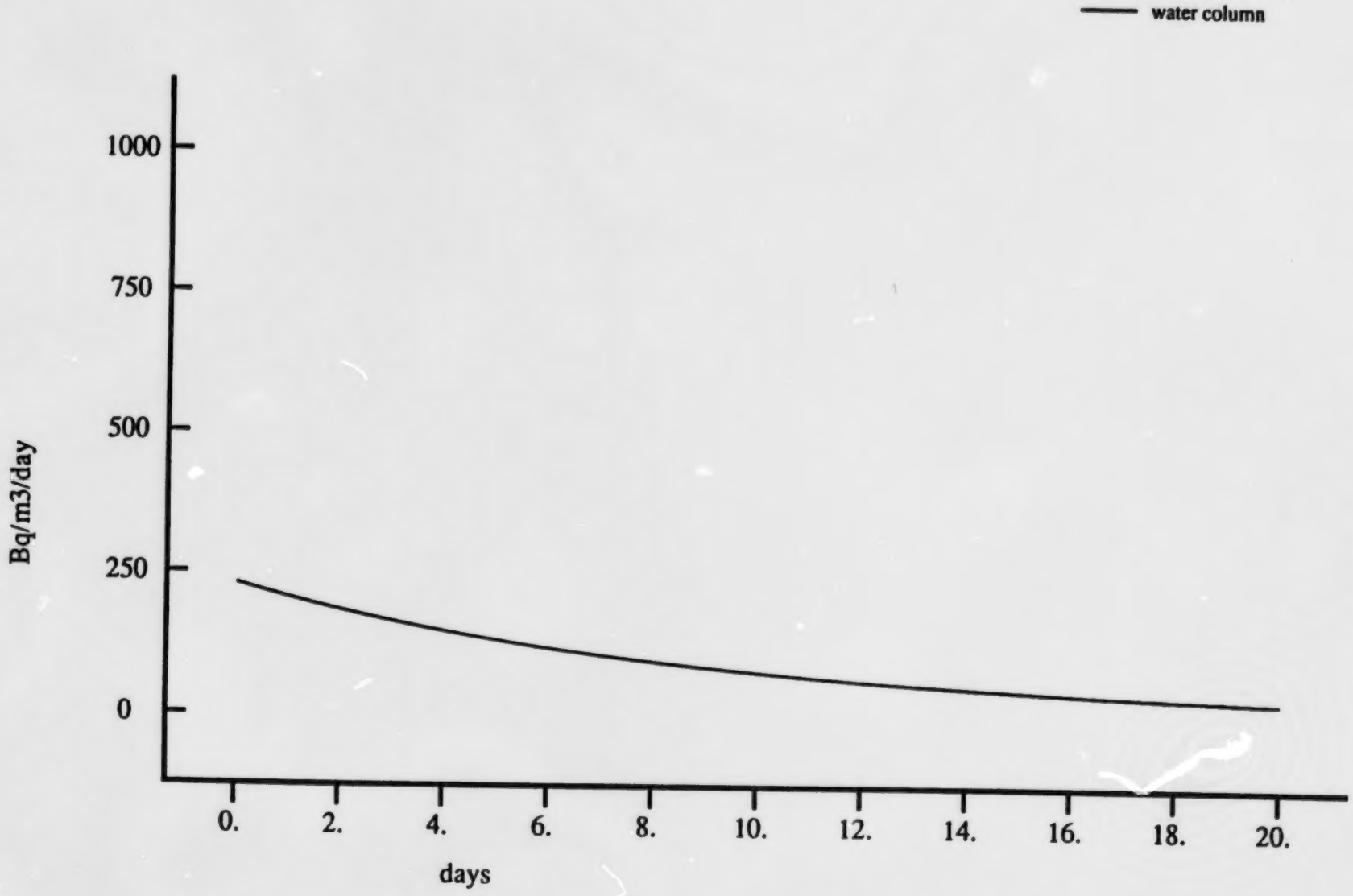
water column
1000
750
500
250
0
Bq/m3/day
0.
2.
4.
6.
8.
10.
12.
14.
16.
18.
20.
days

Radium 226 Sediment Activity vs. Time

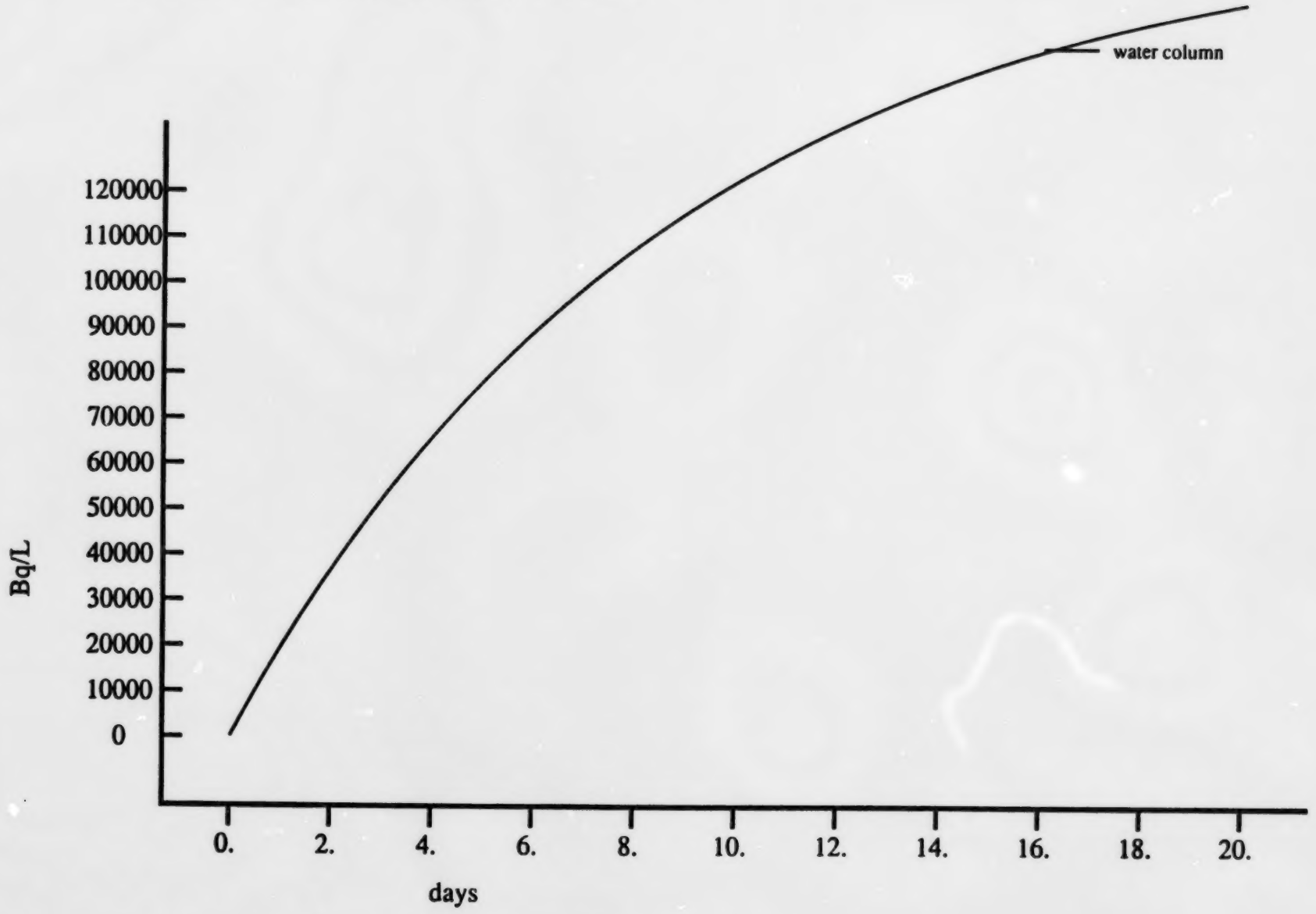

Radium 226 Water Column Activity vs. Time

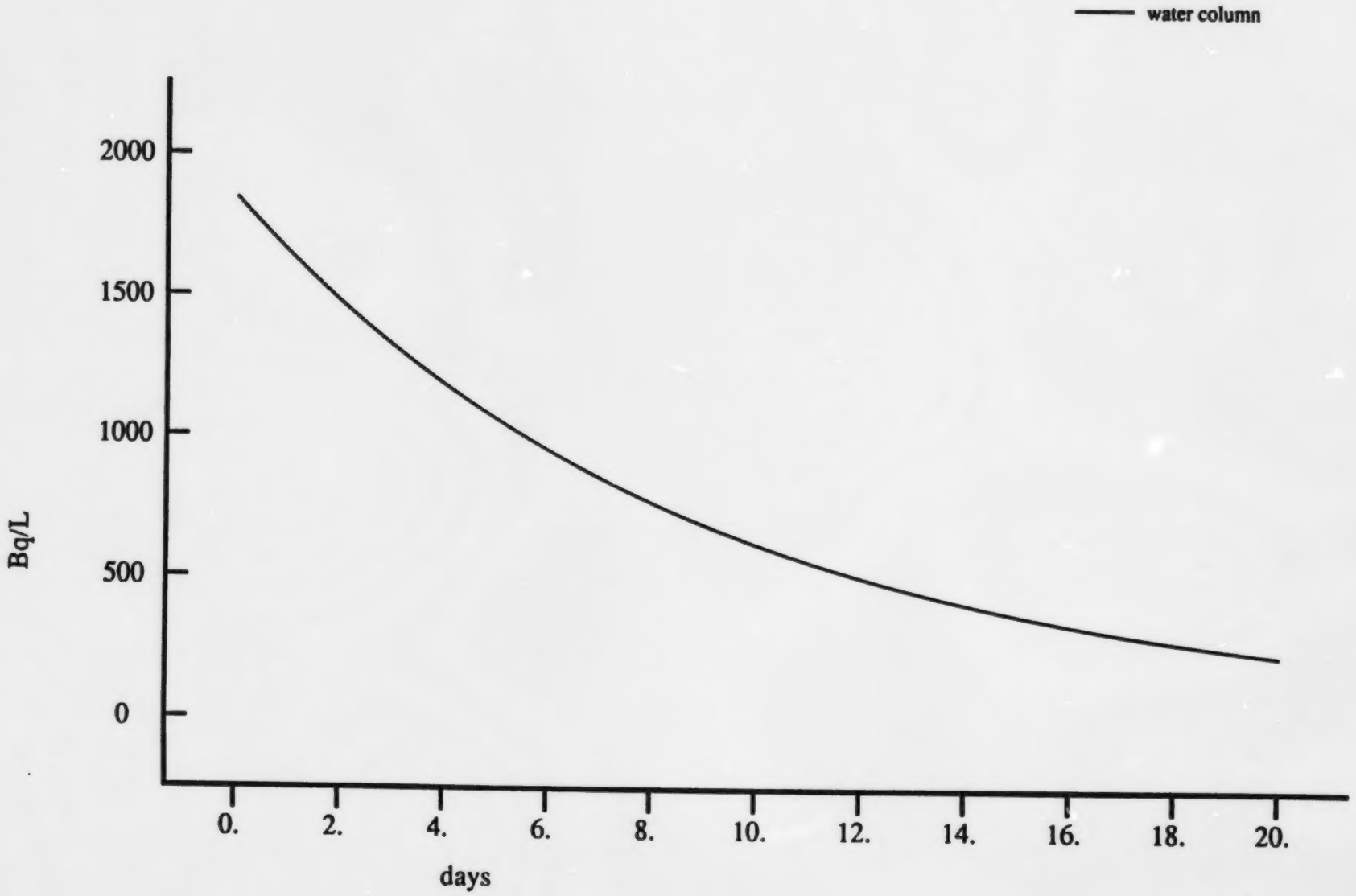

Radium 226 Water Column Activity vs. Time

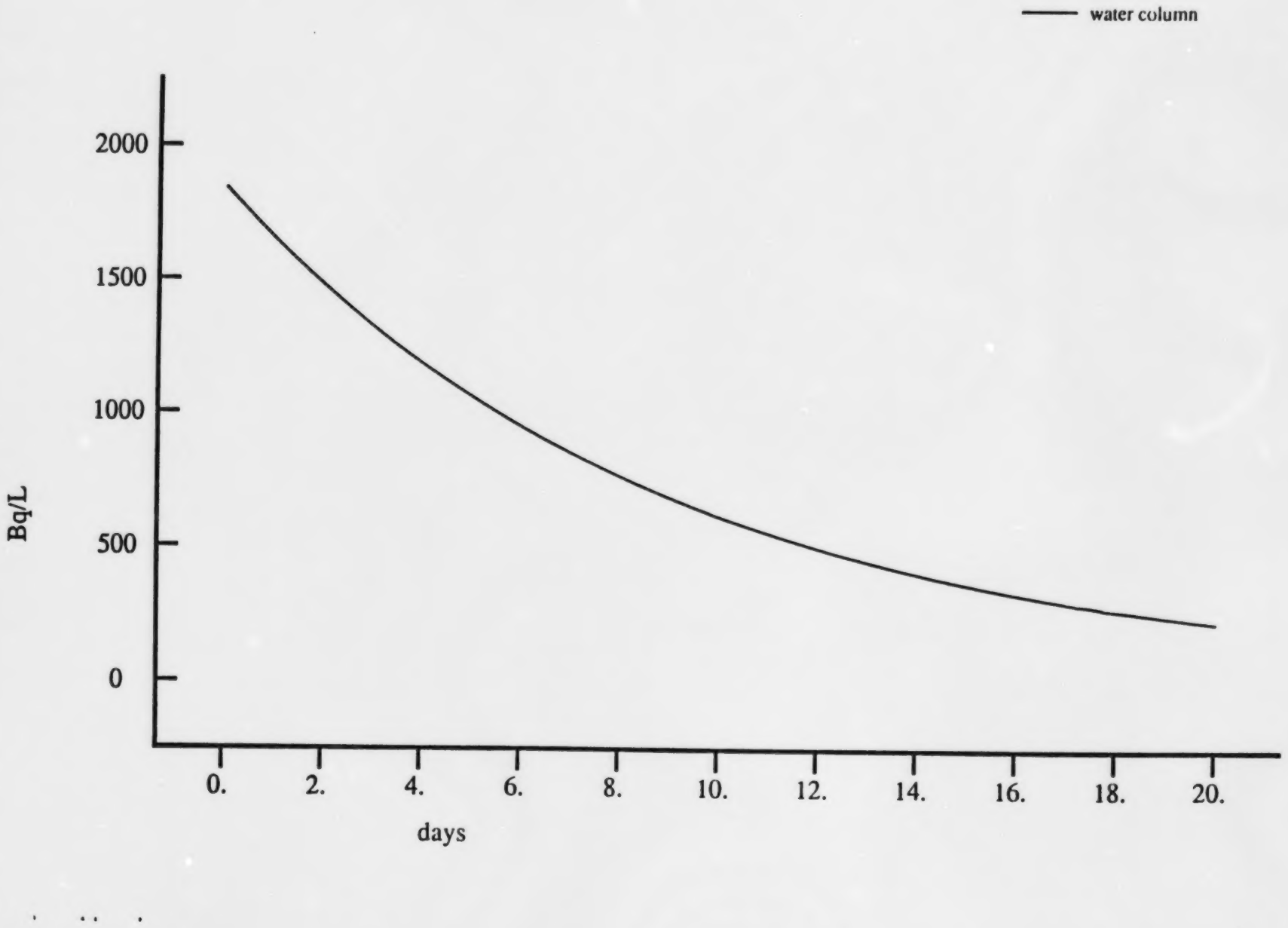

Desorption Rate

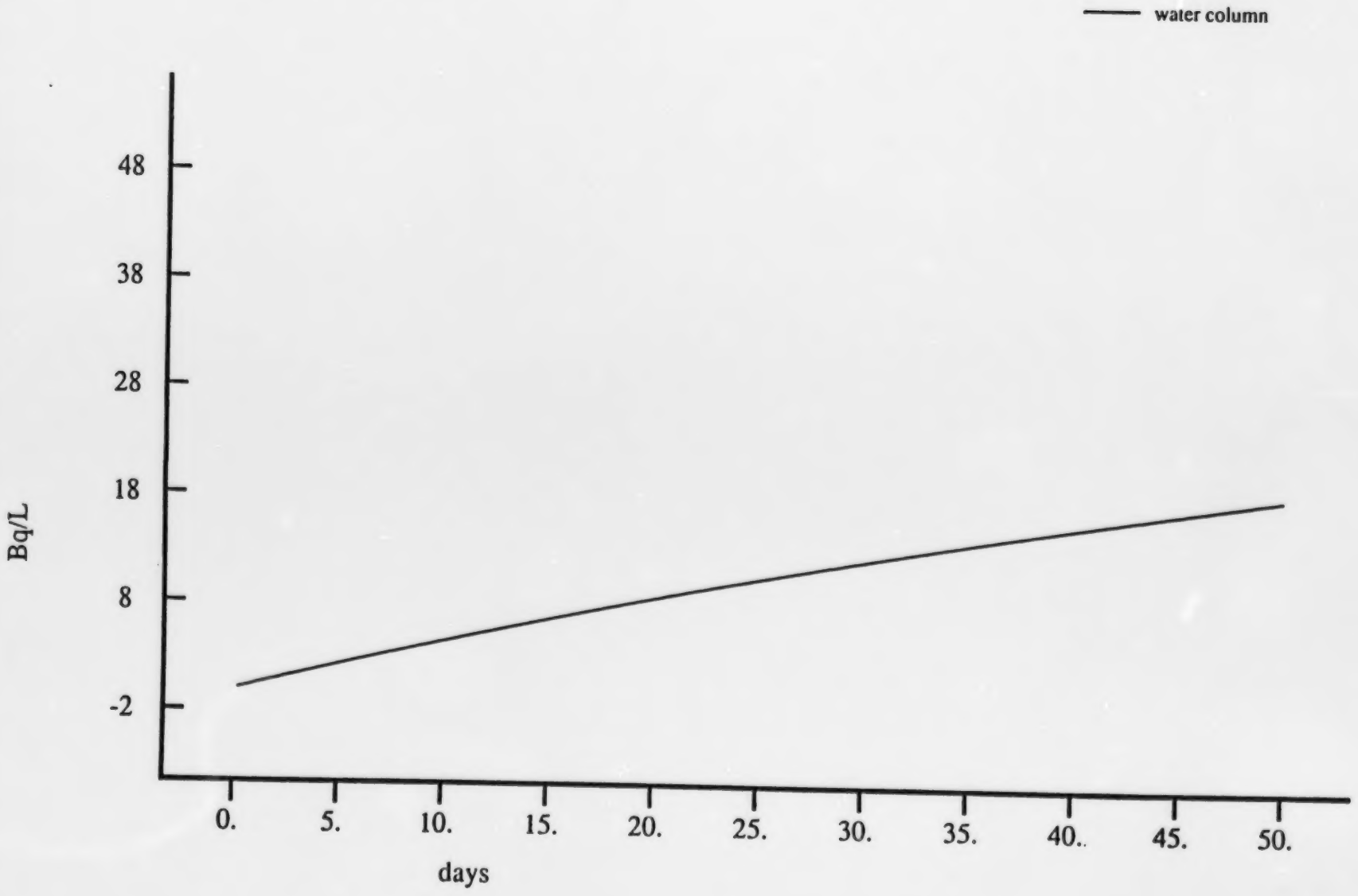

Radium 226 Sediment Activity vs. Time

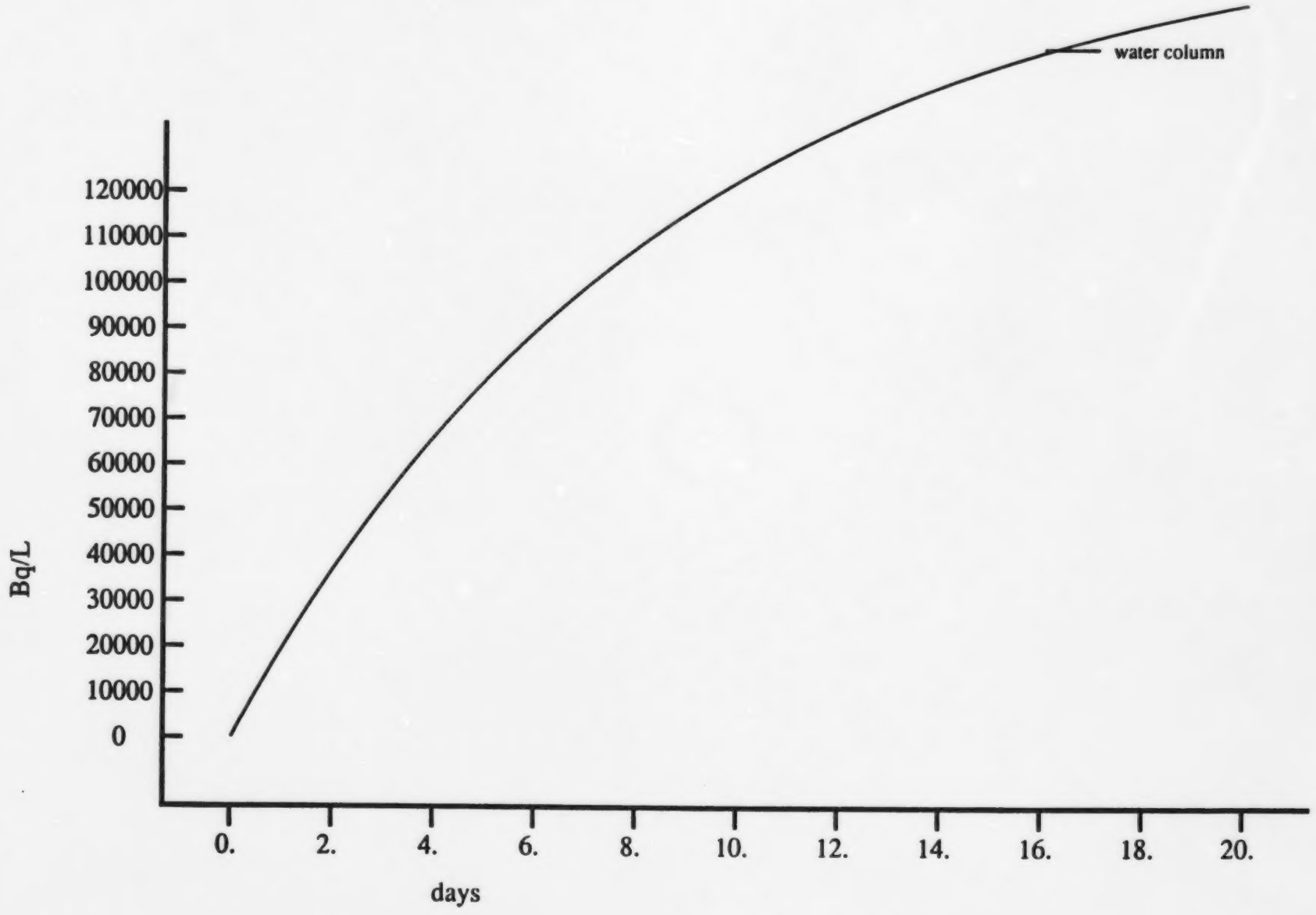

Flux vs. Time

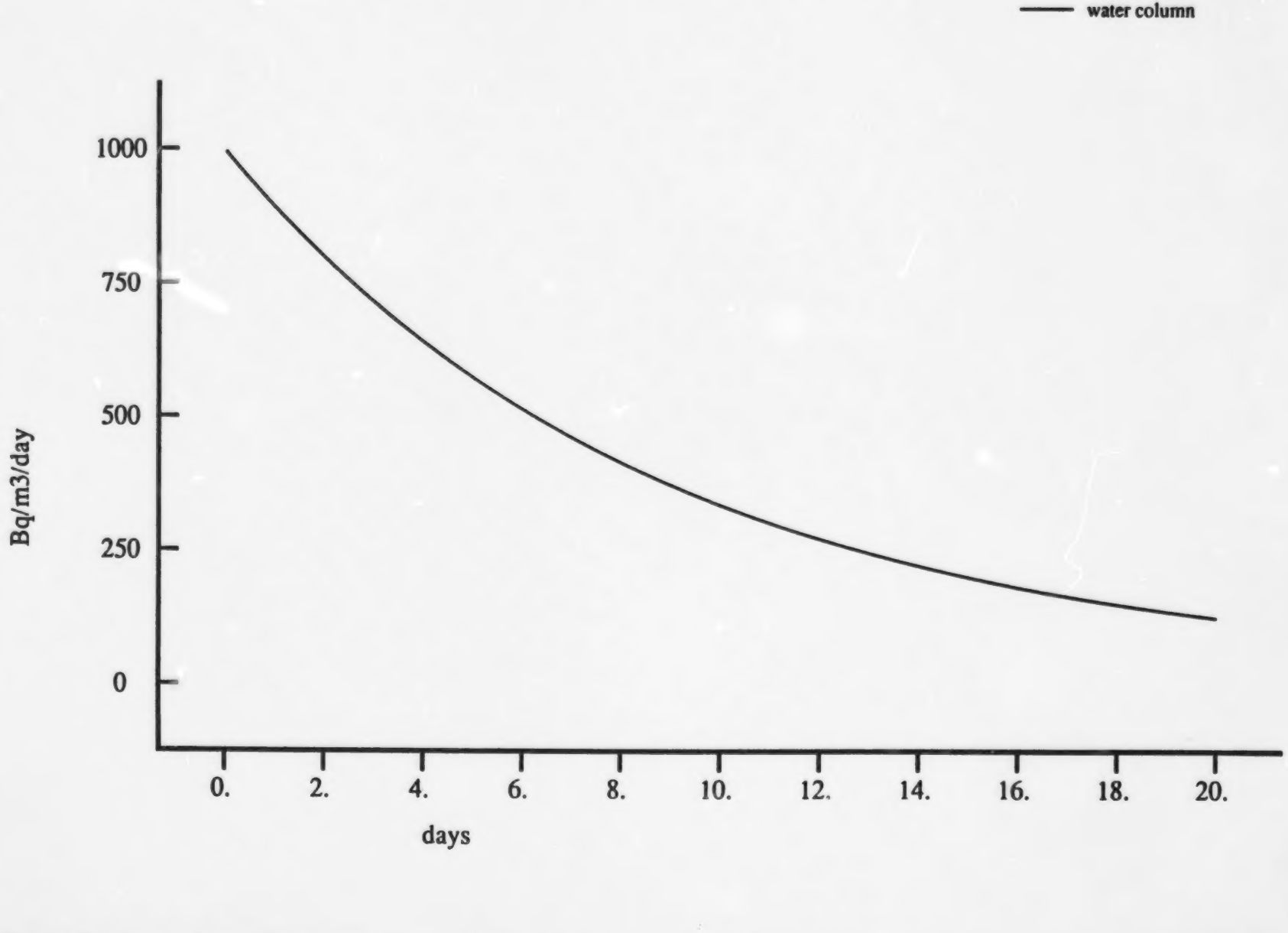
water column
1000
750
500
250
0
Bq/m3/day
0.
2.
4.
6.
8.
10.
12.
14.
16.
18.
20.
days

Radium vs. Time

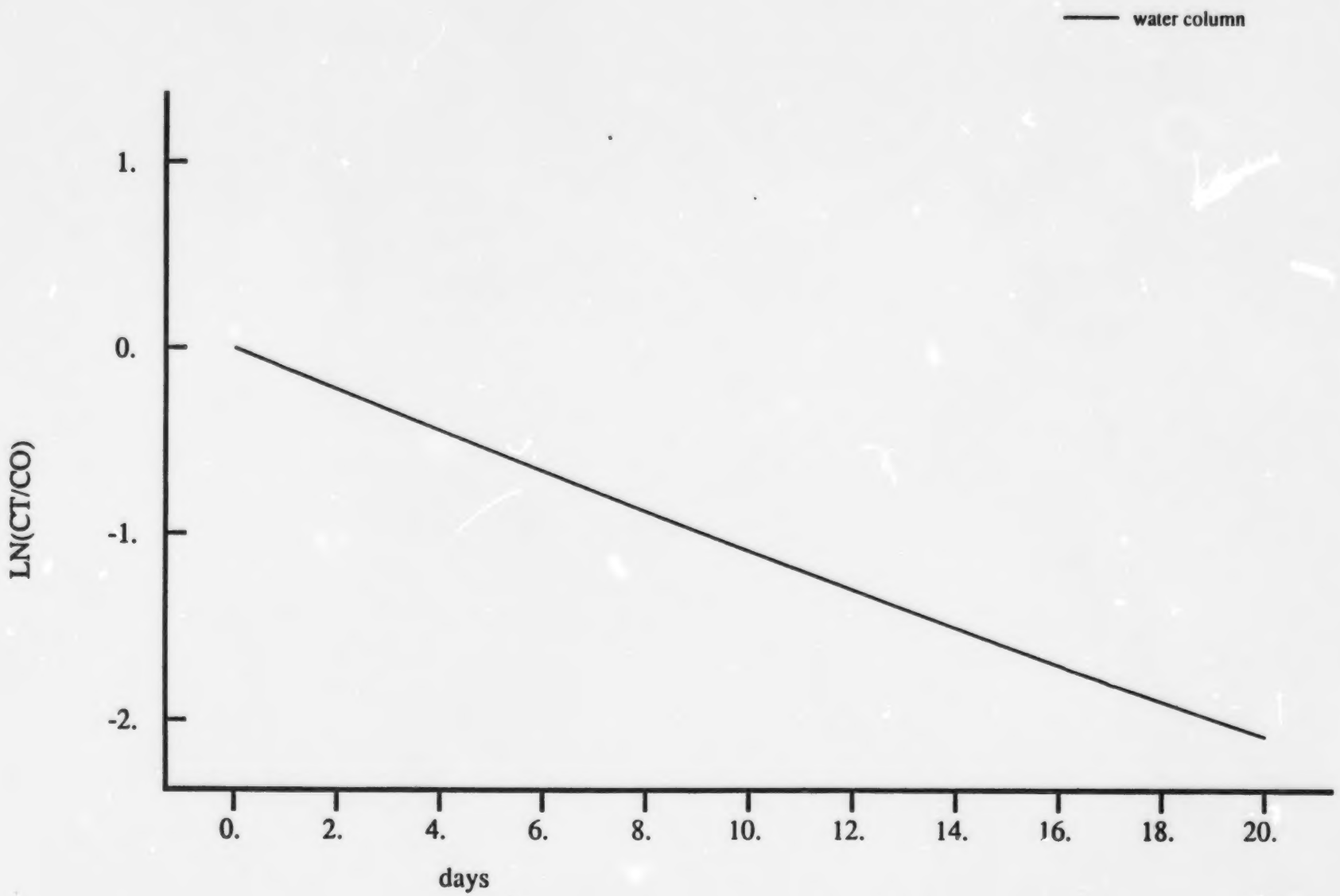

Desorption Rate

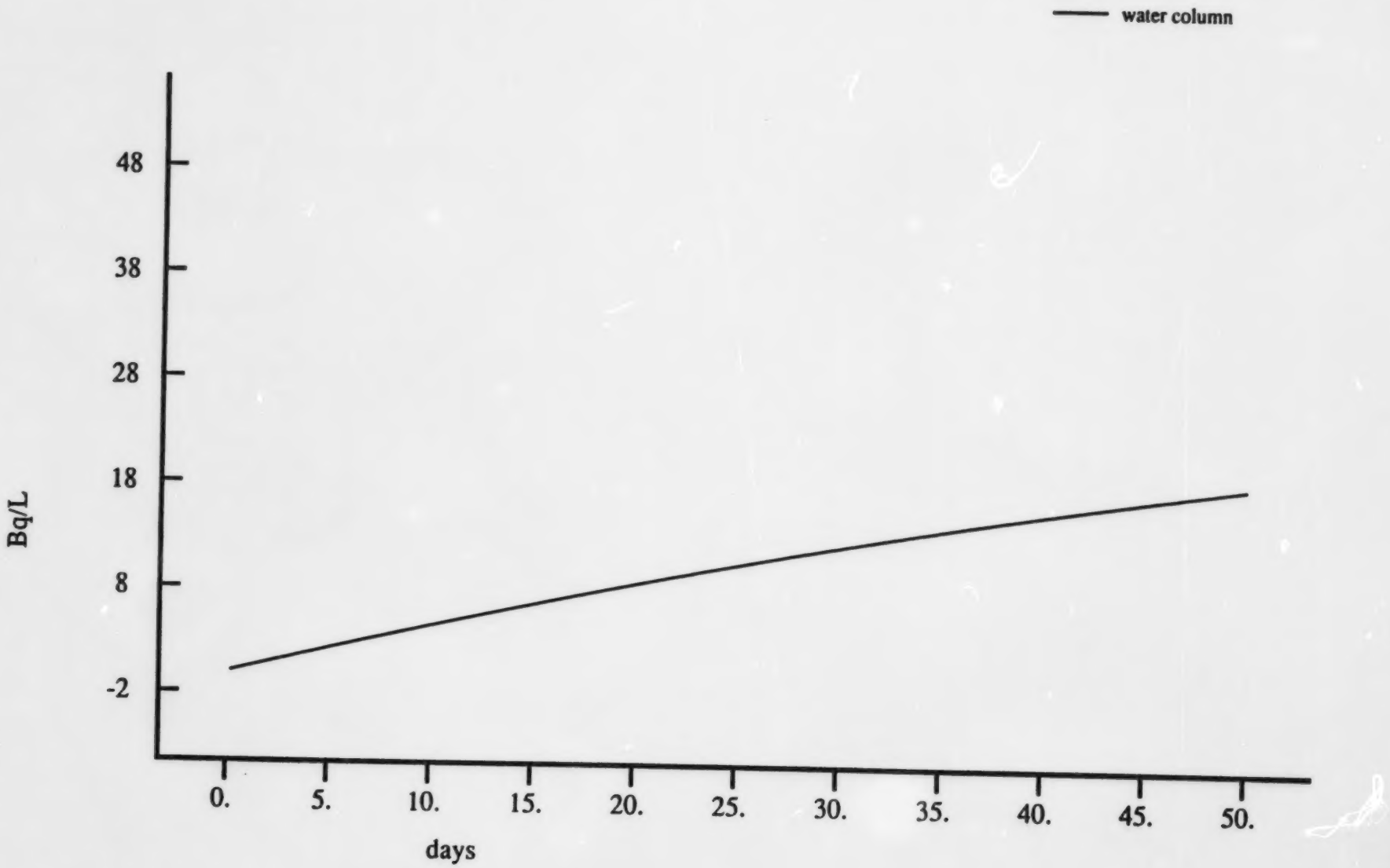

Radium 226 Water Column Activity vs. Time

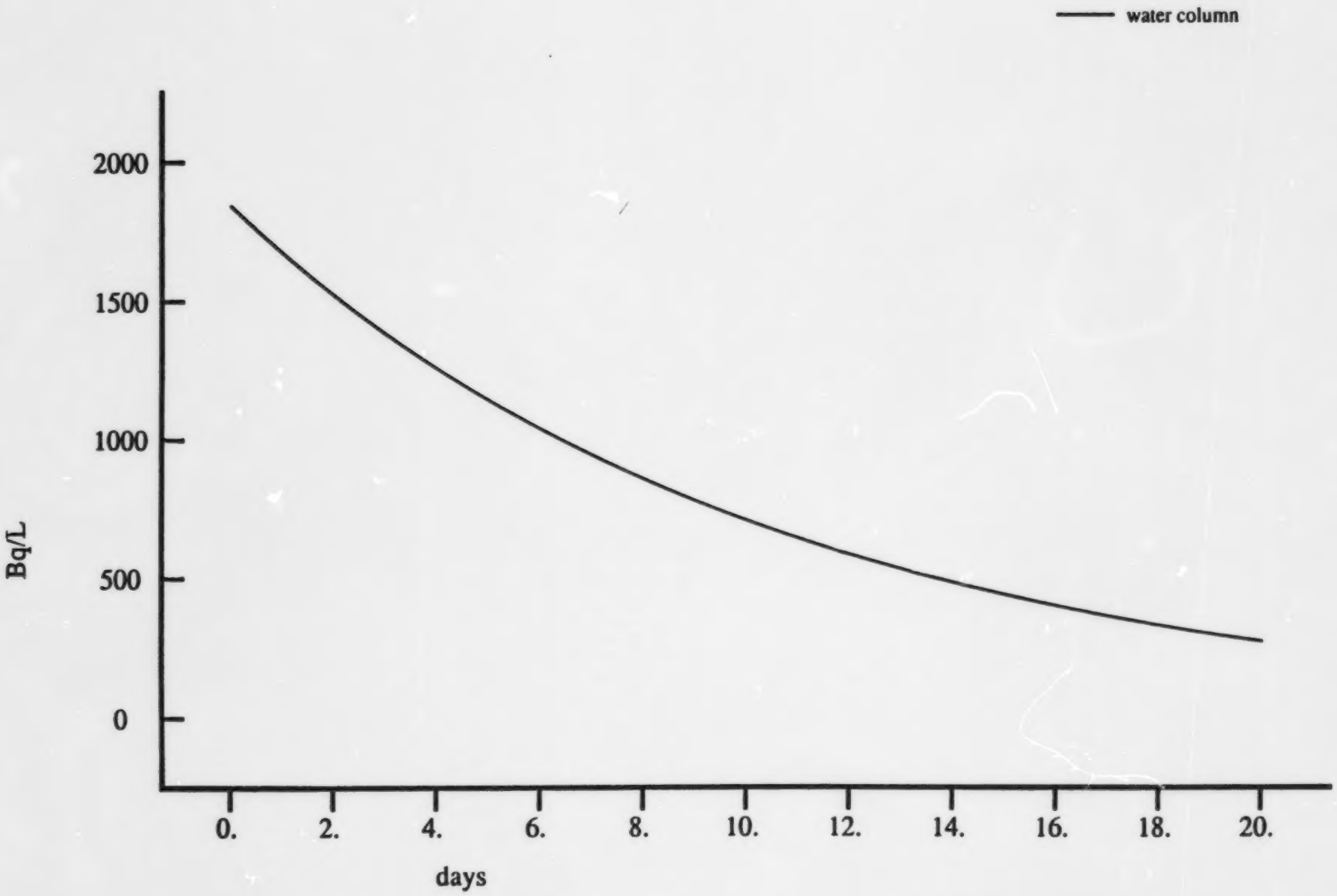

Radium 226 Sediment Activity vs. Time

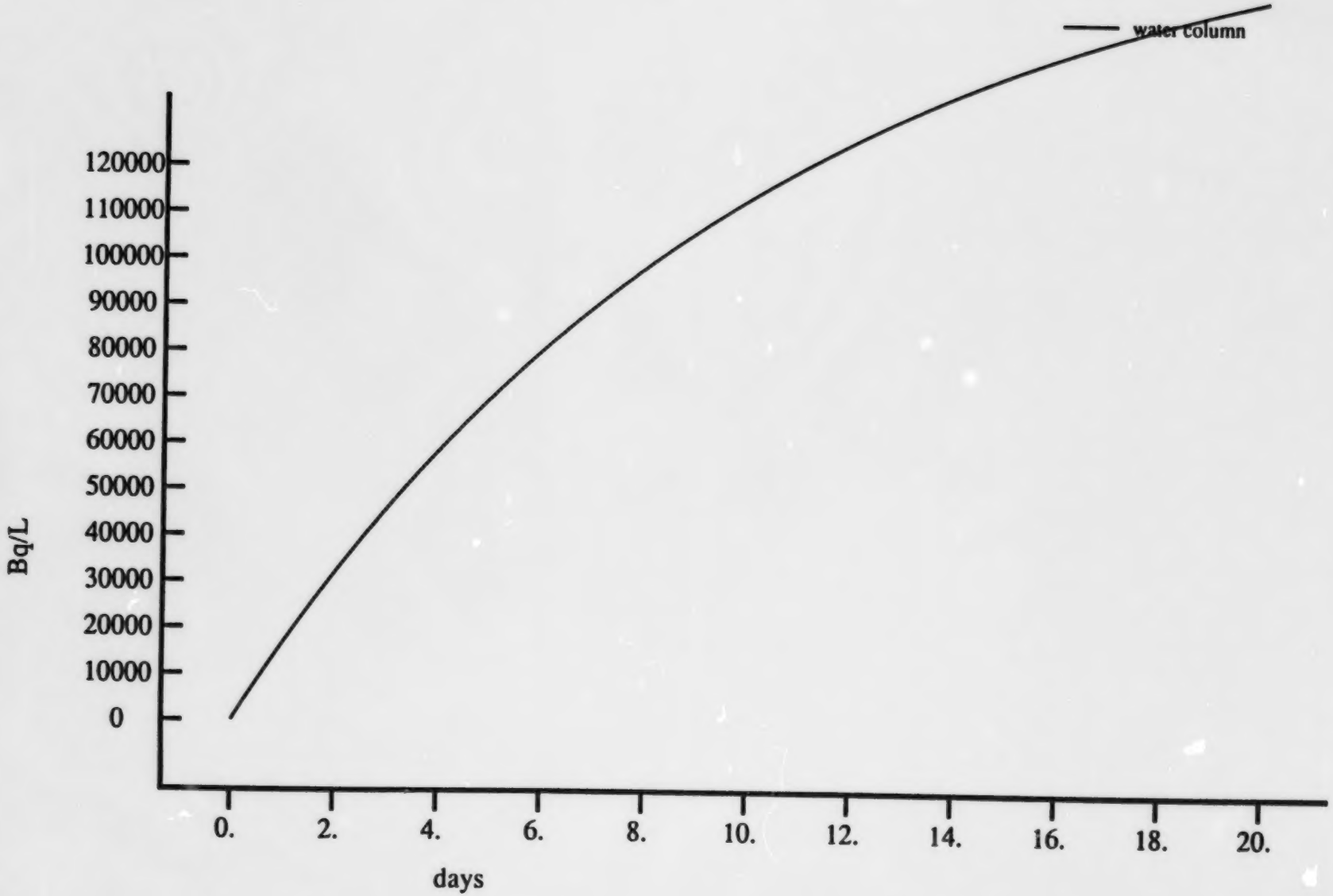

Flux vs. Time

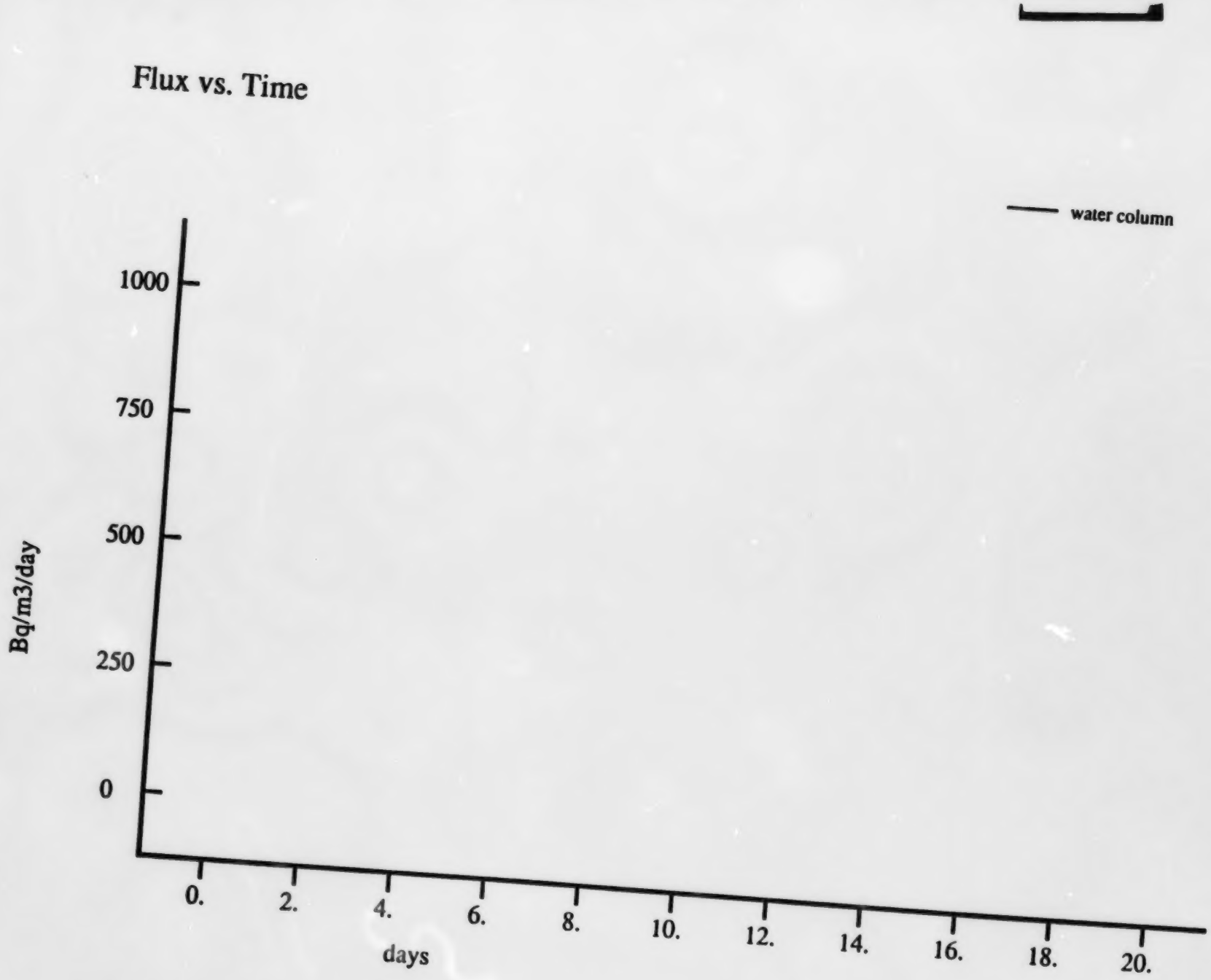
water column
1000
750
500
250
0
Bq/m3/day
0.
2.
4.
6.
8.
10.
12.
14.
16.
18.
20.
days

Radium vs. Time

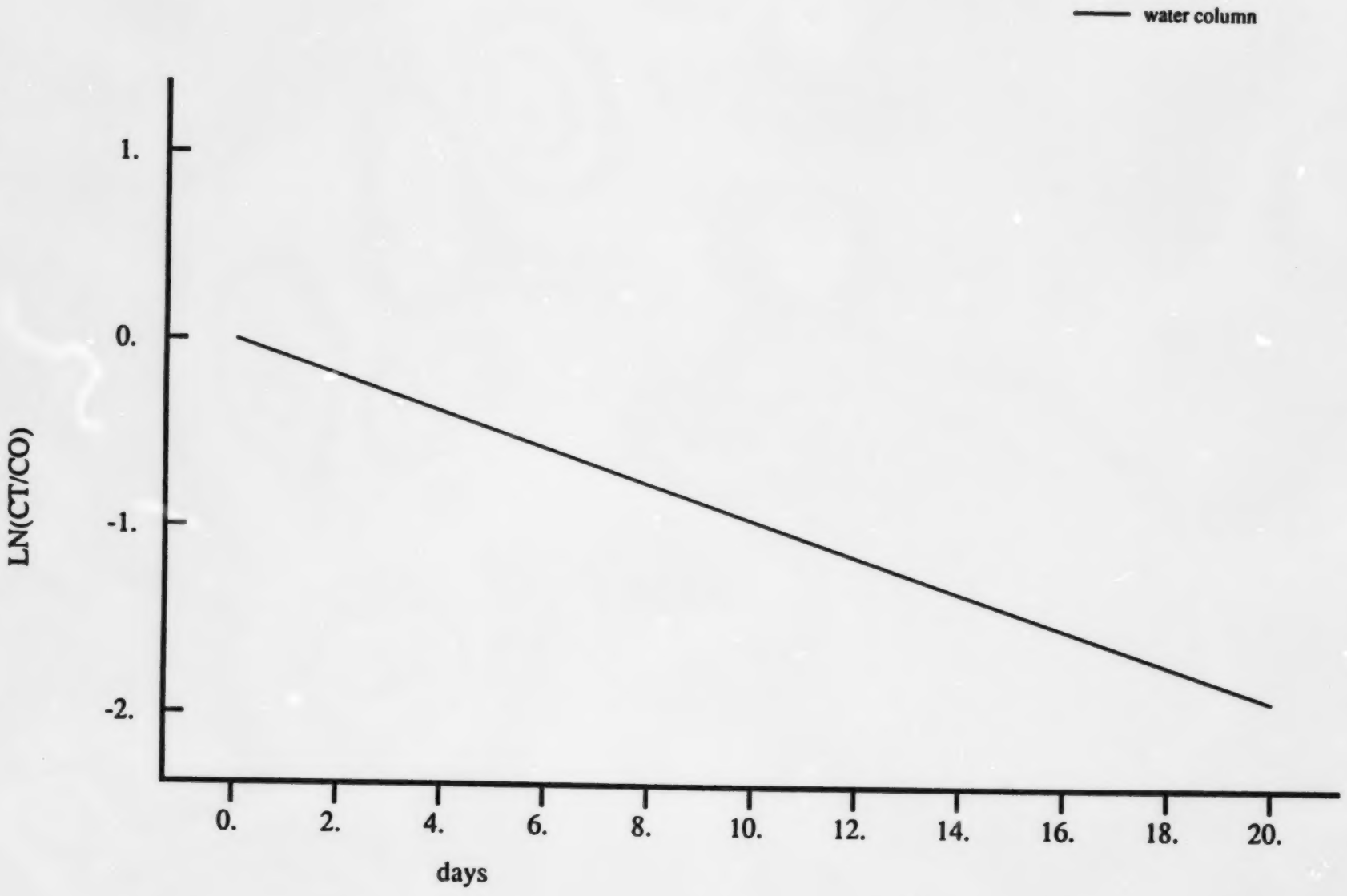

Desorption Rate

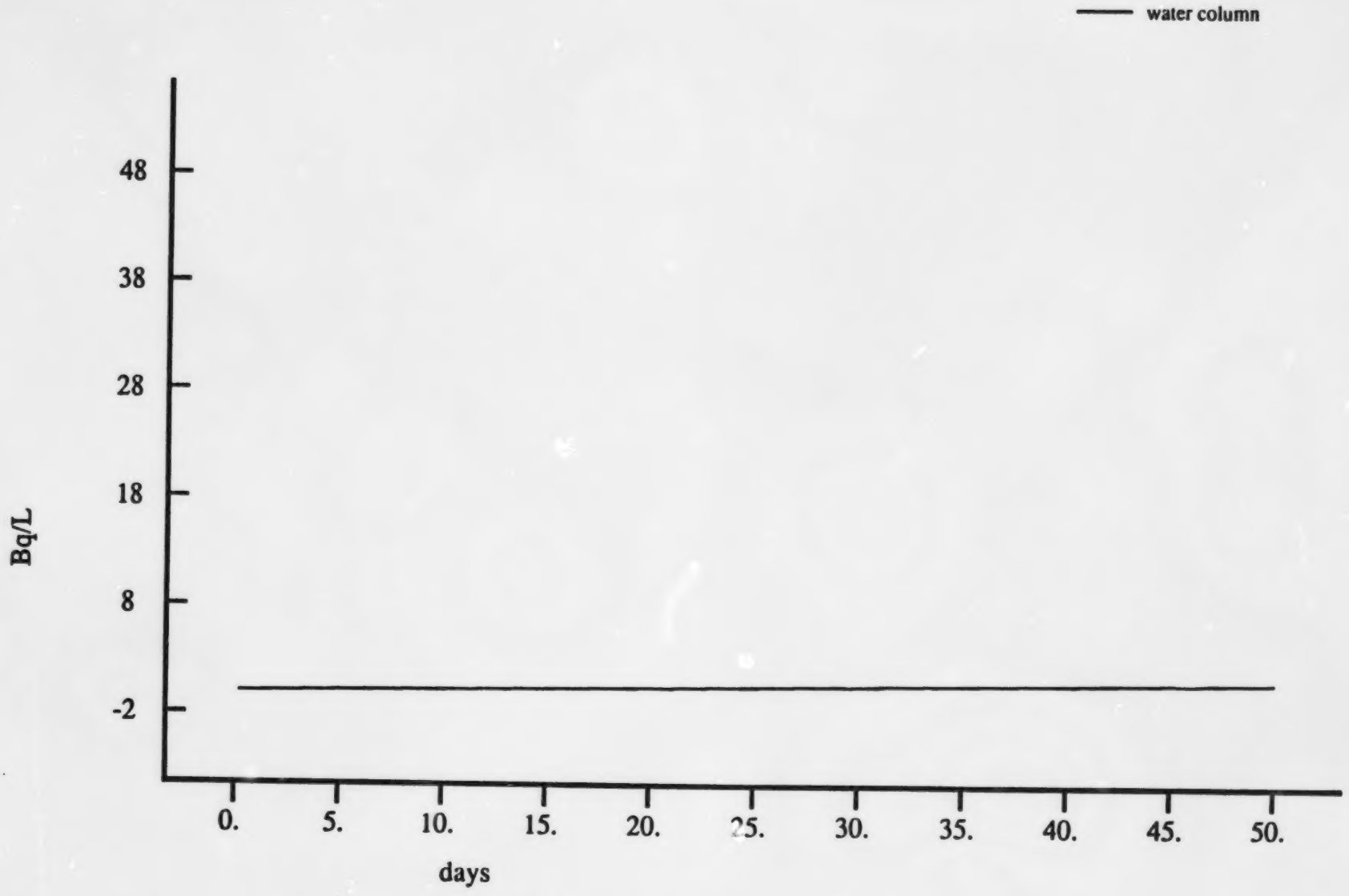

Radium 226 Water Column Activity vs. Time

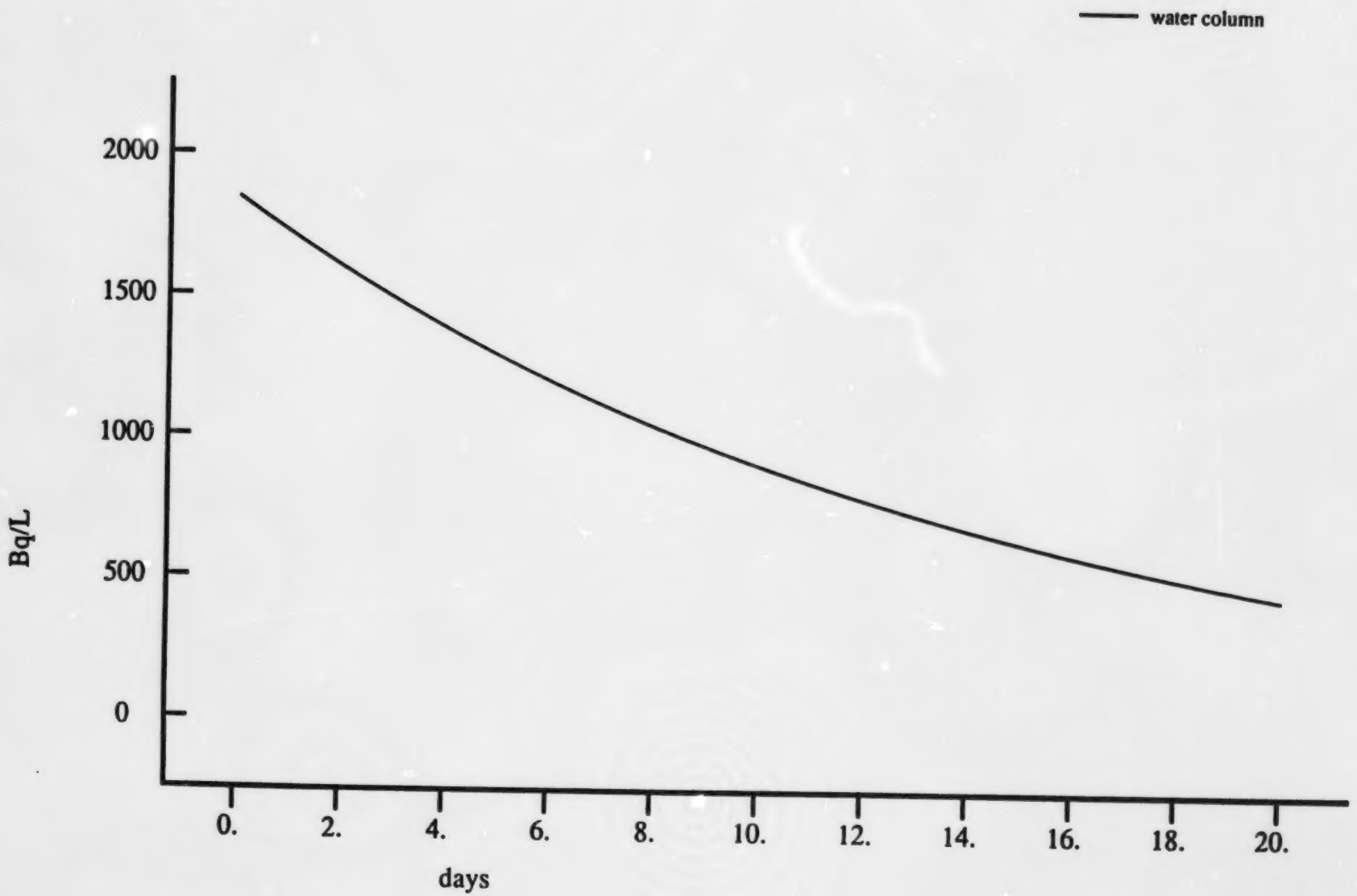

Flux vs. Time

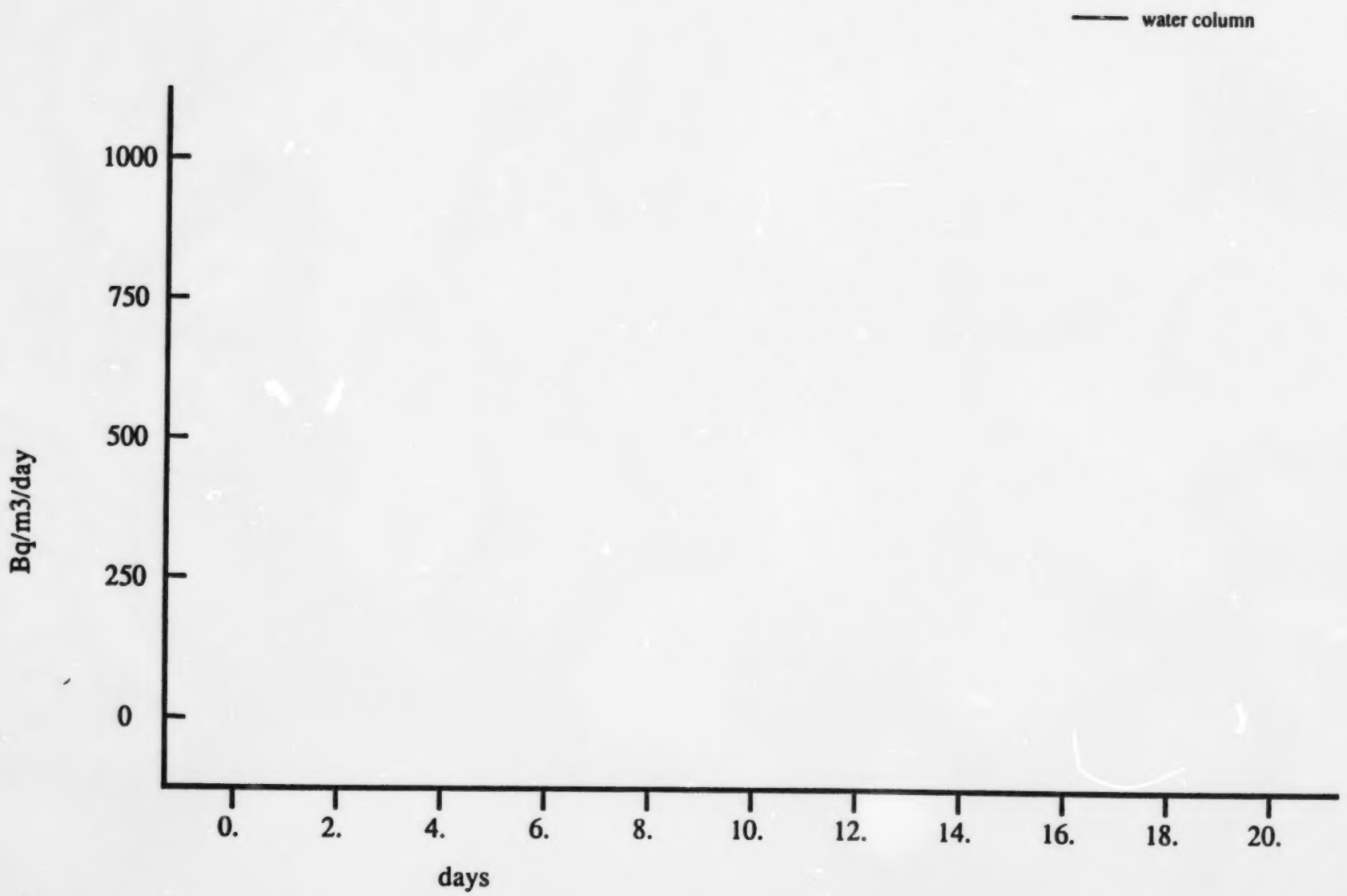
water column
1000
750
500
250
0
Bq/m3/day
0.
2.
4.
6.
8.
10.
12.
14.
16.
18.
20.
days

Radium 226 Sediment Activity vs. Time

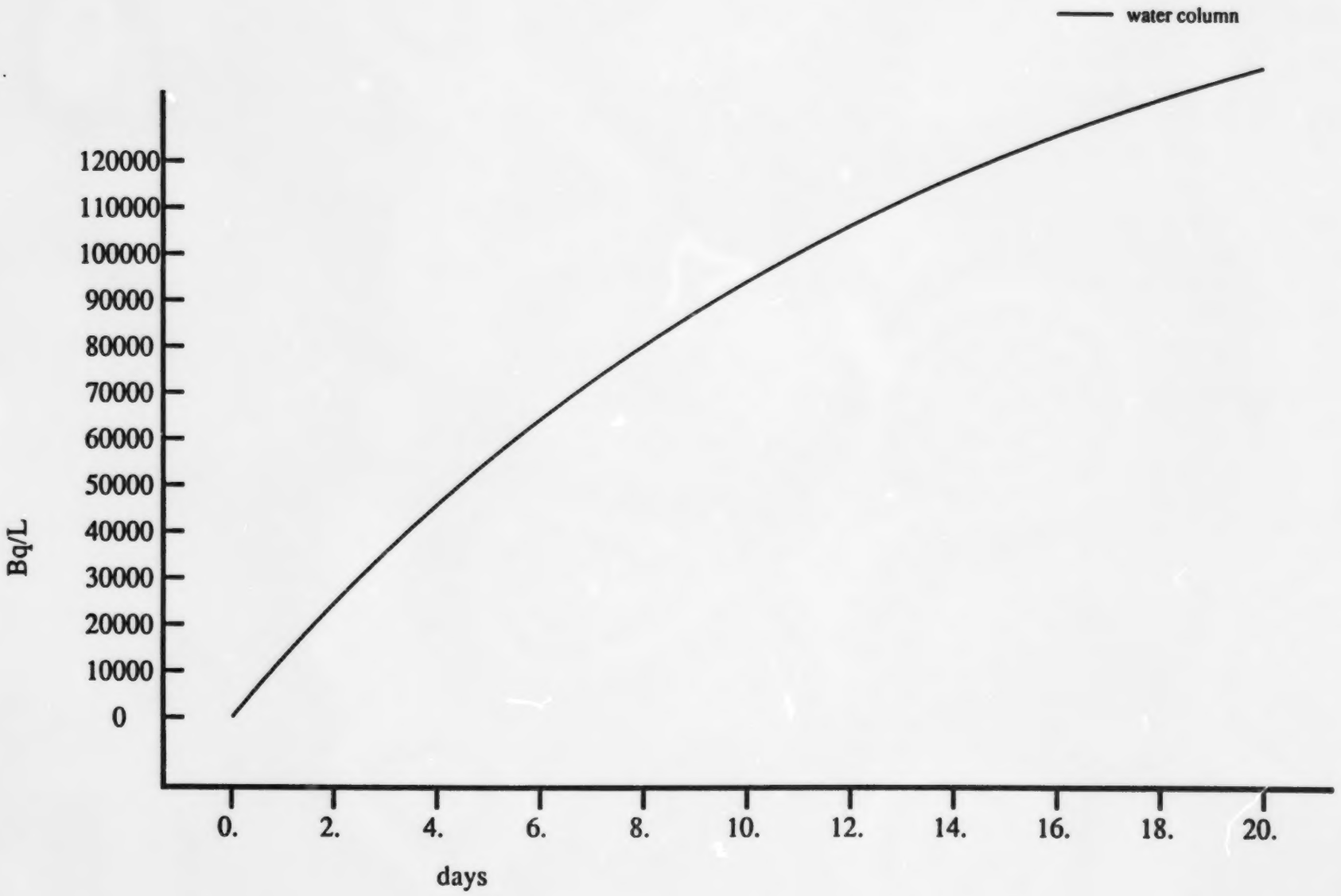

Desorption Rate

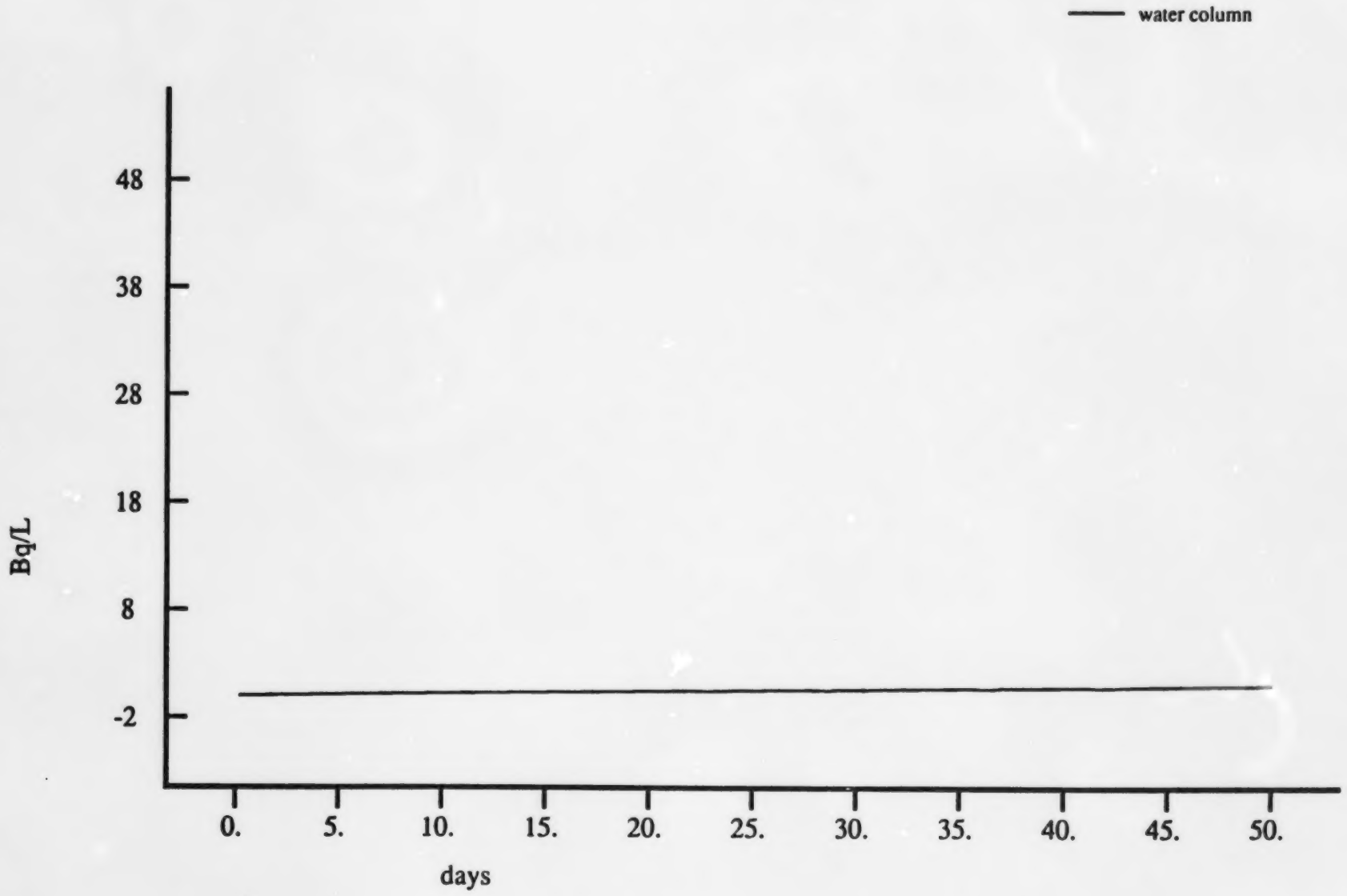

Radium vs. Time

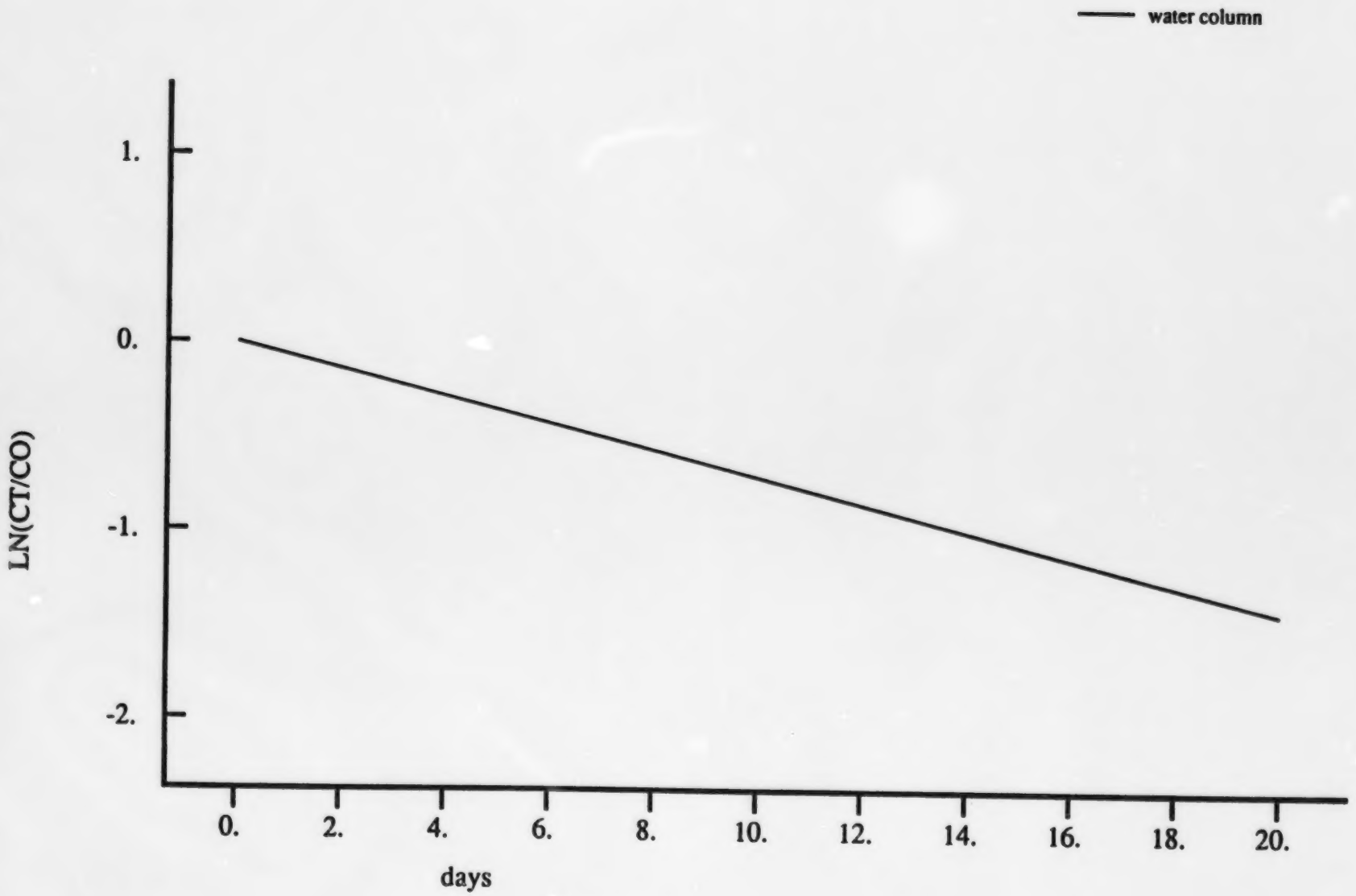

Radium 226 Water Column Activity vs. Time

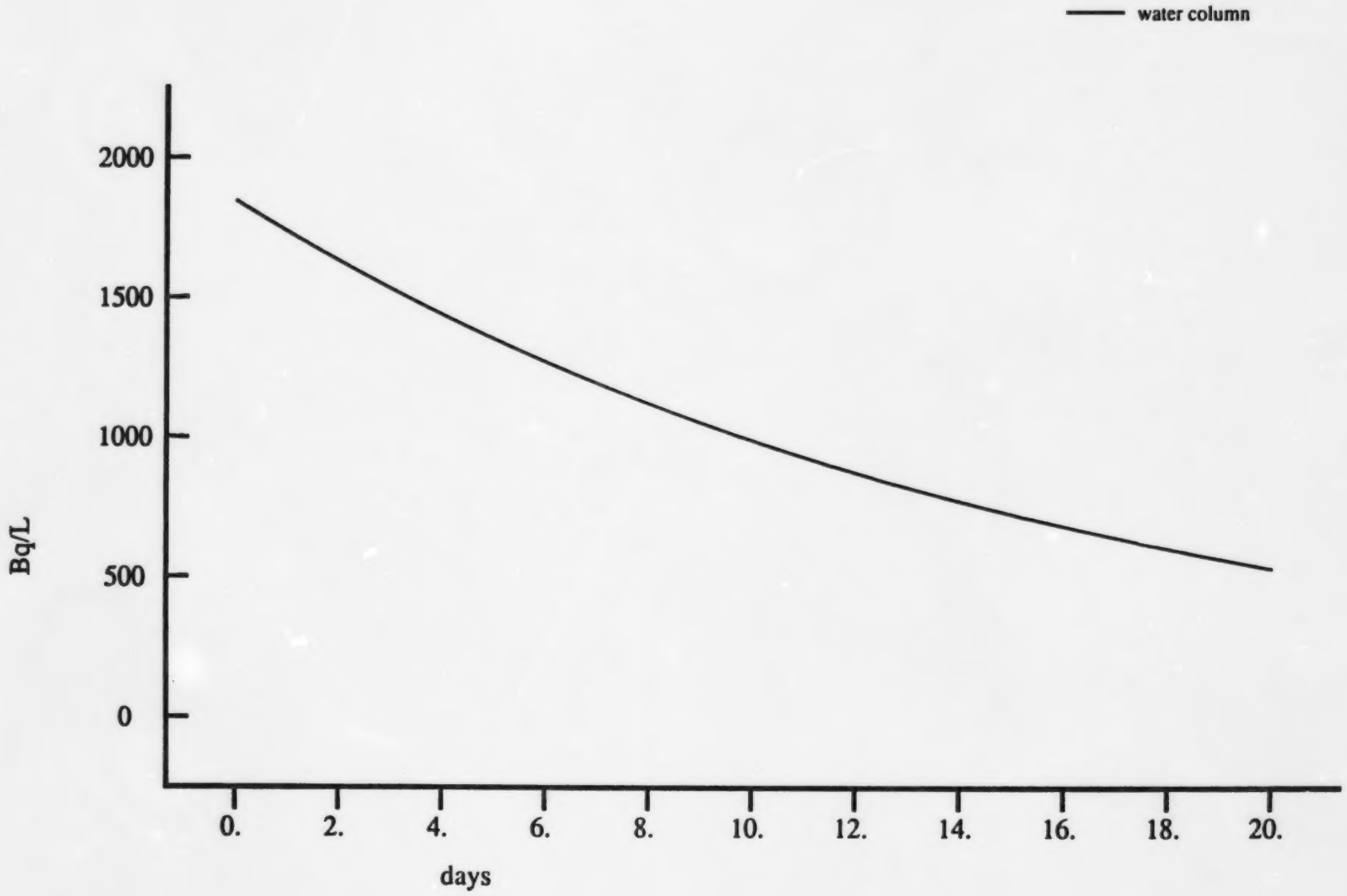

Radium 226 Sediment Activity vs. Time

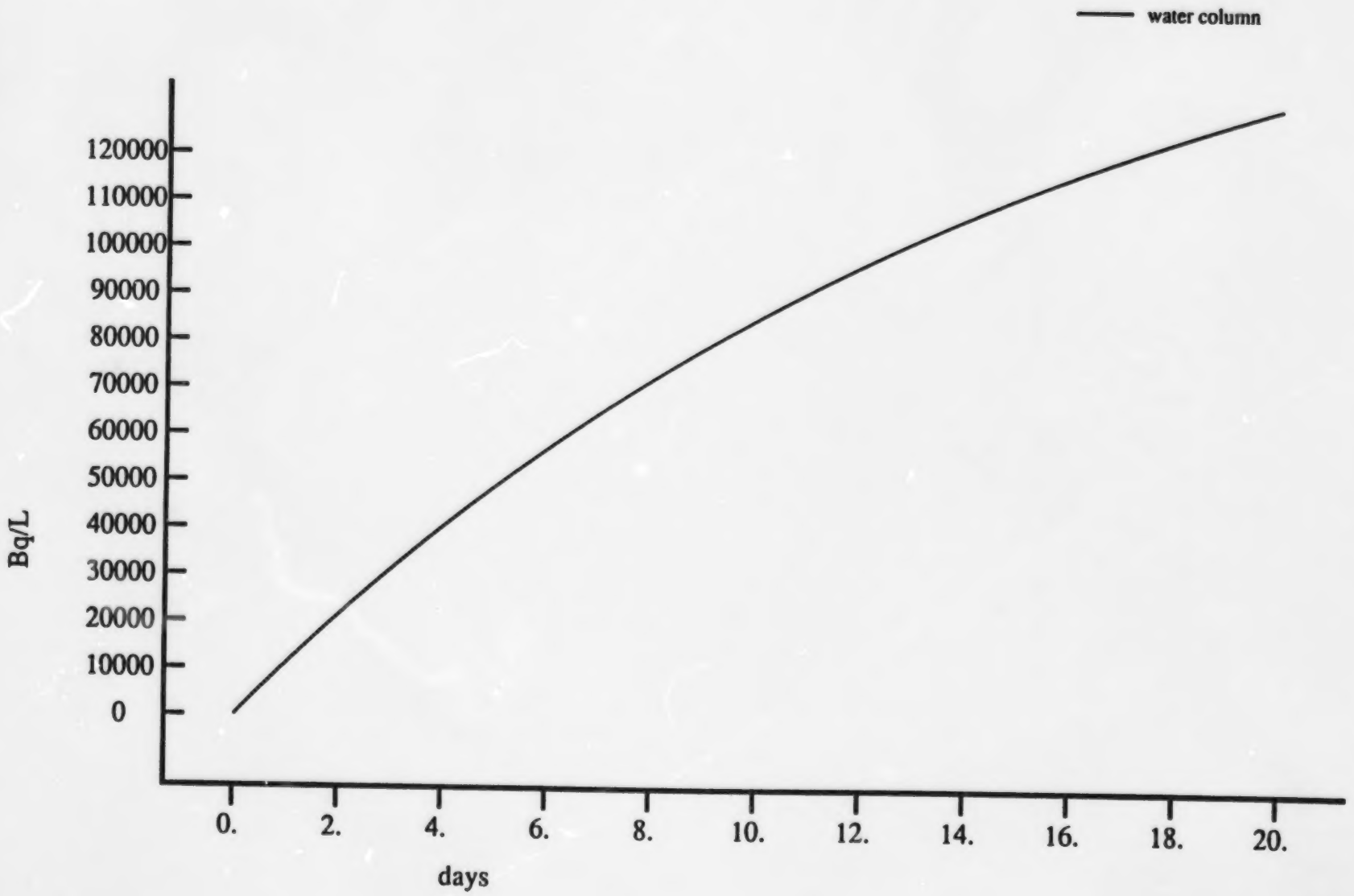

Flux vs. Time

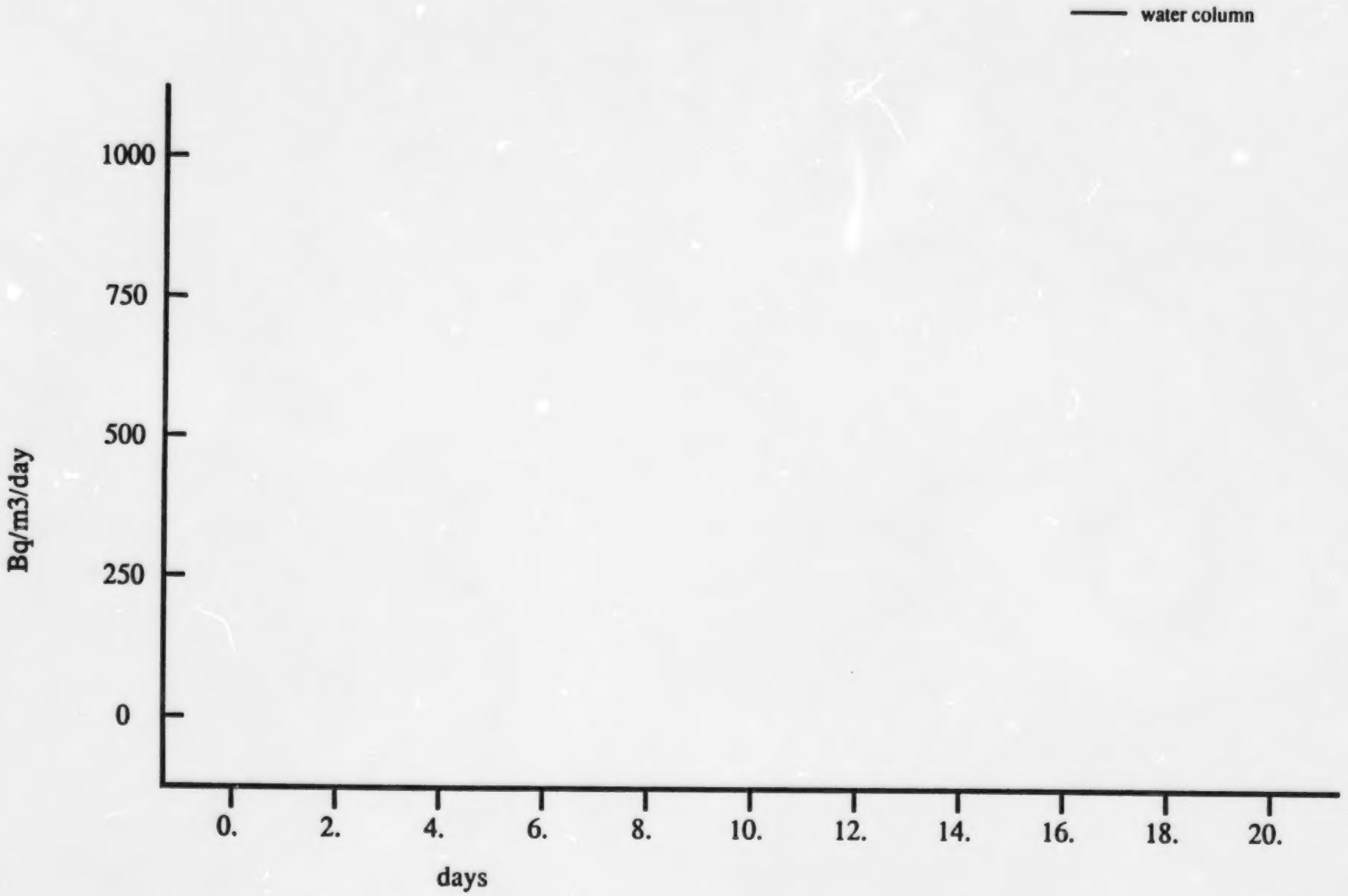
water column
1000
750
500
250
0
Bq/m3/day
0.
2.
4.
6.
8.
10.
12.
14.
16.
18.
20.
days

Radium vs. Time

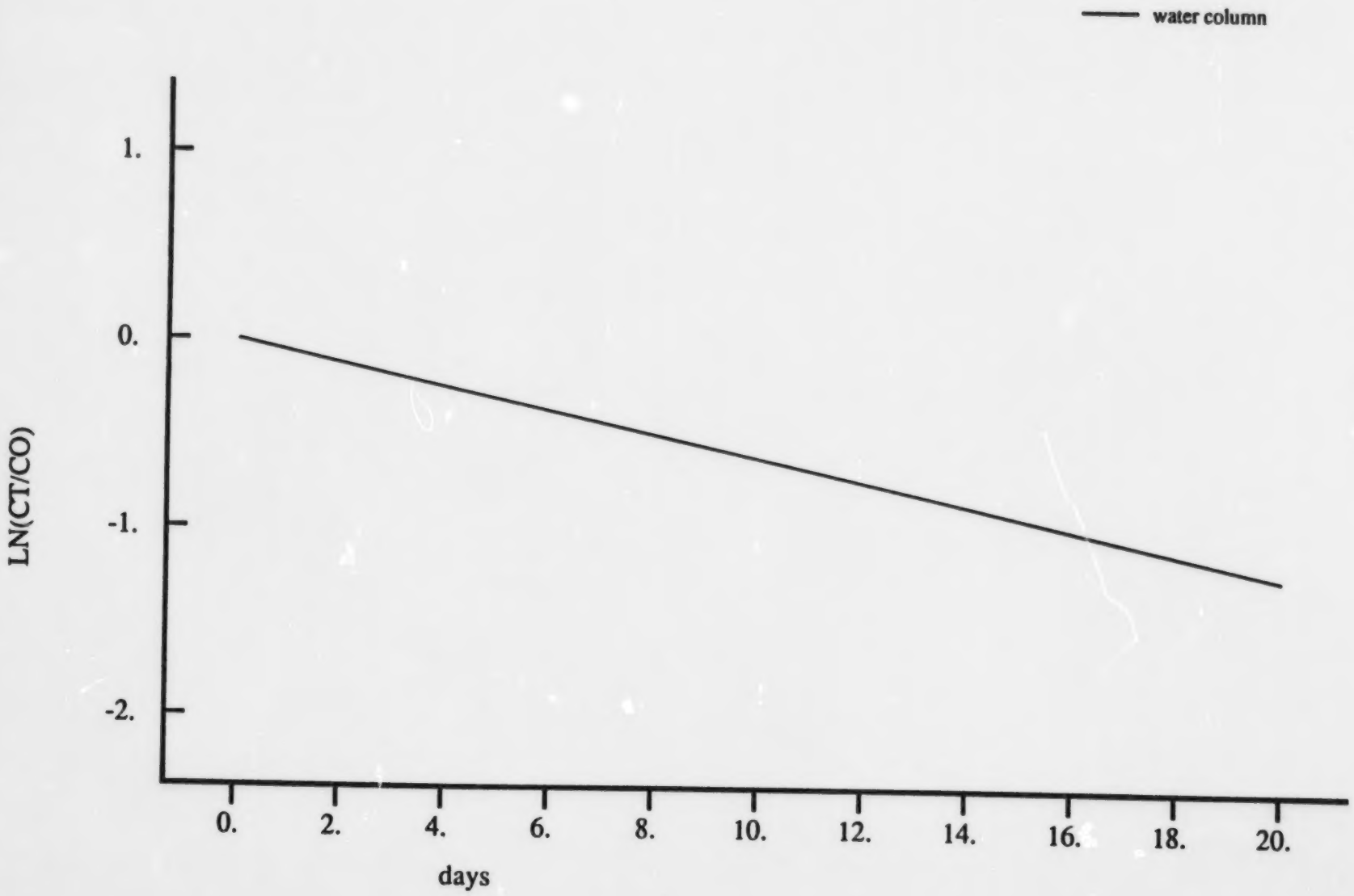

Desorption Rate

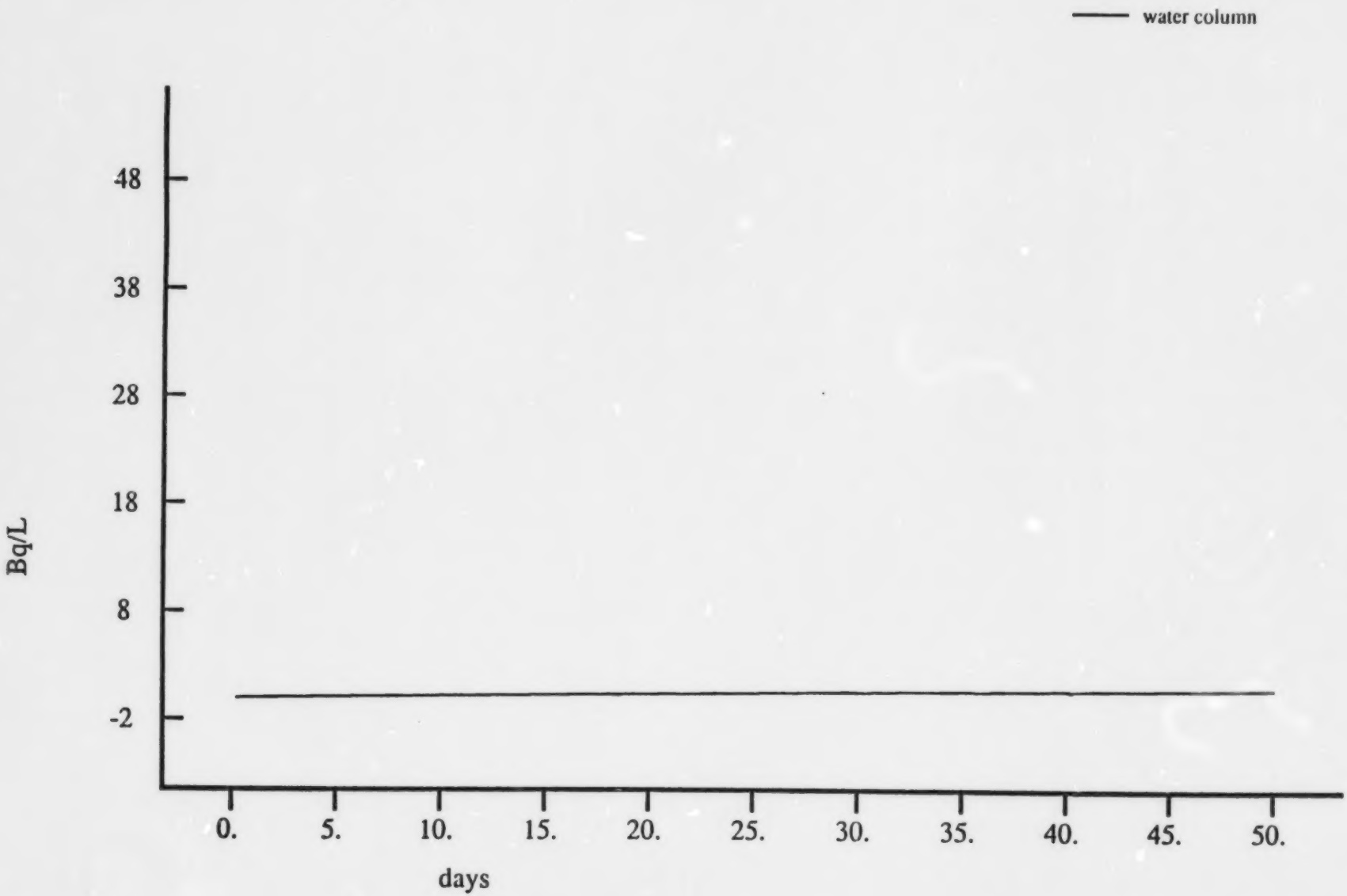

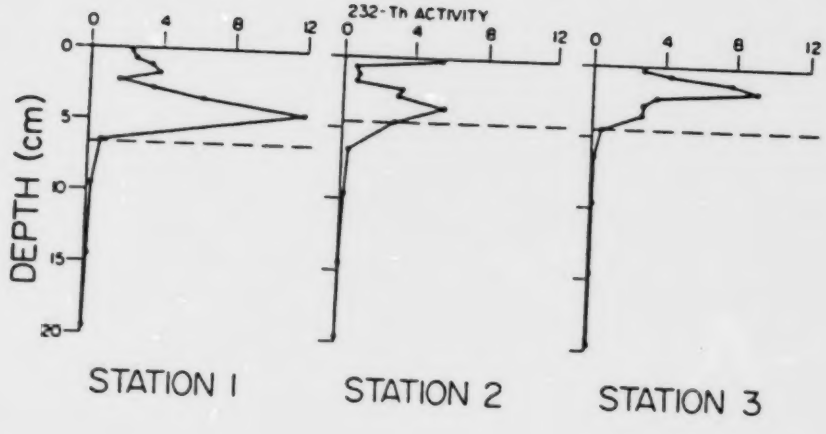

FIGURE 3.5: THORIUM ACTIVITY PROFILES (Bq/g) IN SEDIMENT CORES FROM STATIONS 1, 2 AND 3, 1984. Dashed line corresponds to depth of diatom-inferred pH decline.

Figure 3.6 Iron Concentration Profiles (%) in Sediment Cores From Stations 2, 4 and 5 (100, 40 and 20 m deep respectively)

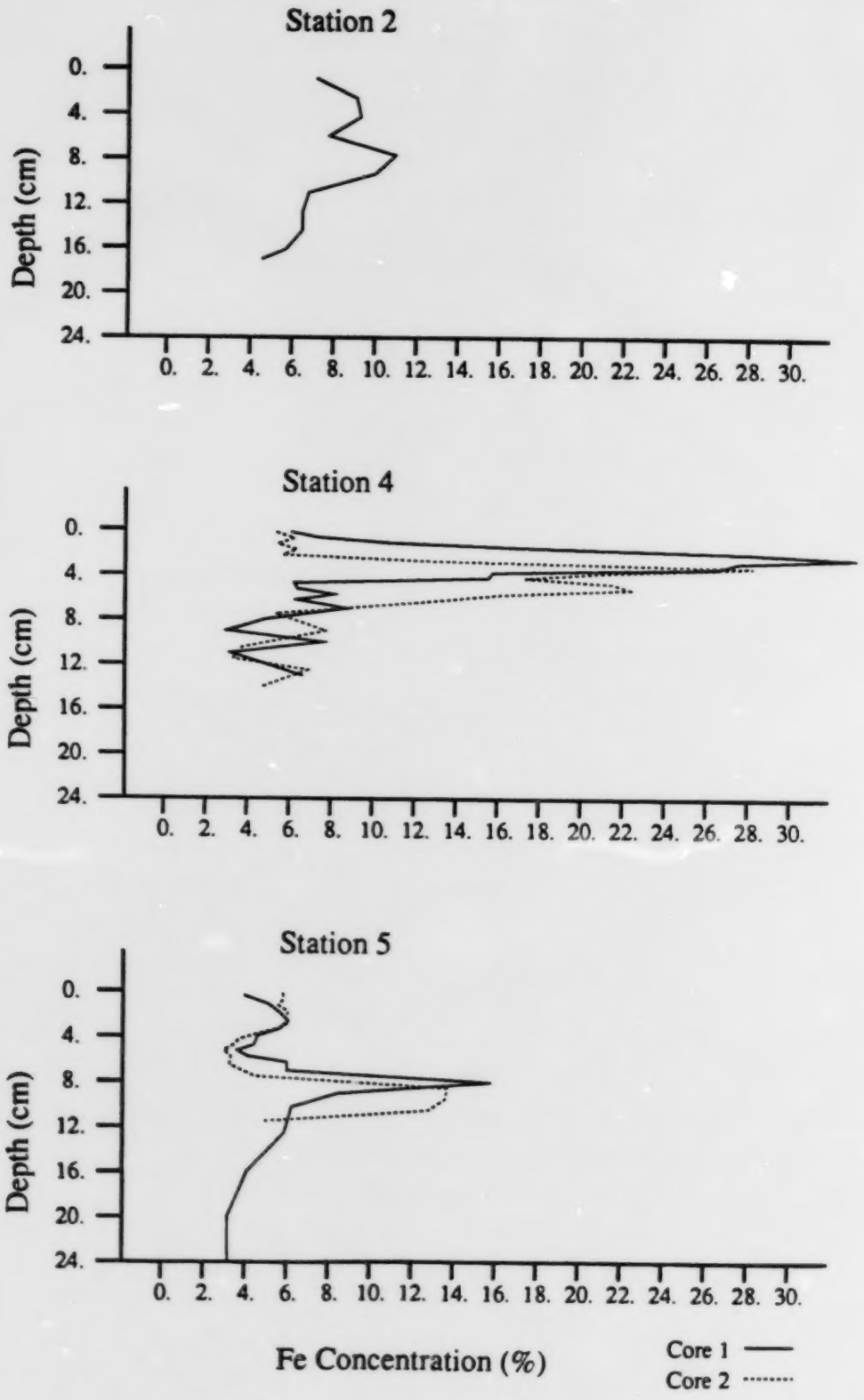

Cornwell (1985) corrected for diagenic Fe and Mn in surficial sediments by estimating sedimentation rates based on sediment Al concentrations and then applying the average Al concentration in deeper sediments to the iron-enriched layers. Although Al profiles are available for three of the five Quirke Lake stations (McKee et al., 1985), concentrations were typically higher in more recent, iron-enriched layers indicating that Al deposition rates have recently increased. The absence of an inverse correlation between sediment Al and Fe in the Quirke cores precludes application of the Al-correction technique.

Average accumulation rates of 141 $g \cdot m^{-2} \cdot yr^{-1}$ for recent sediments and 44 $g \cdot m^{-2} \cdot yr^{-1}$ for pre-mining sediments may be placed in perspective by comparison with data on other Shield lakes. Evans and Rigler (1980a, 1983) reported maxima of 226, 133 and 105 $g \cdot m^{-2} \cdot yr^{-1}$ in three southern Ontario Shield lakes. Whole-lake averages for these three lakes were 45 to 78 $g \cdot m^{-2} \cdot yr^{-1}$. In unproductive Toolik Lake, Alaska, Cornwell (1985) measured sedimentation rates of 12 to 73 $g \cdot m^{-2} \cdot yr^{-1}$. In unproductive Char Lake in the Canadian Arctic, a whole-lake sedimentation rate of 31 $g \cdot m^{-2} \cdot yr^{-1}$ was estimated (de March, 1978). G.J. Brunskill (pers. comm.) estimated average sedimentation rates of 22 to 56 $g \cdot m^{-2} \cdot yr^{-1}$ in four small Arctic lakes in the eastern Keewatin District of Canada. These other data suggest that Quirke Lake has exhibited recent sedimentation rates that are at the high end of the range observed in other Shield lakes, although pre-mining sedimentation rates are typical of lower productivity lakes such as Arctic lakes.

Sediment accumulation rate measurements in Quirke Lake may be used to determine rates of burial following the cessation of mining and milling. Present average sedimentation rates of 1.4 $mm \cdot yr^{-1}$ in Quirke Lake provide an indication of the rate that contaminated sediments will be buried, although average rates may decline slightly if allochthonous inputs are reduced due to a reduction in human activity in the basin. Based on the variation measured in sedimentation rates, accumulation rates may be expected to vary by $\pm$ 1 $mm \cdot yr^{-1}$ around the lake. Sediment compaction will result in a gradual reduction in sediment porosity, from about 97% at the sediment surface to 89 to 90% at a depth of 20 cm (McKee et al., 1985). Thus, a variable but increasing diffusion barrier may be expected to develop over the contaminated sediments of Quirke Lake following the cessation of mining and milling. The decrease in radionuclide levels in post-mining sediments will occur gradually due to continued releases of radionuclides into the watershed from tailings management areas after close-out and subsequent sedimentation

TABLE 3.1: SEDIMENTATION RATES IN QUIRKE LAKE, STATIONS 1 TO 5, 1984 AND 1986

Station	Year Sampled	Sedimentation Rate: Recent Sediments $mm \cdot yr^{-1}$	Recent Sediments $g \cdot m^{-2} \cdot yr^{-1}$	Pre-mining Sediments $mm \cdot yr^{-1}$	Pre-mining Sediments $g \cdot m^{-2} \cdot yr^{-1}$
1	1984	2.4±0.2*	185±14	0.45	55
2	1984	1.6±0.2*	96±7	0.55	64
	1986	2.1±0.2+	80±8	-	-
3	1984	1.6±0.2*	96±7	0.31	34
4-1	1986	0.38±0.02+	67±4		
4-2	1986	0.95±0.06+	199±13		
5-1	1986	1.4±0.1+	198±14	0.15**	24
5-2	1986	1.5±0.1+	205±14		
5-3	1986	1.1±0.1*	147±13		
Means		1.4 (s.d. = 0.6)	141 (s.d. = 57)	0.37 (s.d. = 0.17)	44 (s.d. = 18)

* Values based on diatom analysis.

\+ Values based on thorium analysis.

** Calculated based on an Ambrosia horizon at 5.68 cm and a mean depth of 3.85 cm at Station 5 for the year 1957, determined from one fossil diatom profile and two Th profiles.

Note: Errors in sedimentation rates based on an estimated uncertainty of two years in the appearance of diatom and Th horizons in sediments.

of a portion of these radionuclides. The rate of release from decommissioned tailings will depend on the natural and engineered barriers that are in place at the tailings site.

Present radionuclide accumulation rates in Quirke Lake sediments may be estimated using estimated sedimentation rates and radionuclide activities or concentrations in surficial sediments. McKee et al. (1985) measured radionuclide levels in surficial sediments (top 1 cm) at three water depths (3 m, 10 m and 30 m) along 12 transects around the lake (15 samples per depth) and at Station 1, 2 and 3 at depths of about 100 m.

Sediments at 3 m were frequently sandy and, in most cases, did not appear to be representative of depositional environments. At 10 m, sediments were to be transitional between the depositional environment of deeper areas and the sandier deposits at shallower depths. At 30 m, sediments were similar in appearance to those found at 100 m. Also, the density of benthic invertebrates at 30 m was found to be generally comparable to those found at 100 m, and much lower than densities found at shallower depths (McKee et al., 1985), indicating that the 30 m contour may be defined as within the profundal zone. Geometric mean concentations and coefficients of variation for U-238 and Th-232 decay chain radionuclides at 30 m and 100 m (Table 3.2) may be used in estimating radionuclide sedimentation rates in the lake. There is considerable variation in concentrations for most radiochemical parameters, indicating that deposition rates are variable from location to location. However, given the relatively large number of measurements and wide geographic coverage of the lake, these geometric mean values provide a reasonable estimate of lakewide average concentrations for the 30 m and 100 m depth zones. Concentrations at the 30 m depth zone are assumed to be representative of sediments deposited at 20 to 40 m (Stations 4 and 5), while concentrations at 100 m are representative of sediments deposited at 100 m (Stations 1, 2 and 3).

The average sedimentation accumulation in Quirke Lake is 141 $g \cdot m^{-2} \cdot yr^{-1}$, based on sediment cores from all five locations. As there is no evidence for a consistent effect of depth on sedimentation rate in recent sediments (Table 3.1), this average rate may be reasonably applied to all lake depths within the zone of deposition (water depths of 10 m and greater).

The net sediment loadings in Quirke Lake may be estimated by multiplying the sediment radionuclide activities in the surficial sediment (Table 3.2; becquerels per gram or

TABLE 3.2: MEANS AND VARIATION IN RADIONUCLIDE LEVELS IN SURFICIAL[1] SEDIMENTS OF QUIRKE LAKE, 1984.
Units are Bq/g unless indicated otherwise.

	Lake Depth (m)	Mean[2]	Coefficient of Variation	N	Background[3]
U (ug/g)	30	212	15.9	15	10.6-26.4
	100	803	4.7	6	
Th-230	30	3.43	96.0	15	LE 0.05-0.51
	100	11.3	25.2	6	
Ra-226	30	1.46	263.3	15	0.06-0.28
	100	6.99	36.6	6	
Pb-210	30	3.15	82.3	15	LE 0.3-1.15
	100	15.8	12.1	6	
Po-210	30	4.3	49.0	15	0.17-0.8
	100	13.8	13.1	6	
Th-232	30	1.18	910.3	15	LE 0.05-0.11
	100	4.35	23.3	6	
Th-228	30	0.30	78.0	15	LE 0.05-0.14
	100	1.30	162.7	6	

[1] Sediments sampled from the surface 1 cm.

[2] Geometric mean back-transformed from mean of log values.

[3] Background based on concentrations observed at 14.5 and 19.5 cm in sediment cores from Stations 1, 2 and 3 (McKee et al., 1985).

LE - less than or equal to.

micrograms per gram) by the post-mining sedimentation rates (grams per square metre per year). These estimates are provided in Table 3.3 for the two depth ranges. Po-210 and Th-228 are short-lived (half-lives of 138 d and 1.9 yr, respectively) relative to the period of sediment deposition represented by the surficial 1 cm. Thus, activities of these radionuclides in the surficial layer are largely controlled by the activities of their long-lived grandparents, Pb-210 and Th-232, respectively. Therefore, "accumulation" rates for Po-210 and Th-228 (Table 3.3) include the effects of radioactive ingrowth in the sediments. Pre-mining period sediment loadings cannot be calculated from radionuclide levels in sediments above the Zone 3/Zone 4 pollen boundary, due to the variable degree of downcore contamination (McKee et al., 1987). However, pre-mining loadings may be estimated based on levels of radionuclides in core sections from below the Zone 3/Zone 4 boundary, assuming that sedimentation rates estimated for the 1835-1957 period also apply to these older deposits (Table 3.3). Estimated present mining sediment loadings in Quirke Lake are about two orders of magnitude greater than those estimated for the pre-mining period and greater than one to three orders of magnitude greater than those found in uncontaminated Arctic lakes (G.J. Brunskill, pers. comm.).

Present-day sediment loadings presented here, based on core analysis, and short-term particle flux measurements presented in Section 4 of this report, are in good agreement, indicating that these rates may be validly applied in modelling sediment fluxes in Quirke Lake.

TABLE 3.3: MEAN PRESENT-DAY AND PRE-MINING RADIONUCLIDE ACCUMULATION RATES IN SEDIMENTS AT WATER DEPTHS OF 20 TO 40 m AND AT 100 m[1]. Units are $Bq \cdot m^{-2} \cdot yr^{-1}$ unless indicated otherwise

	Present Rates		
	20-40 m	100 m	Pre-mining Rates[2]
U ($mg \cdot m^{-2} \cdot yr^{-1}$)	29.9	113	0.69
Th-230	484	1,590	L 11
Ra-226	206	986	6.2
Pb-210	444	2,230	L 23
Po-210	606	1,950	19
Th-232	166	613	L 2.6
Th-228	42	183	L 2.5

[1] Calculated from a mean mass accumulation rate of 141 $g \cdot m^{-2} \cdot yr^{-1}$ (Table 3.1) and mean radionuclide levels in surficial sediments for 30 and 100 m depths (Table 3.2).

[2] Calculated from on a mean pre-mining sedimentation rate of 44 $g \cdot m^{-2} \cdot yr$ based on all pollen-dated cores (Table 3.1) and mean concentrations of radionuclides in the bottom two core sections (core depths 14.5 and 19.5 cm) as reported by McKee et al. (1985) for Stations 1, 2 and 3.

4.0 PARTICLE FLUX MEASUREMENTS

4.1 Introduction

The downward flux of materials in lake environments may be measured indirectly through examination of sediment cores, as detailed for Quirke Lake in Section 3 of this report, or directly by particle flux measurements. Collection of settling particles in lakes is normally accomplished using sediment traps. The validity of using sediment traps to measure accumulation rates was demonstrated in efficiency tests by Gardner (1980) and Hargrave and Burns (1980). Problems with this method relate to mineralization within the traps and interference by bottom resuspension (Bloesch and Burns, 1980).

Through measurement of differences in particle accumulation rates at varying distances above the sediments, it is possible to determine the magnitude of sediment resuspension due to disturbance by bottom currents or lake organisms (Rosa et al., 1983). Measurement of the resuspension of bottom sediments is of fundamental interest in terms of geochemical cycling within the lake. Translocation of bottom sediments may play an important role in controlling the distribution of contaminated sediments in Quirke Lake. Resuspended sediments are subject to a different physical-chemical environment in the water column, and contaminant-particle interactions may be altered accordingly. For example, Rosa et al. (1983) found that particles collected near the bottom of Lake Ontario appeared to have acquired an increased metal burden during resuspension events. Furthermore, sediment resuspension will alter the nature of the sediment-water boundary that controls diffusion between these two compartments.

Sediment trap studies were undertaken in Quirke Lake to provide an independent verification of sediment core-derived sedimentation rates (Section 3), and to provide an indication of the importance of sediment resuspension in the lake.

4.2 Methods

Sediment traps were installed in Quirke Lake at Station 5 (20 m deep) and Station 2 (100 m deep) for two periods of 22 to 29 days each between mid-July and mid-August and between mid-August and mid-September 1986. Sediment traps were constructed of 0.2-, 0.5- and 1-m long, 10-cm inside diameter lengths of rigid plastic pipe, with plastic caps

fitted to the bottom. At Station 1, 1-m long traps were installed upright in clusters of three at each of four depths - 2, 5, 10 and 80 m above bottom. At Station 5, traps were installed in triplicate at each of six depths of 0.2, 0.6, 1, 1.8, 5 and 15 m. The 0.2-m and 0.5-m long traps were installed at 0.2 and 0.6 m depths, respectively, while 1-m lengths were used at the other depths. Traps installed at least 2 m above the bottom were maintained at their prescribed depths with a mooring buoyed by a subsurface float. At depths closer to the bottom (Station 5), traps were installed on a resuspension sediment samples (RSS) of a smaller size, but similar design to the one constructed by Rosa et al. (1983) for use in Lake Ontario. The RSS held traps at 0.2 to 1.8 m above bottom by means of a tetrahedral aluminum frame (Figure 4.1). During installation, the RSS was lowered very slowly onto the lake bed, with the final installation monitored by CRT-type sonar, to minimize any effect of sediment disturbance. Traps on the tetrahedron were capped during installation to avoid the introduction of disturbed sediments, and caps were removed remotely 20 min after installation. At the end of the sampling periods, sediment traps were gently raised to the surface, and the trapped material retrieved and transferred to 500 mL vessels. Some losses of sediment traps were encountered during retrieval of traps from the second installation.

Samples were then freeze-dried, weighed on a microblance, and radionuclide contents measured by gamma spectrometry for isotopes of Th and Ra. Total Th (Th-232) and total U (U-238) were analyzed by neutron activation. Particle fluxes were then calculated on the basis of mass or activities per square metre per year. In most cases, triplicate sets of samples were pooled before weighing and analysis. Particle mass and activities were determined for individual traps for one triplicate set (Station 5, first installation, 0.2 m above bottom) to provide an indication of sampling variance.

4.3 Results and Discussion

At the end of each sampling period, sediment traps had accumulated about 0.1 to 0.7 g dry mass of solids each from the water column (Table 4.1). Levels of U-238 decay chain radionuclides were nearly always greater than levels of Th-232 decay chain radionuclides in the accumulated solids. Based on measurements of solids from three experimental replicates as Station 5, coefficients of variation for mass, total U, Th-234, Ra-226, Pb-210, total Th, Ra-228 and Th-228 were 40.0%, 17.8%, 15.9%, 29.4%, 23.3%, 43.9%, 22.4% and 19.3%, respectively.

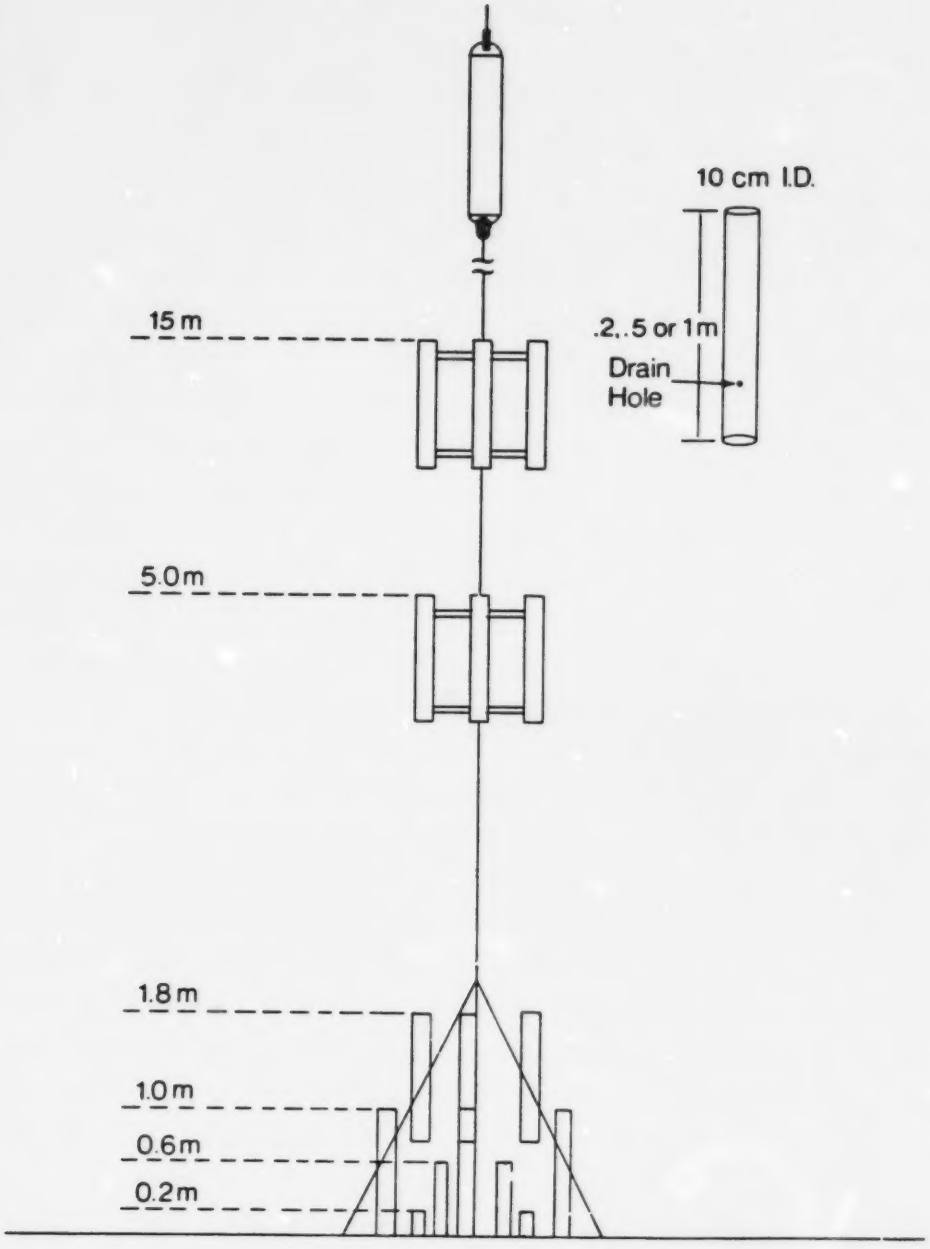

FIGURE 4.1: GENERAL ARRANGEMENT OF RESUSPENDED SEDIMENT SAMPLER (RSS) AND SEDIMENTATION TUBES SPECIFICATIONS (adapted from Rosa et al., 1983)

TABLE 4.1: ACCUMULATED MASSES OF SOLIDS AND RADIONUCLIDE CONCENTRATIONS (Bq/g unless indicated otherwise) IN QUIRKE LAKE SEDIMENT TRAPS, 1986

Experiment No.*	Station	Depth (m above bottom)	No. of Traps in Measurement	Mass (g)	U (ug/g)	Th-234	Ra-226	Pb-210	Th (ug/g)	Ra-228	Th-228
1	2	2	3	0.600	-	5.43	3.35	3.42	-	1.05	1.41
		5	3	0.531	400	6.97	3.70	2.41	43.8	1.25	1.50
		10	3	0.508	335	3.87	2.36	1.95	36.1	0.924	1.02
		80	3	0.453	243	4.01	0.38	1.90	29.2	L 0.36	0.445
	5	0.2	1	0.667	321	2.84	5.36	4.96	286	1.36	1.48
			1	0.334	272	2.48	3.06	3.13	111	0.867	1.11
			1	0.37	388	3.40	5.48	4.71	277	1.08	1.64
		0.6	3	0.926	334	4.4	5.15	4.81	206	1.42	1.60
		1	3	1.35	169	1.80	1.34	1.18	54.9	0.374	0.544
		1.8	3	0.711	238	2.44	1.46	0.759	42.1	0.422	0.604
		5	3	0.423	306	4.52	2.14	2.50	34.9	1.07	0.994
		15	3	0.479	320	4.81	1.51	2.21	49.7	0.82	0.834
2	2	2	2	0.342	418	4.42	3.23	2.38	53.2	1.13	1.60
		5	3	0.507	407	6.04	3.40	4.50	48.2	1.32	1.52
		10	3	0.475	379	5.29	2.69	2.67	48.9	0.942	1.29
		80	2	0.322	211	3.49	0.939	2.34	26.1	0.658	0.239
	5	0.2	1	0.248	225	2.14	1.70	1.89	36.7	0.832	0.595
		0.6	2	0.486	262	3.02	2.10	2.03	56.8	0.328	0.924
		0.6	1	0.213	390	4.16	2.67	2.04	76.5	1.14	1.28
		1	2	0.437	267	3.16	1.55	2.12	47.4	0.481	0.617
		1.8	3	0.870	281	3.09	2.15	2.52	60.1	0.575	0.894
		5	1	0.059	404	6.88	2.49	-	87.1	2.87	1.02
		15	1	0.137	371	3.86	2.12	3.90	70.7	1.12	0.531

* Experiment 1: July-August, duration = 29 days.
Experiment 2: September-October, duration = 22 days.

Using the data in Table 4.1 and the surface area, annual particle and radionuclide settling rates may be calculated, as shown in Table 4.2. Plots of fluxes against the logarithm of distance above the bottom, demonstrate a general increase in flux with increasing proximity to the sediment surface, although linear relationships such as those reported by Rosa et al. (1983) in Lake Ontario were not found. The irregularity may be in part attributed to the fact that our sediment traps sampled different water masses (epilimnion and hypolimnion) which may contain different suspended solids concentrations while, in the study of Rosa et al. (1983), traps sampled depths within 7 m of the bottom, and were confined to the hypolimnion. The trends in mass accumulation rates with depth show less variation at Station 2 (100 m depth) than at Station 5 (20 m depth), although comparisons at depths less than 2 m above the sediment cannot be made because these depths were not sampled at Station 2. The higher mass and radionuclide fluxes near the bottom, especially at Station 5, provide evidence for sediment resuspension, particularly at the shallower station. Transport of resuspended sediments from shallower depths to deeper depths in Quirke Lake would cause sediment focussing, as discussed in Section 3 of this report. This effect was not evident in present sedimentation rates determined from sediment cores, apparently due to the complicating factor of variable post-depositional iron precipitation in bottom sediments, but was apparent in pre-mining sedimentation rates (Section 3 and Table 3.1).

A comparison of the short-term mass accumulation rates determined from sediment trap measurements, with the long-term (30-yr) rates determined from markers in sediment cores collected at the same stations, shows that short-term fluxes of particles in the water column exceed the long-term accumulation rates by 2.3 to 3.4 times (Table 4.3). These differences may be accounted for by higher sedimentation rates than the long-term average during sediment trap measurements, post-depositional oxidation of particulate organic matter, post-depositional dissolution of minerals in settled particles, or resuspension of bottom deposits and eventual transport from the lake. Greater rates of accumulation in sediment traps than in bottom deposits have also been reported in the Great Lakes, where resuspension appears to prevent a large fraction of suspended particulates from becoming a permanent part of the bottom sediment (Bell and Eadie, 1983). Sediment traps were similarly found to yield sedimentation rates of 1.3 to 3.3 times greater than those estimated from Pb-210 dating of cores in Lake Lucerne, Switzerland (Bloesch and Evans, 1982), although resuspension was not considered in explaining the discrepancy in that case. Particle resuspension in Quirke Lake implies

TABLE 4.2: ANNUAL MASS AND RADIONUCLIDE SETTLING RATES* FOR U-238 AND Th-232 DECAY CHAIN RADIONUCLIDES IN QUIRKE LAKE. Values are based on solids from three sediment traps per depth. Expressed as rate measured in first experiment/rate measured in second experiment.

	Station 2				Station 5					
	2	5	10	80	0.2	0.6	1	1.8	5	15
Mass	311/350	275/346	263/324	225/330	710/508	480/477	699/448	368/594	219/121	248/281
U-238	-/147	110/141	88/123	57/70	232/114	160/144	118/119	62/167	67/49	79/104
Th-234	1,690/ 1,720	1,920/ 2,090	1,020/ 1,720	903/ 1,150	2,650/ 1,090	2,110/ 1,610	1,260/ 1,410	899/ 1,840	990/ 831	1,190/ 1,080
Ra-226	1,040/ 1,130	1,020/ 1,180	620/ 872	220/ 310	3,970/ 860	2,470/ 1,090	937/ 694	538/ 1,280	469/ 301	375/ 595
Pb-210	1,060/ 834	663/ 1,560	513/ 866	430/ 770	2,530/ 960	2,310/ 970	825/ 949	280/ 1,500	550/ -	548/ 1,090
Th-232	-/19	12/17	9.5/16	6.9/8.6	171/19	99/30	38/21	16/36	7.6/11	12/20
Ra-228	326/396	344/457	243/305	-/220	860/422	681/275	262/215	155/342	234/347	200/314
Th-228	438/560	410/526	268/418	100/79	1,060/302	770/490	380/276	222/531	218/123	207/149

* Units: $g \cdot m^{-2} \cdot yr^{-1}$ for mass
$mg \cdot m^{-2} \cdot yr^{-1}$ for U-238 and Th-232
$Bq \cdot m^{-2} \cdot yr^{-1}$ for others

TABLE 4.3: COMPARISON OF PARTICLE SETTLING FLUXES WITH NET SEDIMENT ACCUMULATION RATES DETERMINED FROM SEDIMENT CORES IN QUIRKE LAKE ($g \cdot m^{-2} \cdot yr^{-1}$)

	Particle Flux[1]	Net Accumulation[2]
Station 2	303 (225-350)	88 (80-96)
Station 5	429 (121-710)	183 (147-205)

[1] Means and ranges of values reported in Table 4.2.

[2] Means and ranges of values reported in Table 3.1.

that the suspended solids-partition coefficient K_d-settling velocity model applied in the aquatic transport model for radionuclides released into Quirke Lake (BEAK, 1983) is mechanistically oversimplified. Furthermore, return fluxes of radionuclides to the water column are probably strongly influenced by resuspension, and are not controlled simply by diffusion through the bottom sediment-water boundary.

Differences between radionuclide fluxes determined from sediment traps and from sediment cores are less evident than mass flux differences determined by these methods (Table 4.4). Particle fluxes of radionuclides varied considerably between experiments, and among depths as well as between stations (Table 4.2). For Ra-226 and Pb-210, fluxes are greater on settling particles than determined from cores in 50% of the cases. Secular equilibrium was maintained on average between Ra-226 and Pb-210 in the particle fluxes, but average net Pb-210 fluxes to bottom sediments determined from cores were in excess of corresponding Ra-226 fluxes by about two times, suggesting that there may be a greater post-depositional loss of the latter. Average particle fluxes of uranium were nearly the same for Stations 2 and 5, and were also nearly equal to net uranium accumulation rates determined from sediment cores for 100 m depths. Average net fluxes of uranium at lake depths of 20 to 40 m were somewhat lower than observed in the trap measurements. Average uranium activity fluxes exceeded Ra-226 fluxes by about 1.2 to 1.8 times. Secular equilibrium was apparent between Ra-228 and Th-228 in average particle fluxes, but both showed greater activity fluxes than did Th-232. These excesses of Ra-228 and Th-228 in water column particles may be related to a post-depositional remobilization of Ra-228 from bottom deposits. This phenomenon is further suggested by a deficit of Th-228 in bottom sediments (Table 3.2) and generally greater levels of both Ra-228 and Th-228 on water column particulates near the bottom sediments (Table 4.1). Similar excesses of Th-232 decay products have been observed in oceanic waters (Nozaki et al., 1981).

In summary, particle flux measurements indicate that bottom sediments are resuspended into the water column, apparently contributing to mass accumulation rates that exceed long-term net accumulation rates determined from sediment cores. Radionuclide fluxes on these particles were not consistently greater or less than depth-specific, lake-wide averages for U-238 decay chain radionuclides. Differences in average Ra-226/Pb-210 ratios in bottom sediments and suspended sediments appear to suggest a greater remobilization of Ra-226 relative to Pb-210 back to the water column. Similarly,

TABLE 4.4: COMPARISON OF RADIONUCLIDE FLUXES FROM PARTICLE SETTLING WITH NET RADIONUCLIDE ACCUMULATION RATES AT 100 m AND 20-40 m LAKE DEPTHS IN QUIRKE LAKE.
Units are $mg \cdot m^{-2} \cdot yr^{-1}$ for total U, $Bq \cdot m^{-2} \cdot yr^{-1}$ for others.

	U (total)	Th-234	Th-230	Ra-226	Pb-210	Po-210	Th-232	Ra-228	Th-228
Particle Settling[1]									
Station 2	105 (57-147)	1,530 (903-1,920)	-	800 (220-1,130)	840 (430-1,560)	-	51* (28-77)	330 (220-457)	350 (79-560)
Station 5	110 (49-232)	1,410 (831-2,650)	-	1,130 (301-3,970)	1,140 (280-2,530)	-	161* (44-689)	360 (155-860)	390 (123-1,060)
Net Fluxes[2]									
100 m	113	-	1,590	986	2,230	1,950	613	-	183
20-40 m	29.9	-	484	206	444	606	166	-	42

[1] Means and ranges of values reported in Table 4.2.

[2] Values reported in Table 3.3 as lakewide averages.

* Calculated from Th mass fluxes, and a specific activity of 4.03×10^3 Bq/g Th-232.

average Th-228/Th-232 ratios greater than 2 on suspended particules, and less than 0.3 in surficial bottom sediments, suggest much greater post-depositional remobilization of Ra-228 than Th-232.

5.0 MASS BALANCE ANALYSIS FOR QUIRKE LAKE AND THE SERPENT RIVER SYSTEM

5.1 Mass Balance Program

A field program was developed for Quirke Lake to measure the mass balance of U-238 and Th-232 decay series radionuclides. The Ontario Ministry of the Environment, Sudbury office has an existing monitoring program at various stations in the Serpent River system. For this project, larger volumes of water than taken routinely were obtained in order to allow analysis for several radioisotopes. The conventional radioisotopes gathered as a part of the normal MOE program are indicated in Tables 5.1 to 5.3 for the Quirke Lake Inlet, the Quirke Lake Outlet and Panel Discharge. The normal radionuclide parameters encompass radium-226, uranium, dissolved solids, gross alpha and gross beta on the dissolved solids fraction of the sample, particulate solids (suspended solids) and a gross alpha and gross beta measurement of the particulate solids fraction. The normal sampling program consists of six to nine samples per year. To amplify this sampling frequency, the MOE sampling personnel were contracted by BEAK to obtain an extra four sets of samples.

The Ontario Ministry of Laboratory conducts radionuclide analyses for the MOE using their standard procedures (see Appendix A). The techniques for chemical analysis for dissolved solids, uranium and radium-226 measurements proved to be adequate for the levels observed in Quirke Lake. For the other isotopes, namely radium-228, thorium-228, lead-210 and a preliminary scan for thorium-232 and thorium-230, the analytical techniques used by the MOL proved to have inadequate detection limits for water samples. The methods used are summarized in the next paragraph, and in the appendix in detail. Accordingly, a new monitoring program, in which large volumes of samples were obtained, tracers added, and then measurements made as part of this project, was initiated.

The new measurement program consisted of obtaining 50 to 100 L of water for one isotope analysis, addition of a yield tracer to the 50 or 100 L sample, addition of a precipitating agent, and/or neutralizing agent to coprecipitate the isotopes of interest, and subsequent submittal of the chemical precipitate to a radionuclide laboratory for analysis. This sampling program was initiated by collecting one set of samples during the

TABLE 3.1: RADIONUCLIDE DATA FOR QUIRKE INLET (AMPLIFIED MOE MONITORING PROGRAM)

	15 Aug 1986	01 Aug 1986	30 Jul 1986	20 Jul 1986	04 Jul 1986	01 Jul 1986	31 May 1986	19 Apr 1986	23 Mar 1986	26 Jan 1986	31 Dec 1985	24 Nov 1985	03 Sep 1985	Aug 1985	Jan 1985
Pb-210 (Bq/L)	0.093	L 0.04	L 0.04	0.033	L 0.04	L 0.04	0.07	L 0.04	L 0.04	-	-	-	-	-	-
Ra-226 (Bq/L)	$0.090_{\pm}$ 0.004	$0.031_{\pm}$ 0.003	$0.29_{\pm}$ 0.01	$0.056_{\pm}$ 0.003	$0.12_{\pm}$ 0.01	$0.23_{\pm}$ 0.01	$0.098_{\pm}$ 0.003	$0.15_{\pm}$ 0.1	$0.031_{\pm}$ 0.003	0.041	0.039	0.062	0.10	0.07	0.13
Uranium (ug/L)	6	22	9	19	31	8	8	8	0	16	14	8	56	24	39
Dissolved Solids (mg/L)	640	390	640	-	-	-	330	280	840	680	620	650	1,000	800	320
Gross Alpha on DS (Bq/L)	0.71	1.7	0.72	1.13	2.4	0.92	1.1	1.2	2.4	1.6	1.3	0.56	3.9	2.2	2.9
Gross Beta on DS (Bq/L)	1.1	0.8	1.1	2.1	6.8	0.66	0.57	0.59	1.6	1.4	1.2	1.2	1.7	1.6	1.0
Particulate Solids (mg/L)	2	2	10	-	-	-	6	2	2	1	2	2	1	2	2
Gross Alpha on PS (Bq/L)	0.15	0.1	1.1	-	-	-	0.16	0.15	0.17	0.05	0.07	0.19	0.05	0.25	0.27
Gross Beta on PS (Bq/L)	0.15	0.13	0.67	-	-	-	0.13	0.09	0.29	0.04	0.07	0.20	L 0.04	0.25	0.30
Ra-228 (Bq/L)	-	L 0.12	L 0.12	-	L 0.12	L 0.12	L 0.12	L 0.12	L 0.12	-	-	-	-	-	-
Th-228 (Bq/L)	-	-	-	L 0.02	L 0.02	L 0.02	L 0.02	L 0.02	L 0.02	-	-	-	-	-	-

L = less than.

TABLE 3.2: RADIONUCLIDE DATA FOR QUIRKE OUTLET (AMPLIFIED MOE MONITORING PROGRAM)

	15 Aug 1986	01 Aug 1986	30 Jul 1986	20 Jul 1986	09 Jul 1986	01 Jul 1986	31 May 1986	19 Apr 1986	23 Mar 1986	26 Jan 1986	31 Dec 1985	29 Nov 1985	03 Sep 1985	Aug 1985	Jan 1985
Pb-210 (Bq/L)	L 0.04	0.04	L 0.04	0.066	0.048	L 0.04	L 0.04	L 0.04	L 0.04	-	-	-	-	-	-
Ra-226 (Bq/L)	0.065± 0.003	0.072± 0.004	0.039± 0.003	0.087± 0.005	0.072± 0.004	0.05± 0.01	0.035± 0.003	0.011± 0.001	0.028± 0.002	0.083± 0.004	0.14	0.073	0.06	0.06	0.06
Uranium (ug/L)	11	9	9	11	4	L 3	L 3	4	4	17	6	8	10	3	17
Dissolved Solids (mg/L)	390	840	380	-	-	-	76	61	70	400	360	380	320	320	170
Gross Alpha on DS (Bq/L)	0.93	0.87	0.76	0.83	0.55	0.17	0.18	0.28	0.35	2.1	1.4	0.48	0.84	0.57	1.2
Gross Beta on DS (Bq/L)	0.86	1.2	0.85	0.96	0.87	0.15	0.09	0.18	0.14	1.1	0.85	0.90	0.65	0.76	0.29
Particulate Solids (mg/L)	1	L 1	2	-	-	-	1	2	2	6	170	29	1	2	9
Gross Alpha on PS (Bq/L)	L 0.04	0.20	0.05	-	-	-	L 0.04	L 0.04	L 0.04	0.1	1.2	0.21	0.05	0.07	L 0.04
Gross Beta on PS (Bq/L)	0.07	0.18	L 0.04	-	-	-	L 0.05	L 0.04	L 0.04	0.14	0.91	0.30	0.23	0.12	0.08
Ra-228 (Bq/L)	-	L 0.12	L 0.12	L 0.12	L 0.12	L 0.12	L 0.12	L 0.12	L 0.12	-	-	-	-	-	-
Th-228 (Bq/L)	-	-	-	L 0.02	L 0.02	L 0.02	L 0.02	L 0.02	L 0.02	-	-	-	-	-	-

L = less than.

TABLE 3.3: RADIONUCLIDE DATA FOR PANEL DISCHARGE (AMPLIFIED MOE MONITORING PROGRAM)

	15 Aug 1986	01 Aug 1986	30 Jul 1986	20 Jul 1986	04 Jul 1986	01 Jul 1986	31 May 1986	19 Apr 1986	23 Mar 1986	26 Jan 1986	31 Dec 1985	24 Nov 1985	Aug 1985	Jan 1985
Pb-210 (Bq/L)	L 0.04	L 0.04	L 0.04	L 0.04	L 0.04	0.044	L 0.04	0.05	L 0.04	-	-	-	-	-
Ra-226 (Bq/L)	0.13± 0.01	0.073± 0.004	0.19± 0.01	0.098± 0.005	0.083± 0.005	0.49± 0.02	0.058± 0.004	0.29± 0.01	0.58± 0.02	0.048	0.20	0.19	0.19	0.13
Uranium (ug/L)	59	78	60	34	13	360	340	320	300	100	100	100	77	99
Dissolved Solids (mg/L)	150	2,800	2,600	-	-	-	2,800	2,700	2,800	2,400	2,300	2,700	2,200	2,600
Gross Alpha on DS (Bq/L)	3.3	2.6	3.1	2.3	0.76	16	22	22	20	8.1	8.2	8.8	6.3	8.3
Gross Beta on DS (Bq/L)	6.8	7.6	6.7	7.1	1.9	12	10	9	10	7.8	7.6	7.5	7.9	6.8
Particulate Solids (mg/L)	1	5	2	-	-	-	5	2	2	1	2	2	2	2
Gross Alpha on PS (Bq/L)	0.49	2.1	0.75	-	-	-	0.67	0.70	1.0	0.64	0.82	0.78	0.70	0.59
Gross Beta on PS (Bq/L)	0.52	1.1	0.69	-	-	-	2.1	1.3	1.2	0.89	0.95	1.2	0.66	0.95
Ra-228 (Bq/L)	-	L 0.12	L 0.12	-	L 0.12	L 0.12	L 0.12	L 0.12	L 0.12	-	-	-	-	-
Th-228 (Bq/L)	-	-	-	L 0.02	L 0.02	L 0.02	L 0.02	L 0.02	L 0.02	-	-	-	-	-

L = less than.

September field trip for the particle flux measuring program. Subsequently, additional samples were obtained by local personnel in the Elliot Lake area, acidified in 5-gallon containers, and then the 5-gallon containers shipped to Mississauga via ground transport. In Mississauga, the yield tracers were added, the radioisotopes were coprecipitated down to a mass contained in a liquid volume of approximately 400 mL, and then the sample was dried. The dried sample was then submitted to Becquerel Laboratories in Mississauga and Monenco Laboratory, Calgary for analysis.

This technique (addition of the yield tracer to the samples, the coprecipitation steps and final drying of the sample to a small solid form for measurement) is a technique that was initially developed in the oceans and estuaries by such geochemists and oceanographers as W. Broecker, P. Santschii and others. The technique was adapted and used by P. Wilkinson of the Freshwater Institute in Winnipeg for addition to lakes in the Northwest Territories. A detailed description of the procedure is given in the Appendix A1. In this project, the procedures were adapted for use. Minor adaptation include the volumes of water used, and the actual isotopes used as yield tracers. For example, Wilkinson used thorium-228 as a yield tracer for their lake water, whereas it was desired to measure thorium-228 in this project. As a substitute, thorium-234 was used as a yield tracer; however, its short decay half-life (three days) necessitated that the samples be coprecipitated and analyzed within a period of approximately one week from the time of the coprecipitation experiment.

In the new measurement program, the following yield tracers were used. For uranium, neutron activation procedures were used by Becquerel Laboratories (see Appendix: accordingly, yield tracers were not required). For analysis of thorium isotopes (Th-230, Th-232, Th-228), Th-234 was used as a yield tracer. For polonium-210, polonium-208 was used as a yield tracer. For radium-226 and radium-228, radium-224 was used as a yield tracer. For the amplified monitoring program analyzed by the Ontario Ministry of Labour, the analytical procedures for lead-210, radium-226, thorium and uranium are shown schematically in the appendix. Pb-210 is isolated from the water sample by a set of concentration and cleanup procedures, and then its daughter bismuth-210 counted by beta spectroscopy to give an activity for lead-210. Ra-226 is concentrated from solution by barium sulphate precipitation techniques; then a series of steps are taken from which radon ingrowth is allowed and radon counted to give values of Ra-226. For Ra-228, a different set of steps are used to concentrate Ra-228, after which it is counted by the

beta counting of its daughter actinium-228. Thorium is coprecipitated with lanthanum. oxylate; a series of cleanup procedures are then used and a Th-234 yield tracer added. After the cleanup procedures, Th-234 is gamma counted to give yield data and thorium isotopes are counted by alpha spectometry.

For chemical analysis of radionuclides by Becqueral Laboratories, the analytical procedures are also given in the appendix. Briefly, the procedures are as follows. Lead-210, Ra-228 and Ra-224 are directly gamma-counted (Ra-226 by lead-214, bismuth-214 and Ra-228 by its first daughter, Ac-228, while Ra-224 is used as a yield tracer). For uranium, uranium is precipitated and then measured by neutron activation. For the thorium isotopes, Th-234 is added as a yield tracer and the solution is washed and elutriated, then precipitated with lanthanium fluoride. Then Th-232, Th-230 and Th-228 were measured by alpha counting after the Th-234 yield tracer was counted. For Po-210, the Po-208 and Po-210 were extracted from the solid precipitate with HCl; the hydrogen chloride also complexes interfering ions. Then the polonium was plated out and the Po-208 and Po-210 counted.

5.2 Results of Mass Balance Study

The results of the amplified MOE monitoring program are given in Tables 5.1 to 5.3, respectively for Quirke Inlet, Quirke Outlet and the Panel Discharge. The results of the additional field program involving large water volumes conducted in this study are given in Table 5.4 for thorium isotopes, Table 5.5 for radium isotopes, Table 5.6 for polonium isotopes and Table 5.7 for uranium analysis. The data are summarized in Table 5.8 in terms of average activity measured in this program for the different radionuclides for inflow and outflow. For uranium and Ra-226 data measured in this project from the large water volumes, the values are evaluated to ensure that they are consistent with the historical database gathered by the MOE. But, for purposes of mass balance analysis, the MOE database is taken as being the best estimates due to the much larger number of values obtained by the same laboratory. For the thorium isotopes, Ra-228 and Po-210, the values are given in Tables 5.4 to 5.7 are taken as being reasonable estimates of the order of magnitude of their values in surface waters of the Serpent river System (Quirke Lake and the Serpent River at Lake Superior. These values are used to provide an indication of the amount of retention of thorium and other isotopes which are occurring in Quirke Lake. However, for two of these radionuclides, the estimated retention in the

TABLE 5.4: MASS BALANCE ANALYSIS OF THORIUM ISOTOPES FROM LARGE VOLUME

	Sep 1986 (Bq/L)	Oct 1986 (Bq/L)	Nov 1986 (Bq/L)
Quirke Lake			
o Th-228	-	0.0024	0.0027
o Th-232	-	0.00076	0.0009
o Th-230	-	0.0064	0.0053
o Th-234	-	L 0.1	-
Quirke Lke (Outlet)			
o Th-228	Note 1	0.0019	0.0032
o Th-232	Note 2	0.00020	0.00027
o Th-230	Note 3	0.0014	0.0017
o Th-234	Note 4	L 0.1	-
Serpent River			
o Th-228	Note 5	0.00084	0.00090
o Th-232	Note 6	0.000096	L 0.0001
o Th-230	Note 7	0.00024	0.00027
o Th-234	-	L 0.1	-

Notes 1 to 7: Values determined respectively were 0.50, 0.47, 1.9, 1.5, 0.008, 0.0006 and 0.025 Bq/L. Experiments were neutralized using a lime of unknown composition; sample contamination was suspected and data were disregarded.

L = less than.

TABLE 5.5: MASS BALANCE ANALYSIS FOR RADIUM DATA (Bq/L) FOR LARGE VOLUMES

	Sep 1986	Oct 1986	Dec 1986
Quirke Inlet			
o Ra-226	-	0.12	0.23
o Ra-228	-	0.032	0.049
Quirke Lake			
o Ra-226	0.10	0.084	0.090
o Ra-228	0.05	0.027	0.028
Serpent River			
o Ra-226	0.08	0.059	0.052
o Ra-228	0.02	0.016	0.013

TABLE 5.6: MASS BALANCE ANALYSIS FOR POLONIUM DATA (Bq/L) FOR LARGE VOLUMES

	Sep 1986	Oct 1986	Dec 1986
Quirke Inlet			
Po-210	*	0.017	0.021
Quirke Lake			
Po-210	**	0.031	0.022
Serpent River			
Po-210	**	0.0064	0.0040

* No sample provided.

** Analysis not requested.

TABLE 5.7: MASS BALANCE ANALYSIS FOR URANIUM DATA (ug/L) FROM SAMPLE OBTAINED AT SAME TIME AS LARGE VOLUMES

	Sep 1986	Oct 1986	Dec 1986
Quirke Inlet			
U-238	*	34	*
Quirke Lake			
U-238	12	14	*
Serpent River			
U-238	*	1.0	*

* No sample provided.

TABLE 5.8: SUMMARY OF MASS BALANCE RESULTS (concentration units in Bq/L, except Uranium ug/L; fluxes in mg m^{-2} yr^{-1} for total U; Bq m^{-2} yr^{-1} for others)

Radionuclide	Inflow Concentration	Outflow Concentration	% Retention	Net Sedimentation**	Measured Sedimentation Rate	Measured Settling Flux	Ratio of Mass Balance Sedimentation:Measured Sedimentation
Ra-226 (MOE Data)	0.106 (n = 15)	0.063 (n = 15)	0.40	520	200-1,000	970	2.6-0.52
U (MOE Data)	20 (n = 15)	7.7 (n = 15)	0.61	148	30-113	110	5.0-1.3
Ra-226 (Project Data)	0.18 (n = 2)	0.061 (n = 3)	(0.66)*	1,430***	-	-	-
U (Project Data)	34 (n = 1)	13	(0.62)*	250***	-	-	-
Ra-228 (Project Data)	0.041 (n = 2)	0.035 (n = 3)	0.15*	70	-	350	-
Th-228	0.0025	0.0026	0	0	40-180	370	0
Th-232	0.00083	0.00026	0.71	7	170-610	100	0.04-0.01
Th-230	0.0059	0.0013	0.75	50	480-1,600	-	0.1-0.03
Po-210	0.019	0.027	-0.42	(-100)	600-2,000	-	-0.2 to -0.05
Pb-210 (MOE Data)	(0.037)[1]	(0.030)[1]	-	-	440-2,200	1,000	-

* Based on two to three sets of measurement; other data based on 15 sets of estimates.

** Calculated from mass balance (hydraulic loading is 12 m/year)

*** Better estimates are those of MOE data set.

[1] Based on taking activity as one-half detection limit. More than one-half of values are less than detection limit.

lake is viewed as being less precise than those of the estimate of the retention for uranium and Ra-226.

In formulating a mass balance analysis, it is plausible that concentrations measured over time will show a seasonal dependence, particularly as it relates to flow rate. If the substance in surface water is derived from a constant source (such as a constant point source loading, or from dissolution of geological material), then concentrations will decrease as the flow rate increases. If, on the other hand, the substance is particulate in nature, then the concentration of the substance should increase as the flow rate increases because higher flow rates generally are associated with erosional forces which remove the particulate materials from land (via overland flow) and from the stream banks.

The river data for Ra-226 and uranium in Table 5.1 were assessed from this point of view. For the spring period of 1986 (19/04/86, 23/03/86), when substantively higher flow rates occurred in the Quirke Inlet than during the rest of the year, the measured data do not show any consistent pattern in terms of concentrations being higher or lower than the rest of the year. In fact, inspection of the data and plotting over time (not shown) indicates that the variation appears to be random over time, and that there is not a seasonal picture seen in the data. Accordingly, as is typical of many soluble substances which are masked by many processes, it appears that the variation of these two parameters can not be explained by flow rate nor seasonal variability. Seasonal variability does not need to be included in the assessment of mass balance analysis. Accordingly, the estimates of mass balance (e.g., Bq/year loaded to the lake, Bq/year lost in the lake) can be quantified by simply using the average inflow concentrations, the average inlake or outflow concentrations and the average annual flow rates. If there had been a distinct flow concentration relationship, then account must be taken of this flow concentration relationship in deriving the mass balance analysis.

Analysis of the results indicated in Table 5.8 allows the following statements.

1. U-238 and Th-232 decay series radionuclides are present in the following amounts in the Serpent River System. Uranium is of the order of 10 to 20 micrograms/litre and Ra-226 is of the order of 0.05 to 0.1 Bq/L. For the thorium isotopes, Th-232 is of the order of 0.0001 to 0.001 Bq/L, Th-230 is of the order of

0.001 to 0.007 Bq/L, and Th-228 is of the order of 0.002 to 0.003 Bq/L. Po-210 is of the order of 0.01 to 0.03 Bq/L. Ra-228 is of the order of 0.03 to 0.04 Bq/L, and which approximately 25 to 50% of the values of Ra-226.

2. Lead-210 activity levels cannot be assessed at the moment because the available data generally are based upon detection limit values which are of the order of equal to or less than 0.04 Bq/L. In a few instances, lead-210 values of the order of 0.07 to 0.09 Bq/L are noted; however, this is infrequent. Accordingly, the values shown in Table 5.8 are bracketed to indicate the fact that they are mainly derived from detection values. Using Po-210 as a surrogate for Pb-210, the Pb-210 values would be of the order of 0.02 to 0.03 Bq/L, near the detection limit of method used by MOL (LT 0.04 Bq/L).

3. The radionuclides are retained in the lake in the following amounts. Ra-226 is estimated to be retained at the rate of about 40% of the annual loading, while uranium is retained at the rate of approximately 60%. Of the thorium isotopes, a mixed picture is observed. Th-230 and Th-232 are retained at the rate of approximately 70 to 75%. On the other hand, Th-228 shows no retention.

3. All three Th isotopes should act chemically in a similar manner; the chemistry of Th-230 and Th-228 should be controlled by Th-232 because of its large mass. On a gross settling basis, the same portion of Th-228 entering the lake should sediment out as Th-230 and Th-232. Some Th-228 well also be derived from Ra-228 decay in the water column. Using the Th-230 and Th-232 estimates as values of sedimentation rate, Th-228 is retained at the rate of approximately 75% of the inputs. Thus, Th-228 is released from the sediments at the same rate that it settles from the water column so that Th-228 acts conservatively from a point of view of input/output in the lake. The main sources of Th-228 may be sediments in which it decays from Ra-228.

4. With respect to Ra-228, the data suggest that its retention is of the order of 15%, as opposed to the retention coefficient calculated for Ra-226 of 40%. It is possible that the value for Ra-228 may be zero or it could be larger, and nearer to that of Ra-226. However, because the analysis of sediments between Quirke Lake and Serpent Harbour show a differing Ra-228 concentration in sediments

downriver, this suggests that radium is ingrowing in the sediments from Th-232 and then returning to the water column. In this case Ra-228 would behave more conservatively than Ra-226. Accordingly, it is plausible that Ra-228 has a net retention of the order of 10 to 20% as indicated by the data; however, more data are required to establish the precise magnitude.

5. With respect to Po-210, the data (based on two different measurements) suggest that Quirke Lake is acting as an exporter of Po-210. This could be derived from Po-210 ingrowth from lead-210 in the sediments and in the water column and its return from the sediments. Thus the lake could export Po-210 or it could be acting approximately conservatively. The data are not adequate to resolve this potential difference. If the data are taken as indicating that the lake is Po-210 a net exporter of Po-210, this validates the calculations of the previous AECB modelling work (BEAK, 1982; Snodgrass, 1986) which suggested that there was a net export of Po-210 from the lake.

Based upon these inflow/outflow concentration data, the net sedimentation in the lake was calculated from the activity (mass) balances. The results are given in Table 5.8 under the column title "Net Sedimentation". These values are compared to the measured sedimentation rates and the measured settling fluxes summarized previously in Section 4.0 (Table 4.4). The measured sedimentation rates are those values inferred from the sediment concentrations of radionuclides and the sediment chronology data used to estimate accumulation rates. The range of values given is for the shallow stations (the lower value) and the deeper stations (the higher values). Finally, the ratio of the net sedimentation rates calculated from the mass balance to the measured sedimentation rates is given in the last column of Table 5.8. The first value given for the ratio uses the sedimentation rate for the shallow stations; the second ratio value uses the sedimentation rate measured at the deep stations.

The results indicate the following:

1. The amount of radium sedimentation calculated from the mass balance data is bracketed by the measured sedimentation rates. This indicates that the radium mass balance is checked successfully by the measured sedimentation rates.

2. The sedimentation rates from mass balance for uranium are slightly higher than the measured sedimentation rates either at the shallow station or at the deep station. However, sedimentation rates derived from the mass balance are reasonably close to the sedimentation rates measured at the deep station; accordingly, within the coarseness of the measurements, the values are judged to be a reasonable check on each other.

3. There is, for Th-230 and Th-232, a substantive discrepancy between the sedimentation rates inferred from mass balance and the measured sedimentation rates. The sedimentation rates from mass balance are much smaller than the measured settling fluxes for Th-232. One plausible explanation for the discrepancy between the two estimates is that most of the Th-230 and Th-232 entering the lake is associated with particles which were not measured in the influent samples.

4. The measured sedimentation rates for Th-228 suggests that there is a small accumulation of Th-228, whereas the mass balance analysis suggests there is no accumulation of Th-228. Part of this discrepancy could be due to the problems observed in the comparison of the sedimentation rate estimates from the mass balance data to the measured sedimentation rates for Th-230 and Th-232; however, due to Th-228 ingrowth in the lake from Ra-228, it is more plausible that the discrepancy reflects a small net accumulation of Th-228 which cannot be estimated from the mass balance data and its internal formation in the lake. Similar observations would be applied to the comparison of the two sedimentation rates for Po-210.

5. Sedimentation estimates for Ra-228 are not available because the Ra-228 activity has not been adequately characterized in the sediments. Accordingly, a direct comparison between net sedimentation and mass balance measured sedimentation cannot be made. However, settling rates can be used to estimate sedimentation rates if the two are equal. The settling rates of Ra-226 and the sedimentation rates of Ra-226 are approximately equal; accordingly the same is expected for Ra-228. But the sedimentation rates measured from mass balance are lower than measured values, using the settling flux to estimate the sedimentation rate measurements. This is consistent with the mechanism of Ra-228 diffusion out of the sediments and its transport out of the lake.

Accordingly, Ra-228 outflux from the sediments would be larger than the Ra-226 outflux from the sediments because of Ra-228 ingrowth from Th-232, whereas Ra-226 ingrowth would not be significant.

Additional perspective upon the Th-230/Th-232 imbalances can be obtained by examining other analytical data and by reference to the literature.

With reference to an analytical source of error for thorium, the following analytical data were obtained by Beak for samples near the bottom of Quirke Lake.

	Th-230 (Bq/L)	Th-232 (Bq/L)
Diss.	LT .005 - .068	LT 0.005 - 0.013
Particulate	LT .005 - .011	LT .005
Total	LT .01 - .079	LT .01 - .013

These data, thus, tend to corroborate the levels measured in the inflow and outflow and, suggest that the mass balance discrepancy is not due to analytical reasons.

With respect to the literature, one significant mass balance effect is that of Brunskill (pers. comm) similarly found an order of magnitude more Th sedimentation than input from runoff in Saqvacjuac area lakes in the Northwest Territories. Possible unmeasured inputs in claded stream bedload, stream suspended sediments, and shore erosion. His net sediment velocity for Th-230 and 232 was 20 - 80 m/yr, a fast delivery rate to sediments.

5.3 Implications of Mass Balance Study

With respect to one regulatory question which motivated this research, namely, are sediments a substantial long-term source of radionuclides of potential concern, the mass balance analyses described in this section permits the following statements.

1. Of the U-238 and Th-232 decay series radionuclides, lakes should be (a) net sinks for: uranium, Th-230, Th-232 and Ra-226; (b) lakes may be sinks or sources for Ra-228, Th-228 and Po-210. The degree to which sediments are sources for the latter three isotopes requires further assessment.

2. Sediments will be net sources for Ra-228, Th-228 and Po-210.

3. If existing inputs to the Serpent River system were cut off, sediments may be a net source for such isotopes as Ra-226 in a direct sediment-water sense. However, the data of the next few chapters are required to assess its significance.

4. Sediments buried by clean uncontaminated sediment is a slow but constant process in Quirke Lake for decreasing the return rate over time.

6.0 SEDIMENT STUDIES

6.1 Fractionization of Radioisotopes According to a Sequential Extraction Operationally Defined Procedure

6.1.1 Protocols for Chemical Characterization of Sediment

Several protocols for the chemical characterization of sediments have evolved over the past decade. They include:

1. measurement of total metal content;
2. sequential chemical extraction of sediments;
3. measurement of pore water constituents;
4. equilibrium (thermodynamic) analyses and mineral identification; and
5. adsorption studies using "model" and natural surfaces.

Measurement of total metal content involves total digestion or fusion of the sample and measurement of the metal content. This gives reliable estimates of total metal content and hence is the "management" parameter routinely available for assessing "degree of contamination". However, it is not a sufficiently precise parameter because essentially all of the metal content or at least a substantial amount of it may not impact aquatic organisms because it is not "available", e.g., it is not "desorbable". The metals may not be desorbable because they occupy part of the lattice of stable minerals. In some environments, use of a normalizing parameter (e.g., iron) or concentrations deeper in sediments are required to assess the "degree of contamination". For example, trace metals such as nickel and other metals may be high because of their association with hydrous iron oxides; such a phenomena is natural in certain aquatic environments (for amplification of this point see Snodgrass, 1980 for discussion of "normalizing parameters" on Pg. 235-237).

To overcome this lack of specificity, a series of extractive procedures have evolved which aim to define the fraction of total metal content which is availalbe (e.g., Agemian and Chau, 1976, 1977; Jenne et al., 1976; Malo, 1977; Williams et al.; Tessier et al., 1979; Nriagu 1978a,b; 1979a,b; 1980a,b,c). All result in operationally defined chemical fractions about which questions remain about their "process" signficance. But they are

probably the best available approach for obtaining estimates of sediment characteristics and hence will be used in this research.

Some of the procedures involve extraction procedures which may be viewed as research level techniques, (e.g., Williams et al.) while others only measure a proportion of the "available" metal fraction. A few procedures (e.g., Tessier et al., 1977) have been developed at a useful level of complexity while their biochemical significant have been tested to a limited degree. More testing of their biochemical significance is required. The study of Tessier et al. (1979) has been tested by them in further studies (Tessier, 1982) and by others (Mudroch, pers. comm.).

The Tessier procedure operationally defines 5 chemical compartments which have significance to estimating the rate of release of metals. They are:

1. exchangeable (e.g., adsorption),
2. bound to carbonates,
3. bound to iron and managanese,
4. bound to organic matter, and
5. residual.

"Exchangable" metals are conceptually those easily desorbed, and which will come off due to changes in pore water composition. The amount of metal which is reversibly adsorbed is theoretically a function of the concentration in solution and the number of adsorption sites available. Metals bound with carbonates will be susceptible to changes in pH. Iron and manganese oxidizes are thermodynamicaly unstable under anoxic conditions. Metals associated with organic matter may be kept in solution by soluble organic matter (e.g., soluble fulvic acid) or attached to particulate phases. Residual metal should be present as trace impurities in the crystal lattice of primary (e.g., silica sand) and secondary minerals; these minerals should have slow dissolution kinetics (Tessier et al., 1979). Recent evidence (e.g., Lasaga, 1984; Rimsted and Barnes, 1980; BEAK, 1985) now permits one to estimate the dissolution kinetics of some of these minerals.

The method of Tessier was used to attempt to measure the associations of radionuclides, particularly the radium and thorum radioisotopes with different mineral fractions in the

sediments. This method operationally attempts to separate adsorbed, carbonate-associated, hydroxide and oxide-associated, organics, and residual phases by using a set of leaching agents which are known to dissolve these particular components. There is some problem with use of such chemical sequestering techniques because the sequestering agents do not uniquely break down the particulate fractions of concern, but also leach some components of the other fractions. However, within the field of sedimentology and chemical limnology, the Tessier procedure has been and is receiving widespread application as one of the better techniques for trying to gain physical-chemical insights into the mineralogical characteristics of the sediments. Accordingly, within the limits of such a technique as being an operationally defined technique, its results have some validity and are of use for understanding the particulate and soluble phase speciation of radionuclides in the sediment, and for developing insights for using such results in modelling.

6.1.2 Methods

In order to operationally apply the Tessier procedure to Quirke Lake sediments, .1 to .2 mg of Quirke Lake sediment were contacted with the appropriate strength of leaching agents in the appropriate solution volumes as dictated in the procedure. The volume of solution was generally of the order of 8 to 10 mL in order to allow the complete extraction reaction to occur within a centrifuge tube and for the centrifuge tube to be used directly for separations. After separation by centrifuging, the solution was then decanted and the sediment samples washed once or twice as dictated by the Tessier procedure with distilled water. Each time that the sediments were washed, the sample was subsequently separated again by centrification, and the solution decanted. For chemical analysis, the original extractions plus the washwaters were mixed together to give the liquid sample from each extraction for chemical analysis.

For radionuclide analysis, the amount of radioistope which would be obtained for each extraction was unknown; assuming that the activity levels would be insufficient to obtain reasonable detection limits from the extraction, extractions from 10 to 12 g were combined to form one set of solutions for analysis. Hence, solutions from the first extractions from one 12 g lot was combined, solutions from the second extraction of the 12 g were combined, solutions from the third set of extractions from the 12 g sample, and solutions from the fourth extraction of the 12 g sample were combined and

forwarded for radionuclide analysis to the Monenco laboratory. As the results show (see Table 6.1), these solutions gave reasonable detection limits for all samples except for a few (e.g., Pb -210) in which the solution activity was below detection limits. Because most radionuclides came off in one extraction, these detection limits are sufficient for purposes of this experiment because it allows an evaluation of which fraction the nuclide is associated with. However, it does not allow one to determine relative concentrations within the two or three different extractions which are at detection limit. Solutions were also submitted to the National Water Research Institute for radionuclide analysis as a part of the project supported by Environment Canada. In this instance, rather than combining a complete set of up to 12 g equivalent of sample for analysis, a few samples of the order of 1 g and their extractions were combined and used to analyse for one radionuclide (e.g., radium) and then extractions from another set of sediments were used as the aliquot for thorium analysis, etc.

Results from these chemical analysis are given in Table 6.1 in terms of total radionuclide extracted from the particulate extraction procedure. The results indicate the following:

1. In the sorbed fraction, only calcium, manganese and uranium have a significant fraction in this phase.
2. The following elements have a significant distribution in the carbonate, oxide and organic phases, but most of their mass is concentrated in the residual: Al, Ba, Ra-226, Be, Cd, Cr, Cu, Ni, Sr, Th-232, Th-228, Th-230.
3. The following elements are disregarded due to their participation as extraction agents: Mg, Na.
4. In the "oxides of manganese and iron phases", the largest amount of manganese and Tin are in this phase, and a substantial portion of iron. However, there are approximately equal amounts of iron in the "oxide", the organic and the residual phases. Aluminum is also significant in the oxide and organic phase, but its largest amount is in the residual phase consistent with the idea that the largest portion of aluminum is contained in alumino-silicate minerals which presumably do not dissolve significantly in these leaching solutions.
5. The largest portion of uranium is in the carbonate phase.
6. Ra-226 shows a similar distributional pattern to barium, suggesting some possibililty of association.

7. The thorium isotopes are probably not in a hydroxide or oxide form, in comparison to the iron and manganese distributions.
8. Most of the uranium is in a non-residual form, suggesting that it may be potentially more mobile than most of the other elements.
9. The analytical capabilities of ICAP for major elements show an excellent agreement between two samples submitted as blind replicates (4(1) and 4(2) are blind replicates).
10. Replication of chemical extractions (compare No. 1 to No. 2 for all elements in Table 6.1a) shows good reproducibility.

6.2 Mineralogical and Nuclear Emulsion Studies on Quirke Lake Sediments

6.2.1 Introduction

A nuclear emulsion, scanning electron microscope study was undertaken of selected Quirke Lake sediment samples. The objective of this work is to develop a physical/mineralogical basis for the radionuclide associations measured with the chemical extraction procedures.

The dispersed-grain nuclear-emulsion technique was used to evaluate sources of radiation within Quirke Lake sediments; then the samples were examined under scanning electron microscope (model JEOL JMS-840) equipped with x-ray energy dispersive and wave length dispersive capabilities. The wave length dispersive instrument allows identification of various elements on the portion of the sample being examined by the scanning electron microscope, including carbon. The dispersed grain nuclear emulsion technique is a micro-audio radiographic technique which permits the direct observation of the alpha activity on different individual mineral grains or particles which have been dispersed over the surface of an alpha sensitive photographic plate. The size of a mineral grain which can be studied is set by itself in activity and by the resolving power of the optical system used. It is possible to observe in the nuclear emulsion underlying the dispersed sample the sequential decays of individual atoms of Rn-222, Ra-226 and Th-228 which result in the 3, 4 and 5 alpha stars respectively. Because these atoms disperse into the emulsion during the preparation of alpha plate, it is possible by examining these particles under optical microscope to identify sources of activity and identify degrees of particular types of activity. Then by picking these small 20-40

micron size particles off of the nuclear emulsion plate and putting them under the examining system of the SEM, the mineralogy of the particular grains involved can be directly identified.

6.2.2 Results of Nuclear Emulsion and Mineralogy Studies

A variety of particles which were examined by light microscope are shown in Figures 6.1 to 6.9. In addition, a detailed evaluation of what each photograph shows is described underneath each photo. An analysis of the photos indicate that it is difficult to be quantitative with the nuclear emulsion approach; however, it is useful in that it gives a picture of the types of activity that one finds with particular particles and is useful for descriptive purposes.

The following general observations are made from these photographs.

1. There are a series of particles of various sizes and shapes which have alpha activity associated with them; in particular, radium is a potential source for most of the activity but there is also evidence for thorium, lead and uranium in these photographs.
2. In the mineralogical identification with SEM, Ra-226 activity appears to be associated with a variety of particles, including quartz, feldspar, organic matter, and even barium sulphate.
3. Examination of these types of particles under SEM in the areas of intense alpha activity revealed the following types of particles. Three particles on one photo were examined; one particle having a large alpha activity emanating from it appears to be an aluminum-silicate particle with a substantial organic coating associated with it. Another particle nearby was identified as being a small uraniferous grain; the third particle was identified as being primarily a siliceous grain. On another section of the slide, a heterogeneous rough textured grain was examined on which there were alpha tracks emanating but in a non-uniform fashion.

   In examining the section of the whole grain, the SEM work indicated that it was primarily a silicon containing particle with some iron, some aluminum and some barium associated with it. On examaning the site near where the alpha activity

had emanated, a barite inclusion was identified. Also a hexagonally shaped particle containing lots of alpha tracks was identified; detailed examination under SEM shows that it is primarily a barite ($BaSO_4$) with the typical morphology of the barite particle.

In conclusion, it would appear that alpha activity which most plausibly is derived from radium and daughters is associated with a variety of particles in the sediments. It is unclear whether the radium is all co-precipitated with parent solids or is also loosely sorbed to various substances from this work. However, in reviewing the association of radium with the variety of surfaces, it would appear that some of it at least would be sorbed into a variety of services. In addition, the SEM work and occular microscope work would indicate that some of the particles such as aluminum silicate particles, have a coating of organic matter on them, this is typically expected of organic matter associated with sediment minerals. Finally, the analysis indicates that there are a variety of whole grains which would appear to be probably derived originally from ore or tailings. In a review of the operating history of the Quirke Lake system, it is known that one tailings area slumped allowing a mass of tailings to get into the lake over a couple of decades ago. It is possible that this is the source of the minerals such as the uraniferous and the barite grains observed in this work.

The nuclear emulsion - SEM work thus provides some physical basis for the chemical extraction procedure results described previously in section 6.1. The extraction procedure results indicate that radium is associated with a variety of fractions rather than one particular fraction; this is borne out with some degree by the nuclear emulsion results which suggest that radium derived alpha activity is associated with a variety of grains and a variety of phases. The extraction of barium from a variety of phases is borne out by the SEM results becasue they indicate that there are at least one distinct barite phase present in the sediments. These barite particles are probably epigenic in origin and were brought into the lake by mining processes. Because the chemical extraction procedures are relatively selective for other phases, it would suggest that barium itself is also associated with other fractions of the sediments other than strictly barium sulphate. It is possible that the extraction procedures themselves only partially dissolve barium sulphate if barite dissolves with slow kinetics. However, given the relatively quick dissolution of barite which are known to occur, it is more probable that barium is associated with other phases as well.

6.3. Characterization of Adsorption Processes in Quirke Lake Sediments

6.3.1 Description of Adsorption Experiment

An adsorption experiment was conducted in which wet sections of sediment from Quirke Lake sediment cores were mixed with water ($NaHCO_3$ 10^{-3} to 10^{-4} molar). In the first experiment, the solid to liquid ratios of 1:10 and 1:200 were used and the samples were kept under a nitrogen atmosphere to maintain deoxygenated conditions for the sediment sections which were anaerobic. The results from this experiment are given in Table 6.2. In the second experiment, the nitrogen atmosphere was not used but rather the water mixed was purged with nitrogen and then used for mixing with the sediments at a new S:L ratio of 1:500 in order to give better partitioning and counting statistics. In the second experiment, 10^{-4} molar $NaHCO_3$ for the first one of each duplicate and 10^{-3} molar $NaHCO_3$ for the second one of each duplicate described in Table 6.2 were used for the contact solutions.

The experimental procedure consisted of mixing a wet volume of sediment with a given volume of water as dictated by the solid to liquid ratio and counting the activity of injected tracer on the solid and in the supernatant. The S:L ratio in the first experiment was based on some calculated values from the literature; the second set were based on the results from the first set. The sediments were maintained wet in order to maintain the general aerobic or anoxic conditions of the sediment, and to prevent changes in the sediment characteristics as would be effected if one dried the sediments as is often done in these types of experiments. In order to estimate the actual solid content of each sediment section in a wet basis, separate tubes were extruded and the solids concentrations measured.

The sediment and water ($NaHCO_3$) solutions were mixed up in 50 mL centrifuge tubes. For evaluating sorption characteristics, tracers (Th-234, Ra-224, Pb-203) were obtained from Becquerel Laboratories. The Th-234 and Ra-224 tracers were scavanged from appropriate columns while the Pb-203 was obtained from external sources. Each sediment sample was injected with approximately 0.7 mL of tracer solution containing the three isotopes. The tubes were mixed on a shaker for two hours. This contact time was selected as the literature indicates that this is a time frame over which most adsorption occurs; however, in future, it will be necessary to evaluate the sorption

kinetic experimentally to establish the best time for kinetic measurements because some literature suggests a 24-hour period. Because further adsorption could occur over a 24-hour period or longer, these estimates for Kd should be viewed as being lower range estimates.

Once shaking was complete, the centrifuge tube was put into a centrifuge for 20 minutes at 3,500 rpm. The liquid was then decanted into another centrifuge tube and the remaining solids in the centrifuge tube and the centrifuge tube (also 50 mL) containing the liquid was submitted for analysis. The tracers were counted in the decanted liquid and in the solid fraction. From these counts and appropriate background corrections, the Kd values (mL/g) were calculated.

The results are given in Tables 6.2 and 6.3. The data of Table 6.2 (first adsorption experiment), are mainly from a sediment core from a water depth of 20 m in Quirke Lake. In the second set of experiments, a few samples from the 20 m depth station were repeated but most of the measurements were made upon a 100 m core. The counting statistics for the solid phase and for the liquid phase were evaluated. Counting statistics, which provide an indication of the accuracy of the measurement, are defined as being the square root of the total counts on a sample plus background counts divided by the total counts of the sample minus background counts times 100%. If the counting statistics were substantially larger than 10%, the measured values were taken as not being probable values and hence were disregarded in the reporting.

6.3.2 Results

The results indicate the following.

1. There was not a significant relationship between K_D and solid to liquid ratio or the sodium bicarbonate concentration given the overall variability in the estimates of K_D. This precludes the need to examine for coprecipitation or ion exchange effects in this data.
2. There appears to be a trend of higher adsorption values with depth in the sediment for radium. A similar trend is suggested for the adsorption of lead at the 20 m station, but not for thorium. The trends, are, however too noisy to permit definitive conclusions on this point. If the trends were significant, it

would indicate that this would be an additional factor which would need to be evaluated in the modelling work to assess the sensitivity of sediment-water transport.

3. The sorption values (K_D; mL/g) have the following range.

	20 m Station	100 m Station
Thorium	100 - 1,000	200 - 1,200
Radium	40 - 1,500	100 - 17,000
Lead	400 - 1,700	1,900 - 21,000

The thorium and radium values are similar with the lead values being higher. The values for thorium are inconsistent with some literature values which suggest values of the order of 50,000, but they consistent with literature value for radium and lead which are of the order of 500 for radium and 1,000 to 5,000 for lead.

Theoretically, these measured values for thorium can be accepted if it is hypothesized that these represent reversible sorption measurements. Values for thorium of 50,000 and larger may represent non-linear sorption measurements while values measured by Santchi and others for iron (using Fe-59) of the order of one million and larger may result from surface precipitation phenomena in which the aqueous phase concentration is controlled by solubility considerations (Snodgrass, 1986).

These values are used for testing in the modelling work of Section 8.

With respect to other efforts found in the literature for sorption of these isotopes, the data are similar. One of the more imaginative efforts is that of Benes and Streu (1985) who sorbed Ra-224 onto various sediments with different mineral compositions downstream of a wastewater discharge from an uranium mine. Sorption occurred generally in a mixture of hydrochloric acid, sodium hydroxide and distilled water. Experimental variables examined were pH, ionic strength, sulphate (Na_2SO_4) and calcium ($CaCl_2$) concentrations. Then sorption measurements onto particular minerological components (quartz, Kaolinite etc.) were also made.

In this comparison (Benes and Streu, 1985) between total sorption characteristics and sorption calculated from the representing components of the sediments, it was found that the adsorption affinity of the sediments for radium would not be easily derived from their composition or other properties. "No simple correlation with specific surface area, organic matter, oxidic coatings or other components of the sediments was observed. However, an exceptional role of barite (barium sulfate) in the sediments was noted. In the presence of sulfate ions (60 mg/L) this component was responsible for the uptake of the predominant or at least significant part of radium, depending on the barite content of sediments. In the absence of added sulfate ions, the adsorption of radium at pH 5-9 on sediments containing barite was lower than on similar sediments without this component, indicating that other components may be more efficient in radium adsorption."

The sorption measurements of this project and those of Benes and Streu (1985) suggest that additional experiments should be carried out:

1. to characterize sorption characteristics with depth in the sediments;
2. to evaluate the kinetics of adsorption and desorption; and
3. to evaluate the significance of barite with depth in sediments.

It is doubtful, however, that substantive insight into the site of sorption will be obtained using the approach of Benes and Streu (1985) without using wet sediments. The role of sulphate ion would not need extensive investigation for other than the top 1 cm of the sediment because the sulphate concentration in pore water below the 1 cm zone should be negligible due to anaerobic conversion of sulphate to sulphide (and precipitation as sulphide minerals).

TABLE 6.1a: EXTRACTED CONCENTRATION (ug/g)

Fraction	Ag		Al		B		Ba		Be		Ca	
	No. 1	No. 2	No. 1	No. 2	No. 1	No. 2	No. 1	No. 2	No. 1	No. 2	No. 1	No. 2
1	0.77	0.56	82	65	2.7	3.1	12	13	L 0.02	L 0.02	2,700	3,100
2	1.5	1.7	1,300	1,400	4.4	6.2	100	170	0.28	0.23	1,700	2,000
3	3.8	4.3	6,800	6,400	3.5	5.0	410	500	0.46	0.60	1,100	1,300
4	0.37	0.62	8,900	7,700	8.9	5.0	230	160	0.33	0.31	180	310
Residual	L 10	L 10	41,000	45,000	-	-	1,500	1,300	3.3	2.2	4,300	4,200

	Cd		Co		Cr		Cu		Fe		Ir	
	No. 1	No. 2	No. 1	No. 2	No. 1	No. 2	No. 1	No. 2	No. 1	No. 2	No. 1	No. 2
1	0.36	0.72	0.63	0.65	1.7	2.4	2.7	2.9	380	480	L 0.7	L 0.7
2	0.97	1.4	4.4	3.5	5.9	6.8	6.9	1.0	2,700	2,700	L 0.9	L 0.9
3	3.7	3.8	40	31	12	15	17	19	4.0×10^4	3.9×10^4	1.4	L 1.5
4	1.9	0.58	9.2	7.3	13	15	78	81	1.3×10^4	9,700	3.7	2.3
Residual	17	17	L 20	L 20	115	86	48	49	69,000	75,000	L 30	L 30

	K		Mg		Mn		Mo		Na		Ni	
	No. 1	No. 2	No. 1	No. 2	No. 1	No. 2	No. 1	No. 2	No. 1	No. 2	No. 1	No. 2
1	340	430	2.1×10^5	2.1×10^5	3,600	3,900	1.5	1.2	3.4×10^4	3.1×10^4	L 0.24	L 0.24
2	62	180	2.5×10^4	2.4×10^4	8,100	9,400	L 0.31	L 0.29	2.5×10^5	2.8×10^5	1.6	L 0.29
3	180	150	2,600	2,500	3×10^4	3.6×10^4	1.8	L 0.50	2.4×10^4	2.4×10^4	11	15
4	37	L 39	180	150	2,700	3,900	L 0.37	L 0.39	1,000	1,200	5.2	7.7
Residual	9,500	10,800	4,400	4,600	2,000	1,600	64	280	4,900	9,200	L 20	L 20

	Pb		Si		Sn		Sr		V		Zn	
	No. 1	No. 2	No. 1	No. 2	No. 1	No. 2	No. 1	No. 2	No. 1	No. 2	No. 1	No. 2
1	L 0.97	1.5	140	162	L 0.73	L 0.72	4.6	5.8	L 0.12	L 0.12	0.68	0.97
2	13	12	650	760	L 0.93	7.6	8.1	11	L 0.16	L 0.15	31	44
3	86	110	1,400	1,300	77	32	5.0	6.0	4.5	6.2	56	78
4	110	140	2,000	1,700	4.1	1.2	2.5	3.5	1.3	4.2	27	34
Residual	250	170	-	-	L 25	L 25	110	110	62	56	86	106

	Zr		Th-232*		U		Th-228*		Ra-226*		Th-230*	
	No. 1	No. 2	No. 1	No. 2	No. 1	No. 2	No. 1	No. 2	No. 1	No. 2	No. 1	No. 2
1	0.19	0.10	0.002	0.0017	63	72	0.0056	0.0029	0.029	0.02	0.014	0.015
2	3.1	4.4	0.069	0.094	340	270	0.053	0.10	0.12	0.15	0.47	0.64
3	5.0	5.0	0.12	0.14	160	140	0.16	0.20	0.94	1.4	0.27	0.95
4	6.3	7.7	0.10	0.10	31	26	0.077	0.14	0.57	0.41	0.56	0.69
Residual	110	120	1.1	1.0	18.3	21.2	0.68	0.63	4.4	3.8	3.8	4.8

	Pb-210*	
	No. 1	No. 2
1	L 0.048	L 0.048
2	L 0.062	L 0.039
3	1.6	1.8
4	L 0.074	L 0.077
Residual	3.4	3.2

* Units = Bq/g

TABLE 6.1b: CONCENTRATION EXTRACTED (ug/g)

Fraction	Ag	Al	B	Ba	Be	Ca	Cd	Co	Cr	Cu	Fe	K
1	1.9	34	9.5	43	0.085	3,500	L 0.27	17	220	11	110	300
2	0.55	1,900	3.0	110	0.25	1,400	0.35	20	21	6.2	1,900	35
3	0.71	5,800	7.9	110	0.42	380	1.5	18	16	5.6	3.4×10^4	51
4(1)	0.61	7,500	L 0.16	120	1.6	660	0.41	6.6	12	78	1.3×10^4	L 41
4(2)	0.41	7,200	L 0.16	120	1.4	620	L 0.41	5.3	10	78	1.4×10^4	L 41
Residual	L 0.7	4.1×10^4	-	1,000	1.1	8,800	L 1	L 7	89	16	3.1×10^4	2.0×10^4

	Mg	Mn	Mo	Na	Ni	P	Pb	Si	Sr	Th	Ti	V
1	5.7×10^3	410	19	6.9×10^4	35	260	L 1.3	2.2×10^4	L 0.27	4.6	L 0.27	L 0.27
2	3.6×10^4	340	10	5.2×10^3	5.9	59	88	8.5×10^4	3.8	35	3.5	2.1
3	3,400	610	L 10	3.8×10^4	9.6	40	170	23×10^4	2.0	40	7.1	16
4(1)	1,400	150	L 8	2,200	7.0	180	88	22×10^4	4.1	48	16	11
4(2)	480	150	L 8	940	6.1	190	86	25×10^4	4.1	46	17	11
Residual	6,000	440	L 30	1.7×10^4	28	980	10	-	170	110	2,300	55

	Zn	Zr
1	L 0.27	3.0
2	30	5.9
3	44	12
4(1)	33	121
4(2)	40	12
Residual	75	130

TABLE 6.2a: K_D VALUES (mL/g) FROM FIRST ADSORPTION EXPERIMENT

Section (cm)	Depth	Th-234	Ra-224	Pb-203
0-1	20 m	230	36	420
0-1	20 m	225	82	750
1-5	20 m	127	160	930
1-5	20 m	590	150	2,100
1-5	20 m	109	110	670
1-5	20 m	430	120	1,900
5-7	20 m	650	250	2,200
5-7	20 m	-	130	3,600
7-12	20 m	-	180	4,700
12-25	20 m	350	120	4,000
12-25	20 m	2500	220	3,000
12-25	20 m	800	160	3,800
12-25	20 m	-	-	6,000
12-25	20 m	-	-	-
12-25	20 m	-	-	-
0-1	100 m	200	67	760
0-1	100 m	450	260	1,400

TABLE 6.2b: K_D VALUES (mL/g) FROM SECOND ADSORPTION EXPERIMENT

Depth	Section	Th-234	Ra-224	Pb-203
20 m	1-5 cm	-	170	3,300 - 10^{-4}M $NaHCO_3$
20 m	1-5 cm	-	180	2,900 - 10^{-3}M $NaHCO_3$
20 m	5-7 cm	-	690	12,000
20 m	5-7 cm	-	760	9,700
20 m	7-12 cm	-	870	8,400
20 m	7-12 cm	-	960	15,000
20 m	12-25 cm	-	1,390	17,000
20 m	12-25 cm	-	1,530	8,300
100m	1-5 cm	-	110	1,900
100m	1-5 cm	790	1,100	5,900
100m	1-5 cm	770	1,200	2,800
100m	1-5 cm	-	120	4,900
100m	5-7 cm	-	1,500	21,000
100m	5-7 cm	-	-	2,900
100m	5-7 cm	870	-	3,900
100m	5-7 cm	-	1,400	10,000
100m	7-12 cm	-	2,400	20,000
100m	7-12 cm	1200	17,000	1,600
100m	7-12 cm	1200	9,000	1,500
100m	7-12 cm	-	2,300	13,000
100m	12-25 cm	2500	2,000	13,000
100m	12-25 cm	270	0	4,600
100m	12-25 cm	200	5,100	4,600
100m	12-25 cm	-	3,500	-

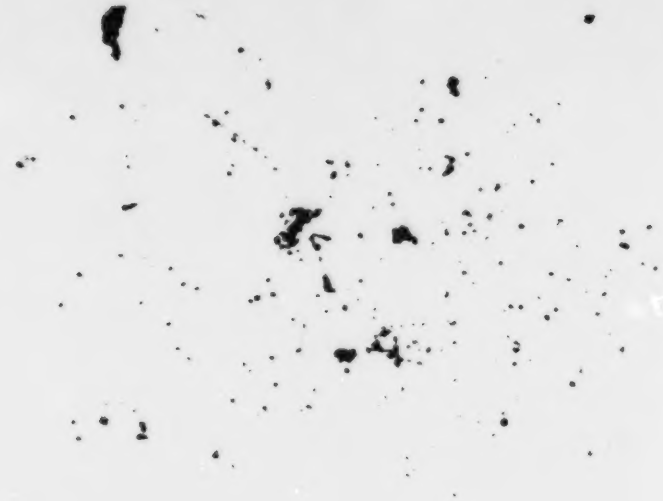

FIGURE 6.1:

Photomicrograph No.: KK-7

Sample No: Quirke Lake #1
Laboratory No.: WS-5
Exposure: 37 days
Magnification: Ocular 10x; Objective 53x (oil)

A photomicrograph of a 2-track alpha star whose vertex originates at the surface of a small particle associated with an aggregate of very small brown particles. In general, the population of 2-track stars is essentially forbidden. The occurrence of 2-track stars whose vertices are in the emulsion, i.e., stars produced by the decay of radionuclides surrounded on all sides by the emulsion, is extremely small (less than 10 stars after a 500-hour exposure). (See Figure 3). Most 2-track stars that occur in the emulsion are observed to have their vertices very close to either the upper or lower surface of the emulsion. Because of the very low natural abundance of 2-track stars, it is believed that most stars with only two branches, either associated with particles or in the emulsion, are actually incomplete 3-, 4-, or 5-track stars whose other branches fell outside of the emulsion and, consequently, did not leave tracks.

The interpretation of the 2-track star in photomicrograph KK-7 is that it was produced by the decay of a Ra-226 atom attached to the surface of the particle and that two of the four alpha particles emitted during the sequential decay of the atom entered the hemisphere overlying the emulsion and were not recorded. It is less likely that the source atom was part of a 5-track star from the decay of Th-228 because these stars are less abundant. It is least likely that the source atom was Rn-222 because of the chemical properties of radon gas.

Note the short, single track in photomicrograph KK-7, lying above and to the left of the 2-track star. The radionuclide which produced this single track cannot b e associated with a specific particle and is believed to have entered the emulsion from the distilled water used to disperse the sample. Although on the basis of track length it could be assigned to either U-238 and its long-lived daughters or to Th-232, the relatively high concentration of U-238 (482 mg/g) compared to Th-232 reported for this sample suggests that U-238, U-234, or Th-230 is a more likely candidate. See also Figure 1. The number of short, single tracks at the upper surface of the emulsion which do not appear to be associated with a specific particle as well as the short, single tracks in the emulsion is relatively large.

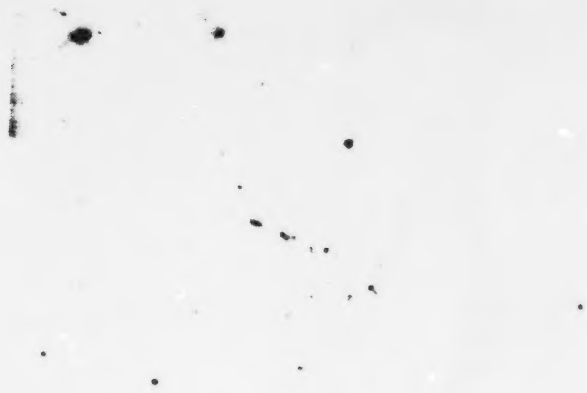

Figure 6.2

Photomicrograph No.:	MH-6
Sample No:	FS Th-232 Standard
Laboratory No.:	Th-1
Exposure:	35 days
Magnification:	Ocular 10x; Objective 100x (oil)

A photomicrograph of a 5-track alpha star whose vertex lies within the alpha-sensitive photographic emulsion. The population of 5-track stars is dominated by the sequential decay of Th-228/Ra-224/Rn-220/Po-216 and either Bi-212 or Po-212 in the Th-232 decay chain. In contrast, the 3- and 4-track star populations are principally products of Rn-222 and Ra-226, respectively, in the U-238 series (see Figure 6). For long exposures (in excess of 90 days), the presence of even relatively low concentrations of Th-232 compared to U-238/U-235 can be expected to be the major source of 5-track stars. Only in those cases where Th-232 is essentially absent would assignment of any significant number of 5-track stars to the decay of Th-227 in the U-235 decay chain have a reasonable chance of being correct.

A preliminary survey of the alpha-star populations in the emulsion of the Quirke Lake #1 alpha plate (WS-5) suggests that the 5-track stars are roughly half as abundant as the 4-track stars. On the basis of limited track-length observations as well as the ratio of 4 to 5-track stars it appears that the 5-track stars are most probably produced by the decay of Th-228 or from samples containing Ra-228 which has had sufficient time to come into equilibrium with its daughter Th-228. The sample is reported to contain approximately 1.6 to 2.0 B/g of Th-228. The mode of occurrence of the Th-228 has not been identified. However, at least part of the Th-228 in Sample WS-5 is sufficiently weakly bound so that it can be taken into solution in the distilled water used to disperse the sample in the preparation of the alpha plate. The Th-232 would, of course, produce only short single tracks (alpha-particle energy, 4.0 MeV) whereas small particles of thorium containing minerals or recent coprecipitates of Th-232 and Th-228 would produce multiple tracks with at least a few of the characteristic, maximum length 8.8 MeV alpha tracks.

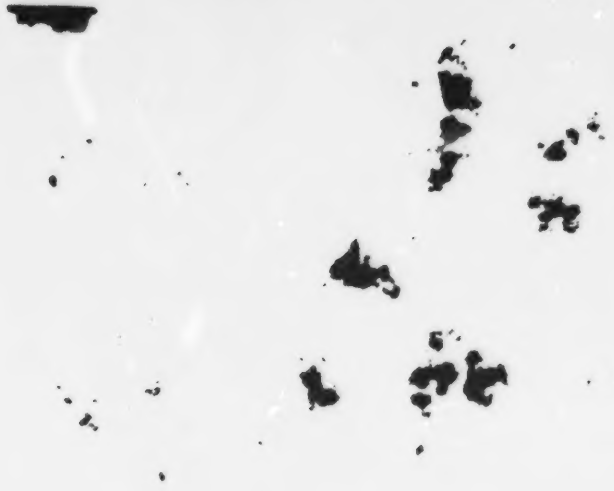

Figure 6.3

Photomicrograph No.:	JJ-5
Sample No:	Quirke Lake #1
Laboratory No.:	WS-5
Exposure:	37 days
Magnification:	Ocular 10x; Objective 53x (oil)

Photomicrograph JJ-5 is a representative microscope field containing numerous, small aggregates of light brown to brown particles found in the alpha-plate preparation of Sample WS-5. These aggregates of small brown particles may consist of a mixture of iron oxides and organic material.

Two of the particles in the photomicrograph, the central particle and the elongate particle to the left and below the central particle, are associated with short, single alpha tracks. The single alpha track which can be observed near the particle above the central particle originates elsewhere. Although it is possible that in this case the two particles and their associated single tracks may, in fact, each represent just one branch of a 3-, 4-, or 5-track star, it is not probable. A more likely explanation for the general observation that almost all of the alpha activity associated with the small aggregates of brown particles is limited to short, randomly-oriented, single tracks is that the parent radionuclides are limited to the principal single track emitters, U-238,U-234, Th-230, Th-232 and possibly Pb-210/Po-210. It should be noted, however, that if colloidal precipitates form which contain even relatively small numbers of atoms of Pb-210/Po-210 the alpha activity of these very small particles may be intense because of Po-210's relatively short half-life (138 days). A comparable number of atoms of the very much longer half-lived single track emitters might not result in a single alpha decay. In view of the absence of sequential decays and colloidal concentrations of Pb-210, the most probably interpretation of the short, random, single-track alpha activity associated with many small brown particles is that it is due to the presence of low concentrations of the long-lived radionuclides in the U and Th series.

Figure 6.4

Photomicrograph Nos.:	JJ-6 and JJ-7
Sample No:	Quirke Lake #1
Laboratory No.:	WS-5
Exposure:	37 days
Magnification:	530x, Ocular 10x; Objective 53x (oil)

Photomicrograph JJ-6 (left) is focused on the alpha tracks in the underlying emulsion and shows the alpha activity associated with a large particle. Photomicrograph JJ-7 (right) is focused on the alpha active particle.

This particle is approximately 0.08 by 0.05 mm in size. In general, these large particles are very abundent and they are usually light brown to brown in transmitted light. These particles appear to be composed of aggregates of much smaller brown particles and small, birefringent mineral grains (typically quartz and feldspar) which are covered or dusted with very small brown particles. Under crossed polaroids, these large aggregates of small brown particles appear to be reddish brown in color. The relief of the particle is relatively high. This translucent brownish material may be a mixture of iron oxides and/or organic material.

The alpha-track activity associated with the large aggregate of brown particles (JJ-6) is moderate and consists of a number of short to medium length single tracks whose origins appear to be localized within a small area in the interior of the particle. On the basis of projection of the alpha track back into the particle it would appear to be unlikely that the alpha activity was limited to a single point source or colloidal-sized particle. The particle JJ-7 was surrounded by approximately 45 single alpha tracks including the steeply-dipping tracks that are out-of-focus in the photograph JJ-6. Considering the specific alpha activity of the source area and the track lengths, the radionuclides most probably responsible for this activity are either Ra-226 and its daughter or Pb-210/Po-210.

(over)

Figure 6.4 (cont'd)

The alpha-track count of the particle in JJ-6 is somewhat higher than the alpha activity typically associated with the larger aggregates of brown particles. The source of the alpha activity in most of the large particles appears to be more uniformly distributed throughout the aggregates and the orientations of the alpha tracks appears to be random as might be expected if the source of the alpha activity was not confined to one very small area.

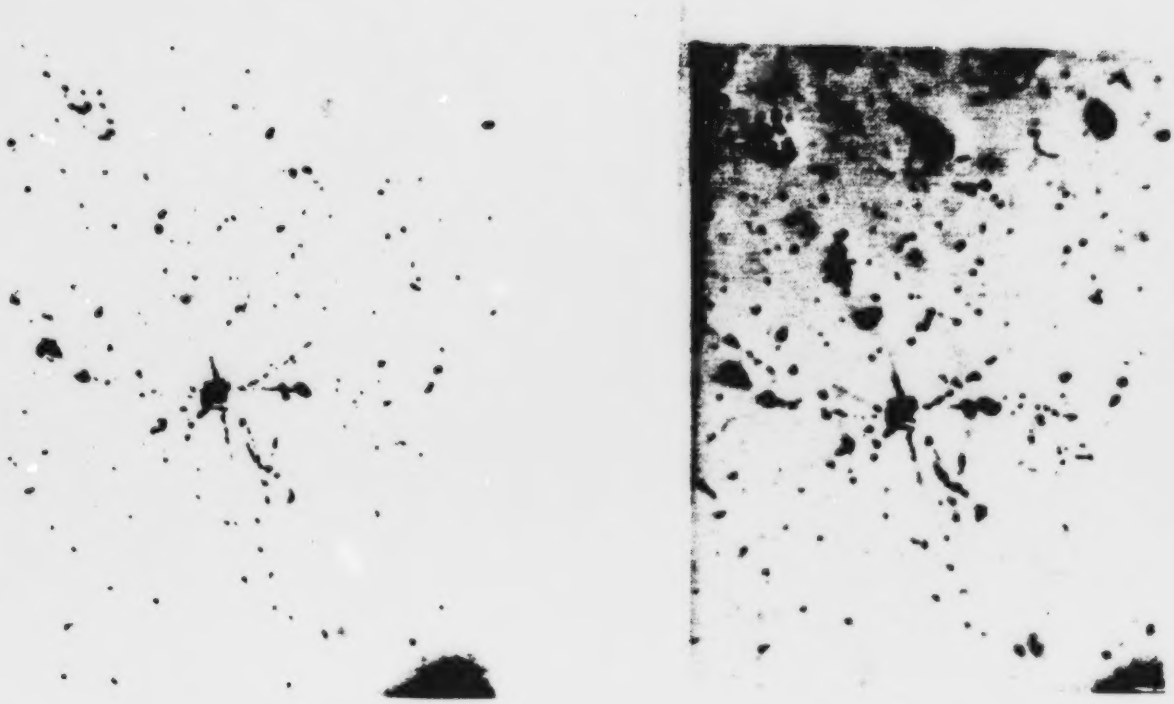

Figure 6.5

Photomicrograph Nos.: KK-3 (left) and KK-4 (right)
Sample No: Quirke Lake #1
Laboratory No.: WS-5
Exposure: 37 days
Magnification: Ocular 10x; Objective 100x (oil)

Photomicrograph KK-3 (left) is focused on the alpha tracks in the underlying emulsion and shows the alpha activity associated with a small aggregate of microcrystallites. Photomicrograph KK-4 (right) is focused on the alpha-active particle and suggests the microcrystalline nature of the aggregate. The crystallites are yellowish-brown in color, birefringent under crossed polaroids and, as can be seen, exhibit moderately high relief.

With one exception, the alpha tracks associated with the particle KK-3 are relatively short (Note magnification is 1000x). The tracks do not appear to be randomly-oriented, possibly because the particle itself is very small, but, rather they appear to converge on a small area within the microcrystalline aggregate. On the basis of alpha-track length and specific activity, the alpha activity may be due to the concentration of a small number of Pb-210/ Po-210 atoms in a colloidal-sized particle within the microcrystalline aggregate.

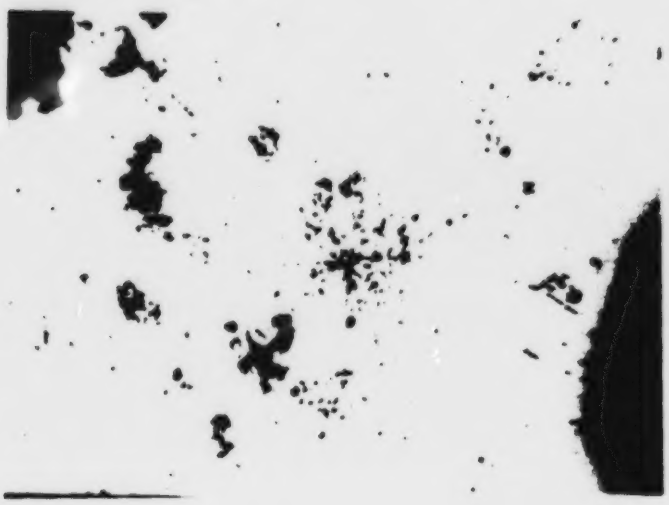

Figure 6.6

Photomicrograph No.:	KK-8
Sample No:	Quirke Lake #1
Laboratory No.:	WS-5
Exposure:	37 days
Magnification:	Ocular 10x; Objective 53x(oil)

A photomicrograph of two small alpha-active euhedral crystals associated with an aggregate of small brown particles. The crystals are pale yellow in color, do not appear to be birefringent under crossed polaroids, and have low to moderate relief. The alpha activity of these two particles is noticably higher than the alpha activity associated with the particle KK-4. As can be seen, the number of long tracks with these two particles is also clearly greater. The alpha track lengths and the specific activity of the crystals strongly suggest that this alpha activity is most probably produced by Ra-226 and its three alpha-emitting daughter products.

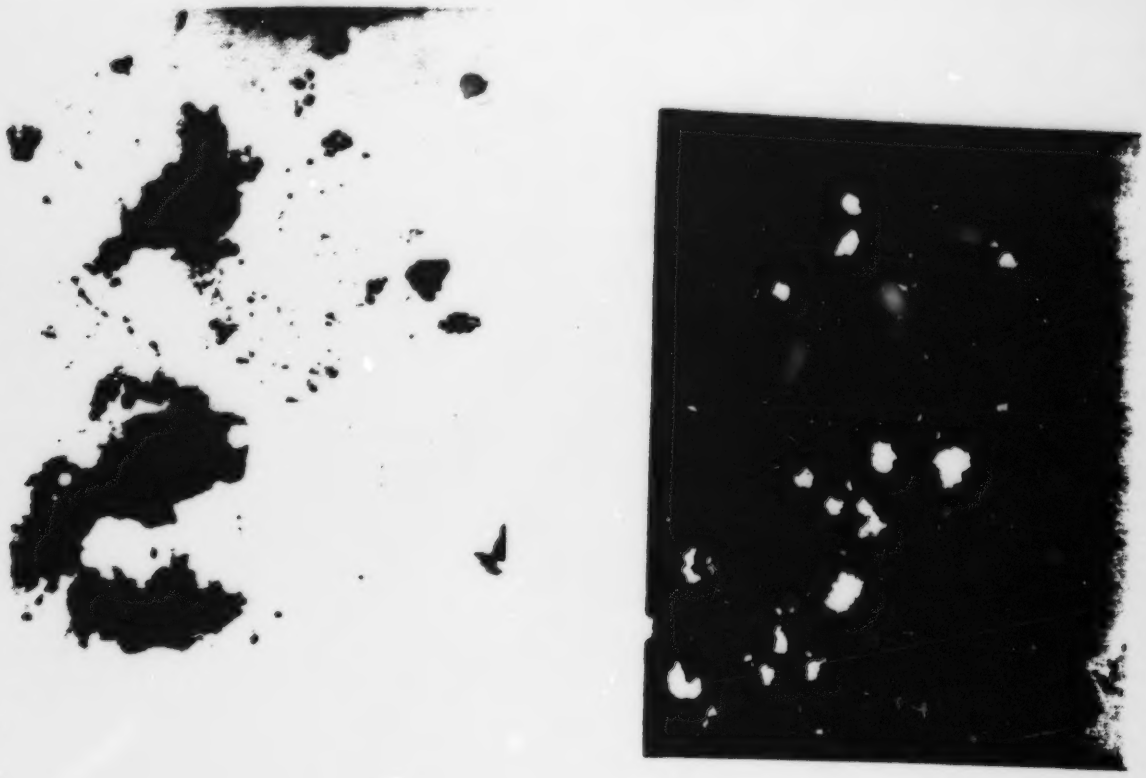

Figure 6.7

Photomicrograph No.:	KK-5 (left) and KK-6 (right)
Sample No:	Quirke Lake #1
Laboratory No.:	WS-5
Exposure:	37 days
Magnification:	Ocular 10x; Objective 53x(oil)

Photomicrograph KK-5 (left) is focused on a small clear to pale yellow crystalline platelet and its associated alpha activity. Photomicrograph KK-6 (right) shows the same field under crossed polaroids and the birefrigence of the platelet. In addition, photomicrograph KK-6 also shows the birefringence of many of the small quartz and fieldspar fragments which are included in the larger aggregate of brown particles on either side of the alpha-active platelet.

Compared to the alpha activity of the two euhedral crystals in photomicrograph KK-8, the alpha activity of the platelet is low but clearly higher than the much larger aggregates of brown particles. Although the single long track suggests the decay of a Po-214 atom, the remaining alpha tracks do not appear either to have a common vertex or to be associated with the sequential decay of a single atom of Ra-226. A possible explanation of the observed alpha activity of this platelet is that the activity is a consequence of the sequential decay of several Ra-226 atoms of which only 5 alpha tracks were recorded, the remaining alpha particles having trajectories in the hemisphere above the emulsion.

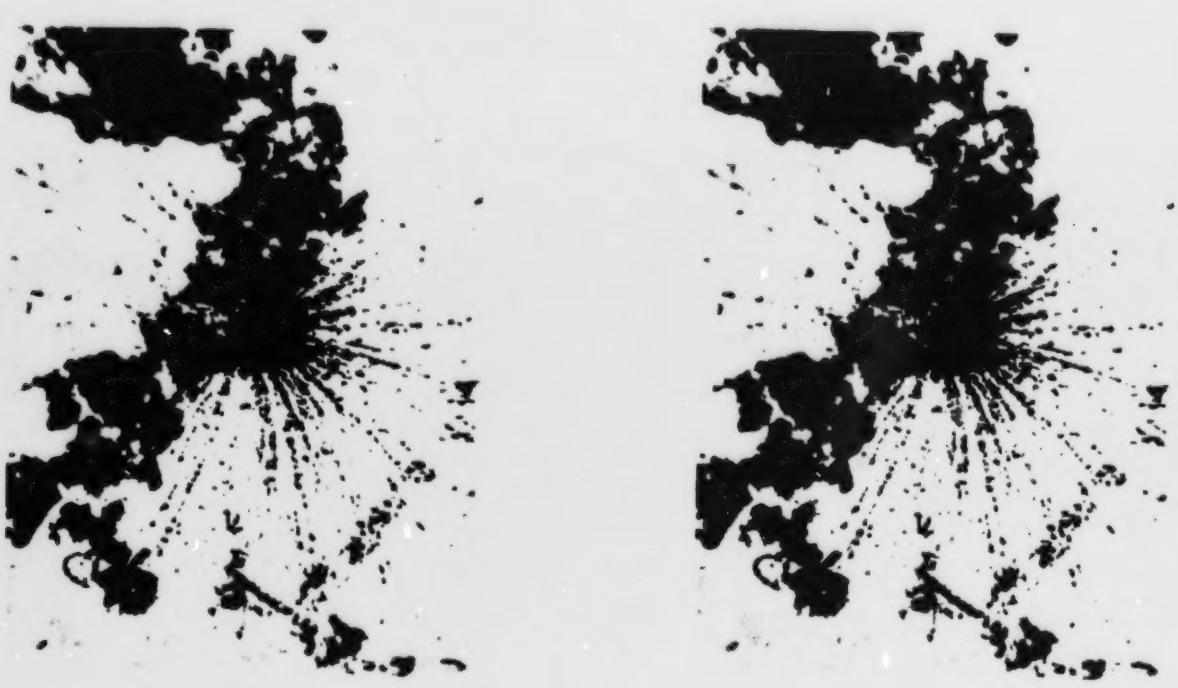

Figure 6.8

Photomicrograph No.:	JJ-8 (left) and KK-1 (right)
Sample No:	Quirke Lake #1
Laboratory No.:	WS-5
Exposure:	37 days
Magnification:	Ocular 10x; Objective 53x(oil)

Photomicrograph JJ-8 (left) is focused on the intense alpha activity associated with a small, rounded, brown to grayish particle. Photomicrograph KK1 (right) is focused on the source particle. Details of the source particle are difficult to see because the density of the alpha tracks in the source area prevents observing the particle in transmitted light. Both the track lengths and the specific alpha activity of the source suggest the particle contains Ra-226 and/or Ra-228.

Figure 6.9

Photomicrograph No.: KK-2
Sample No: Quirke Lake #1
Laboratory No.: WS-5
Exposure: 37 days
Magnification: Ocular 10x; Objective 53x(oil)

Photomicrograph of a small to very small, intensely alpha-active particle. On the basis of the area defined by the convergence of the alpha-tracks, this particle is smaller than the alpha active particle in photomicrograph KK-1. The density of the alpha tracks precludes observation of the source particle in transmitted light. Both the track lengths and the high specific activity suggest the presence of Rn-226 and/or Ra-228 and their alpha-emitting daughter products.

7.0 EXPERIMENTAL FIELD MEASUREMENT OF RADIUM TRANSPORT BETWEEN SEDIMENT AND WATER

In this chapter, movement of radium and barium between sediments and water were experimentally measured under controlled conditions in a shallow Shield lake. The results from these measurements and the prior data for Quirke Lake are interpreted and generalized in Section 8 using modelling techniques.

7.1. Background

There is considerable evidence that the loss of nuclide activity from water to sediments is an important term in nuclide mass balances in fresh waters. The transport rates, mechanisms of nuclide transport, and significance of diffusion of radionuclides back from sediments to water are unclear. It is also unclear how useful the behaviour of barium is, as an analog for radium. In the experiments described below, Ra-226 and Ba-133 transport between waters and sediments were determined in enclosures (limnocorrals) in a shield lake. These measurements provide information on the potential remobilization of radionuclides from sediments in lakes following the cessation of aqueous inputs from uranium mining and milling.

7.2 Methods

Ra-226 and Ba-133 were added to six columns of Perch Lake water and sediments isolated in limnocorrals. Perch Lake is a small, shallow (mean depth 2 m) dystrophic lake located on the property of Chalk River Nuclear Laboratories. Six limnocorrals containing Perch Lake water were used in the experiments: two contained Perch Lake water only (i.e., controls), two received an addition of humic matter and two limnocorrals received additional particulate organic matter collected from the lake bottom.

The limnocorrals (or "bags") were constructed from 6 mil polyethylene tubing 0.78 m in diameter. To the bottom of each was attached a stainless steel cylinder open on both ends (41 cm high by 76 cm dia, 0.16 cm steel). The tubing was inserted through the cylinder and drawn up around the outside of the cylinder and held in place with waterproof tape.

Two flexible pvc hoops were used for each bag, one for support and the other attached to the supporting raft. The middle hoop was taped to the outside of the bag about halfway between the sediments and the surface, to keep the bag from collapsing. The top of the bag was attached to a floating "raft" or wooden support securely anchored inside a log boom.

The bags were installed from the surface by carefully lowering through the support raft the bag with bottom cylinder and support hoop attached. The bottom cylinder was allowed to passively sink into the soft sediments (about 0.3 m), and the bag was drawn inside and over the top hoop, which was then screwed (approximately 0.20 m above the lake surface) to the raft. Lake water was added to the bags until the walls were reasonably taut. To minimize the effects of corral installation on subsequent experiments the corrals were installed 1 day before any experiment started.

Radioactive isotopes were used in these experiments since they were easily measured in trace quantities, did not alter the concentrations of stable elements, and provided a well defined initial source term. About 3 MBq of each isotope dissolved in 1 L of distilled water were injected as a soluble inorganic salt into the water at the start of the experiment. Nuclides used in the experiments include: Na-22, Mn-54, Co-57, Fe-59, Ni-63, Zn-65, As-74, Se-75, Te-99, Sn-113, I-125, I-131, Ba-133, Cs-134, Ce-141, Hg-203, Pb-210, Ra-226, Th-232, U-238 and Am-241. The nuclides were injected into the bags using positive pressure through a tygon base equipped with a T-junction at the bottom. The tubing was raised and lowered through the water column continuously during injection to ensure complete mixing. Radionuclides evaluated as a part of this project were Ba-133 and Ra-226.

Sampling the water started the day after injection, and continued every second day for 2-3 weeks. Composite water samples were collected by reversing the injection procedure; raising and lowering the tubing while drawing water under a vacuum. Duplicate 4 litre samples were taken from each bag each sampling day. Duplicate subsamples of the water were taken and filtered through 0.4 um nucleopore polycarbonate filters to measure the particulate content. The filters were dried in a dessicator and weighed.

A cylindrical sediment trap (height:diameter ratio = 5:1; Bloesch and Burns, 1980) was suspended about 0.5 m above the bottom in each bag to measure particulate fluxes. Traps also were installed at the same depth in the lake (suspended from the raft) to monitor fluxes outside the corrals. On each sampling day the sediment trap contents were collected and filtered through pre-weighed glass-bire filters (Gelman, type AE, 0.45 pm). The filters were dried, weighed and the activity of each isotope measured.

In each experiment, plastic strips made from the same material as the limnocorral walls were cut (2.5 cm x 2 m), weighted with lead weights, and suspended along the inside walls in a control bag to measure uptake of the radionclides by the plastic. On each sampling day, 2 strips were removed, rinsed with lake water, and placed in a 500 ml polyethylene bottle containing 50% aqua regia. After allowing the radionuclides to desorb into the solution, the contents of the bottle were analyzed to measure nuclide activity.

On June 5, 1986, 0.1 mCi of Ba-133 and 0.02 to 0.1 mCi of Ra-226 were added to the six experimental systems. The concentration of activity in the water, on the plastic, in sediment traps, and on the particulate phase were measured 24 hours after injection and subsequently every second day for approximately 3 weeks. At the end of this period any residual nuclide activity in the water was washed out of the limnocorrals by diluting it into the much larger lake volume. At this point all of the Ra-226 and Ba-133 activity was in the sediments, and radionuclide free water was overlying the sediments. New plastic was placed for the limnocorral and the limnocorral was resealed into the sediment. After the limnocorral was sealed, two 4.5L of water were collected a few times each week over a six week period and the radionuclides concentration measured in each sample. This provides an estimate of the significance of back difussion of Ba-133 and Ra-226 from the sediments to the water.

Water samples were counted in fixed geometry on a Ge(Li) detector coupled to a 4,096 channel analyser to determine the activity of the isotopes by gamma ray spectroscopy. Because the activity of the Ra-226 supplied for the experiments was significantly less than originally anticipated (1mCi), the counting statistics for Ra-226 using gamma spectroscopy were poor. Therefore, the activity of Ra-226 was also determined by liquid scintillation counting. Water samples were first run through an ion exchange column, then sealed in a glass vial with a suitable solvent, and left for 21 days. Following the ingrowth of Rn-222 and its daughters, the samples were counted in a Beckman LS 235

liquid scintillation system. Since this is a very time consuming process, the analyses of Ra-226 activity extended over a large period of time. The activity of Ba-133 was analysed in all experimental systems using gamma spectroscopy.

The activity of Ba-133 was analyzed simultaneously by gamma spectroscopy using a Germanium or a Germanium-Lithium drifted crystal detector. Impulses were analyzed on a Canberra Series 40 multichannel analyzer. Water samples were gamma counted in 1.4 L Marinelli beakers to optimize counting efficiency. Filters were counted intact and plastic strips counted in a 500 mL bottle. The counters were calibrated for all geometries using sources prepared in an identical manner to the samples.

7.3 Results

Concentrations of all tracers added to the enclosures decreased following their addition to the water. The behaviour of all radiotracers usually was bracketed by observations of Fe-59 and Na-22. During the first approximately 14 days the nuclide activity decreased exponentially from the water column. Loss rates of all nuclides studied ranged from 2% to 12% per day, very similar to the rates of loss (3% to 8% day^{-1}) measured by Santschi et al. (1986) and Schindler et al. (1980) in enclosure experiments at ELA. Later in the experiment, the loss rates decreased. Similar observations were reported by Nyffler et al. (1986) and Santschi et al. (1986). Changes in concentration of stable element analogs were much smaller and the stable Fe concentration increased slightly during the experiments (Chant and Cornett, 1987).

A series of experiments were performed in 1985 and 1986 to assess the reproducibility of the measured loss rates (Chant and Cornett, 1987). Variability between duplicate water samples collected simultaneously was low (average coefficient of variation approximately 2.7%). Loss rates measured in duplicate experiments run at the same time were also similar. Differences in loss rates between June and July were significantly larger (up to 8% d^{-1}) and may reflect different particle fluxes and/or turbulent mixing within the limnocorrals.

Ra-226 and Ba-133 concentrations measured in the water decreased in all experiments (Figure 7.1). The decrease was loglinear for approximately 2 weeks. After that period the rate of isotope transport from water to sediments may have decreased. Since the

FIGURE 7.1

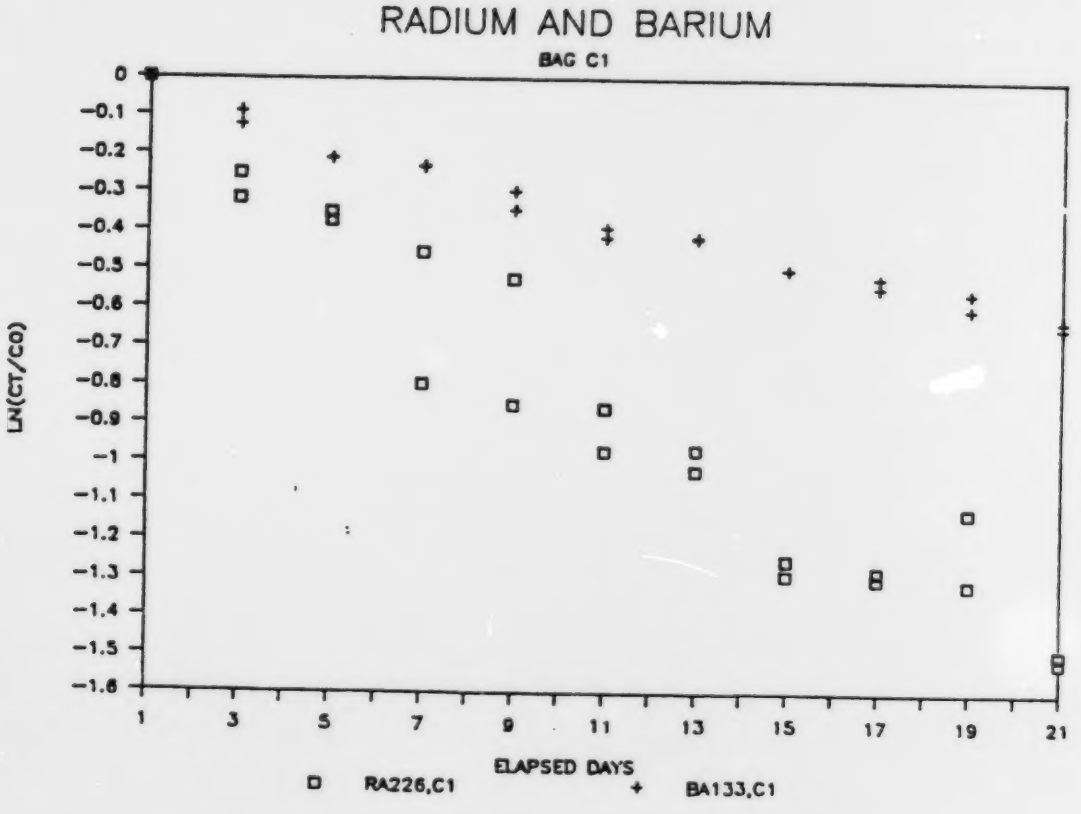

LOSS RATES OF RADIUM-226 AND BARIUM-133 IN LIMNOCORRALS

count statistics from the gamma spectrometry analyses of Ra-226 were poor, Ra-226 was also analysed by measuring the concentration of Rn-222 in secular equilibrium with the Ra parent. Figure 7.2 shows that the results of both analyses agree very closely. However, there are some discrepancies at lower count rates and we are currently investigating this discrepancy. It is possible that the slight low bias in Rn-222 count rates is caused by leakage of Rn-222 from the vials. The concentration of isotopes measured in the two control systems agreed very closely (Figure 7.3). The first order rate constant for water to sediment transport was calculated by least-squares regression (Table 7.1). Over the 19 day period of the experiments, Ra-226 was transported from water to sediments at rates of 5-9%/day. Ra-226 was transported 2 - 3 times more rapidly than Ba-133 (Table 7.1, Figure 7.1). These results are interpreted as suggesting that barium is not a good analog for radium in freshwater systems.

The transport of Ba-133 from the sediments into the water was measured in all bags while the return of Ra-226 from sediments were measured only in two bags (one control; one humic material treatment). Figure 7.4 illustrates that Ba-133 is desorbed from the sediments and transported into the overlying water. Ra-226 is similarly transported (Figure 7.5), however, the desorption rate of Ra-226 from the sediments is slower than that for Ba-133 and plateaus more rapidly. This is consistent with the hypothesis that Ba-133 and Ra-226 act differently.

In comparing the effect of humic acids and particulate materials (Table 7.1), it is obvious that the humic substances did not measurably affect the transport of Ra-226 or Ba-133 (the loss rates for these two treatments are essentially the same as the control bags) despite more than doubling the humic acid content in the humic acid treatments. Accordingly, complexation reactions with the humic substances and Ra-226 or Ba-133 would appear to be minimal. This phenomenon was not uniformly observed because certain radiocations applied to the humic treatment showed a measurable decrease in loss rates.

Doubling particulate concentrations approximately doubled the removal rates for both Radium-226 and Ba-133. This shows that particulate movement by settling processes is also, therefore, a significant method for removal of radiocations from the water column. This perturbation must, however, be viewed with some circumspection because the suspended solids concentration in the "Particulate" treatment was maintained by

FIGURE 7.2

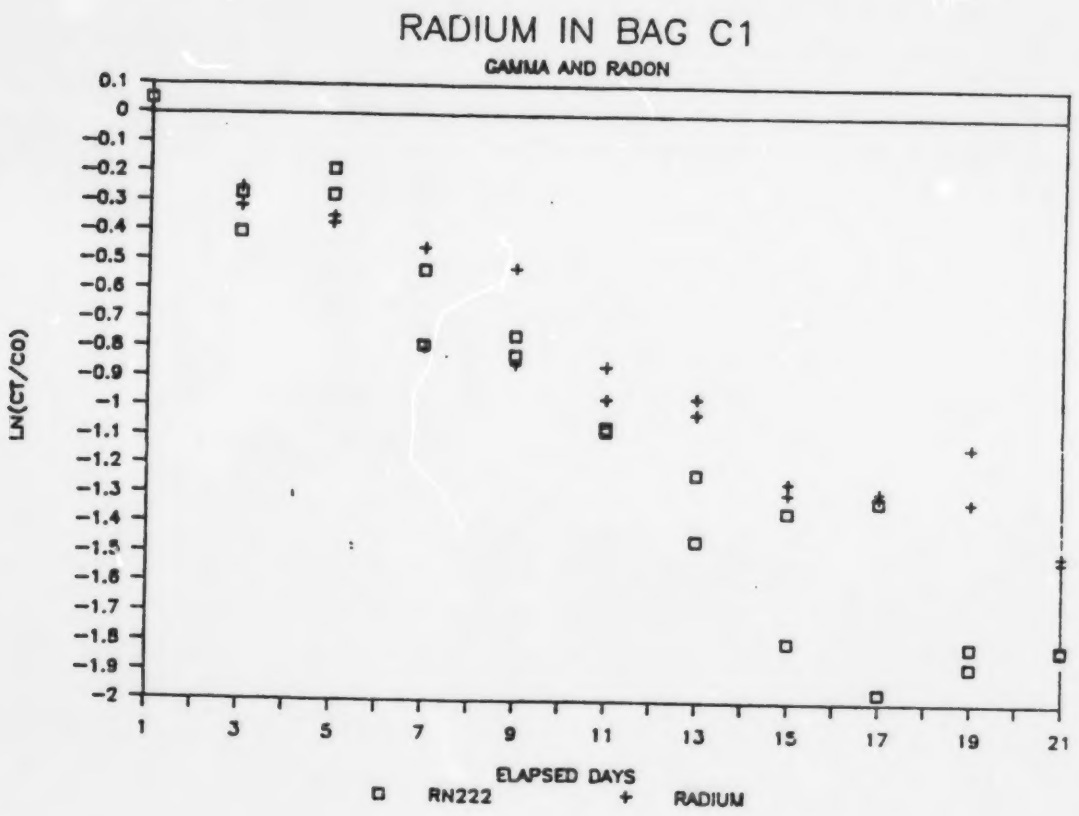

COMPARISON OF Ra-226 FLOXES USING GAMMA SPECTROSCOPY AND RADON-222 COUNTING

FIGURE 7.3

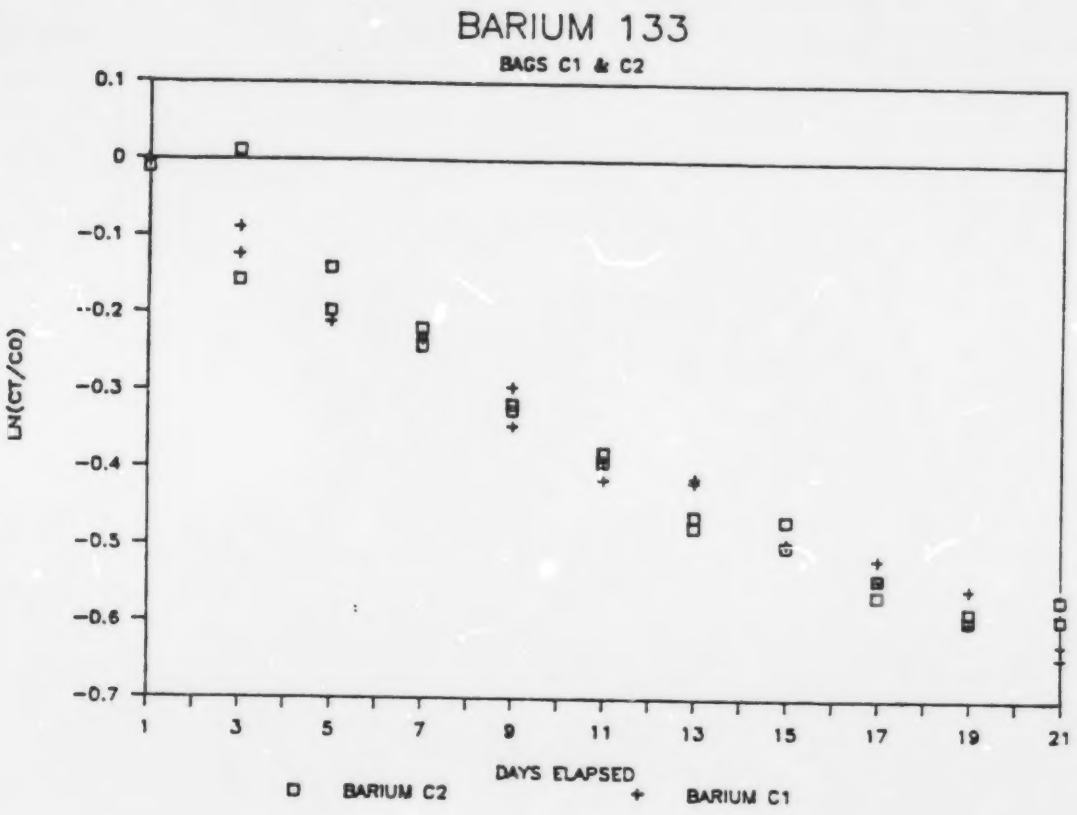

COMPARISON OF LOSS RATES OF BARIUM-133 IN TWO CONTROL BAGS

TABLE 7.1: LOSS RATES FROM LIMNOCORRALS (PLUS OR MINUS/STANDARD DEVIATION)

Description of Corral	Number	Loss Rate (%/day) Ra-226	Ba-133
Control	1	7.1 ± 0.5	3.53
	2	5.6 ± 0.7	3.57
Humic Treatment	1	6.6 ± 0.4	3.53
	2	5.2 ± 0.5	3.1
Particulate Matter Treatment	1	13.7 ± 0.4	6.53
	2	13.5 ± 0.5	5.07

Other Chemical Parameters for the Different Treatments

Limnocorral	Number	Suspended Solids Concentration (mg/L)	Humic Acid Concentration (mg/L TOC)	Water Column Kd(ml/g)
Control	1	2.8	10	430,000
	2	1.5	10	-
Humic Treatment	1	7.9	27	36,000
	2	7.1	26	160,000
Particulate Treatment	1	6.5	10	200,000
	2	7.5	10	170,000

FIGURE . 7.4

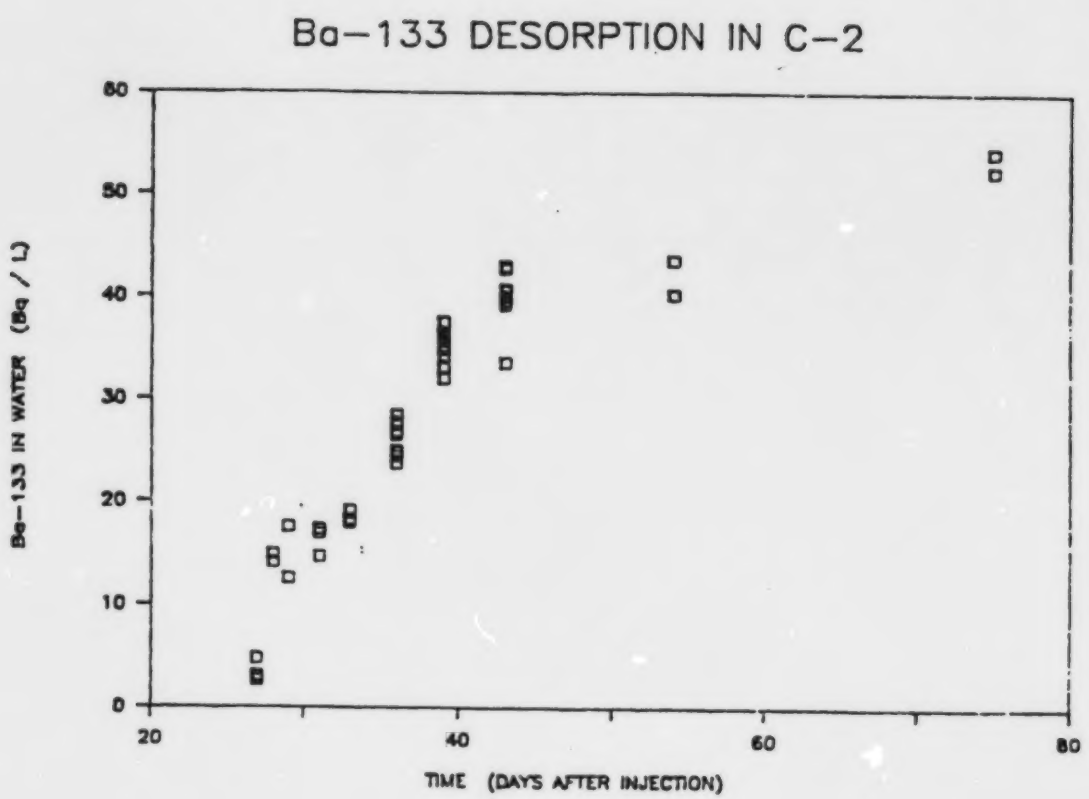
Ba-133 DESORPTION IN C-2
Ba-133 IN WATER (Bq / L)
0
10
20
30
40
50
60
20
40
60
80
TIME (DAYS AFTER INJECTION)

Fig. 7.5 Desorption Rate Data

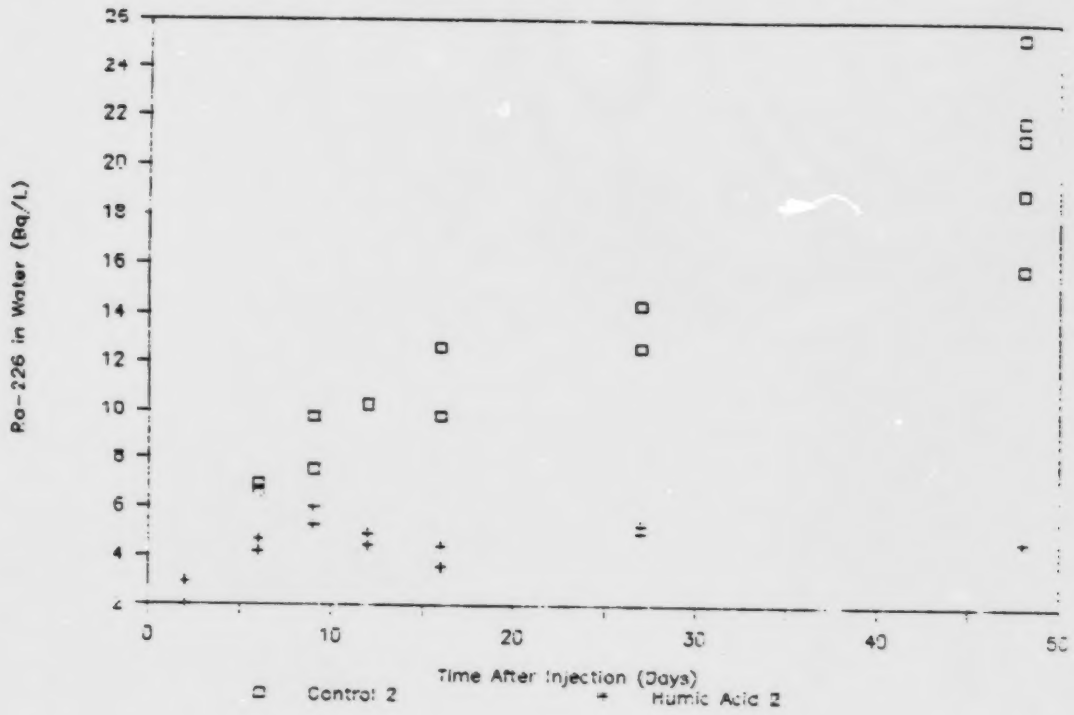

periodic addition of the suspended solids (illite clay) to maintain elevated levels. Accordingly, the net removal reactions would involve a complex series of additional adsorption reactions of the radiocations onto the added particles. Due to the probable rapid sorption kinetics of Ra-226 and Ba-133 (e.g. 100 gm $ml^{-1}d^{-1}$), these additional reactions should not substantially affect the removal ratio estimates. If, sorption kinetics were important, the observed loss rate due to settling would be lower than the actual loss rates.

The observed K_D values and the percent of the radionuclide which was particulate is given in Table 7.1. The K_D values vary by about an order of magnitude.

Throughout the experiments, particulate material (less than 0.40 um) was collected in sediment traps and analyzed to determine the fluxes of particles and nuclides from the water column. Duplicate sediment traps were also deployed in the lake to test the hypothesis that seston fluxes in the lake and in the enclosures were equal. Traps in the lake were suspended from the limnocorral frame immediately adjacent to the enclosures. The average particulate flux inside the enclosures (0.53 ± .17 g dry weight $m^{-2}d^{-1}$) was only 40% of the flux measured in the lake, (2.2 ± 1.2 g dry weight $m^{-2}d^{-1}$) (Figure 7.6). A second difference between enclosure and lake particulate fluxes was the significantly larger variance in lake-trap catch (Figure 7.6). The daily particulate flux in the lake sediment traps was correlated with the maximum wind speed measured during the same period at a meteorology tower located about 50 m from the lake shore (R^2-0.50, p less than 0.01) while the flux within the enclosures was not correlated with wind speed. Trap catch variance between dates was significantly larger than the within-day variance measured in duplicate traps (p less than 0.01).

The observed settling fluxes caught in the traps for Ra-226 are given in Figure 7.7 (7.7a: the controls; 7.7b: the humic treatment; 7.7c: the particulate treatment). The difference between corrected and uncorrected as an estimate of the radioisotope activity associated with the solution phase in the centrifuged particulate matter contained at the bottom of a centrifuge tube. The rates show a general decrease in flux rate over time, consistent with that of the water column data. This reflects the K_D values inferred from the radium-226 distribution between water and sediments (summarized in Table 7.1) being consistent over time.

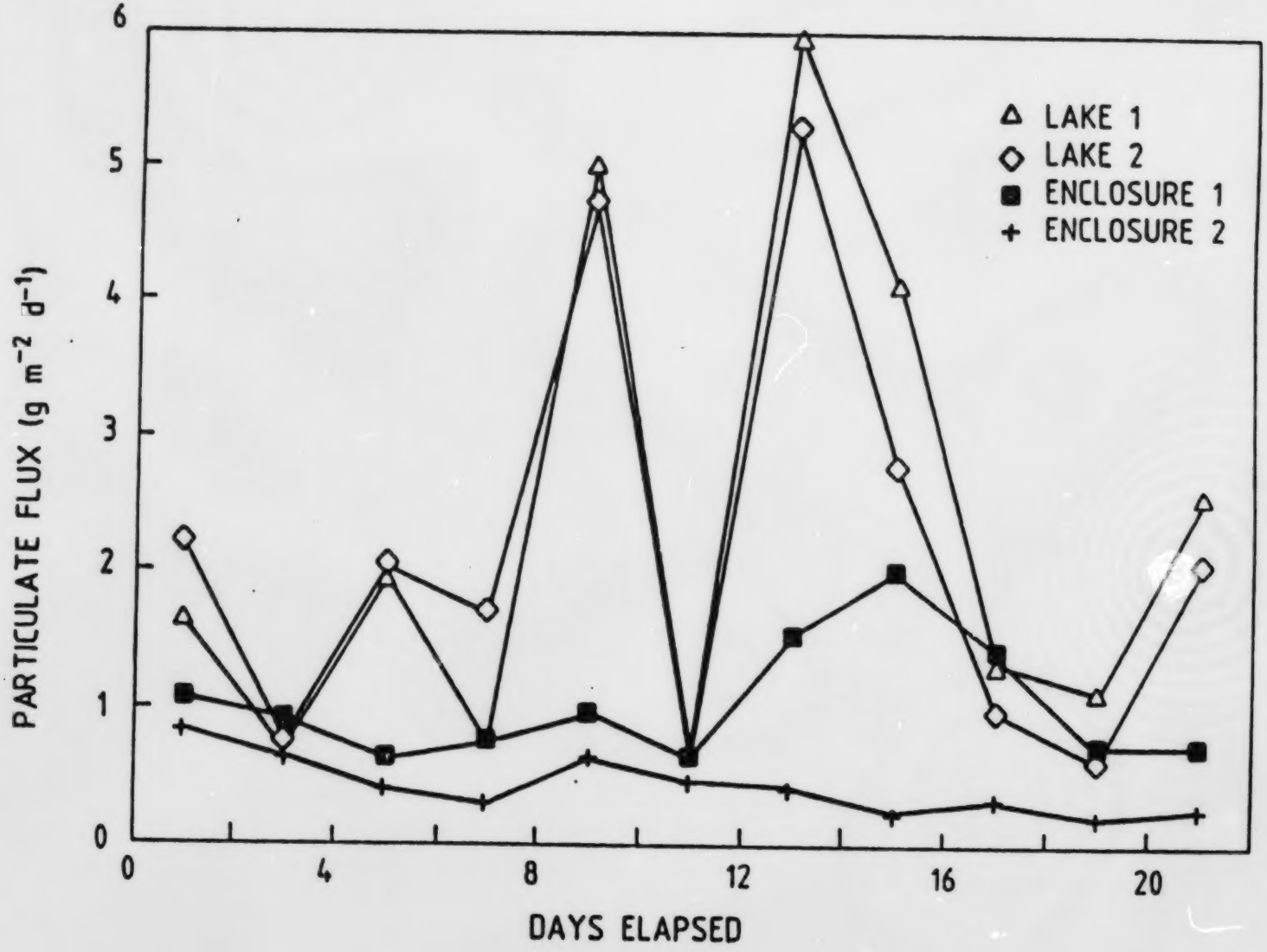

FIGURE 7.6: VARIATION OF PARTICULATE FLUX IN CONTROLS (1-2) AND IN PERCH LAKE

FIGURE 7.7a: SETTLING RATE OF Ra-226 IN CONTROL

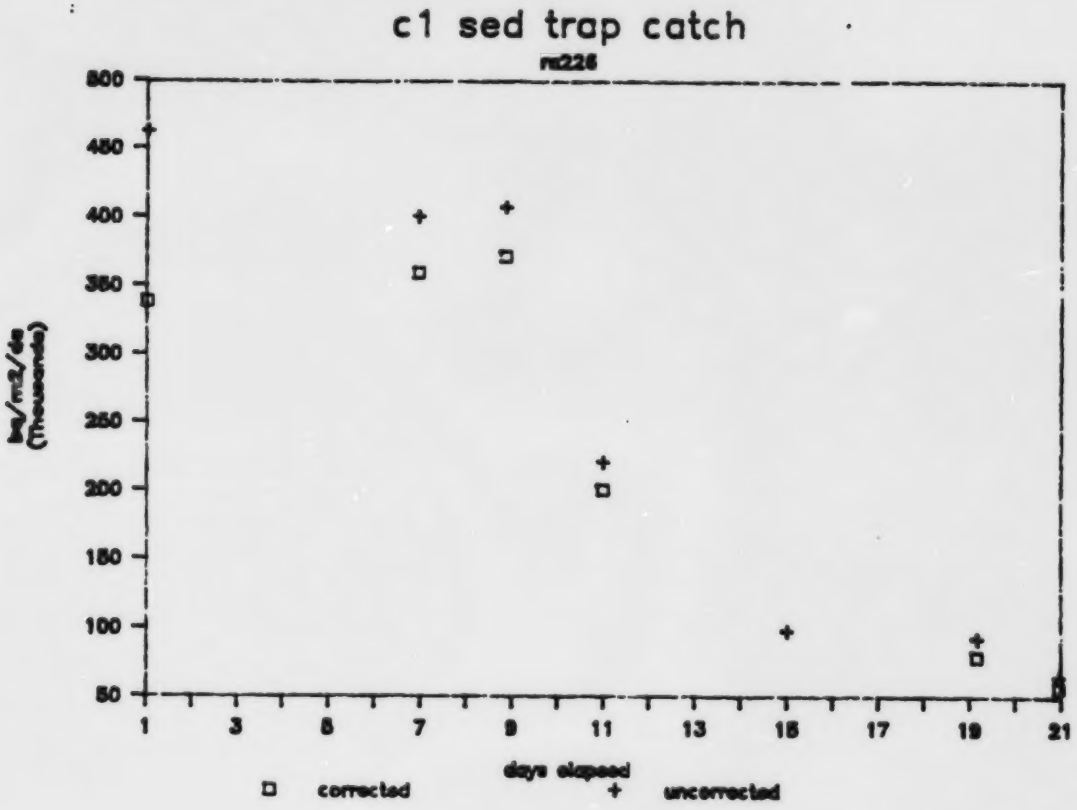

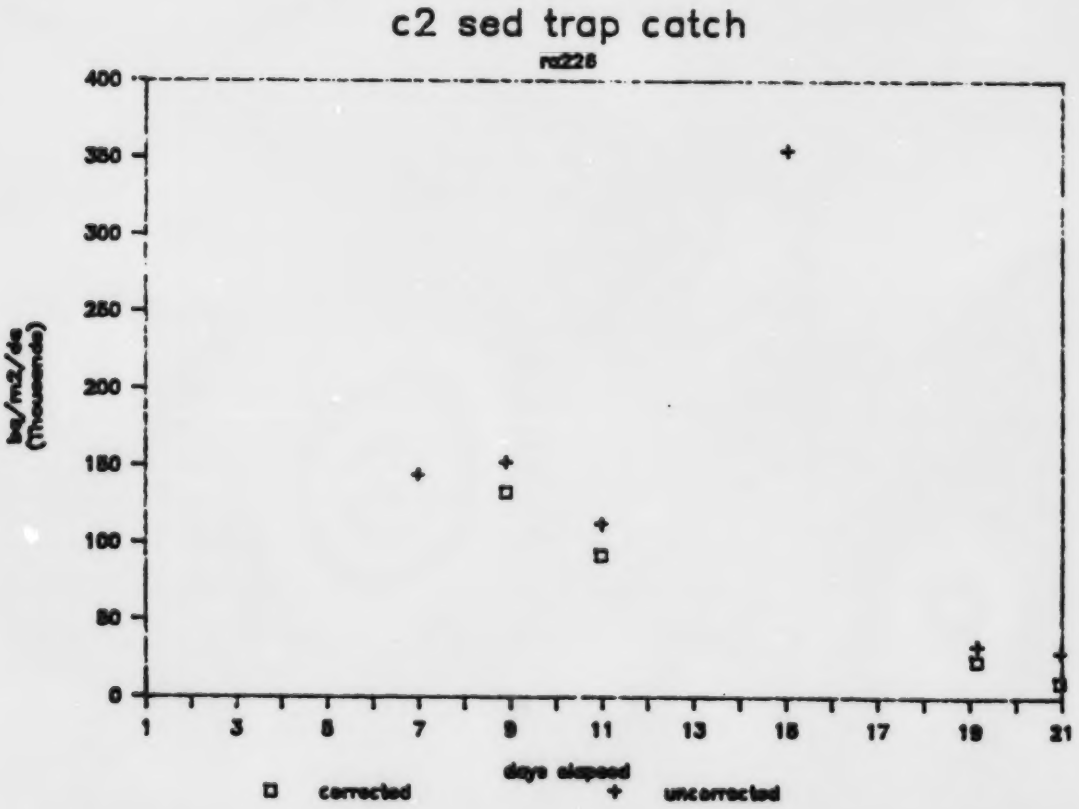

FIGURE 7.7b: SETTLING RATE OF Ra-226 IN HUMIC ACID LIMNOCORRALS

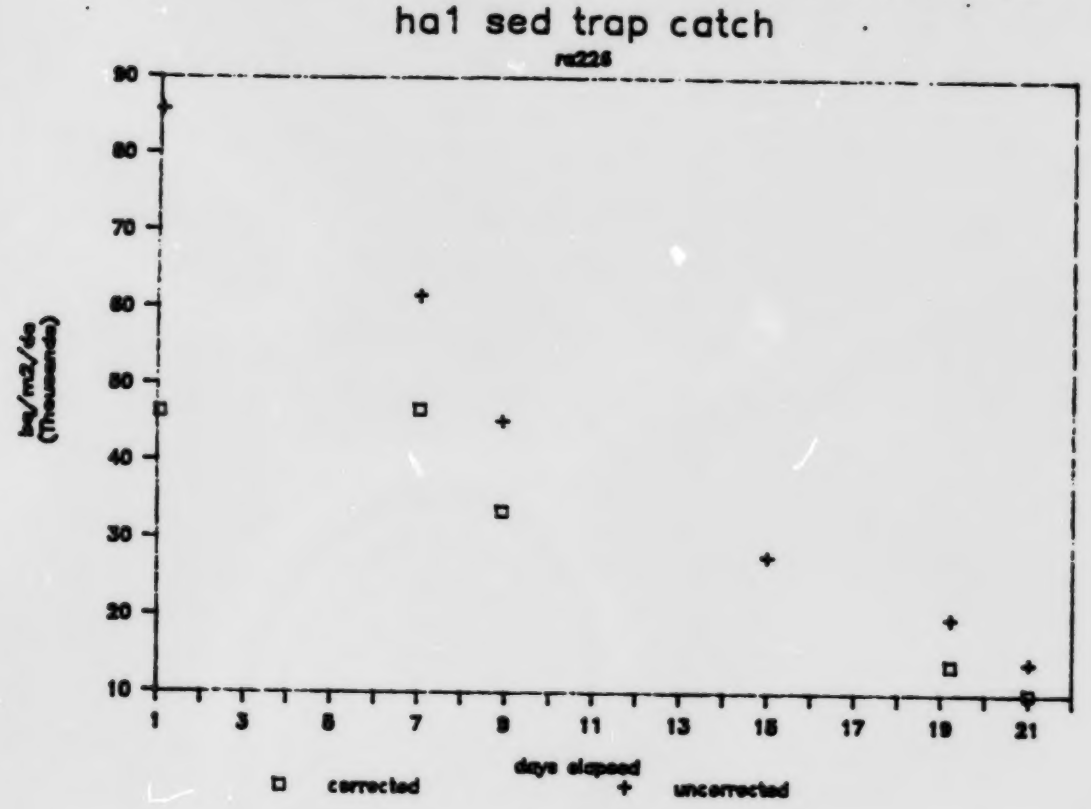

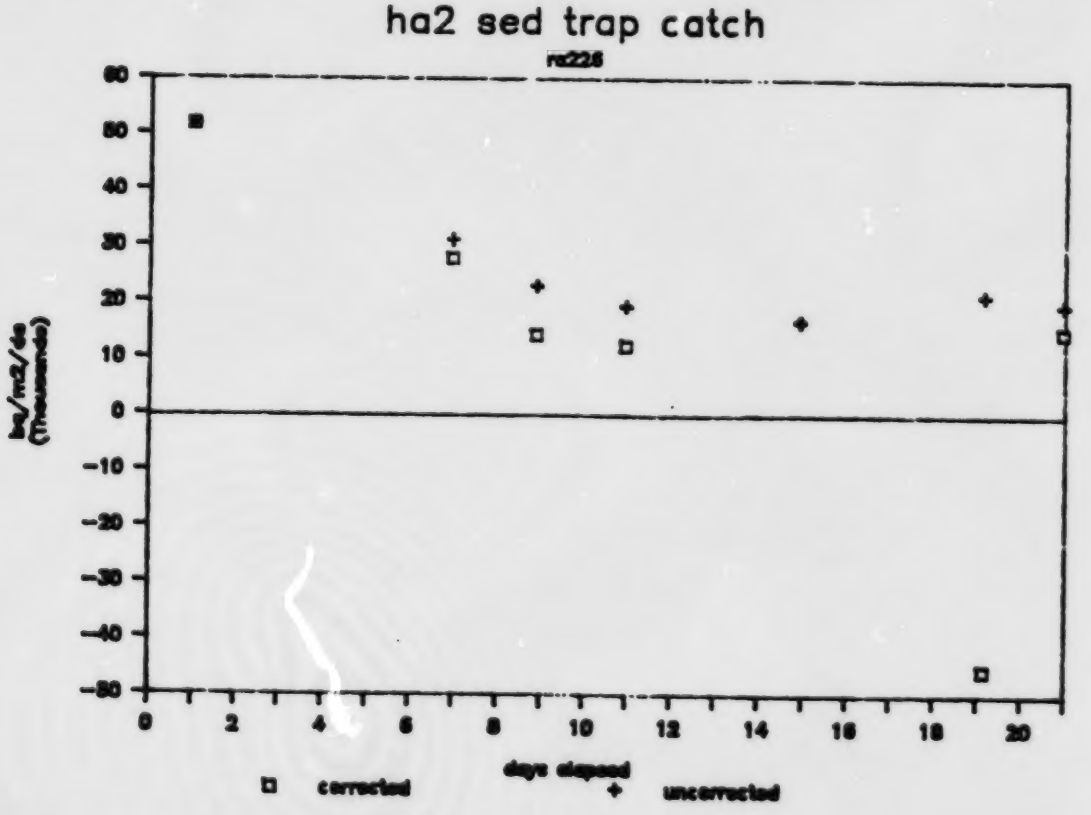

FIGURE 7.7c: SETTLING RATE OF Ra-226 IN SEDIMENT-SPIKED LIMNOCORRALS

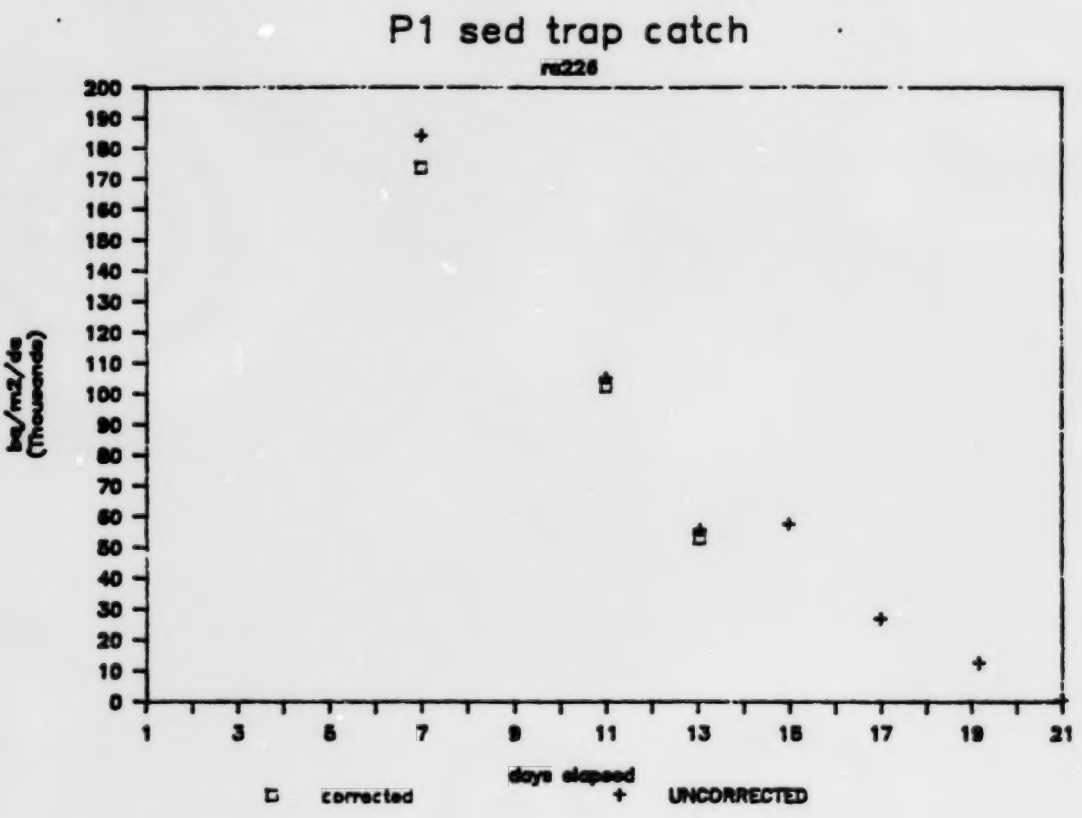

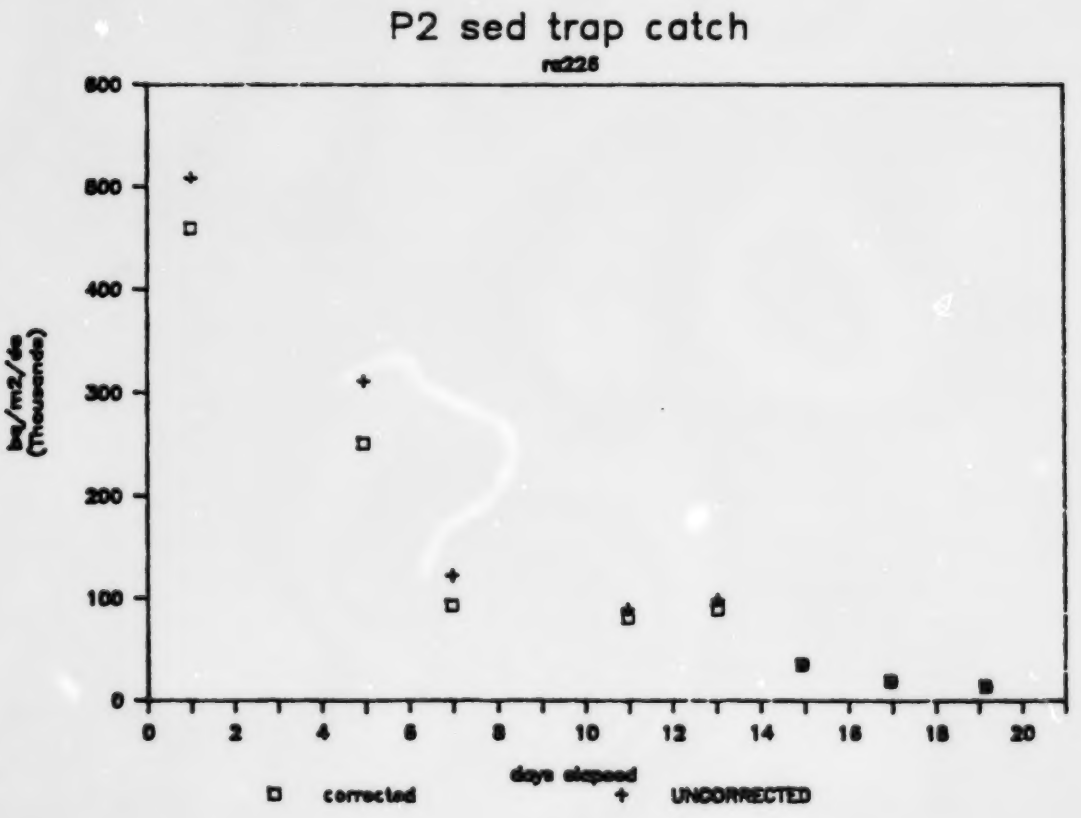

7.5 Relative Importance of Settling and Diffusion

The initial estimates of settling flux (during the first four days of the experiment were compared to the observed removal rate (see Table 7.2). Within the limits of the variance of the estimates of settling flux, the settling rate can explain the observed removal rate.

Diffusion from water into the bottom sediments cannot be measured directly in the limnocorrals; however, estimates of the probable magnitude can be made (Snodgrass, 1986). If the molecular diffusion coefficient for radium-226 (ca 1×10^{-5} m^2/d) is divided by an estimate of the thickness of the laminar sublayer (200 um; Santschi et al, 1984), the mass transfer coefficient (k_s), see Table 7.2, has a value of 0.05 m/d. Such a value can be used to calculate removal due to diffusional processes and the diffusional effect compared to the observed removal rate. This comparison is also presented in Table 7.2 for two different values of the mass transfer coefficient: 0.05 and 1.0 m/d. Provided these are reasonable estimates of the mass transfer coefficient, diffusion can also explain the order of 50-100% of the observed removal rate in the controls and in the humic acid treatment. However, a smaller fraction of removal can be explained by diffusional processes in the particulate treatment. Assuming that similar diffusional processes occur in all six limnocorrals, then diffusional processes are approximately 50% less in the particulate treatment than in the control or in the humic acid treatment.

These calculations, however, may be used to determine the relative magnitude of diffusional and settling processes. Because back-diffusion (sediment desorption in Figure 7.4, 7.5) is lower than the adsorption process (Figure 7.1-7.3), it is plausible that settling may be the dominant mode of transport of Ra to the sediment. Modelling procedures are required to evaluate the probable difference. These procedures are used in the next section to assess the relative importance of settling and diffusion.

7.6 Other Sources of Error in the Limnocorral Experiments

Additions of several non-particle reactive tracers were made to the limnocorrals to measure their volumes and to monitor for leakage. Fluoride (NaF) and bromide (KBr), rhodamine dye (Rh-WT), Na-22 and humic acids were used in different experiments. The results of these additions are detailed by Cornett and Chant (1987); their discussion is extracted herein for completeness. Concentrations of all these tracers decreased during

TABLE 7.2: COMPARISON OF LOSS RATES TO SETTING AND CALCULATED DIFFUSION

Limnocorral	Observed Removal Rate at t = O $Bq/m^2/day$	Ratio of Settling to Observed Rate at Time Zero	Ratio of Calculated Diffusional Flux to Observed Rate at Time Zero	
			$k_s = .05$	$k_s = 0.1$
Control 1	440,000	0.8	.4	0.7
Control 2	130,000	1.2	.4	0.9
Humic 1	160,000	0.4	.4	0.8
Humic 2	350,000	1.0	.5	1.0
Particulate 1	100,000	1.0	.2	0.4
Particulate 2	50,000	1.3	.2	0.4

the experiments (Figure 7.8a from Cornett & Chant, 1987). Initial loss rates of F^- and Br^- (6% d^{-1}) and rhodamine (4% d^{-1}) were much more rapid than loss rates of Na-22 (1.0-1.8% d^{-1}) and humic acids (0.6% d^{-1}). These losses could indicate slow leaks. However, the loss rates were very consistent in replicate experiments and Na-22, Br, F and humic acid concentrations reached equilibria after rapid initial losses. Since these tracers were not volatile, nor taken up by the plastic or measured on suspended seston or in sediment traps, the loss is interpreted to result from diffusion from the water into the sediments and sorption onto the matrix. Rhodamine concentrations decrease throughout the experiments. Since this tracer could not be used to monitor the integrity of the enclosures we did not analyze its behaviour further. Rhodamine may have disappeared from the water by photochemical oxidation, sorption onto plastic, or particles or bottom sediments. In two cases, Na-22 concentrations changed abruptly. We interpreted these events to indicate that the bottom of a limnocorral lifted out of the sediments during storms and settled in again, resealing the system. The resulting sudden leakage, dilution and subsequent resealing was evident from the sudden change in Na-22 concentration (Figure 7.8b, Cornett & Chant, 1987). Subsequent concentrations measured in the bag were corrected for the dilution in tracer concentration.

All nuclides except Na-22 were measured on the plastic enclosure walls. After 21 days tracer accumulation on the walls ranged from 0% (Na-22) to 6% (Sn-113) of the initial amount of tracer added (Figure 7.9; Chant & Cornett, 1987). This was not a large amount of activity relative to the loss to the sediments. The uptake of the radioisotopes by the plastic was gradual during the first 14 days, then increased rapidly and was accompanied by accelerated epiphytic growth on the bag walls (Figure 7.9). Activities of Ra, Sn, and Fe on the bag walls and epiphytes after 21 days were less than 20% of the activity left in the water. This was significant when compared to the amount left in the water column. However these isotopes were not irreversibly attached to the enclosure walls. When pieces of labelled plastic were placed in unlabelled lake water, the tracers rapidly reappeared in the solution (unpublished data). The only large change in sediment trap flux within the enclosure occurred in enclosure 1 shortly after this system was disturbed and leaked (Figure 7.8b). Since this change in particle flux did not occur in the replicate limnocorral the altered flux probably was induced by disturbance of the enclosure. During the experiments, Perch Lake was not thermally stratified at the enclosure site. In other concurrent studies in Perch Lake (Risto et al., 1987) resuspension of bottom sediment and associated contaminants were the dominant terms in the mass

FIGURE 7.8a: BEHAVIOUR OF NON-PARTICULATE REACTIVE TRACERS (AFTER CORNETT AND CHANT, 1987)

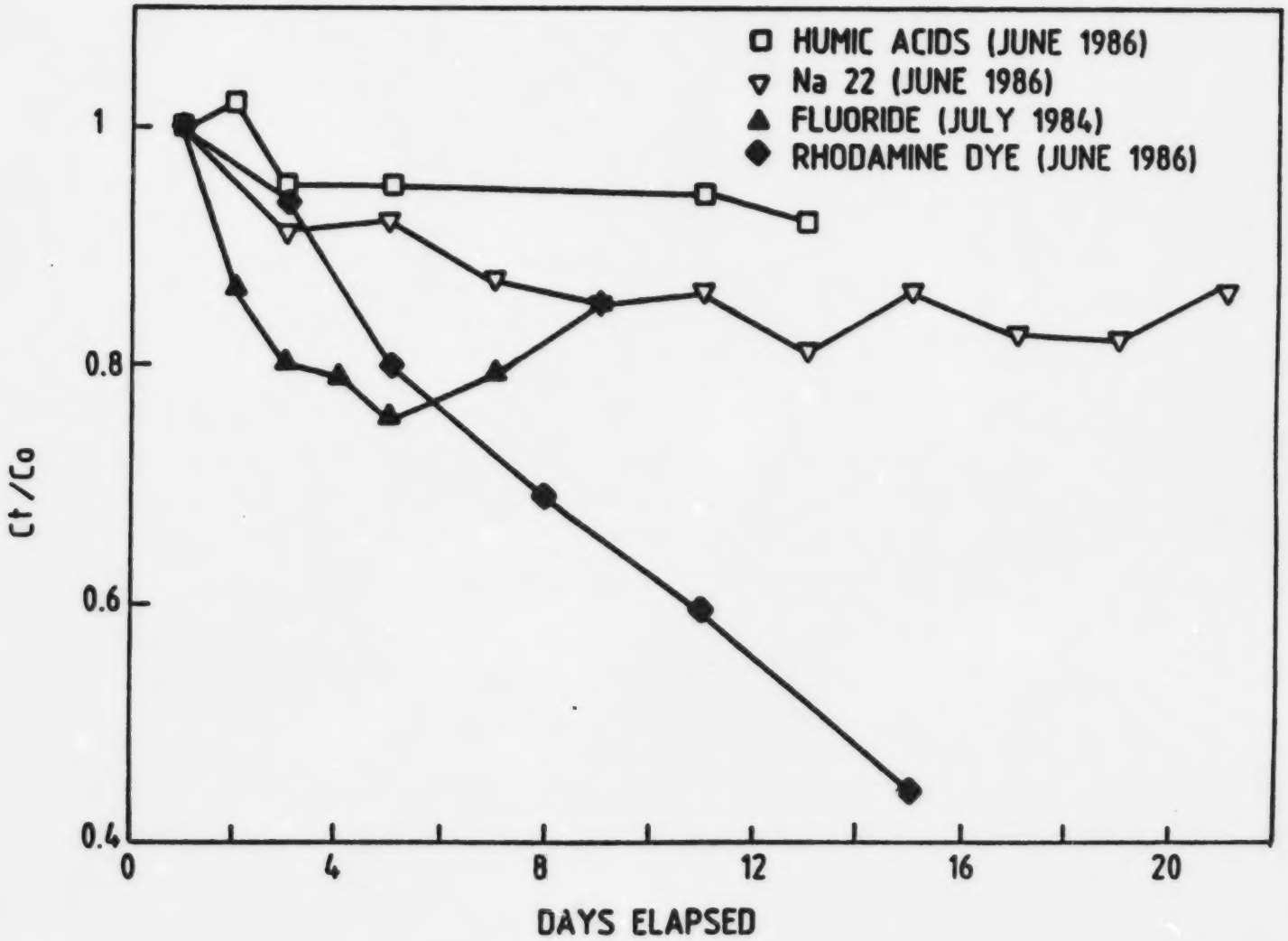

FIGURE 7.8b: LOSS OF Na-22 FROM A LIMNOCORRAL DURING A STORM EVENT

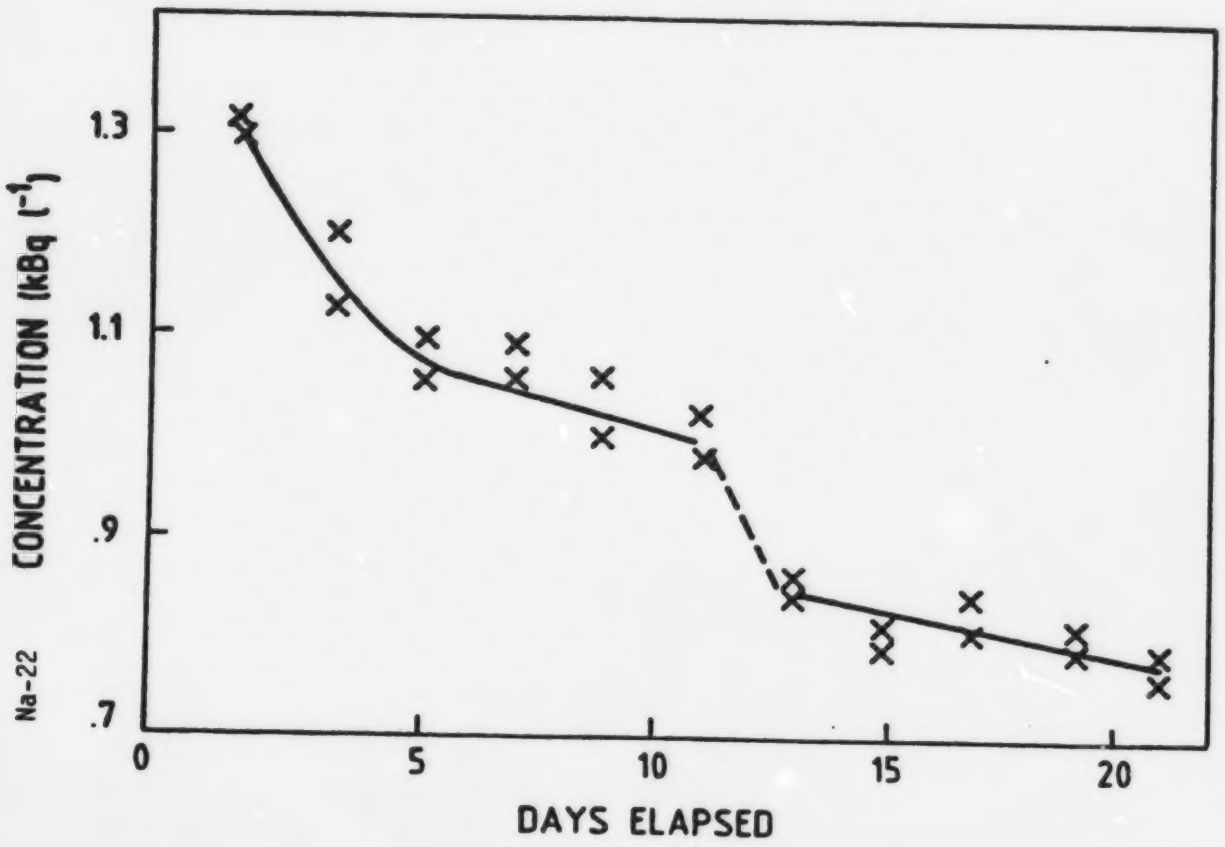

FIGURE 7.9: ACCUMULATION OF VARIOUS RADIONUCLIDES ON LIMNOCORRAL WELLS (AFTER CORNETT AND CHANT, 1986)

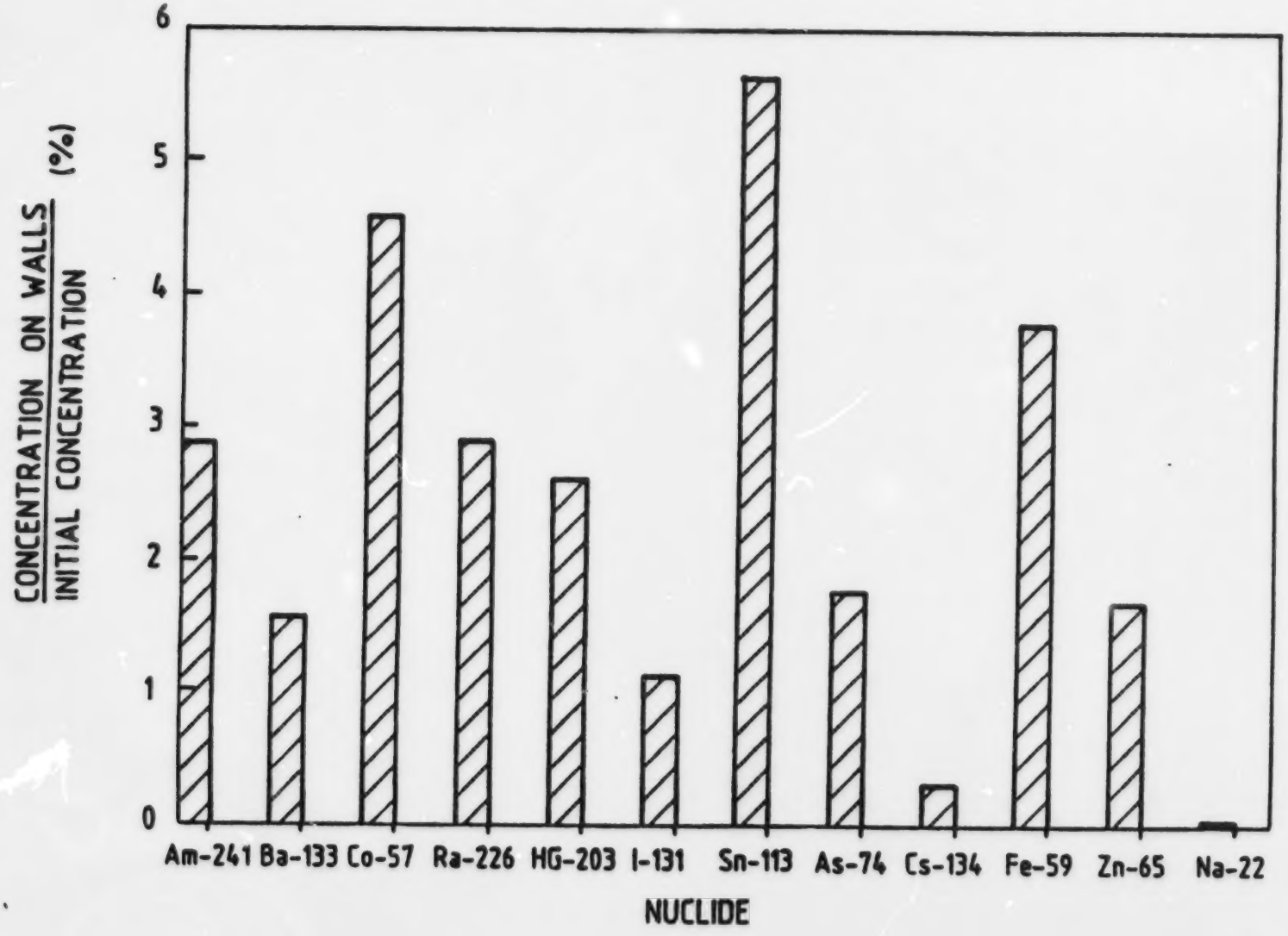

FIGURE 7.10: FLUX OF Na-22 IN SEDIMENT TRAPS (AFTER CORNETT AND CHANT, 1987)

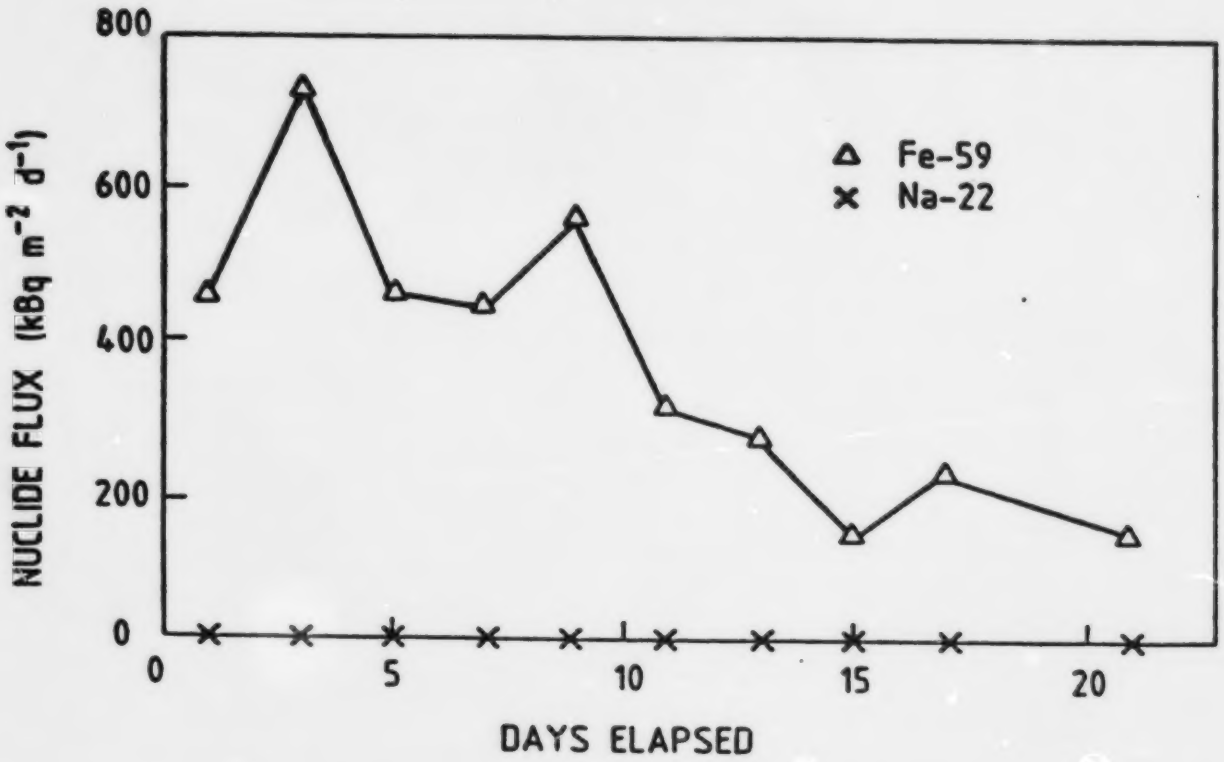

balance during unstratified periods. The different particulate fluxes in the lake and in the enclosure are interpreted to indicate that resuspension was much more important outside than inside the enclosures. Smaller catches also could be explained by a reduced nutrient supply lowering productivity or decreased turbulence slowing settling velocities within the enclosures. Temperature and Eh measurements inside and outside the enclosures indicated that the water was oxic, well mixed vertically (0-2 m) and there were no thermal density gradients ($\pm 1^{o}C$ in 2 m) which could retard particle settling. Temperatures measured outside the enclosures were equal ($\pm 2^{o}C$) to those measured within the enclosures.

Evaluation of nuclides attachment to particulate material (greater than 0.40 pm) in the water and in the traps identified significant fractions (4.8% Cs-134 to about 100% Co-57) to be particulate bound for all nuclides except Na-22. No Na-22 was measured on particles suspended in the water or in the sediment traps (Figure 7.10).

Sediment cores of the soft gyttja (porosity greater than 96%, loss on ignition = 50%) within the enclosures were collected at the end of the experiments (Chant & Cornett 1987). All nuclides added to the water were measured in the sediments. The highest nuclide concentrations (except Na-22) were measured in the surficial 1 cm slices. Na-22 activity in the sediments was constant in the top 14 cm of the cores while Fe-59 decreased below the interface and concentrations in the 5-6 cm slice were greater than 6% of the Fe-59 in the top slice. The distribution of activity was much deeper in the cores than expected. Mixed layers determined from Pb-210 dating suggest bioturbation and physical mixing were restricted to the 0-3 cm horizon and measured concentrations of macrobenthos were very low (unpublished data). Calculations (next section) indicate that all nuclides should diffuse less than 10 cm below the interface and that diffusion of nuclides that are sorbed to particles should be negligible. It is probable that coring and sectioning smear sediment and tracers deeper into the core than that found in undisturbed natural systems (Chant, unpublished data).

8.0 MODELLING ANALYSES OF THE SEDIMENT AND WATER TRANSPORT OF U-238 AND Th-232 DECAY SERIES RADIONUCLIDES

The objective of this research project was two-fold. First, to develop an experimental database for assessing the potential importance of radionuclide release from lake and riverine sediments previously contaminated with uranium mill discharges over the long-term. Secondly, to develop a database for assessing the calibration and mechanisms derived in the previous model developed for the Atomic Energy Control Board (BEAK, 1982). In this section, the structure of that model is reviewed, and this model and additional models of differing degrees of complexity are used to assess the field and laboratory results described in Chapters 1.0 through 7.0.

8.1 Structure of Model Used in Previous Studies

The basic model was previously developed and applied to the chain-link system in a diagnostic and comparative fashion, and was used as the lake component for pathway calculations of critical group dose rate and for the collective effective incomplete dose equivalent commitment to populations located in a local area, the Great Lakes area and the North Atlantic. In this context, the Serpent River system and particularly discharges of U-238, U-235 and Th-232 decay series radioisotopes to Quirke Lake were used as a model morphology and geometry for evaluating these doses to the particular populations.

For each lake, a three-box model was developed. It includes the water column "box" and anaerobic (surface) sediment "box", and a deeper anaerobic sediment "box", which then transfers material to deeper anaerobic sediments which are considered to be non-reactive in terms of transferring materials to the overlying lake water. For each box, ten compartments were used; one compartment for particles (suspended in the water column or contained in the sediment boxes), and one compartment for each of nine radionuclides (U-238, U-234, Th-230, Ra-226, Pb-210 and Po-210 of the U-238 decay series chain and Th-232, Ra-228 and Th-228 radionculides of the Th-232 decay chain). For each Radionuclide compartment, a mass balance was calculated using the definitional figure given in Figure 8.1; inflow occurs to the lake of particulate and dissolved materials, loading from point sources, outflow, adsorption, sedimentation of the adsorbed radionuclides across the bottom of the lake, ingrowth from the parent

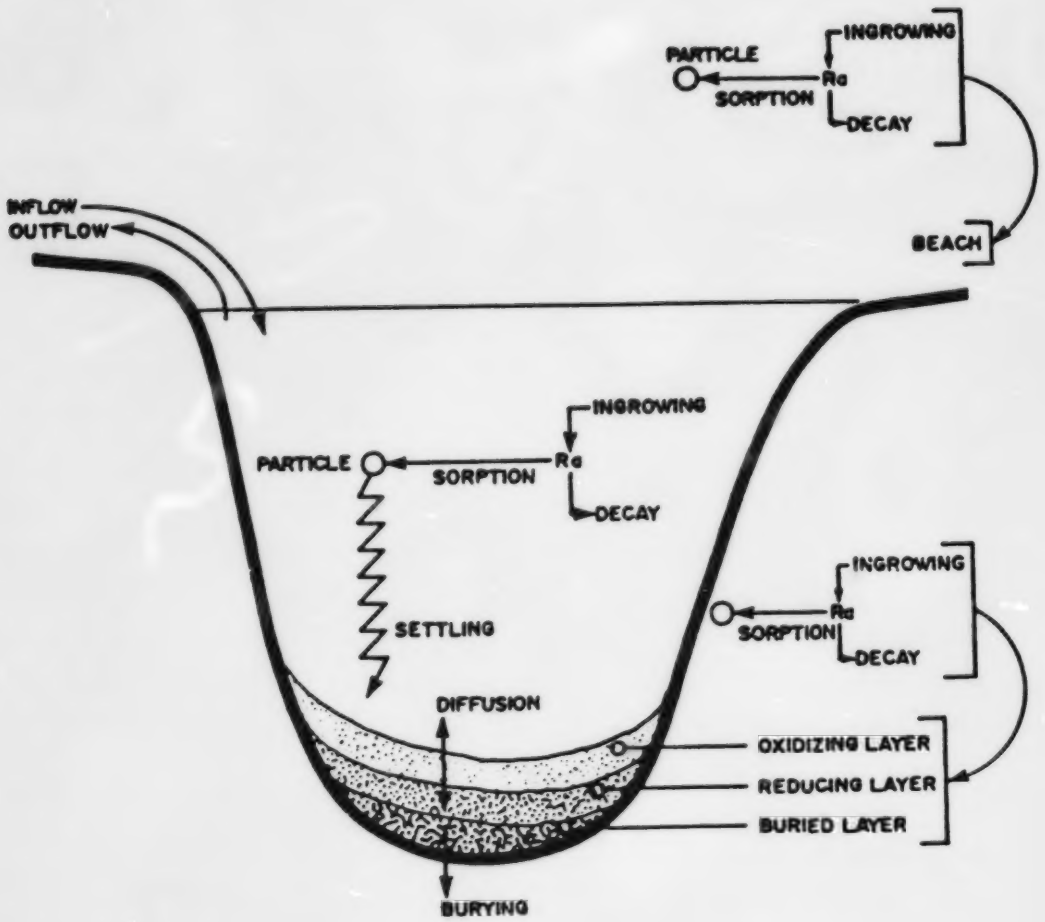

FIGURE 8.1: MAJOR MECHANISMS IN LAKE MODEL

radionuclide, and radioactive decay (first order kinetics). In addition, diffusion occurs between the water column and aerobic sediment, and between the sediment compartments. Adsorption is treated using a linear distribution coefficient for both the water column and sediments.

The resultant time-dependent equations for the water column, the surficial sediments and the deeper sediments are given in Table 8.1, together with a definition of symbols. In Equation 1, the first term describes inputs from land-based sources; the second term lost by settling; the third lost by radioactive decay; the fourth term lost by outflow (Q is the outflow); and the fifth term, diffusion across the sediment-water boundary. In Equation 3, the first term describes an input into the sediment from water column by settling; the second lost by decay; the third lost by sedimentation; the fourth diffusion across the sediment-water boundary; and the fifth diffusion between the surface and river sediment boxes. In Equation 5, the first term describes sedimentation from the surface to the anerobic layer; the second, decay and loss by sedimentation; and the third diffusion between the surface and anaerobic layers. Equation 5 assumes that diffusion between the anaerobic layer and deeper sediments is negligible. Equations 6 and 8 describe the sediment porewater concentrations as a function of sediment properties; f is the fraction of c in the water column that is particulate (see Equation 7), while f_s is a fraction of c_s that is particulate (see Equation 8) in the surficial sediments and f_a is the particulate fraction in the anaerobic layer (see Equation 9).

In recent work, it has become clear that particle erosion and deposition which are the mechanisms not considered in this previous model, are of potential importance in affecting radionuclide transport between the water column and the sediments. The elucidation of the importance of these mechanisms in sediment-water transport was one of the main foci of this study. Accordingly, this mechanism was adapted for inclusion in this model as well. This importance is borne out by the field data from the limnocorrals and analyzed in Chapter 7.0 in which a net settling flux is maintained by "deposition and erosion". Also, the depth profiles of mass accumulation in Quirke Lake from the settling lake data described in Chapter 4.0 indicates that particle erosion and deposition has occurred in this deep lake even at depths of 80 to 100 m of water.

To obtain insights into the predictions of this model, a steady-state analysis was carried out. The steady-state form of the model is given in Table 8.2 with the same symbols as given previously in Table 8.1. The major differences in this case are that the effects of

TABLE 8.1: MODEL EQUATIONS

$$V\frac{dC}{dt} = W - gfCA - KCV - QC - k_s[(1 - f)C - C_{pw}]A, \quad (1)$$

or

$$\frac{dC}{dt} = \frac{L_a}{Z_m} - \frac{gf}{Z_m} + K + \frac{1}{t_w} \cdot C - \frac{k_s}{Z_m}[(1 - f)C - C_{pw}]. \quad (2)$$

for the surficial sediment layer:

$$V_s\frac{dC_s}{dt} = gfCA - KC_sV_s - g_sC_sA - k_s[(1 - f_s)C - C_{pw}]A + k_d[(1 - f_a)C_a - C_{pw}]A, \quad (3)$$

or

$$\frac{dC_s}{dt} = \frac{gfC}{Z_s} - (K + \frac{g_s}{Z_s})C_s - \frac{k_s}{Z_s}[(1 - f)C - C_{pw}] + \frac{k_s}{Z_s}[(1 - f_a)C_a - C_{pw}]. \quad (4)$$

and for the deep sediment layer:

$$\frac{d}{dt}C_a = \frac{g_sC_s}{Z_s} - (K + \frac{g_s}{Z_a})C_a - \frac{k_s}{Z_a}[(1 - f_a)C_a - C_{pw}]. \quad (5)$$

where $C_{pw} = (1 - f_s)C_s$. (6)

$$f = \frac{F\,SS}{1 + F\,SS}. \quad (7)$$

$$f_s = \frac{F_s\,M/E}{F_s\,M/E + 1}. \quad (8)$$

$$f_a = \frac{F_a\,M_a/E_a}{F_a\,M_a/E_a + 1}. \quad (9)$$

Symbols

A	Surface area of lake (m^2)
C	Concentration (activity) of radionuclide in water column (g/m^3)
C_a	Concentration (activity) of radionuclide in anaerobic sediment (g/m^3)
C_s	Concentration (activity) of radionuclide in sediment (g/m^3)
C_{pw}	Concentration (activity) of radionuclide in porewater (g/m^3)
D	Diffusion coefficient (m^2/day)
E	Porosity of surficial sediment
E_a	Porosity of anaerobic sediment
f	Fraction of radionuclide that is particulate in water column
f_a	Fraction of radionuclide that is particulate in anaerobic sediment
f_s	Fraction of radionuclide that is particulate in surficial sediment
F	Adsorption coefficient in water column (l/kg)
F_a	Adsorption coefficient in anaerobic sediment (l/kg)
F_s	Adsorption coefficient in surficial sediment (l/kg)
g	Settling rate of particulates (m/day)
K	Radionuclide decay rate (day^{-1})
k_s	Sediment-water transport coefficient
K_D	Linear distribution coefficient (l/kg)
L_a	Unit area loading of radionuclides (g/m^2/day)
M	Dry bulk density of surficial sediment (kg/l)
M_a	Dry bulk density of anaerotic sediment (kg/l)
Q	Outflow rate (m^3/day)
t	Time (day)
t_w	Hydraulic detention time (day)
SS	Suspended solids concentration (kg/l)
V	Volume of lake water (m^3)
V_s	Volume of sediment (m^3)
W	Radionuclide loading rate to lake (g/day)
Z_a	Depth of anaerobic sediment (m)
Z_m	Mean lake depth (m)
Z_s	Depth of surficial sediment (m)

TABLE 8.2: STEADY-STATE FORM OF MODEL EQUATIONS

The steady-state concentration in the water column is:

$$C = \frac{\dfrac{L_a}{Z_m}}{\underbrace{\dfrac{gf}{Z_m}}_{\text{Settling of particulate}} + \underbrace{K}_{\text{Decay}} + \underbrace{\dfrac{1}{t_w}}_{\text{Out-flow}} + \underbrace{\dfrac{k_s}{Z_m}\dfrac{(1-f)C - C_{pw}}{C}}_{\text{Diffusion}}}. \qquad (1)$$

or

$$C = \frac{\dfrac{L_a}{Z_m} + \dfrac{k_s C_{pw}}{Z_m}}{\dfrac{gf}{Z_m} + K + \dfrac{1}{t_w} + \dfrac{k_s(1-f)}{Z_m}}, \qquad (2)$$

and in the sediment is

$$\frac{C_s}{C} = \frac{gf + k_s(1-f)}{k_s(1-f_s) + g_s + KZ_s} \qquad (3)$$

Model calibration.

(a) Water column

G = 25 m/yr
$k_s = D/\text{del } Z = 10^{-3}$ m/d to 10^{-3} m/day
SS = 0.4 mg/l
K_D for water = 100 times sediment value

(b) Sediment

	E	RHO	RHO_s	Z_s	g_s
Shield	0.95	1.02 g/cc	1.4 g/cc	.04 m	0.2 mm/yr
Great Lakes	0.88	1.07 g/cc	1.6 g/cc	.02 m	1.5 mm/yr

ingrowth from radionuclides from parent daughter are ignored in order to make the steady-state analyses practicable and understandable.

To understand the effects of the ingrowth from the parent and decay to a daughter, the time scales of two processes; decay rates of their radionuclides, and settling burial rates can be used to estimate the effects of ignoring the ingrowth decay phenomena. The decay half-life of the radionuclides are respectively U-238 4.5×10^9 yrs; Th-230 8.1×10^4 yrs; Ra-226 1,620 yrs; Pb-210 22 yrs; Po-210 138 days. The time to bury surficial sediment in two generic types of lakes are 200 years for the Shield lake (assuming a depth of 4 cm for the zone to be buried), and 13 yrs for the Great Lakes (assuming a depth of burial of two sediments). For the burial rates given in Table 8.2, ingrowth and radioactive decay would be significant for both Pb-210 and Po-210, particularly in the Shield Lakes and also in the Great Lakes sediments, but not for the other radionuclides. This assessment is based upon comparing the relative magnitudes of the two time scales. If the time scale for radioactive decay of a particular radionuclide is less than the sediment burial time, it will approach secular equilibrium within the burial time frame. Therefore, the sediment burial rates of these two systems would also significantly impact the sediment burial characteristics of Ra-228 (half-life = 6.7 years and Th-228 (decay half-life = 1.9 yrs.).

The model was also used to calculate the relationship of sedimentation and diffusion in the sediments, and sediment burial by the material removed from the water column by settling processes. This gives the net accumulation (settling flux) which occurs with sediment burial. The results are given in Table 8.3. In this analysis, gross settling minus entrainment of sediments which returns sediments to the water column is formulated into a net settling flux as expressed by the equations described in Tables 8.1 and 8.2. At steady-state, the effect of gross settling minus sediment erosion is the same as treating the overall process as being a net settling process as described in the equations. Only when non-steady-state effects are considered in a model such as would be of concern for evaluating the response of lakes to changes in land-based loadings, would the dynamics of sediment erosion significantly affect the model calculations. In fact, the net effect of sediment erosion is to increase the rate of cycling of radionuclides between the sediment and the water. But the net long-term effect as compared to the steady-state effect is negligible. This can be proven by derivation of the appropriate equations and application of a sensitivity analysis.

Table 8.3 Net accumulation of settling flux (%).[a]

Radionuclide	Lake[b]	Condition		
		$k_s = 10^{-3}$ m/day	$k_s = 10^{-4}$ m/day	$k_s = 10^{-5}$ m/day
^{238}U	S	80	30	1.8
	Gt	83	36	7.3
^{230}Th	S	67	18	1.5
	Gt	99.8	98	35.0
^{226}Ra	S	18	4	1.5
	Gt	67	21	6.9
^{210}Pb	S	10	4	1.5
	Gt	64	42	6.7
^{210}Po	S	0.3	0.4	1.3
	Gt	4	4	6.0

[a] Net accumulation equals flux of radionuclide buried below surface zone divided by flux of radionuclide settling into sediment from water column.
[b] S, Shield Lake; Gt, Great Lake.

Net accumulation described in Table 8.3 is defined as the portion of the settling flux that is retained in the deep sediments; hence, it is the portion of the settling flux that was measured and described as the sedimentation rate in Chapter 4. The net radionuclide accumulation in the sediments calculated for the different radionuclides is given as a function of three different estimates of the mass transfer coefficient, K_s: 10^{-5}, 10^{-4} and 0.1 m/day. As described later, a value for K_s of 0.1 m/day is roughly the value indicated by field data. The former two values, 10^{-5} and 10^{-4}, are plausible values for some substances over very short-term time scales in which the diffusion coefficient is molecular (i.e., of the order 10^{-5} m^2/day), but where the gradient thickness of the order of 1 metre. Such a large gradient is generally only measured in very undisturbed hypolimnetic waters of lakes, in thermocline regions of fairly stable lakes, and/or in the deep oceans.

The calculations indicate that as this mass transfer coefficient, K_s, increases from 10^{-5} to 10^{-4} m/day, there is a substantively small portion of the radionuclides which remain in the sediments. For values for K_s of 0.1 m^2/day and larger, only a few percent of the radionuclides settling to the sediments actually are retained in the sediments. For all conditions, only a few percent of Po-210 settling to the sediments is buried in the deep sediments. This low accumulation rate of Po-210 is caused by its decay, rather than by loss from the sediment diffusion processes. The net accumulation of Po-210 increases as K_s increases because, of all the radionuclides, it alone has a net diffusion gradient towards the sediments; i.e. due to radiological decay of Po-210 in the sediments, the porewater concentration of Po-210 is calculated to be lower than in the water column, and hence the net diffusional gradient is towards the sediments. All of the radionuclides are calculated to have a net gradient from the sediment porewater to the water column.

These calculations then permit observations concerning the effect of diffusional processes upon settling and hence overall sediment water transport processes. They are:

1. within the range of values tested in the calculations for the absorption coefficient of 500 to 50,000 mL/g, diffusional processes minimize the net removal of radionuclides from the water column caused by settling processes; and

2. if diffusional and settling processes remove, radionuclides from the water column over the long-term, then the values for the absorption coefficient in the sediment must be substantially larger by the range tested in these data.

An assessment of the range of absorption coefficients tested in these calculations can be made by reference to Section 7.0. The linear distribution coefficient values obtained in the short-term experiments for radium and thorium are of the order of 500 to 2,000 mL/g, while the values of the distribution coefficients for lead-210 are of the order of 1,000 to 5,000 mL/g. Accordingly, the values used in these calculations would appear to be reasonable.

In addition, the values tested in this set of calculations assume that the absorption coefficient for radionuclides on suspended material in water is 100 times that of the value for bottom sediments. This type of relationship was based upon suspended solids, K_D relationships observed previously by O'Connor and Connelly (1980). They found that, typically, there was a one-half order to one order of magnitude decrease in the K_D as the suspended solids concentration was decreased over an order of magnitude. Whether such a relationship is, in fact, real, or simply an artifact of experimental procedures has been a question of concern for several years now, particulary since about 1982. To some researchers, it is plausible that such a relationship should occur, but it is the general opinion of many researchers that it is an experimental artifact. To date, few reasonably good explanations, theoretical derivations or experimental measurements have been obtained to prove that the relationship exists. In some work, it is most probable that the relationship does not exist, and that the relationship is caused by the absorption of other materials where behaviour is masked by the sample sorption of the radionuclides. For example, ion exchange, coprecipitation, and even precipitation are the types of processes which are required to explain it. If such a relationship does not exist, then the flux from the water column to the sediments could be even smaller than that calculated here, and hence the effects of diffusion would be even greater than those described in the calculations of Table 8.2 the rate of diffusion into sediments.

8.2 Sediment Transport Dynamics

Assuming negligible decay, the diffusion rate of radioisotopes in the sediments can be calculated using the following formula:

$$\frac{Cpw}{C^{o}pw} = \text{erfc}\left[\frac{z}{2(at)^{0.5}}\right] \qquad (8.1)$$

Here Cpw is the porewater concentration at depth z.

$C^{o}pw$ is the porewater concentration at z = 0

a is equal to fED

f is the fraction of the radionuclide which is particulate

E is the porosity

D is the diffusion coefficient (m^2/d)

t is time

erfc is the complementary error function

This equation is obtained by using Laplace transforms to solve the diffusion adsorption equation. The equation was used to calculate the depth situation of radionuclides in the sediments using different values of the distribution coefficient and sediment porosity values which are typical of the Quirke Lake and Chalk River sediments. The resultant calculations are given in Figure 8.2 for different values of the linear distribution coefficient, K_D (values ranging from 10 to 1,000 mL/g). In general, the calculations show that, if the distribution coefficient is much greater than approximately 50, then the net penetration of material in the sediments by diffusional processes is small over the time frame of the limnocorral experiment. This implies that the diffusion of material in these sediment cannot explain very much of the depth penetration observed in the limnocorral sediment. It suggests that the depth penetration has to be due to either mixing because of benthic macroinvertebrates, or smearing of effects from the coring procedure. Hence, the depth penetration data from the core cannot be used with certainty in aiding the evaluation of transport calculations in these sediments. It also suggests that, the 200 um thick fluid zone of diffusional resistance and absorption in the top mm of the sediments are the main sediment-water layers which are involved in removal processes. Deeper sediment zones would be involved in short-term sediment-water transport if the sediments are substantially disturbed by erosional processes or if settling processes cause significant depth penetration of the material into the sediments.

Figure 8.2a

Depth Penetration into Sediments for Kd=10 L/kg
For Pore Water Concentration

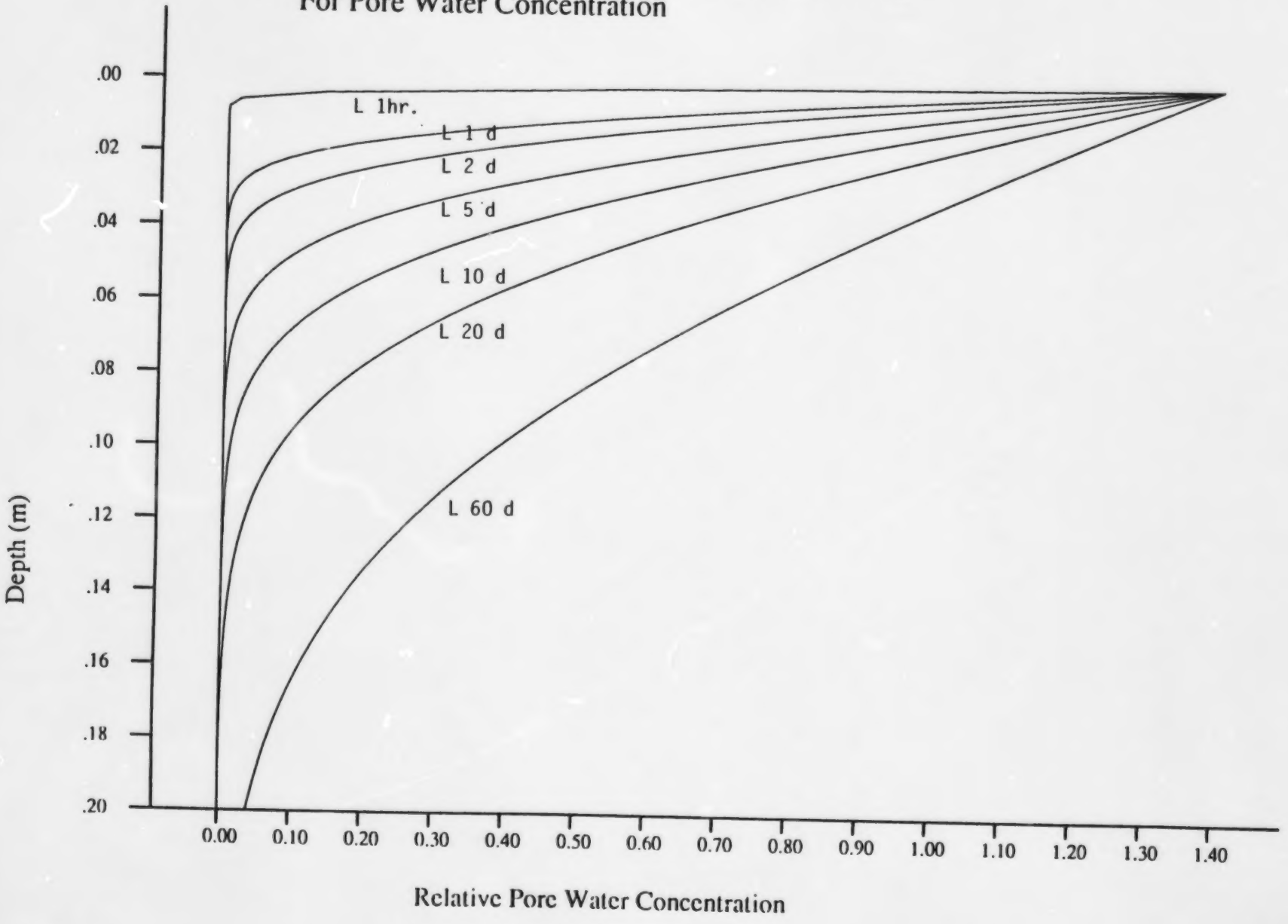

Figure 8.2b

Depth Penetration into Sediments for Kd=50 L/kg
For Pore Water Concentration

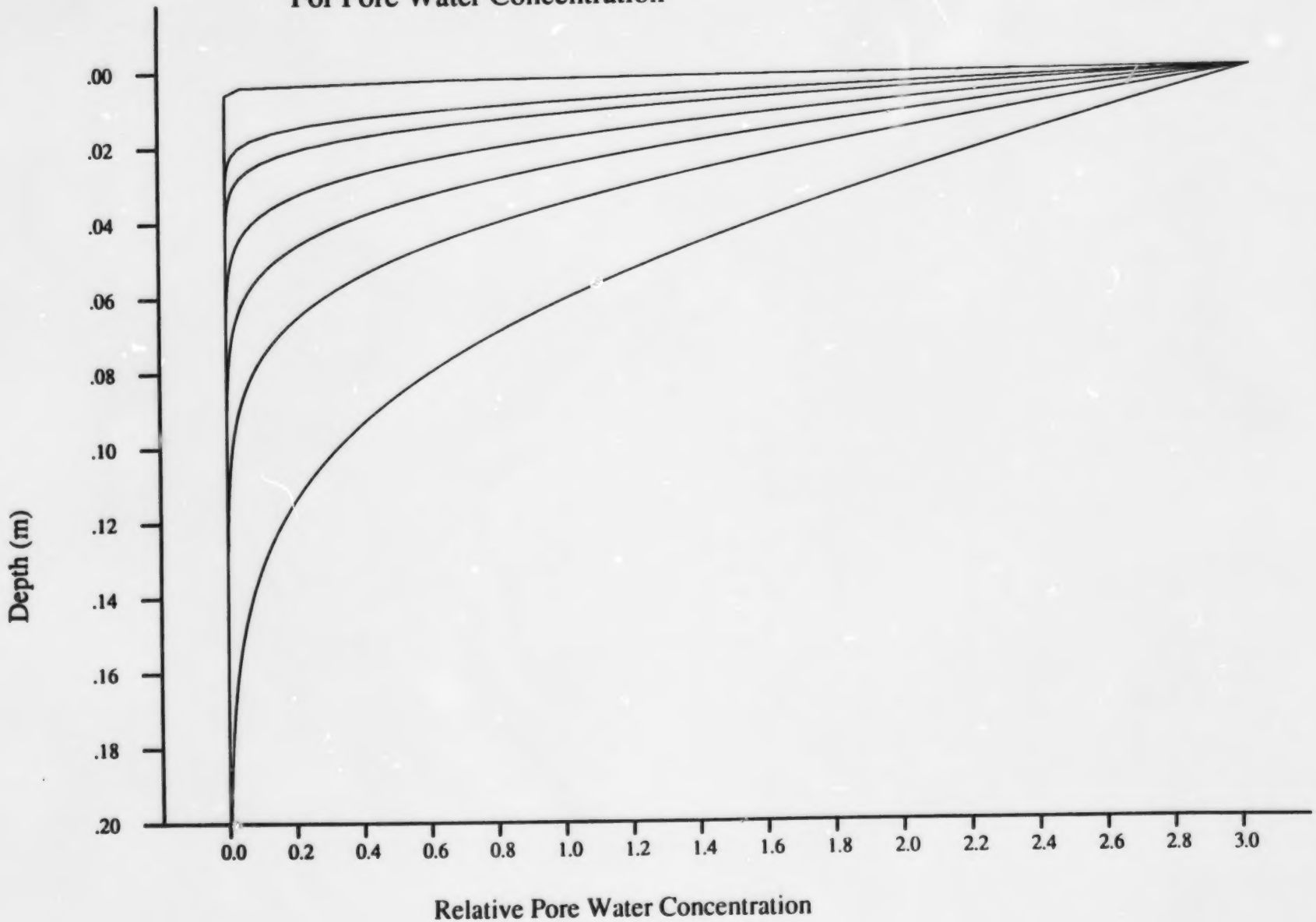

Figure 8.2c

Depth Penetration into Sediments for Kd=100 L/kg
For Pore Water Concentration

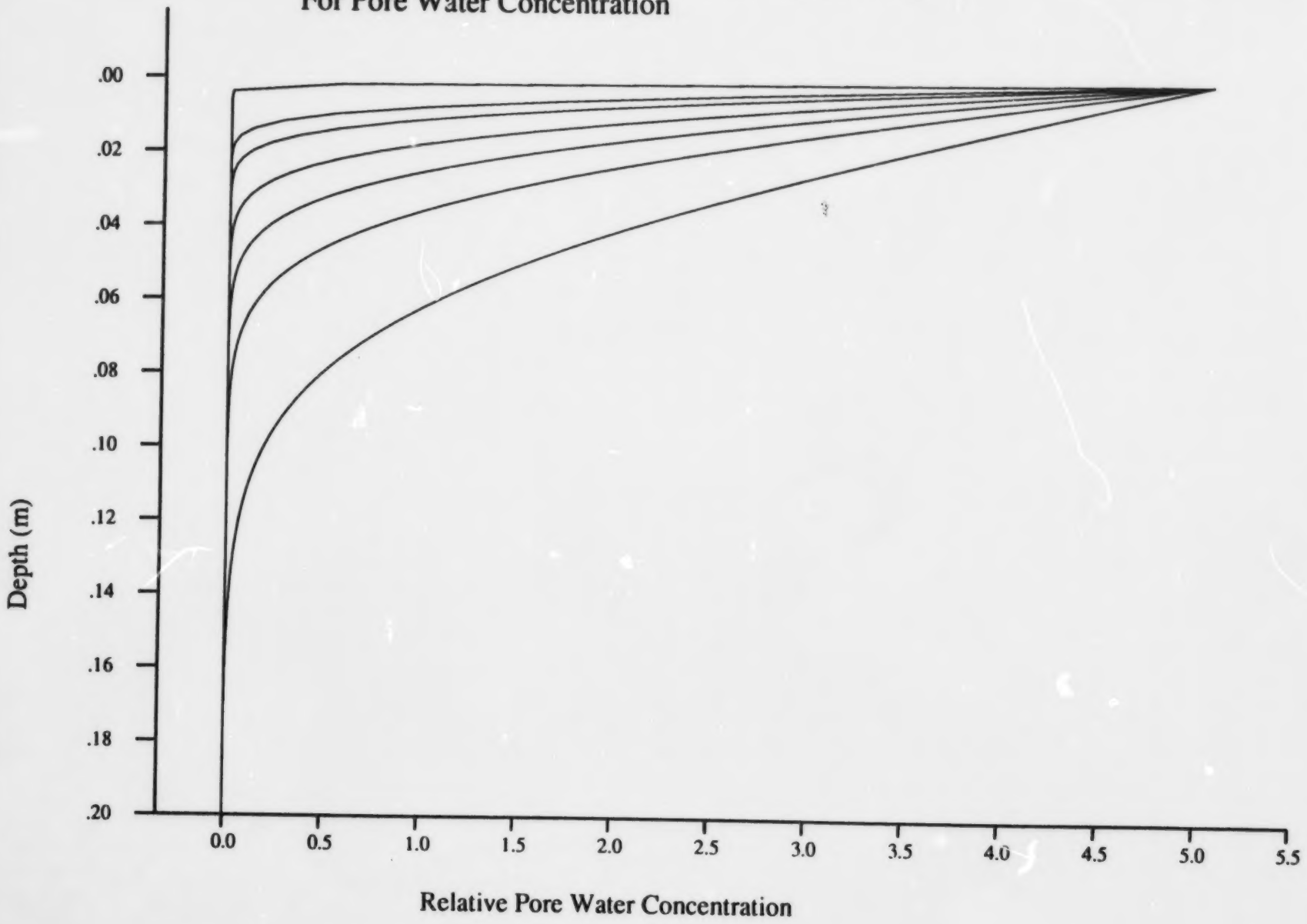

Figure 8.2d

Depth Penetration into Sediments for Kd=500 L/kg
For Pore Water Concentration

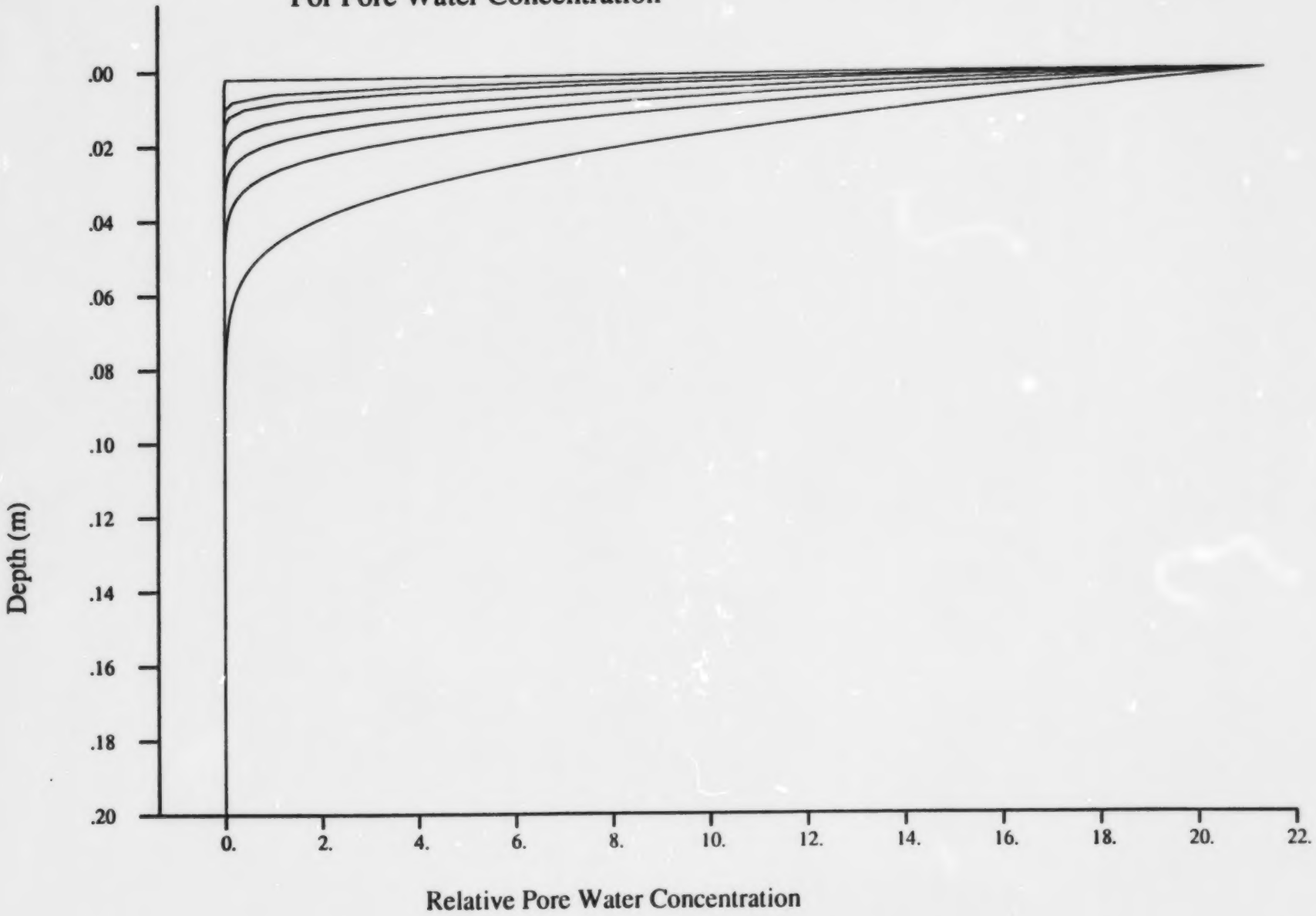

Figure 8.2e Depth Penetration into Sediments for Kd=1000 L/kg
For Pore Water Concentration

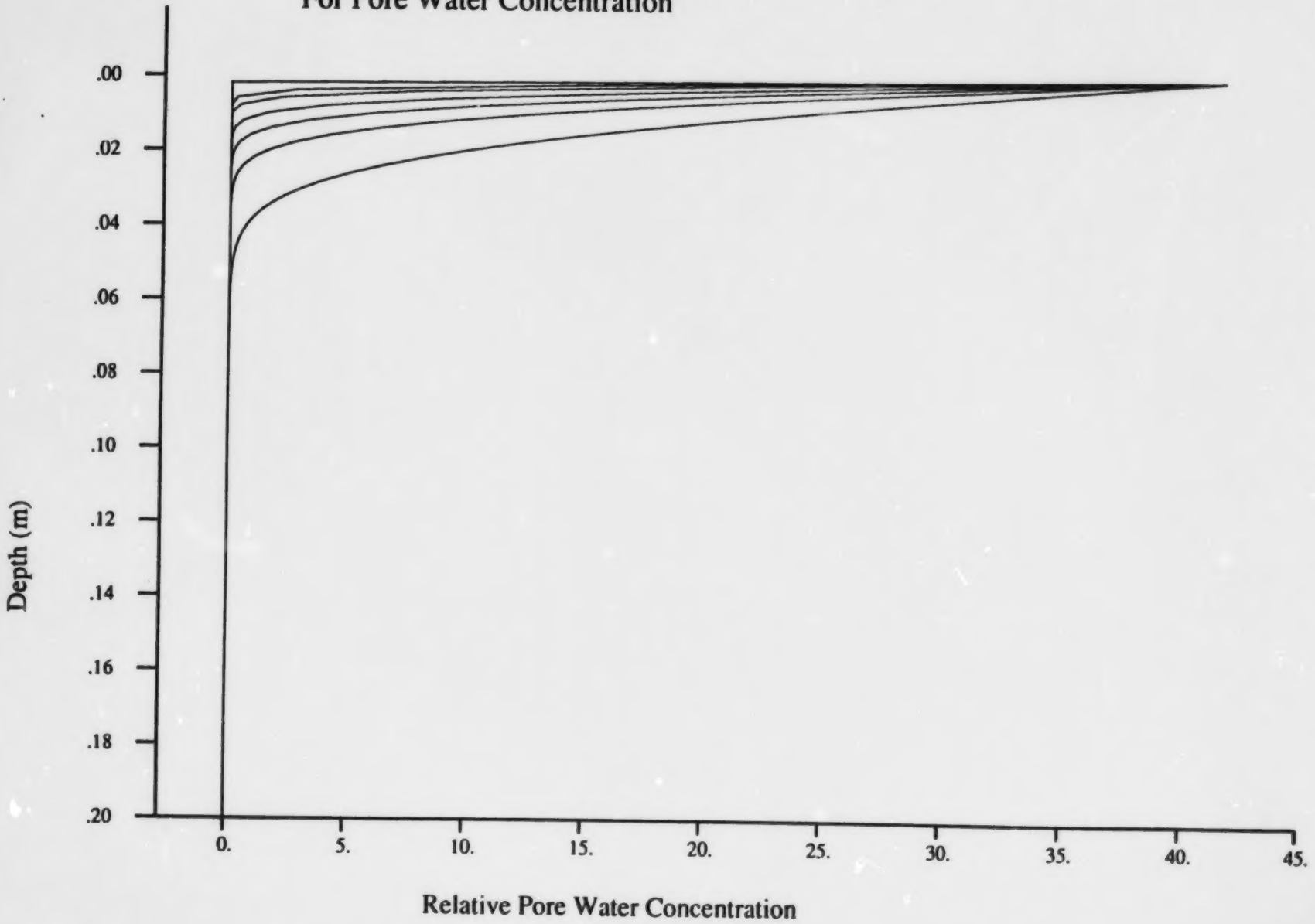

8.3 Modelling of the Results of the Field Experiments Using a Kinetically-Controlled Sediment Adsorption, Sediment Settling and Diffusion Model

A model formulated by Santschi (1985) was algorithmed and formulated into a probabilistic simulation format. The representation of the model is shown schematically in Figure 8.3 in which water column, fluid film and various sediment compartments are shown. The model basically shows the following details. The system is divided vertically into a series of boxes which include the well-mixed water column, a fluid layer (described as a diffusive boundary layer), and a number of sediment layers (algorithmed in this study as being 20 layers) with the surficial layer being considered to be anaerobic. Each sediment box can be divided into an equal or unequal thickness; in this work, it was divided into equal thicknesses. These compartments were then used to calculate a mass balance for the flux of particles and radionuclides attached to these particles, and the diffusion of these particles and of the radionuclides between the boxes.

The horizontal division of the system represents the aqueous phase, the adsorbed phase and a matrix (solid) phase. K_1 and K_{-1} are adsorption and desorption rate constants between the porewater and the sorbed phases, K_2 and K_{-2} are rate constants for transfer of the sorbed material into the matrix material on the solid phase. D^i_{eff} and D^i_p are the porewater diffusion coefficients and sediments respectively, and W, PRS and SR represent wall diffusion, particle resuspension and particle settling rates, respectively.

This model has been used by Santschi to simulate the removal of radioisotopes from limnocorrals for several radionuclides. The derivation of the kinetic rate constants for adsorption and desorption were obtained from laboratory studies. The results of the model simulation as shown in Figure 8.4. Overall, the model does a reasonable job of simulating observed removal characteristics for various limnocorrals in which either removal or other perturbations have been induced to cause a removal and then a subsequent release from the sediments back into the water column for six radionuclides (Cs-134, Zn-65, Mn-54, Co-60, Fe-59 and Sn-113).

In this work sorption constants (K_D's) were measured, but the actual kinetics of adsorption and desorption were not measured. Accordingly, to simulate removal characteristics from the water column and release from the sediments back to the water

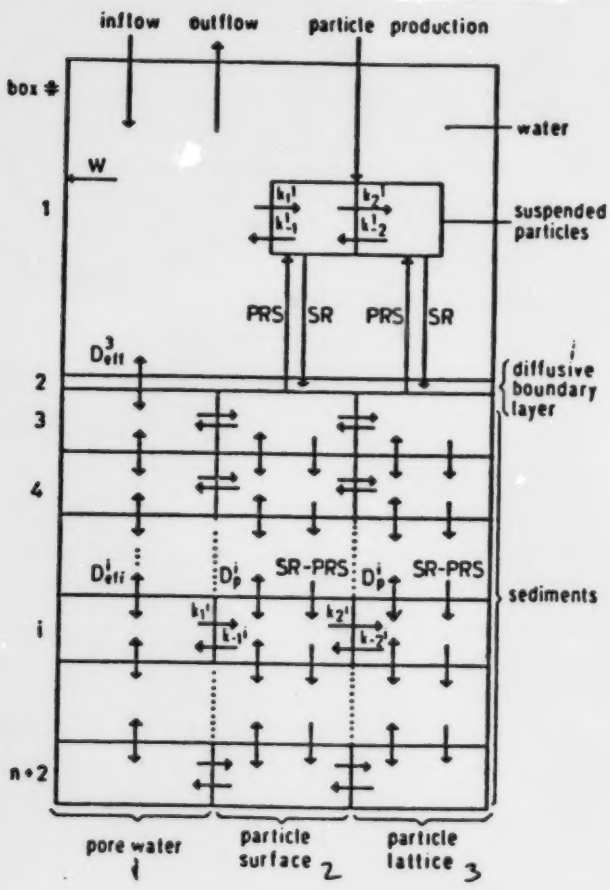

FIGURE 8.3: REPRESENTATION OF SEDIMENT-WATER TRANSPORT BY SANTSCHII ET AL (1985)

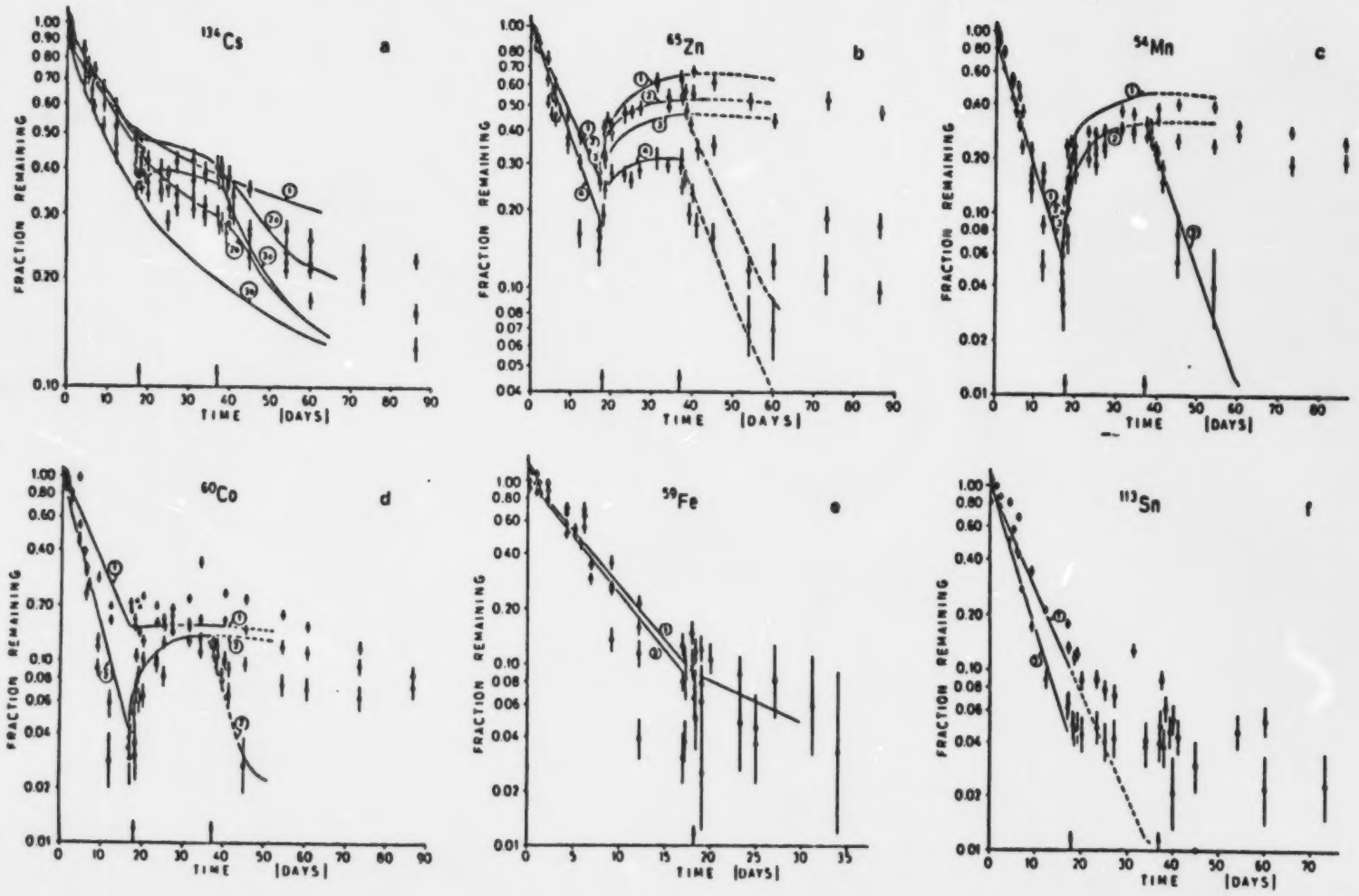

FIGURE 8.4: VALIDATION OF SANTSCHII ET AL (1985) MODEL

column, and to provide a perspective for the sediment-water fluxes measured in Quirke Lake, the values for the kinetic adsorption and desorption coefficients were inferred from the experimental database. Using the values of Santschi et al. for desorption which are typically fairly constant for ali radionuclides, the kinetic adsorption rate constant can then be estimated given the value for K_D.

The model system used for simulation emulates fairly closely the data for the limnocorrals in Perch Lake, including the particle concentrations, the depth of the water column, and the sorption sediment surface characteristics. The simulation results were made for a substance modelled after Ra-226 in which the K_D is approximately 500 mL/g. Simulations are presented in Figure 8.5 for the removal from the water column. The results indicate that, with the calibration chosen, the removal rate is quite quick and then is slower. Simulations were also made of sediment release, but the results aait future indepth analysis before presentation in a report.

An adequate calibration study of this model to explain both removal from the water and release from the sediments awaits future work. Further studies are required to determine which coefficients substantively influence the patterns shown in Figure 8.5. A testing of the ability of the model to predict both removal and release, its scale-up to Quirke Lake scale, and simplification of its results into the modelling format of Table 8.1 awaits future work.

8.4 Evaluation of the Limnocorral Data Using a Simple Model

In previous work, the model used previously for the AECB in the northern Ontario application was simplified and a steady-state analysis developed for analyzing limnocorral data. The model is described as Equation 8.2.

$$v_s = gf + k_s(1-f) \qquad (8.2)$$

Here, the symbols are as previously defined. The first term of Equation 8.2 describes the net effective removal velocity of the particulate fraction while the second term describes the net effective removal from the water column of soluble substances. v_s is a removal velocity which is derived directly from the limnocorral data; it basically describes the removal of total concentrations of radionuclides. Such removal

characteristics have been used previously in developing models for phosphorus in a large number of lakes in North America, Europe and Asia. Hence this provides a useful perspective for analyzing radionuclide data obtained from limnocorrals and/or field studies in the field of nuclear isotope and radionuclide transport.

The model is summarized in Figure 8.6. The plot shows the effect of removal plotted against the percent particulate for a range of mass transfer coefficients. The lines shown assume that the particulate settling velocity is 25 m per year. Shown also on the graph are a few removal velocity estimates obtained by others from limnocorral work for radioisotopes of zinc, selenium, mercury, cobalt and iron. As well, below the "percent particulate" axes (the x axis) is a water column distribution coefficient (K_D, mL/g) for the assumption that the suspended solids concentration is 2 mg/L. Removal velocities observed in the limnocorrals are plotted as a function of the percent particulate on Figure 8.6. In general, the removal velocities for the particulate materials (based upon the sediment mass balance of Ra-226) are of the order of 0.2 to 0.3 m/day for the control limnocorrals, of the order of 0.05 to 1.0 m/day for the humic control limnocorrals, and approximately an order of magnitude greater for the particulate treatment limnocorral. The results indicate that the removal rates are close to those observed in other limnocorrals except for the removal of the particulate fraction which is over an order of magnitude faster. This suggests that the use of the illite clay is not representative of particles typical of lake systems and hence that they should not be considered directly for evaluating their effect on removal characteristics in other lakes. Hence, the net settling velocity of the particulate treatment is excessive in comparison to the other limnocorrals.

If the particulate settling velocity of the suspended solids in the control bags are of the order of 25 m/year, then diffusion processes are required to explain the removal characteristics observed in the sediments. This suggests that diffusion would control removal of much of the radionuclides observed in the limnocorrals in these experiments.

8.5 Model Validation Studies With Limnocorral and Quirke Lake Data

In this section, the model previously used (Table 8.1) is revised to account for sediment erosion and then the calibration used in the BEAK (1982) study, is compared with the limnocorral and Quirke Lake data. The revised model equations are:

Figure 8.5

Monte Carlo Simulation of Santschi Model
+/- 2 Standard Deviations

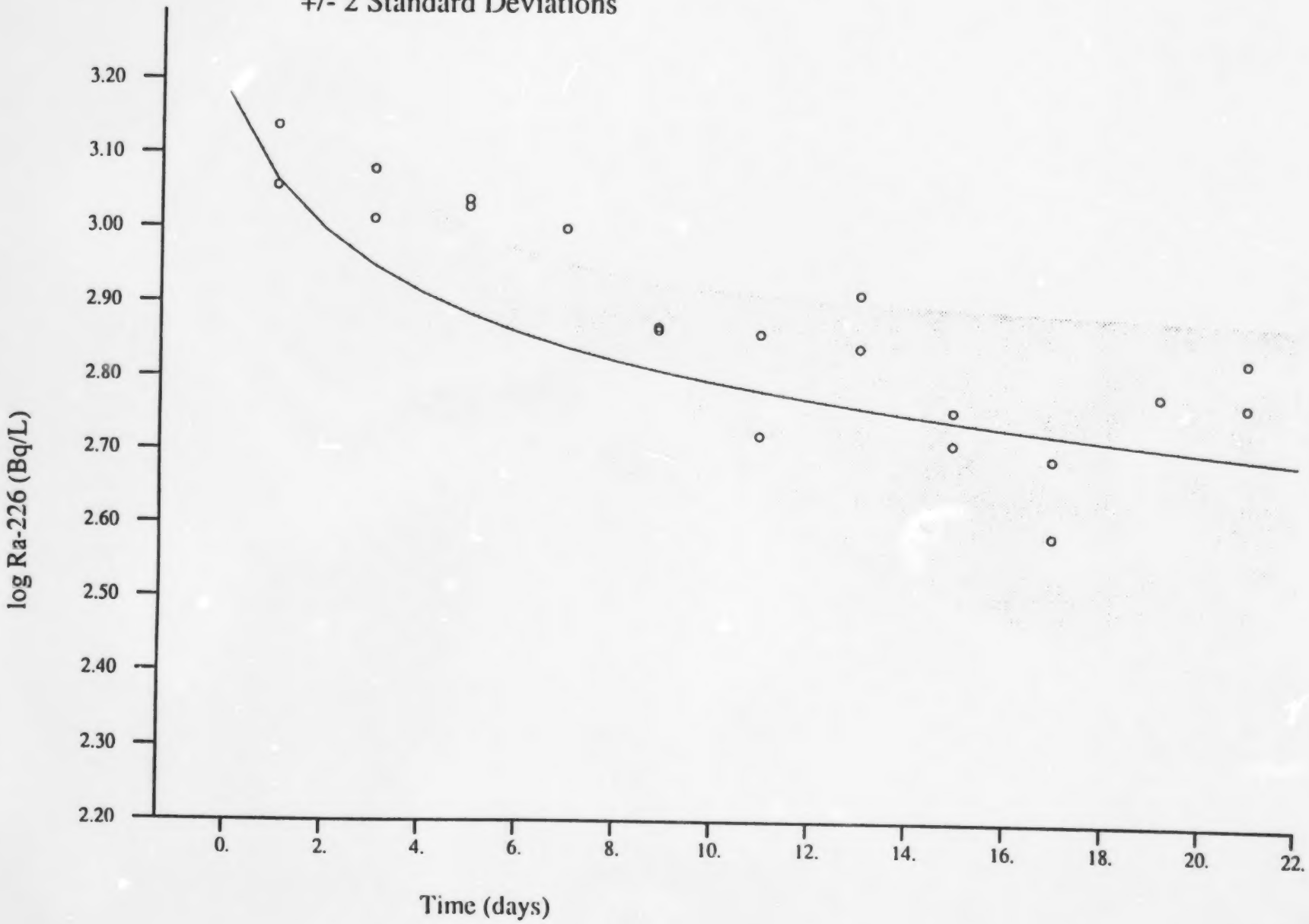

FIGURE 8.6 Effective removal volocity (Eq. 8.2) as a function of percent particulate.

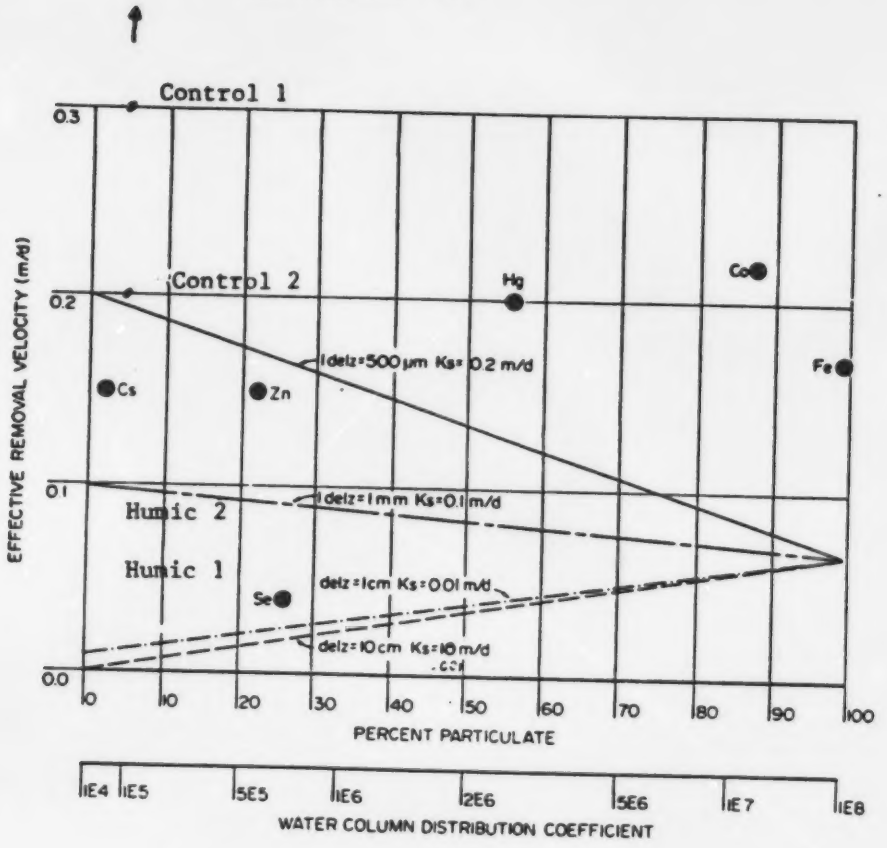

$$\frac{dC}{dt} = A_{11} - A_{12}C + A_{13}C_s$$

$$\frac{dC_s}{dt} = A_{11} + A_{22}C - A_{23}C_S$$

where: $A_{11} = \frac{La}{Z_m}$

$$A_{12} = \frac{(gf}{Z_m} + K + \frac{1}{t_w} + \frac{K_s(1-f)}{Z_m}$$

$$A_{13} = \frac{k_s}{Z_m}(1-f_s) + \frac{E_r}{Z_m}$$

$$A_{21} = 0$$

$$A_{22} = \frac{gf}{Z_s} + \frac{k_s}{Z_s}(1-f)$$

$$A_{23} = (K + \frac{g_s}{Z_s} + \frac{k_s}{Z_s}(1-f_s) + E_r)$$

Here E_r is the sediment erosion rate (m/day) of the surficial layer of sediment and the other symbols are as defined in Table 8.1.

With the revised model, there are ten coefficients which require specification with lake data and three model coefficients whose calibration is being tested by application of the model from lake to lake. The suspended solids concentration (SS), the sediment erosion rating (E_r), the sediment dry bulk density (M), the sediment porosity (E), the sediment burial rate (g_s), the sediment dry bulk density (Ps), the particle settling rate (g), the radionuclide loading (W), the lake mean depth (Z_m) and the hydraulic residence time (t_w) are lake specific. The decay rate constant (K) and the diffusion coefficient (D) are radionuclide specific. If sediment reworking by macroinvertebrates or other benthos is significant, D becomes lake specific. The depth of the active sediment interchanging

with the overlying water (Z_s) is calculated from equation 8.1. Thus, the following model coefficients require calibration: the adsorption coefficient in the sediment F_s; the relationship between F, the adsorption coefficient on the water column, and F_s; and the sediment-water transport coefficient, k_s.

In the previous application of the model, F was set equal to 100 F_s based upon literature relationships and k_s was taken as ranging from 10^{-5} m/d to 10^{-3} m/d based upon arguments of this coefficient being a mass transfer coefficient. The mass transfer coefficient can be approximated as the diffusion coefficient divided by a concentration gradient thickness. The above values for k_s are based upon a molecular diffusion coefficient of the order of 10^{-5} m^2/d for Ra-226 and a gradient thickness ranging from 1 m to 1 cm. Analysis of limnocorral data from Northern Ontario (see Figure 8.6), however, suggest that k_s should be of the order of 0.1 to 0.1 m/d for several nuclides.

The approach of this study was to check the model calibration with the limnocorral data and to conduct model validation studies with Quirke Lake. The model calibration was checked with the following data from "Control 2" limnocorral: Ra-226 flux data into the sediment (Figure 7.3) and efflux data (Figure 7.5) from the sediments/

Field measurements of F for suspended solids in the water column of the control limnocorral gave a value for F of 430,000 L/kg (Table 7.1). This value is different than the calibration of BEAK (1982) which was 50,000 L/kg. Accordingly, model simulation was used to evaluate values for the F-F_s relationship and k_s. The resultant values were: F_s = 10F_s and k_s = 0.2 m/d.

Comparison of the model predictions to observed data for the control (Figure 8.7) indicates that a good fit is obtained qualitatively and statistically (at a 95% level) for both loss of Ra-226 from the water column and tje efflux back from the sediment. However, the calculated flux to the sediment (defined as Flux = fgC is lower than observed in the sediment traps. Also, this calibration results in the model under predicting removal of Ra-226 from the water column of the limnocorral to which particulate matter was added (Figure 8.8). This is caused (Figure 8.6) by the effective removal rate in the particulate-treated limnocorrals being substantially higher than the controls despite the particulate-treated limnocorral having approximately the same percentage particulate fraction. The particulate addition has approximately the same

Figure 8.7a Ra-226 Removal from Control

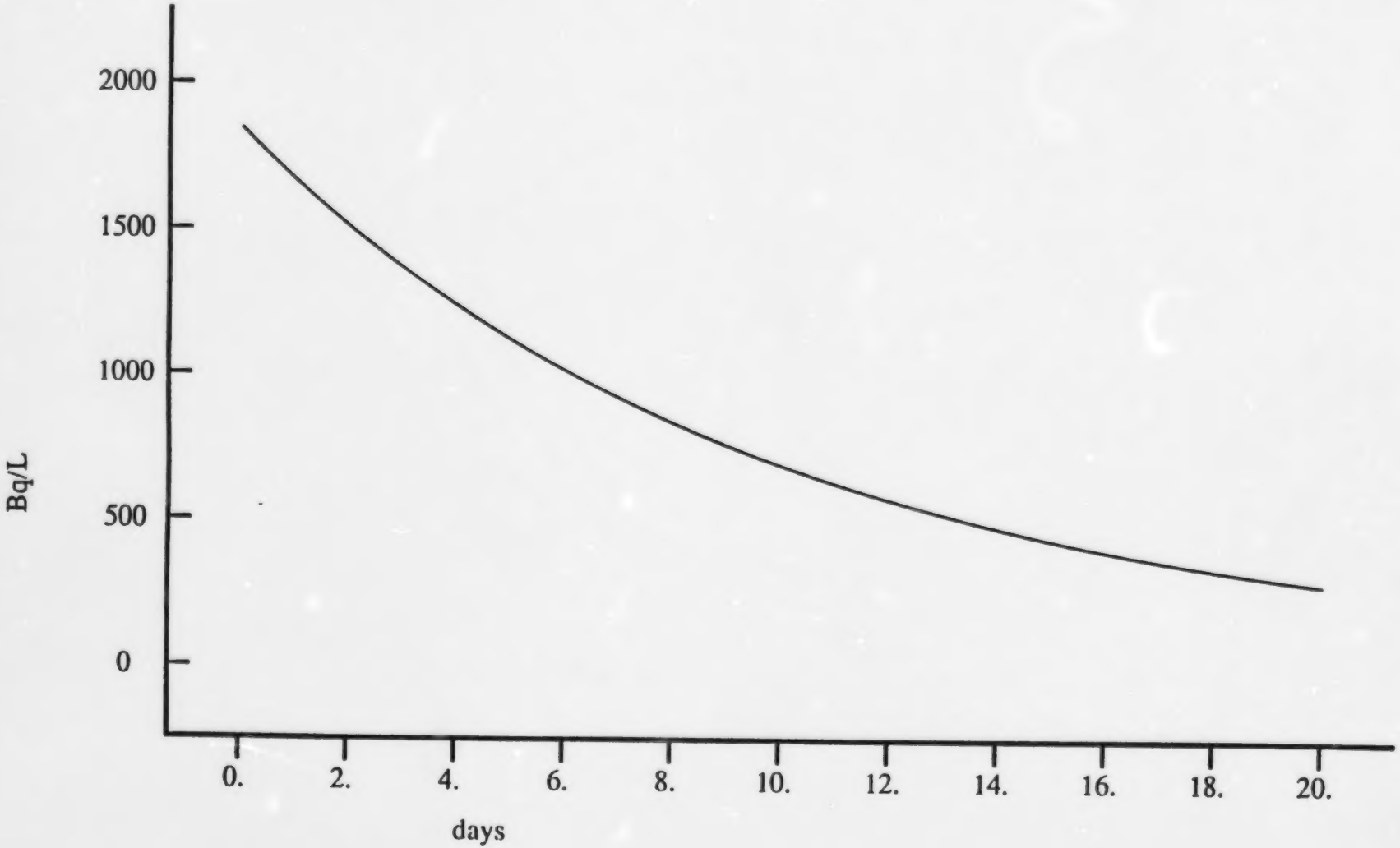

Figure 8.7b Ra-226 Activity in Sediments in Control

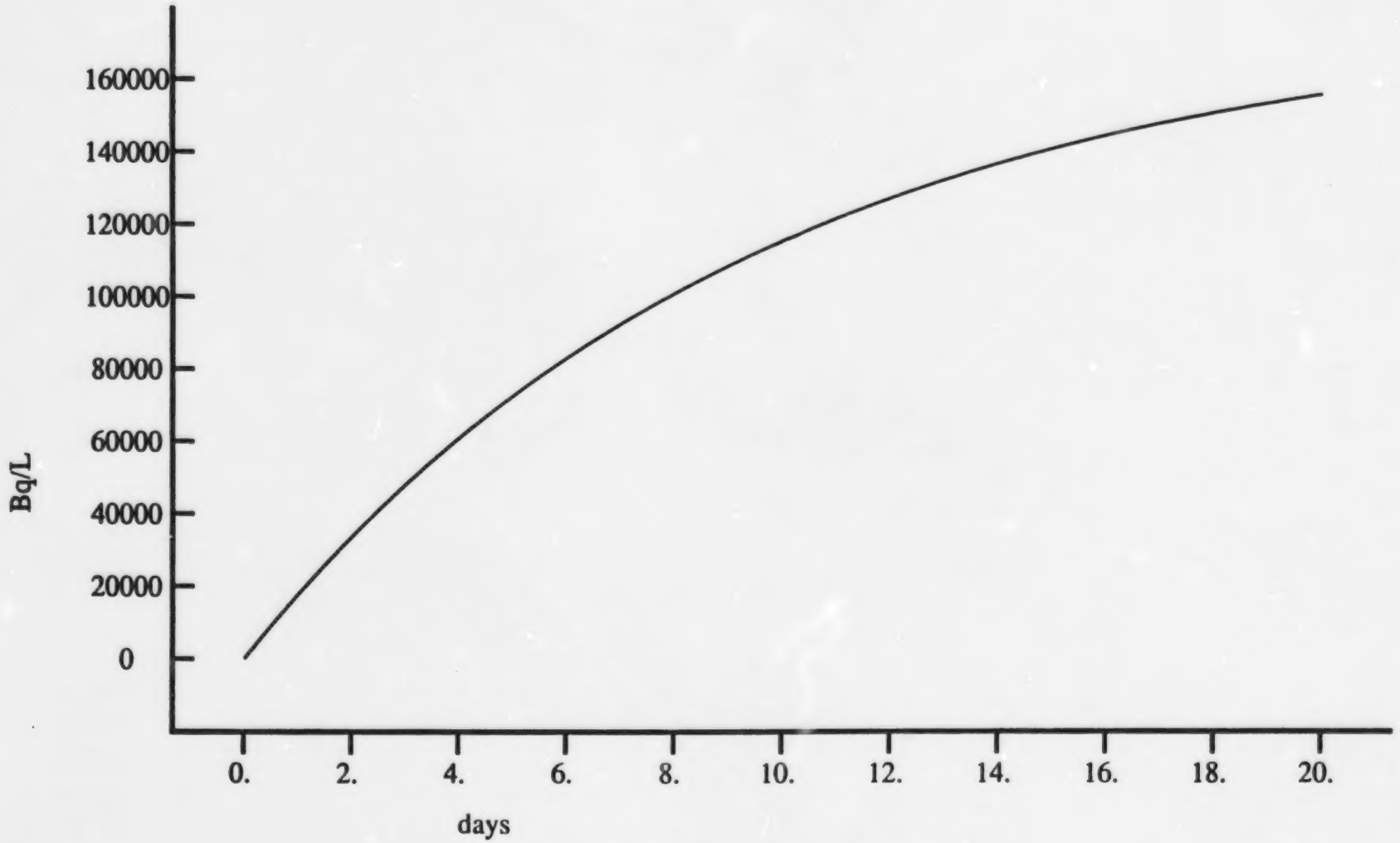

Figure 8.7c Ra-226 Flux from Water in Control

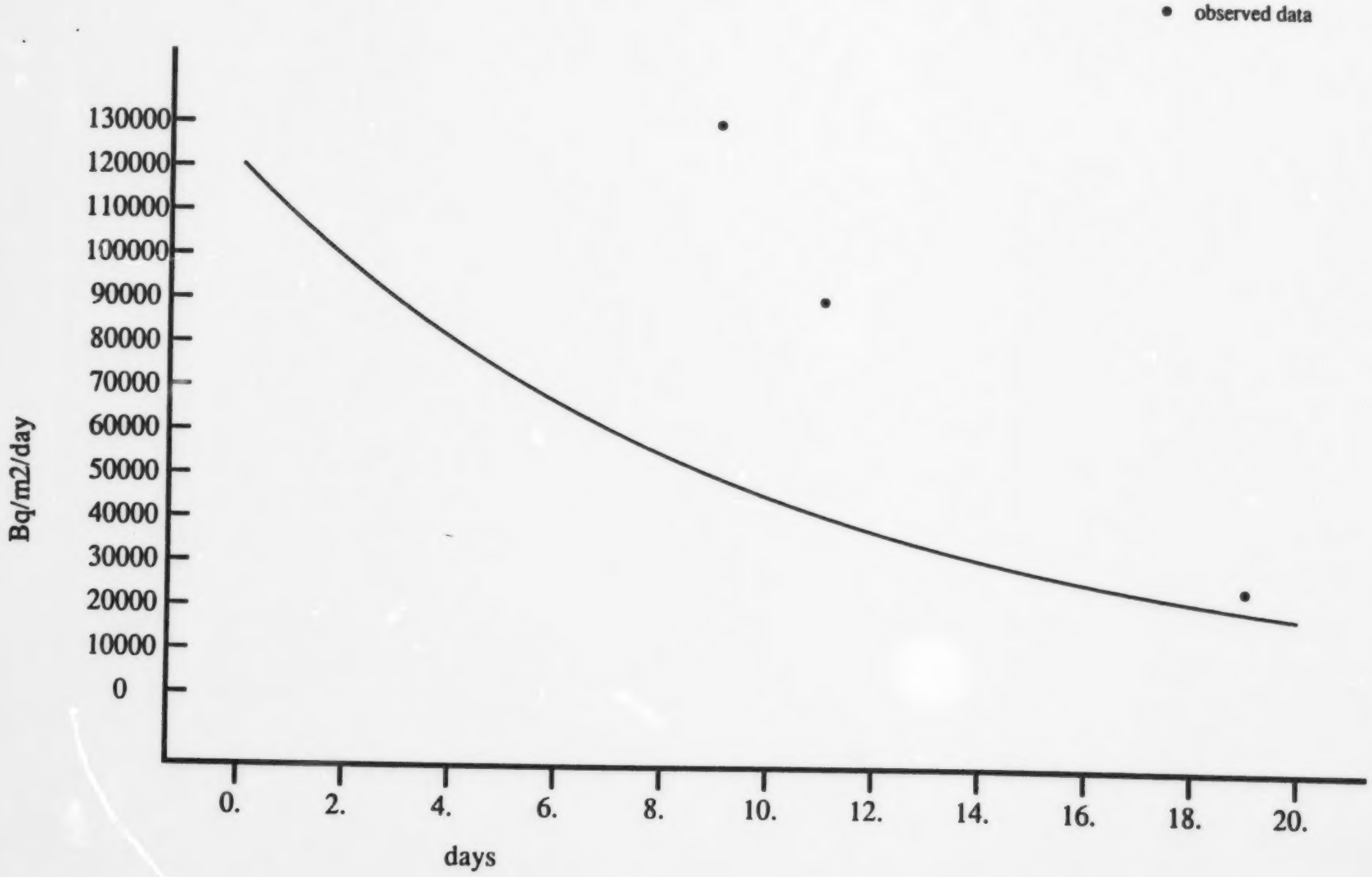

ıre 8.7d ln Ra-226 Removal from Control

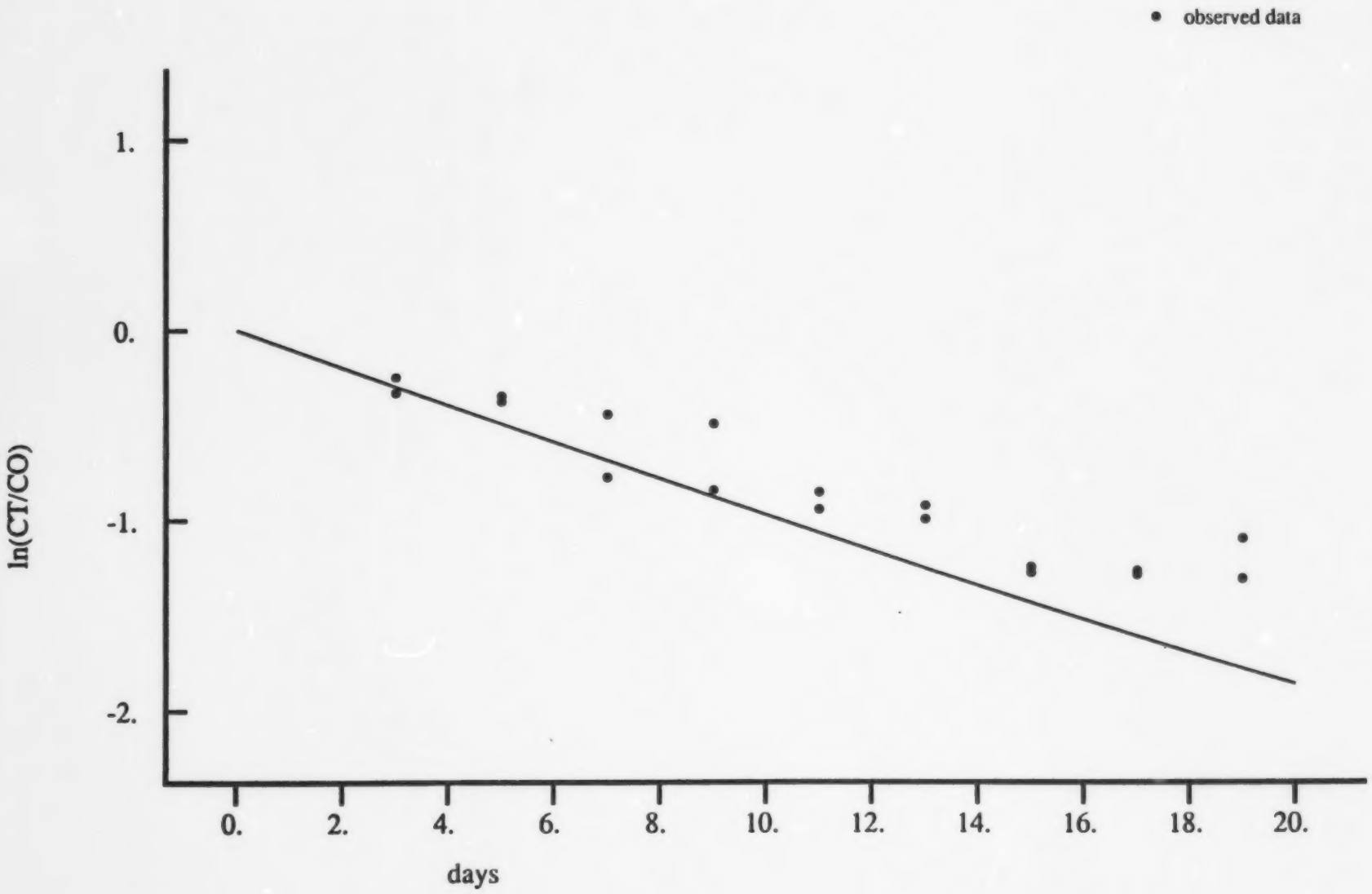

Figure 8.7e Ra-226 Desorption Rate in Control

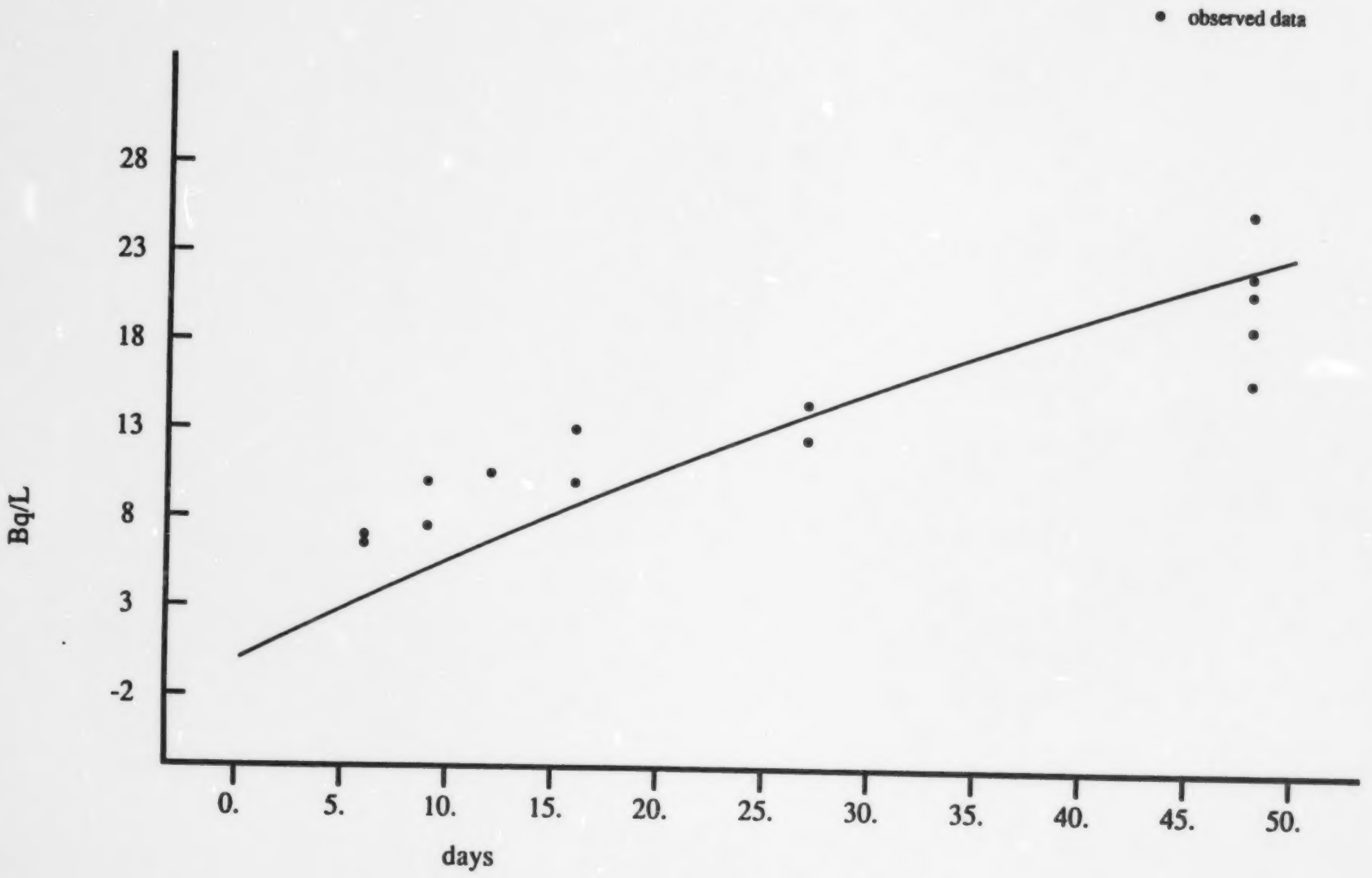

Figure 8.8a Ra-226 Removal in Particulate Addition

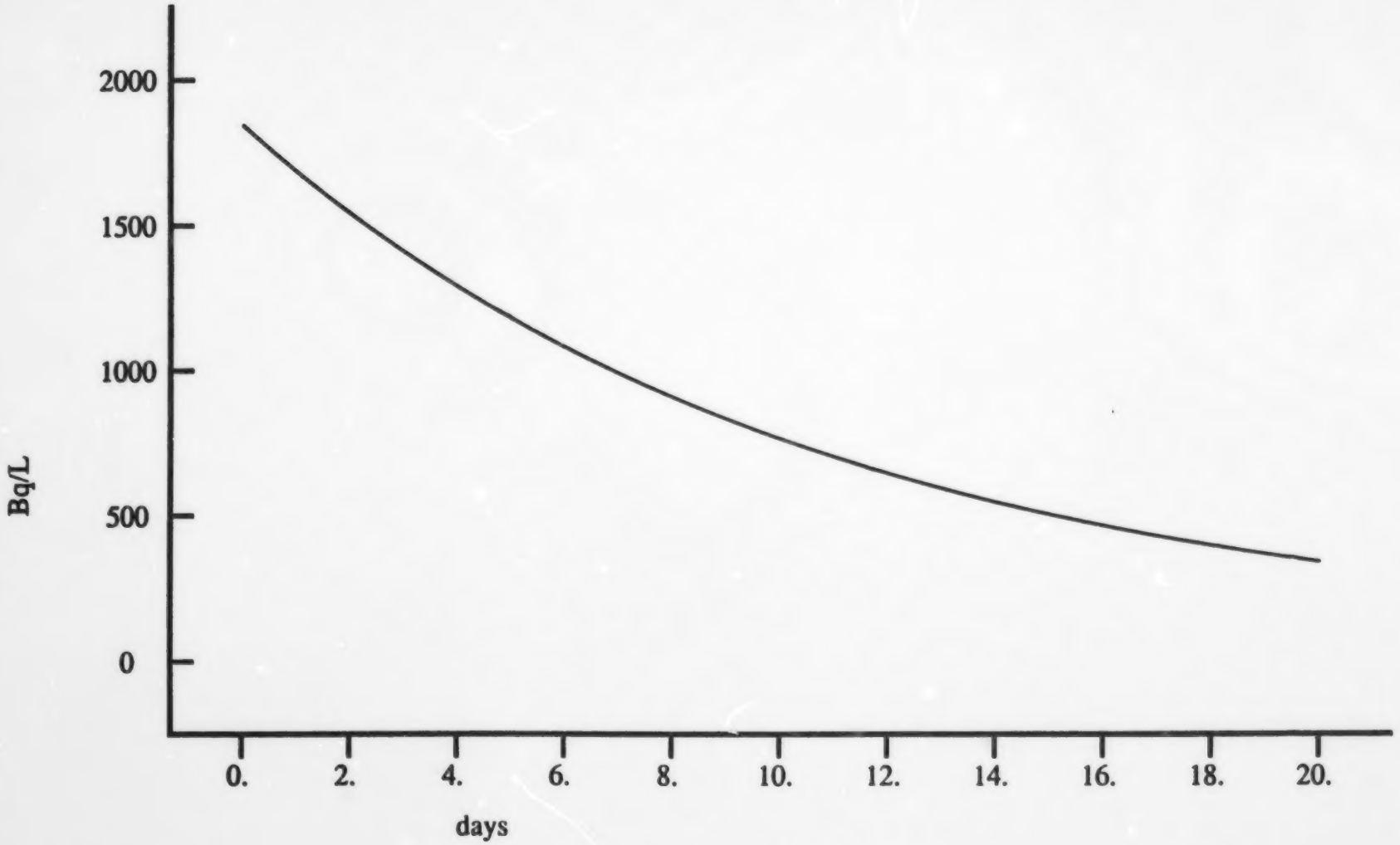

Figure 8.8b Ra-226 Activity in Sediments in Particulate Addition

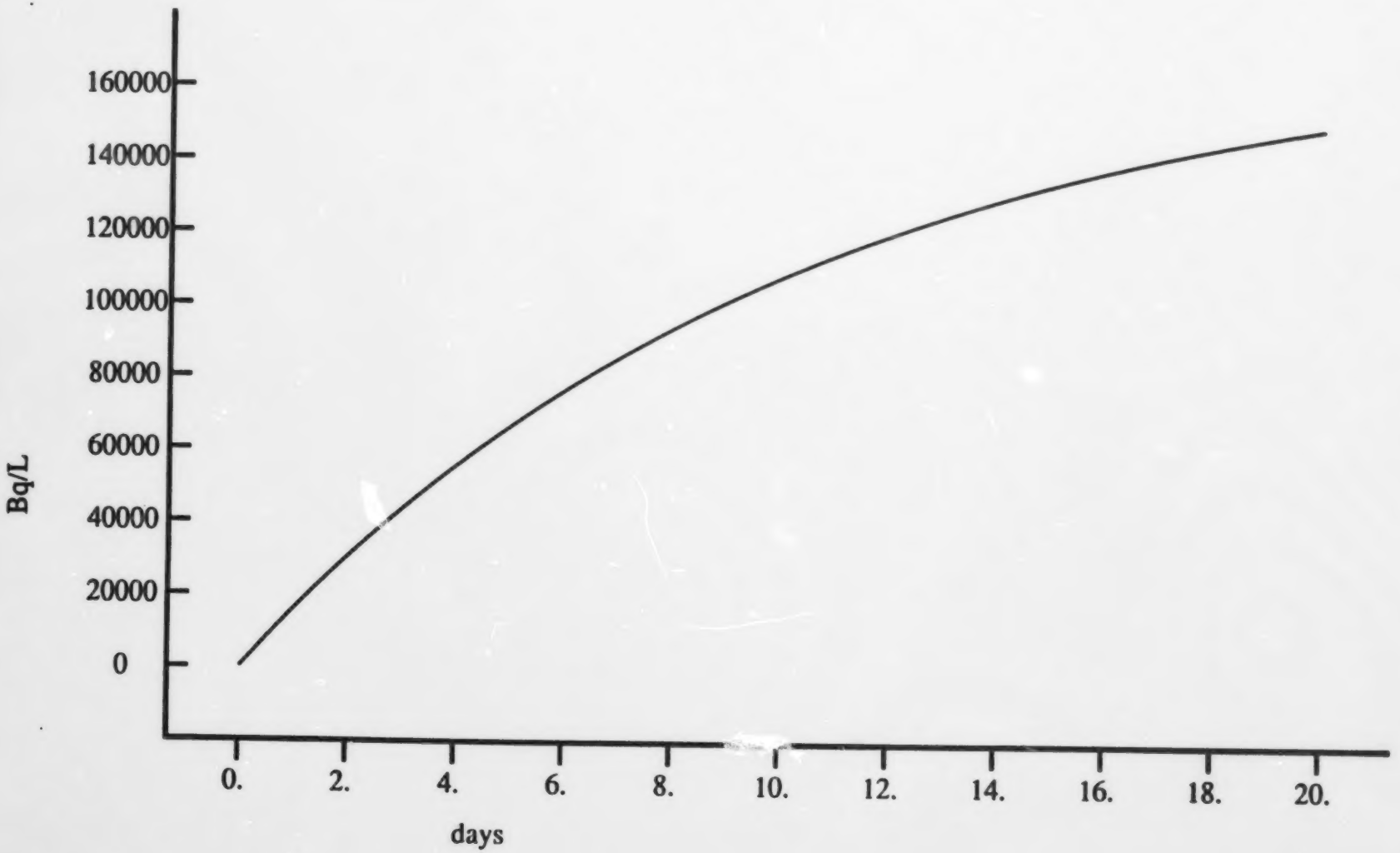

Figure 8.8c Ra-226 Flux from Water in Particulate Addition

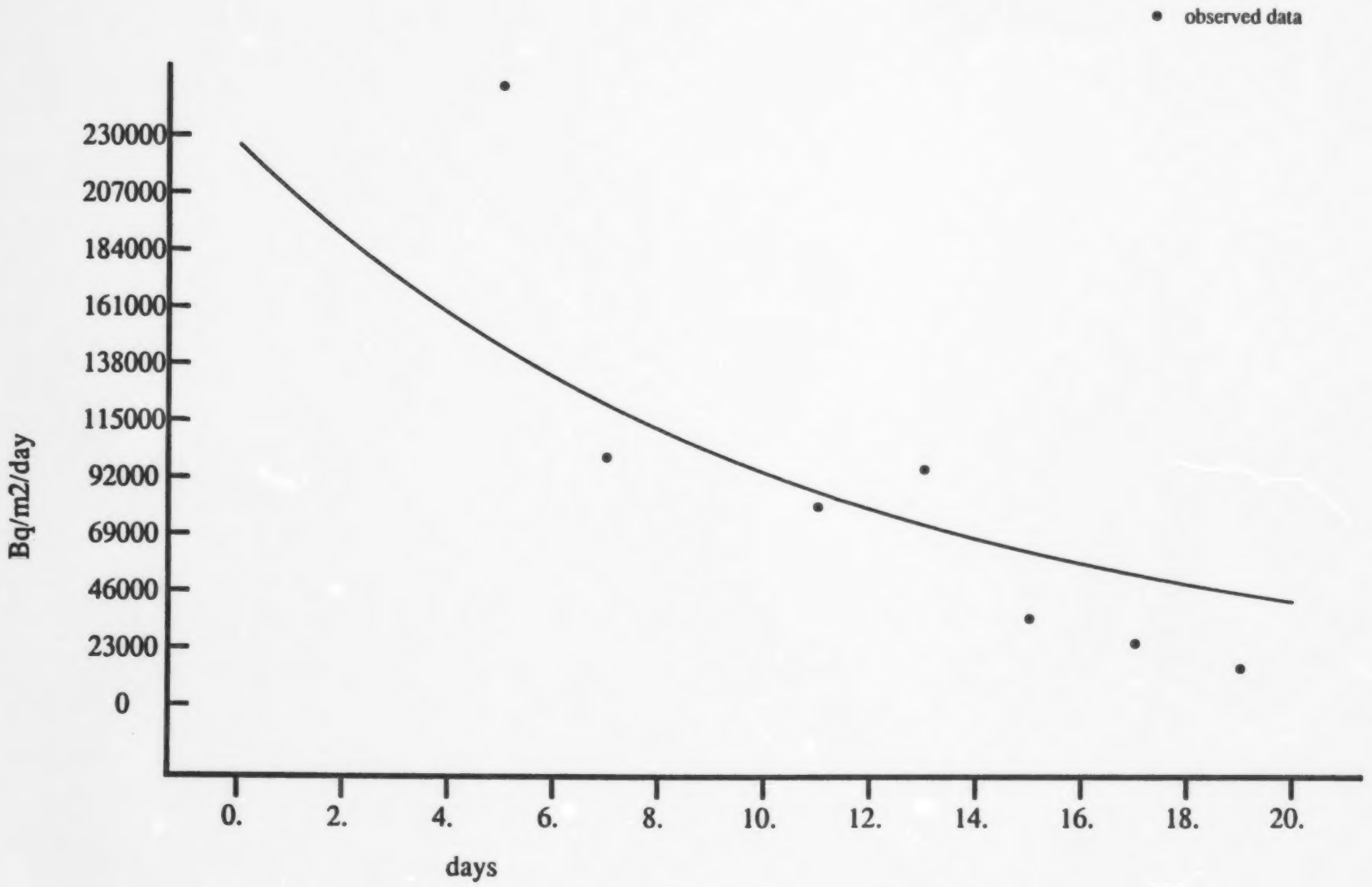

Figure 8.8d ln Ra-226 Removal from Particulate Addition

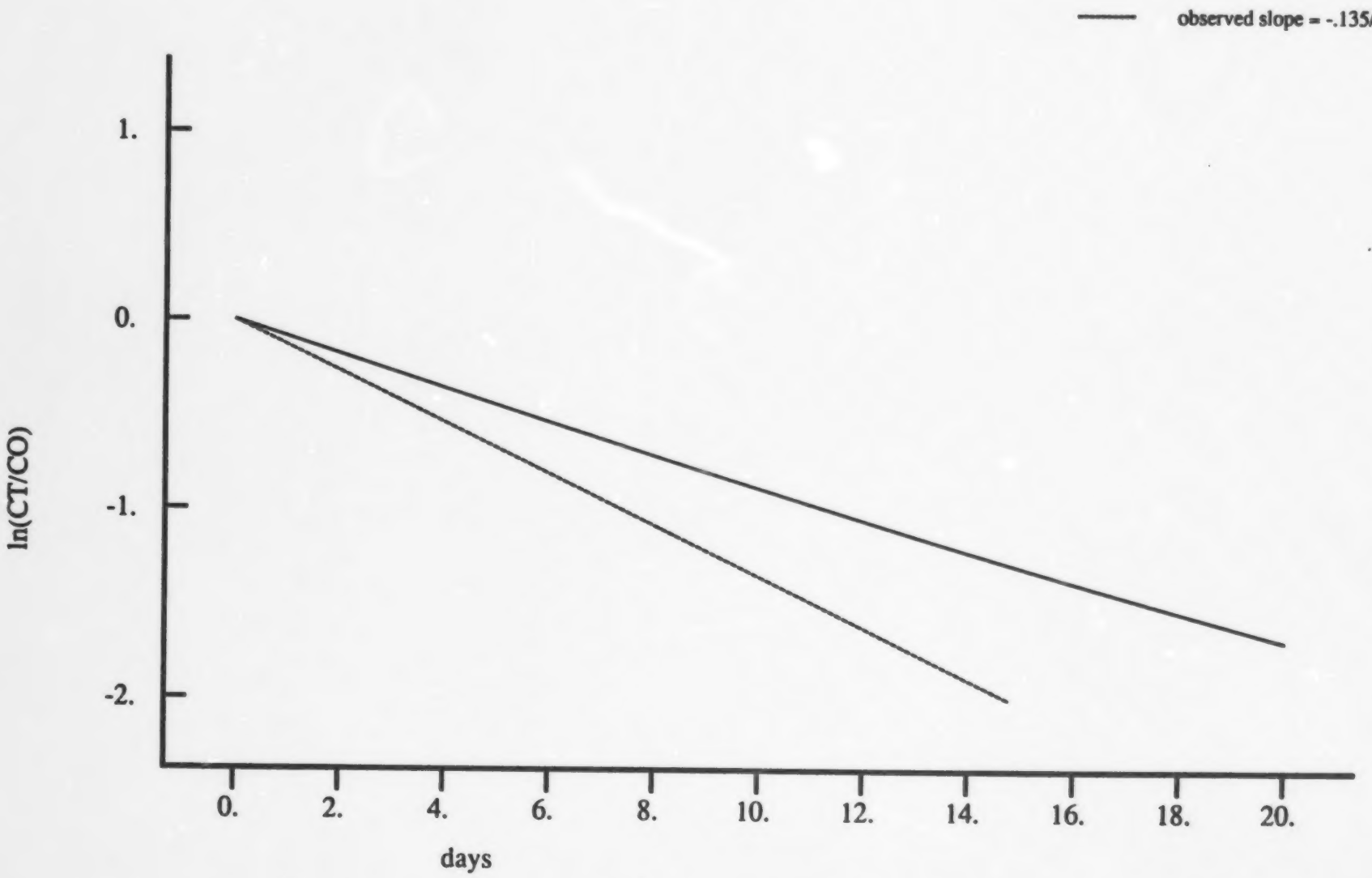

Figure 8.8e Ra-226 Desorption Rate in Particulate Addition

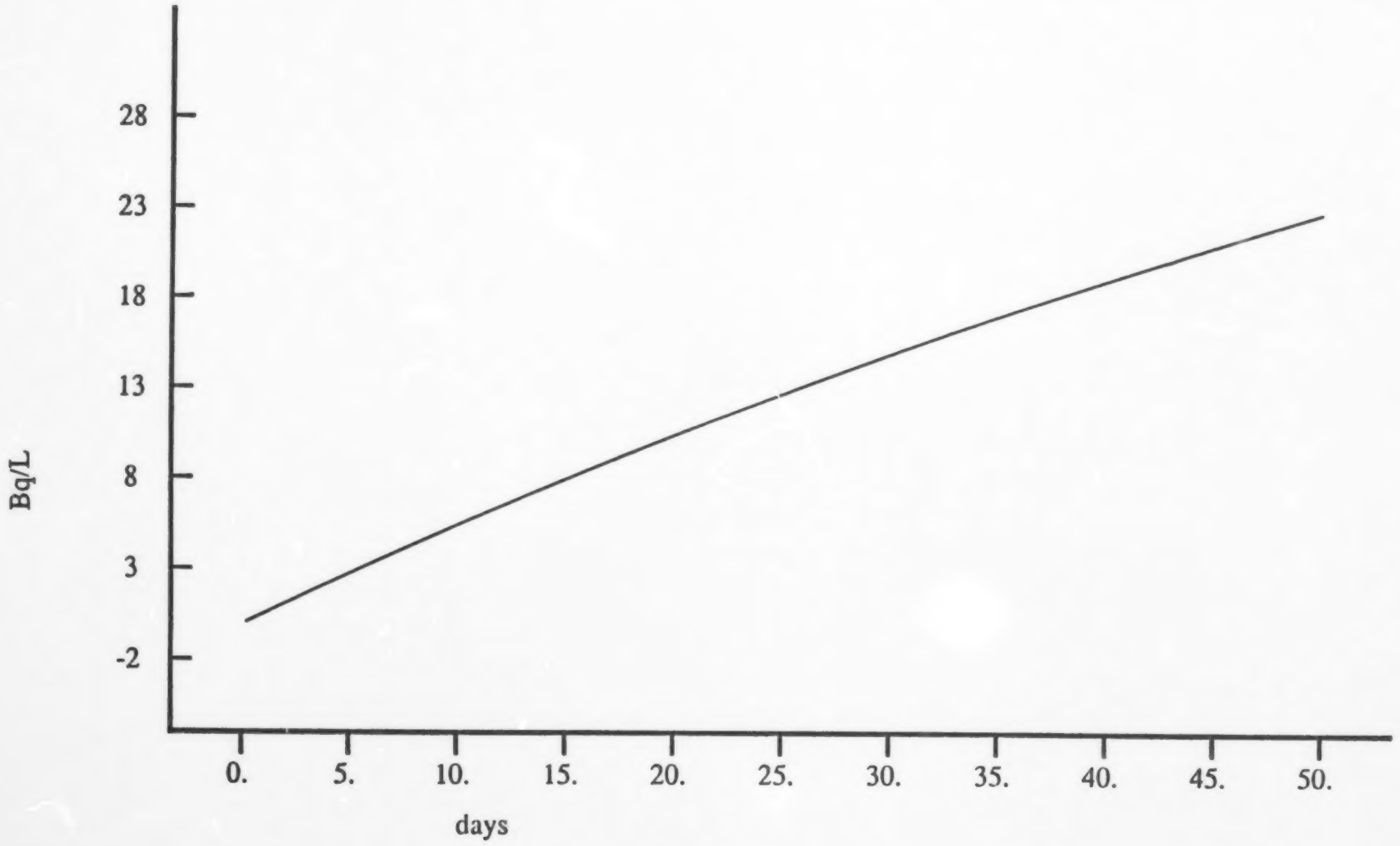

water column sorption constant as the controls; hence, the particulate addition has a higher settling velocity than used in the model simulation.

Comparison of model predictions with observations for Quirke Lake water (Figure 8.9a) and sediments (Figure 8.9b) indicate that the model over predicts removal from the lake by a small amount and too much accumulation in the sediment (observed sediment values are 70 Bq/L, ranging from 20 to 120 Bq/L). Decreasing the sediment-water mass transfer coefficient by 50% results in better agreement (Figure 8.10a,b) but there is still excessive sediment accumulation predicted by the model, if the hypothesis is valid: that the sediments are at a higher activity level than steady-state concentration would predict, given the current water column activity. However, due to the rapid time to steady-state predicted by the model (Fgure 8.9) between sediments and water, a steady-state condition between the sediment and water column may be plausible.

Future work will require further checks upon the model calibration achieved in this study, measurements of sorption coefficients, and studies upon the physiochemical form of Ra-226 in sediments to increase confidence in these model calculations.

Figure 8.9a Ra-226 Activity in W Column of Quirke Lake

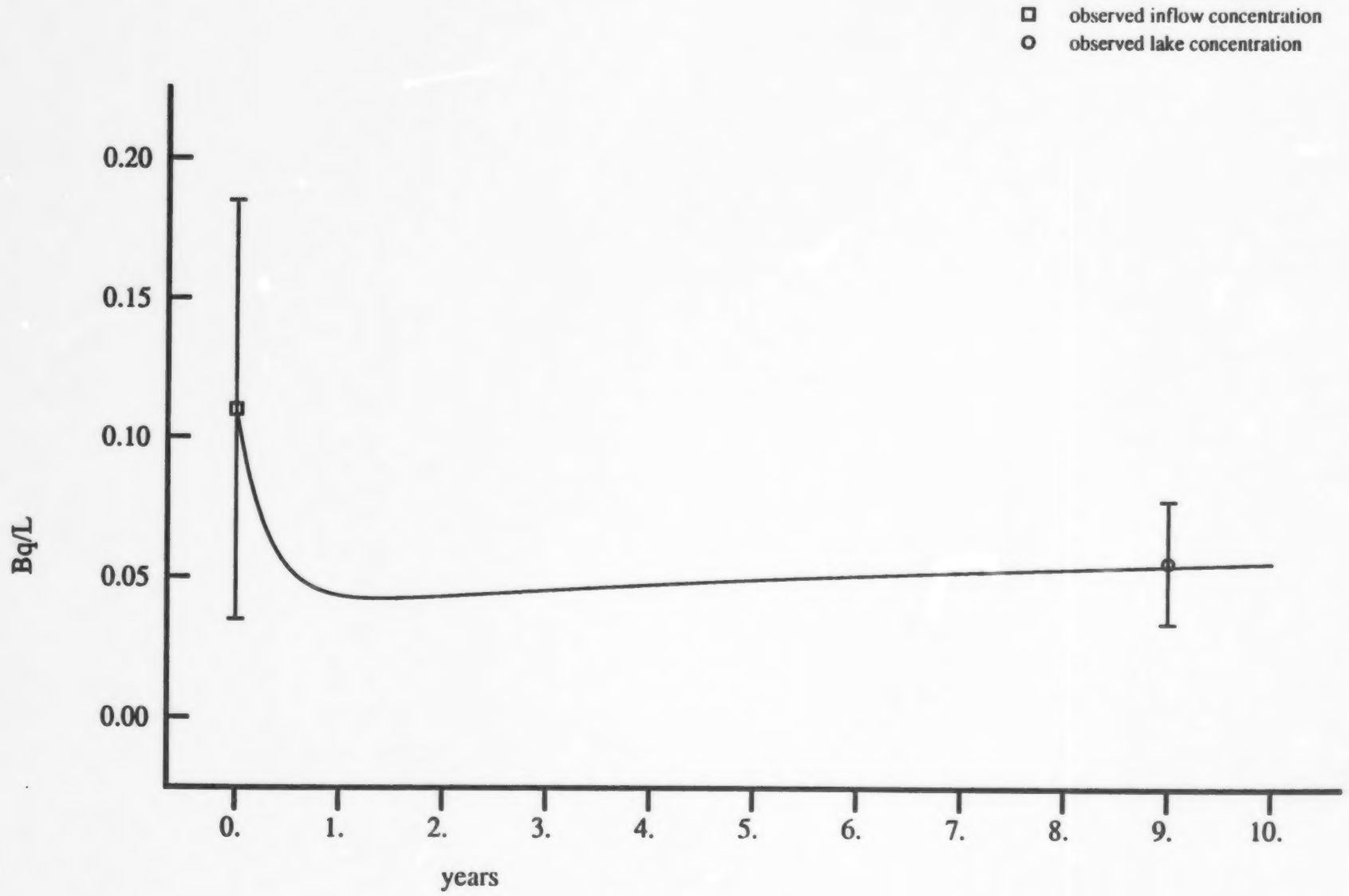

Figure 8.9b Ra-226 Activity in Sediments of Quirke Lake

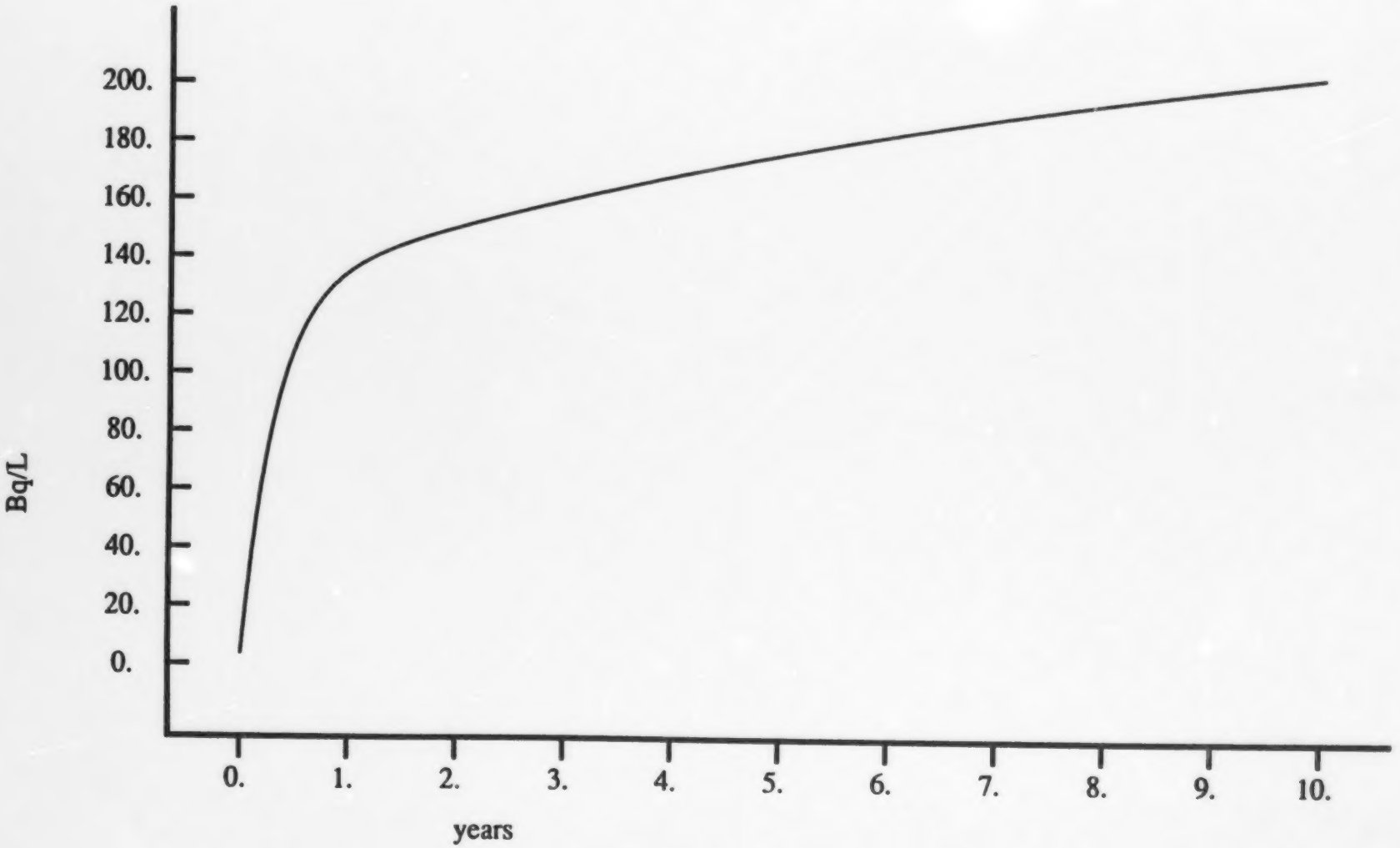

Figure 8.10a Ra-226 Activity in Water Column of Quirke Lake for KS = 0.1

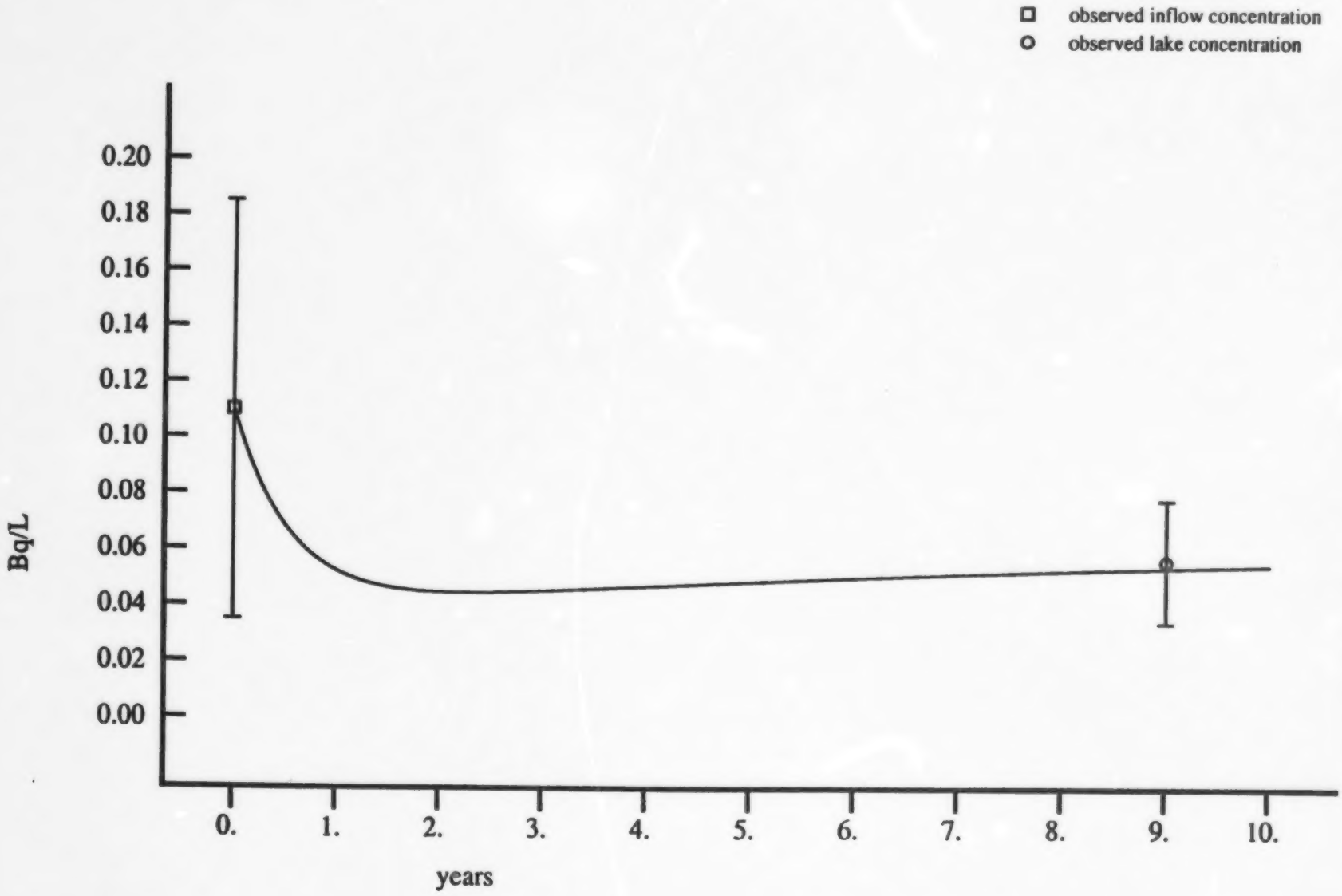

Figure 8.10b Ra-226 Activity in Sediments of Quirke Lake for KS = 0.1

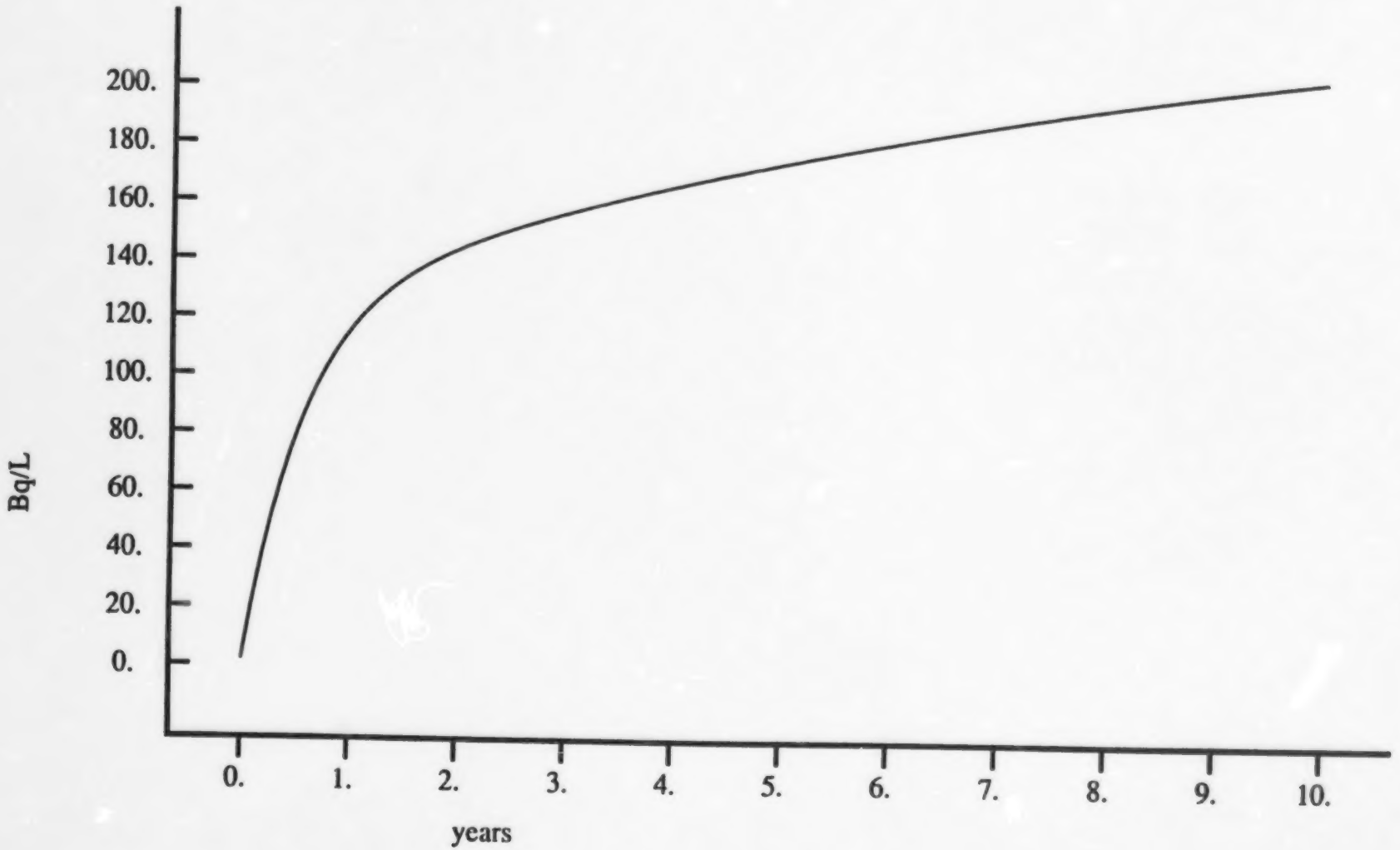

9.0 SUMMARY

Uranium mining and milling operations have been carried out in the Elliot Lake, Ontario region since 1955. Quirke Lake, situated near the headwaters of the Serpent River watershed, receives aqueous discharges from mill process wastes, mine waters and tailings seepage. These discharges typically contain high concentrations of U-238 and Th-232 decay chain radionuclides, as well as metals and other inorganic materials. Once released into the environment, these radionuclides are transported through environmental pathways and may impact radiologically on human receptors and natural biota.

BEAK developed a mathematical model for the AECB to predict aqueous transport and consequence (dose commitment) due to releases of radionuclides into Quirke Lake. This model provided a framework for testing the sensitivity of model outcome (dose) to environmental processes, and provided focus for defining the necessary environmental measurements for model calibration and fine-timing. A study of radionuclide sedimentation undertaken for the Ontario Ministry of the Environment determined radionuclide accumulation rates in the deep basis of Quirke lake.

BEAK undertook the present study to carry out a series of field and laboratory measurements to develop a better understanding of watershed processes affecting radionuclide transport in the upper Serpent River system, and to provide information for calibration and refinement of the radionuclide transport model.

Sedimentation rates were measured at various water depths in Quirke Lake using sediment cores and analysis of core profiles of fossil pollen, fossil diatoms and total thorium to estimate whole sediment accumulation rates in recent years (since the beginning of uranium mining and milling) and over the long-term (over the previous 150 years). Average sedimentation rates in Quirke Lake were estimated at 141 $g.m^{-2}.yr^{+}$ for recent sediments, and 44 $g.m^{-2}.yr^{-1}$ for pre-mining sediments. Based on average radionuclide activities measured in the surfical sediments around Quirke Lake, present radionuclide sedimentation rates were found to be in the range of 500 - 2,000 $Bq.m^{-2}.yr^{-1}$ for Th-230, Pb-210 and Po-210, 200 - 1,000 $Bq.m^{-2}.yr^{-1}$ for Ra-226, 30 - 110 $mg.m^{-2}.yr^{-1}$ for U, 170 - 610 $Bq.m^{-2}.yr^{-1}$ for Th-232, and 40 - 180 $Bq.m^{-2}.yr^{-4}$ for Th-228. These accumulation rates are about two orders of magnitude greater than rates observed in the pre-mining sediments.

Sediment traps were used to collect particles settling from water column in Quirke Lake, and to measure radionuclide activities on the collected particles. These measurements were used to provide a measurement of sediment resuspension at the sediment-water interface, and to provide an independent verification of sediment core-derived sedimentation rates. Erosion of the bottom sediments was found to contribute to higher particle and radionuclide settling rates with increasing proximity to the sediment-water interface. This resuspension may contribute to the translocation of contaminated sediments within the lake, and to downstream export. Mass accumulation rates determined by sediment traps were greater than those measured from sediment cores, apparently due to the effects of resuspension. Radionuclide fluxes measured by sediment trap were in reasonable agreement with fluxes measured by sediment core for most radionuclides (mean values differed generally by a factor of 2 or less). Discrepancies in the Ra-226/Pb-210 ratios in bottom sediments and suspended sediments suggest greater remobilization of Ra-226 of Pb-210 back to the water column. Ratios of Th-228/Th-232 in bottom and suspended sediments similarly suggest much greater post-depositonal remobilization of Th-228 (probably via Ra-228) than of Th-232.

A mass balance analysis for seven U-238 and Th-232 decay series radionuclides was performed on Quirke Lake, using measurements of water-borne radionuclide concentrations and measured sedimentation rates. The results indicate that Ra-226, uranium, Th-230 and Th-232 are mostly retained within Quirke Lake, but that Ra-228 and Th-228 are retained much less than their sister radioisotopes. This is caused by ingrowth from their parents within the lake. The measured sedimentation flux agrees with that calculated from the mass balance for uranium and Ra-226, but is over an order of magnitude higher than the mass balance calculated flux for Th-230 and Th-232. It is possible that particulate components are difficult to measure in the inflow. A similar observation was made independently by researchers working on Keewatin District lakes.

Mineralogical, chemical extraction and adsorption studies were performed on the sediments of Quirke Lake. The results suggest that Ra-226 and barium are distributed throughout various sediment fractions (adsorbed, carbonates etc.) Distinct grains of barite and uraninite were identified. The measured adsorption values are similar to literature values for Pb-210 and Ra-226, but were below literature values for Th. A possible explanation for the literature values based upon coprecipitation, precipitation and ion exchange concepts was advanced.

Ra-226 and Ba-133 were spiked into a limnocorral to ascertain their removal velocities. The observed removal velocities are similar to values observed for other radionuclides. A large fraction of the removal can be explained by sedimentation but diffusion into bottom sediments can also explain the removal rate. Modelling techniques or other field measurements are required to determine the relative significance of settling and diffusion for controlling radionuclide removal.

To scale short-term (limnocorral) measurements to the long-term (Quirke Lake), the model previously developed for the AECB was used to evaluate the data gathered in this project. As well, other models which are simpler and more complex were used. The results from all models provide insights into radionuclide behaviour but do not provide definitive conclusions. The models can explain the short-term removal rates, using settling fluxes and diffusional fluxes to explain removal. But using these values of diffusional processes, the models calculate that the long-term patterns of sediment accumulation which are typically observed, cannot be maintained because diffusion would remove too much material. This suggests that diffusional fluxes may have a lower effect in the long term than in the short term. It shows that the scale-up of limnocorral data to lake scale requires further evaluation. It suggests that settling processes may be the main mechanism for removal of radionuclides to the sediments over the long-term with the significance of diffusion being mainly to release radionuclides back to the water column.

The model previously developed for the AECB was modified to account for complexation and particle erosions. Its predictions agree reasonably well with observations for the influx and efflux of Ra-226 in the limnocorral. It predicts slightly high values for Ra-226 accumulation in Quirke Lake. Further studies are required to test its degree of validation.

With respect to the impact of sediments upon water column activity over the long-term, the data of this project have shown that sediments will be a net source of Ra-228, Th-228, Po-210 and possibly Pb-210. The magnitude of the sediments as a source for Ra-226 and other thorium isotopes is unclear without further evaluation.

This project suggests the need for more experimental measurements. These include:

(i) a field program to evaluate thorium mass balances.

(ii) experimental measurement of the kinetics of adsorption and desorption of the U-238 decay series radionclides and modelling studies to assess the long-term release rate of these nuclides from the sediments.

(iii) validation studies of these measurements with data gathered in this project.

(iv) a synthesis of the modelling results initialed in this project.

10.0 REFERENCES

Agemian, H. and A.S.Y. Chau. "A Study of Different Analytical Extraction Mthods for Nondetritial Heavy Metals in Aquatic Sediments". Arch. Environ. Contam. Toxicol., 6, pp. 69, (1977).

Agemian, H. and A.S.Y. Chau. "Evaluation of Extraction techniques for the Determination of Metals in Aquatic Sediments". Analyst (Great Britain), 101, pp. 761, (1976).

Appleby, P.G. and F. Oldfield. 1983. The assessment of Pb-210 data from sites with varying sediment accumulation rates. Hydrobiologia 103: 29-35.

BEAK (1985). Descriptive Algorithm Developemnt for Physical, Chemcial and Biological Processes Operational in Uranium Mill Tailings. Report to CANMET, EM&R.

Battarbee, R.W. 1973. A new method for the estimation og absolute micro-fossil numbers, with reference especially to diatoms. Limnol. Oceanogr. 18: 647-653.

Beak Consultants Limited (BEAK). 1983. An approach to the calculation of dose commitment arising from different methods for the long-term management of uranium mill tailings through aquatic pathways. Atomic Energy Control Board, Research Rep. No. INFO-0097.

Bell, G.L. and B.J. Eadie. 1983. Variations in the distribution of suspended particles during an upwelling event in Lake Michigan in 1980. J. Great Lakes Res. 9: 559-567.

Bloesch, J. and N.M. Burns. 1980. A critical review of sedimentation trap technique. Schweiz. Z. Hydrol. 42: 15-55.

Bloesch, J. and R.D. Evans. 1982. Lead-210 dating of sediments compared with accumulation rates estimated by natural markers and measured with sediment traps Hydrobiologia 92: 579-586.

Brunskill, G.J. and P. Wilkinson. 1987. Annual supply of ^{238}U, ^{230}Th, ^{226}Ra, ^{210}Pb and ^{210}Po to Lake 239 (Experimental Lakes Area, Ontario) from terrestrial and atmospheric sources. Can. J. Fish. Aquat. Sci. 44 (in press).

Brunskill, G.J., D. Povoledo, B.W. Graham and M.P. Stainton. 1971. Chemistry of the surface sediments of sixteen lakes in the Experiamental Lakes Area, norethwestern Ontario. J. Fish. Res. Board Can. 28: 277-294.

Carignan, R. and R.J. Flett. 1981. Postdepositional mobility of phosphorus in lake sediments. Limnol. Oceanogr. 26: 361-366.

Chant, L. and R.J. Cornett. 1987. Measuring Contaminant Transport Rates Between Water and Sediments using Limnocorrals. CRNL Manuscript.

Charles, D. 1985. Relationships between surface sediment diatom assemblages and lakewater characteristics in Adirondack lakes. Ecology 66: 994-1011.

Chiu, N.W. and J.R. Dean. 1984. Analytical methods manual, National Uranium Tailings Program. A Report by Monenco Consultants Limited for Energy, Mines and Resources Canada.

Cornwell, J.C. 1985. Sediment accumulation rates in an Alaskan arctic lake using a modified ^{210}Pb technique. Can. J. Fish. Aquat. Sci. 42: 809-814.

Dave, R.B. and D.C. Anderson. 1984. Methods of pH calibration of sedimentary diatom remains for reconstructing history of pH in lakes. Hydrobiologia 120: 69-87.

DeMarch, L. 1978. Permanent sedimentation of nitrogen, phosphorus and organic carbon in a high arctic lake. J. Fish. Res. Board Can. 35: 1089-1094.

Delorme, L.D., S.R. Esterby and H. Duthie. 1984. Prehistoric pH trends in Kejimkujic Lake, Nova Scotia. Int. Rev. Gesamten Hydrobiol. 69: 41-55.

Dickman, M., S. Dixit, J. Fortescue, R. Barlow and J. Terasmae. 1984. Diatoms as indicators of the rate of lake acidification. Water Air Soil Pollut. 21: 375-386.

Earle, J.C., H.C. Duthie and W.A. Glooschenko. 1987. Spatial variabillity of diatoms on the surface sediment of Precambrian Shield lakes. In: F. Round (Ed.). Proc. Ninth Int. Diatom Symp., Bristol, U.K. (in press).

Energy, Mines and Resources Canada (EMR). 1981. Report of the National Technical Planning Group on Uranium Tailings Research.

Environment Canada. 1985. Historical streamflow summary, Ontario, to 1984. Inland Waters Directorate, Water Resources Branch, Water Survey of Canada, Ottawa.

Evans, R.D. and F.J. Rigler. 1980a. The measurement of whole lake sediment accumulation and phosphorus retention using lead-210 dating. Can. J. Fish. Aquat. Sci. 37: 817-822.

Evans, R.D. and F.J. Rigler. 1980b. Calculation of the total anthropogenic lead in the sediments of a rural Ontario Lake. Environ. Sci. Technol. 14: 216-218.

Evans, R.D. and F.J. Rigler. 1983. A test of lead-210 dating for the measurement of whole lake soft sediment accumulation. Can. J. Fish. Aquat. Sci. 40: 506-515.

Gardner, W.D. 1980. Field assessment of sediment traps. J. Mar. Res. 38: 41-52.

Hargrave, B.T. and N.M. Burns. 1979. Assessment of sediment trap collection efficiency. Limnol. Oceanogr. 24: 1124-1135.

Huhn, F.J. 1974. Lake sediment records of industrialization in the Sudbury area of Ontario. M.Sc. Thesis, University of Toronto, Toronto, Ontario. 84 p.

Hustedt, F. 1939. Systematische and okologische Unterschungen uber die Diatomeen-Flora von Java. Bali, und Sumatra. Arch. Hydrobiol. Suppl. 16: 274-394.

International Joint Commission (IJC). 1983. Report on Great Lakes water quality. Appendix on radioactivity. Great Lakes Water Quality Board, Report to the International Joint Commission.

Kemp, A.L.W. and N.S. Harper. 1976. Sedimentation rates and a sediment budget for Lake Ontario. J. Great Lakes Res. 2: 324-340.

Kemp, A.L.W., C.I. Dell and N.S. Harper. 1978. Sedimentation rates and a sediment budget for Lake Superior. J. Great Lakes Res. 4: 276-287.

Kipphut, G.K. 1978. An investigtion of sedimentary processes in lakes. Ph.D. Thesis, Columbia University, New York, NY. 180 p.

Lasaga, A.C. (1984). "Chemical Kinetics of Rock-Water Interactions". J. Geophys. Res., 89(B6), (June 10), pp 4009-4025.

Lush, D.L., W.J. Snodgrass and P.M. McKee. 1982. Aquatic pathway variables affecting the estimation of dose commitment from uranium mill tailings. p. 483-503. In: Management of Wastes from Uranium Mining and Milling. International Atomic Energy Agency, Vienna, IAEA-SM-262/9.

Malo, B.A. "Partial Extraction of Metals from Aquatic Sediments". Environ. Sci. Technol, 11(3), pp. 277-282, (1977).

McAndrews, J.H. 1981. Lake Quarternary of Ontario: temperature trends from the fossil pollen record. p. 319-333. In: W.C. Maheney (Ed.). Quarternary Paleoclimate. GeoAbstracts, Norwich.

McAndrews, J.H. and M. Boyko-Diakonow. 1987. Pollen analysis of varved sediment at Crawford Lake, Ontario: evidence of Indian and European farming. In: Geology of Canada and Greenland. Geological Survey of Canada, Ottawa, Ontario (in press).

McAndrews, J.H., A.A. Berti and G. Norris. 1973. Key to the Quarternary pollen and spores of the Great Lakes region. Royal Ontario Museum Miscellaneous Publication. p. 61.

McKee, P.M., D.R. Hart, A.J. Burt, H.C. Duthie and J.H. McAndrews. 1985. A survey of the benthos and sediments of Quirke Lake. A Report to the Ontario Ministry of the Environment, Northeastern Region.

McKee, P.M., W.J. Snodgrass, D.R. Hart, H.C. Duthie, J.H. McAndrews and W. Keller. 1987. Sedimentation rates and sediment core profiles of ^{238}U and ^{232}Th decay chain radionuclides in a lake affected by uranium mining and milling. Can. J. Fish. Aquat. Sci. 44: 390-398.

Merilainen, J. 1967. The diatom flora and the hydrogen ion concentration of the water. Ann. Bot. Fenn. 4: 51-58.

Neame, P.A., J.R. Dean and B.G. Zytaruk. 1982. Distribution and concentrations of naturally-occurring radionuclides in sediments in a uranium mining area of northern Saskatchewan, Canada. Hydrobiologia 91: 353-361.

Nozaki, Y., Y. Horibe and H. Tsubota. 1981. The water column distributions of thorium isotopes in the western North Pacific. Earth Planet. Sci. Lett. 54: 203-216.

Nriagu, J.O. (Ed.) (1976). Environmental Biogeochemistry. Ann Arbor Science. Ann Arbor, 2 volumes.

Nriagu, J.O. (Ed.) (1979b). Copper in the Environment. Wiley, 2 volumes.

Nriagu, J.O. (Ed.) (1980a). Calcium in the Environment. Wiley, 2 volumes.

Nriagu, J.O. (Ed.) (1980b). Nickel in the Environment. Wiley, 2 volumes.

Nriagu, J.O. (Ed.) (1980c). Zinc in the Environment. Wiley. 453 pp.

Nriagu, J.O. (1983). "Arsenic enrichment in lakes near the smelters at Sudbury, Ontario". Geoch. et Coscomch Acta, 47. p. 1623-1526.

Nriagu, J.O. (Ed.) (1978a). The Biogeochemistry of Lead in the Environment. Wiley, 2 volumes.

Nriagu, J.O. (Ed.) (1978b). Sulphur in the Environment. Wiley.

Nriagu, J.O. (Ed.) (1979a). The Biogeochemistry of Mercury in the Environment. Elsevier. 696 pp.

Nyffeler, U.P., P.H. Santschi and Y.-H. Li. 1986. The relevance of scavenging kinetics to modelling of seidment-water interactions in natural waters. Limnol. Oceanogr. 31: 277-292.

Renberg, I. and T. Hellberg. 1982. The pH history of lakes in southwest Sweden, as calculated from the subfossil diatom flora of the sediments. Ambio 11: 30-33.

Rimsted, J.D. and H.L. Barnes (1980). "The Kinetics of Silica-Water Interactions". Geochem. Cosmochem. Acta., 49, pp. 1683-1699.

Risto, B., R.J. Cornett and L. Chant. 1987. Resuspension of sediments and contaminants in a small Shield lake. In: Proceedings from the 4th International Symposium on the Interaction between Sediments and Water, Melbourne, Australia.

Robbins, J.A. 1978. Geochemical and geophysical applications of radioactive lead. p. 285-393. In: J.O. Nriagu (Ed.). The Biogeochemistry of Lead in the Environment. Elsevier/North Holland, Amsterdam, The Netherlands.

Robbins, J.A. and E. Callender. 1975. Diagenesis of manganese in Lake Michigan sediments. Am. J. Sci. 275: 512-533.

Rosa, F., J.O. Nriagu and H.K. Wong. 1983. Particulate flux at the bottom of Lake Ontario. Chemosphere 12: 1345-1354.

Santschi, P.H., P. Bower, U.P. Nyffeler, A. Azevedo and W.S. Broecker. 1983. Estimates of the resistance to chemical transport posed by the deep-sea boundary layer. Limnol. Oceanogr. 28: 899-912.

Santschi, P.H., U.P. Nyffeler, R.F. Anderson, S.L. Schiff, P. O'Hara and R.H. Hesselein. 1986. Response of radioactive trace metals to acid-base titrations in controlled experimental ecosystems: evaluation of transport parameters for application to whole-lake radiotracer experiments. Can. J. Fish. Aquat. Sci. 43: 60-77.

Schindler, D.W., R.H. Hesslein, R. Wagemann and W.S. Broecker. 1980. Effects of acidification on mobilization of heavy metals and radionuclides from the sediments of a freshwater lake. Can. J. Fish. Aquat. Sci. 37: 373-377.

Smithson, G.G. 1979. Radiochemical procedures for determination of selected members of the uranium and thorium series. CANMET Rep. 78-22.

Snodgrass, W.J. (1980). "Distribution and Behaviour of Nickel in Aquatic Environment". Nickel in the Environment. (J.O. Nriagu ed) pp. 203-274.

Snodgrass, W.J., D.L. Lush, P.M. McKee and R.R. Walker. 1983. An approach to the calculation of dose commitment arising from different methods for the long-term management of uranium mill tailings through aquatic pathways. Atomic Energy Control Board Report, INFO-0097.

Snodgrass, W.J., D.L. Lush, R.R.Walker and W. Bell. 1986. Particle-based lake model for calculating dose commitment. p. 229-241. In: P.G. Sly (Ed.). Sediment-Water Interactions. Springer-Verlag, New York, NY.

Stockmarr, J. 1970. Tablets with spores used in absolute pollen analysis. Pollen Spores 13: 615-621.

Taylor, M.C. 1986. Surficial sedimentary diatoms-limnological relationships in Canadian Shield lakes. M.Sc. Thesis, University of Waterloo, Waterloo, Ontario. 199 p.

Tessier, A., P.G.C. Campbell and M. Bisson (1979). Sequential Extraction Procedure for the Speciation of Particulate Trace Metals. Anal. Chem, 51(7), pp. 844-851.

Tessier, A., P.G.C. Campbell and M. Bisson (1982). "Particulate Trace Metals Speciation in Stream Sediments and Relationships with Grain Size: Implications for Geochemical Exploration". J. Geochem. Explor, 16, pp. 77-104.

Warwick, W.F. 1980. Palaeolimnology of the Bay of Quinte, Lake Ontario: 2800 years of cultural influence. Can. Bull. Fish. Aquat. Sci. 206: 117.

APPENDIX A.1

Method of Concentration of Radionuclides from Bulk Lake Samples

APPENDIX A.1: METHOD OF CONCENTRATION OF RADIONUCLIDES FROM BULK LAKE SAMPLES

Fifty to 200 litre samples of lake water were collected using two types of apparatus: surface sampling by inserting 20 L buckets into the water and pumping the water from depth. Samples were not filtered in order to allow a measurement of total radionuclide content. The water samples were acidified to pH 2 by addition of nitric acid for sample preservation before shipping to BEAK's laboratory.

Thorium, polonium and lead are precipitated from the water sample as hydroxides and collected on an iron-hydroxide floc. Added analytical tracers (U-232, Th-228, Po-209 and stable lead) were allowed to equilibrate for at least one hour, with the acidified (pH 1.5) water sample contained in a 50 to 210 L plastic vessel. After mixing in 2 g of Fe^{3+} (as $FeCl_3$ solution), the pH was increased to 9 to 10 with NaOH, and as large as possible flocs are formed by gentle stirring of the sample. When the floc had settled to the bottom, the supernatant water was siphoned off and the flocculant precipitate poured into a smaller container and centrifuged down. The residual solids were dried overnight ($70^{\circ}C$) in an aluminum dish. The solids were then transported to Becquerel Laboratories for analysis.

Ra-226 and Ra-228 were precipitated by addition of sulphuric acid and barium chloride to the 50 L or 200 L vessel. After one hour was allowed for completion of the coprecipitation reaction, small pin-point, poorly-settling solids were in the water. These solids were coagulated by addition of $FeCl_3$ and pH adjustment, similar to procedures for thorium. Then, the solids were concentrated and dried before shipping for radionuclide analyses.

APPENDIX A.2

Chemical Methods of Analysis by Ministry of the Environment (Ministry of Labour)

LEAD-210 IN WATER

WATER

LET STAND AT LEAST 30 DAYS FOR LEAD-210/BISMUTH-210 EQUILIBRIUM

+ HYDROCHLORIC ACID TO 4M
LEAD CARRIER, BISMUTH CARRIER, ASCORBIC ACID

EXTRACT SEVERAL TIMES WITH 1% DDTC
NOTE TIME

DDTC LAYER

+ 50% SODIUM BISULFATE, NITRIC ACID

HEAT GENTLY TO EXPEL CHLOROFORM

HEAT TO CHAR

WET-ASH WITH NITRIC ACID

EVAPORATE TO DRYNESS

RESIDUE

+ NITRIC ACID, WATER

DILUTE TO 25 mL WITH WATER

1 mL

+ PERCHLORIC ACID
12% THIOUREA

DILUTE TO 10 mL

MEASURE ABSORBANCE AT 470 mμ

DETERMINE BISMUTH CONCENTRATION

24 mL

+ BISMUTH CARRIER, AMMONIUM HYDROXIDE TO pH 8

HEAT IN WATER BATH

CENTRIFUGATE

DISCARD

PRECIPITATE

BISMUTH HYDROXIDE

+ HYDROCHLORIC ACID
WATER

HEAT IN WATER BATH

PRECIPITATE

BISMUTH OXYCHLORIDE

WASH WITH WATER AND METHANOL

MOUNT

COVER WITH AL FOIL (7 MG/CM^2)

BETA-COUNT AFTER 10. H DECAY TIME

NOTE TIME OF COUNT

CENTRIFUGATE

DISCARD

AQUEOUS LAYER

DISCARD

APRIL 1983

RADIUM-226 IN WATER

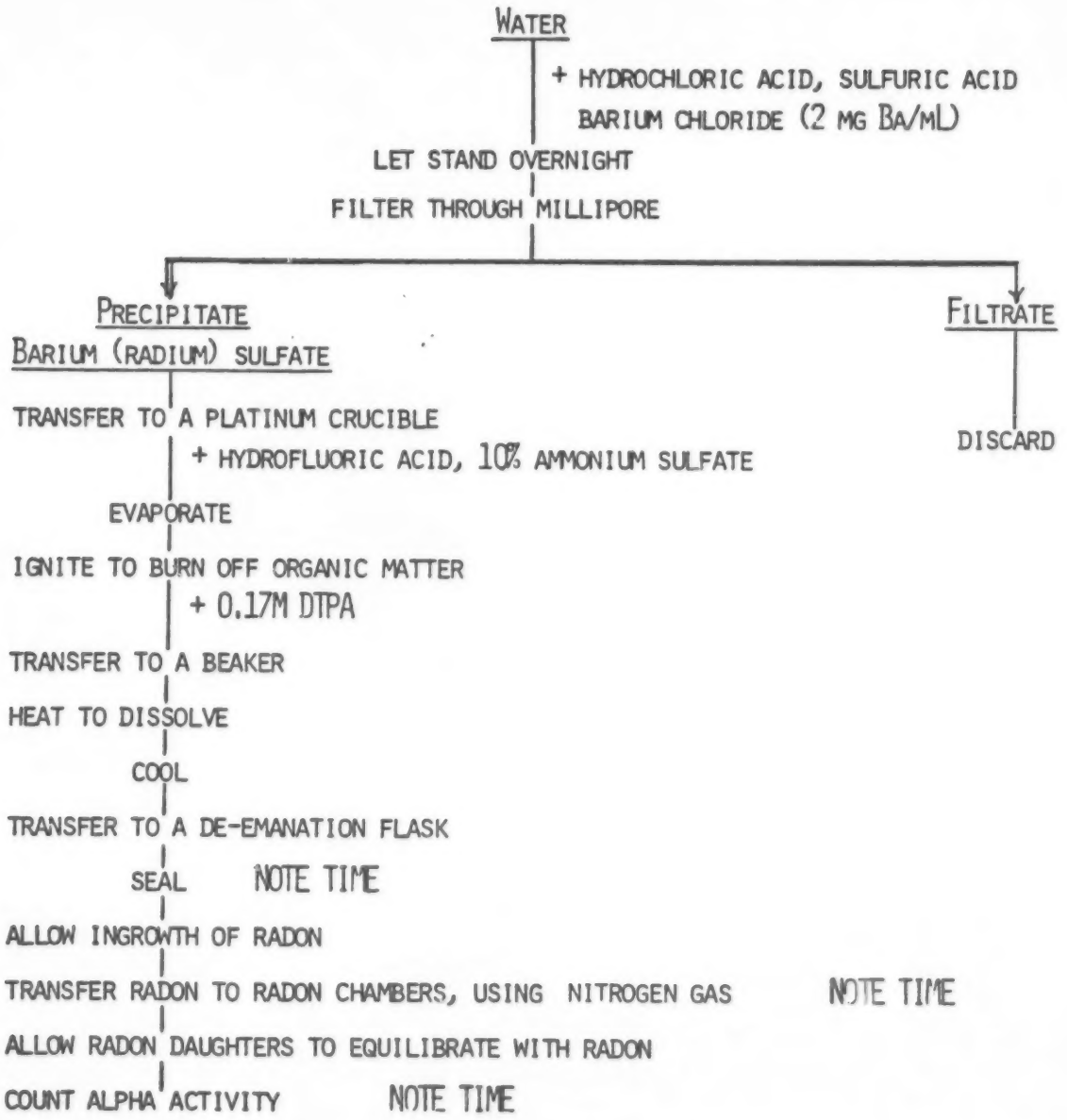

APRIL 1983

RADIUM-228 IN WATER

ACIDIFIED WATER SAMPLE

+ SULFURIC ACID, POTASSIUM SULFATE

HEAT TO BOILING

+ 3.2% LEAD NITRATE

PRECIPITATE

INSOLUBLE SULFATES ON FILTER

WET-ASH WITH NITRIC ACID

EVAPORATE TO DRYNESS

+ POTASSIUM SULFATE, SODIUM SULFATE & SULFURIC ACID

FUSE

COOL

+ SULFURIC ACID-HYDROCHLORIC ACID SOLUTION

FILTRATE

DISCARD

CENTRIFUGATE

DISCARD

PRECIPITATE

LEAD (RADIUM) SULFATE

+ 0.17M DTPA

HEAT IN WATER BATH

CENTRIFUGATE

+ 0.45% BARIUM CHLORIDE, 20% SODIUM SULFATE

WATER, 6M ACETIC ACID

DIGEST

PRECIPITATE

SILICA

DISCARD

PRECIPITATE

BARIUM (RADIUM) SULFATE

+ 0.17M DTPA

HEAT IN WATER BATH

+ 20% SODIUM SULFATE, WATER, 6M ACETIC ACID

NOTE TIME

DIGEST

CENTRIFUGATE

DISCARD

APRIL 1983

RADIUM-228 IN WATER (cont'd)

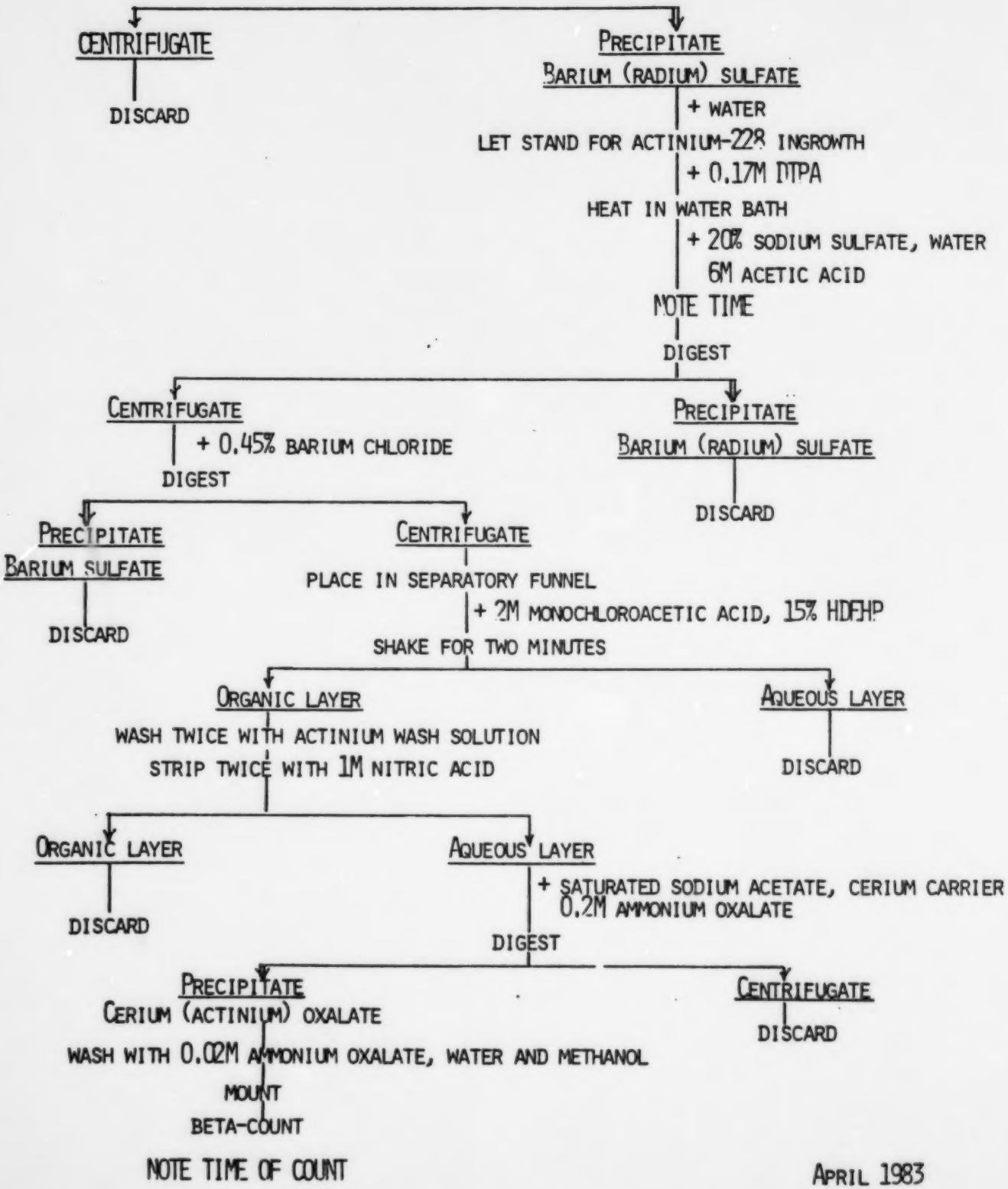

NOTE TIME OF COUNT

April 1983

THORIUM IN WATER

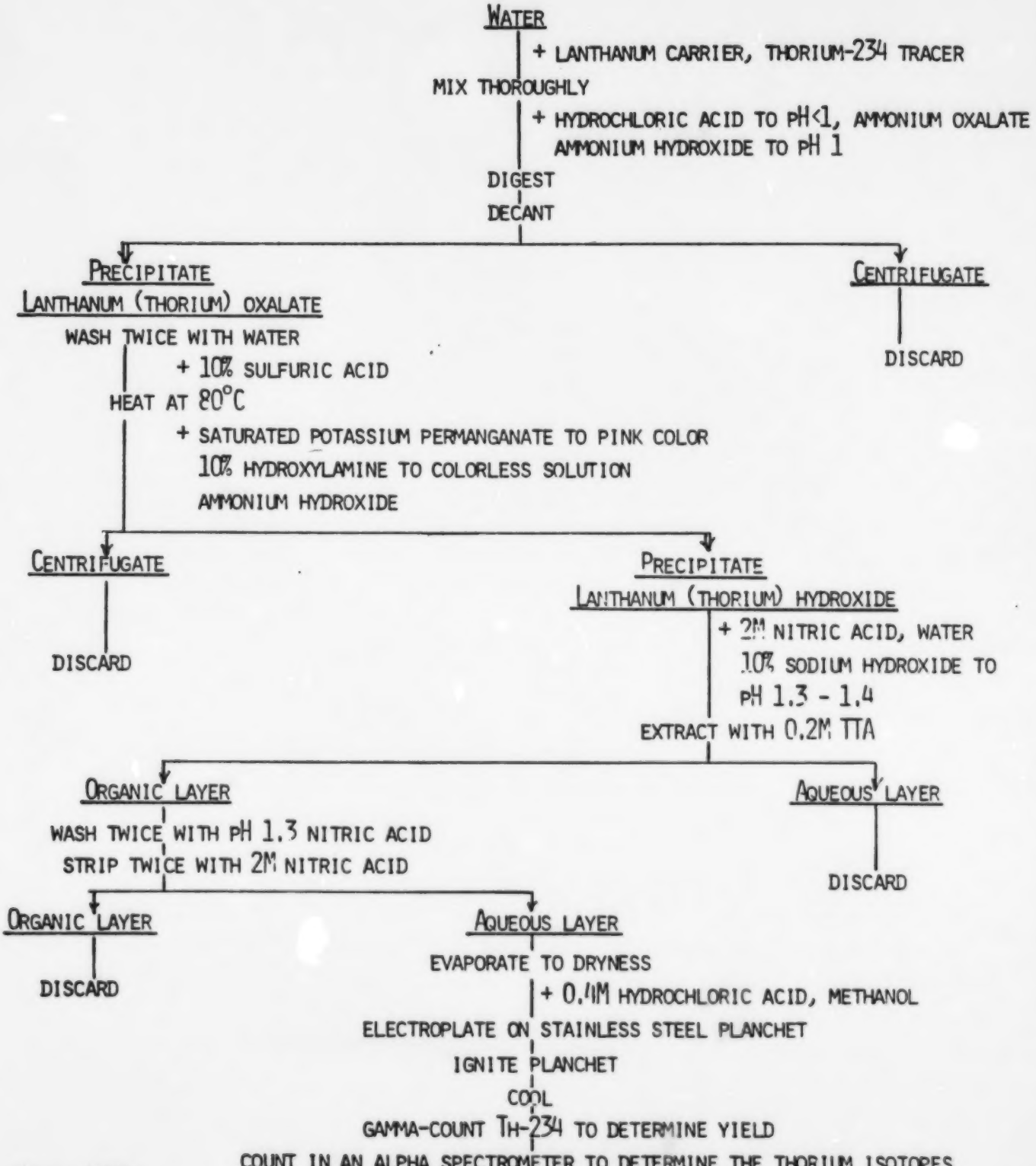

APRIL 1983

THORIUM IN WATER

WATER

+ LANTHANUM CARRIER, THORIUM-234 TRACER

MIX THOROUGHLY

+ HYDROCHLORIC ACID TO pH<1, AMMONIUM OXALATE
AMMONIUM HYDROXIDE TO pH 1

DIGEST

DECANT

PRECIPITATE
LANTHANUM (THORIUM) OXALATE

WASH TWICE WITH WATER

+ 10% SULFURIC ACID

HEAT AT 80°C

+ SATURATED POTASSIUM PERMANGANATE TO PINK COLOR
10% HYDROXYLAMINE TO COLORLESS SOLUTION
AMMONIUM HYDROXIDE

CENTRIFUGATE

DISCARD

CENTRIFUGATE

DISCARD

PRECIPITATE
LANTHANUM (THORIUM) HYDROXIDE

+ 2M NITRIC ACID, WATER
10% SODIUM HYDROXIDE TO
pH 1.3 - 1.4

EXTRACT WITH 0.2M TTA

ORGANIC LAYER

WASH TWICE WITH pH 1.3 NITRIC ACID

STRIP TWICE WITH 2M NITRIC ACID

AQUEOUS LAYER

DISCARD

ORGANIC LAYER

DISCARD

AQUEOUS LAYER

EVAPORATE TO DRYNESS

+ 0.1M HYDROCHLORIC ACID, METHANOL

ELECTROPLATE ON STAINLESS STEEL PLANCHET

IGNITE PLANCHET

COOL

GAMMA-COUNT TH-234 TO DETERMINE YIELD

COUNT IN AN ALPHA SPECTROMETER TO DETERMINE THE THORIUM ISOTOPES

APRIL 1983

APPENDIX A.3

Chemical Methods of Analysis by Monenco Laboratories
Calgary, Alberta

APPENDIX A.3: METHODS OF ANALYSIS BY MONENCO LABORATORIES CALGARY, ALBERTA

Sample Preservation and Preparation

Liquids: Water samples for dissolved radionuclide analysis were assumed to have been field-filtered and preserved prior to shipment to the laboratory. Any water samples for total radionuclide analysis were also acidified in the field; they were subsequently digested in the laboratory prior to analysis.

Solids: Solids were dried at 50°C and ground to ensure sample homogeneity. Prior to drying the moisture content was measured. Solid samples were dissolved by KF-pyrosulfate fusion for the determination of radium and thorium and by digestion using a hot concentrated mixture of nitric, perchloric and hydrofluoric acids, followed by a pyrosulfate fusion for the determination of lead and polonium. Subsamples for radionuclide analysis exceeded 0.5 gm in order to minimize uncertainty due to the counting statistics.

Summary of Analytical Methods

All samples were analyzed according to the procedures outlined in the "Analytical Methods Manual - National Uranium Tailings Program" by Dean and Chiu (1984). They are in summary:

- Radium-226, Radium-223 - High Resolution Alpha Spectrometry (HRAS) (Ba-133 Tracer)
- Th-232, Th-230, Th-228 - HRAS (Th-234 Tracer)
- Radium-228 - Indirect measurement of daughter, Actinium-228, a beta emitter
- Lead-210 - Indirect measurement of daughter, Bismuth-210, a beta emitter
- Polonium-210 - HRAS (Po-208 Tracer)
- Uranium - Delayed neutron activation (solids), fluorimetry (liquids)
- Uranium Ratio (U-234, U-234, U-238) - HRAS (after isolation of uranium)

Specified Analytical Procedures

Po-210

Summary: Indirect measurement of daughter, bismuth-210.

Method: One must allow 30 days for the ingrowth of Bi-210, a beta emitter, to achieve an equilibrium of greater than 98%. A carrier solution of stable lead and bismuth was added prior to digestion. Bismuth was then solvent-extracted, subsequently precipitated as bismuth oxychloride and beta-counted to meaure Bi-210, the first daughter of Pb-210. The absolute detection limit for Pb-210 was 0.05 Bq (Dean and Chiu, 1984).

Po-210

Summary: Polonium-210 - HRAS (Po-208 Tracer)

Method: A tracer solution of Po-208 was added prior to digestion. The polonium isotopes were deposited on a nickel disc and determined by alpha spectroscopy. The overall chemical yield was determined by the recovery factor Po-208. The detection limit for Po-210 was 0.01 Bq.

Ra-226

Summary: Radium-226, Radium-223 - High Resolution Alpha Spectrometry (HRAS) (Ba-133 Tracer)

Method: A tracer solution of Ba-133 was added prior to digestion. Radium was coprecipitated with $PbSO_4$, subsequently dissolved and isolated by coprecipitation with $BaSO_4$. The overall chemical yield was determined by gamma counting of Ba-133; Ra-226 was then determined by alpha spectroscopy. The detection limit for Ra-226 was 0.01 Bq (Dean and Chiu, 1984).

Ra-228

Summary: Indirect measurement of daughter, Actinium-228, a beta emitter.

Method: Radium-228 and other radium isotopes were separated by coprecipitation with lead sulphate, re-dissolved and purified by coprecipitation with barium sulphate. The barium (radium) sulphate was stored to allow the ingrowth of Ac-228, the first daughter of Ra-228 and known to grow into equilibrium with Ra-228 by virtue of its short half-life. Actinium-228 was then separated from the radium isotopes by coprecipitation with cerous hydroxide which was then beta-counted to a detection limit of 0.05 Bq (Dean and Chiu, 1984).

Ra-223

Summary: High Resolution Alpha Spectrometry (HRAS, Ba-133 Tracer)

Method: Radium isotopes were collected as described for Ra-226 and determined by alpha spectroscopy. While the alpha energy of Ra-226 was clearly separate from Ra-223 and Ra-224, the alpha energies of these latter two isotopes (5.71 and 5.68 MeV, respectively) are too close to permit resolution. In the natural environment, Ra-224 was not expected to be present in significant amounts, but it was found to occur in waste tailings strems in other NUTP projects. In such cases, its presence affected the precision of the Ra-223 measurement. The Ra-224 contribution, if any, was quantified and subtracted by measurement of its daughter products Bi-212 and Po-212 by alpha counting techniques. The detection limit of Ra-223 was 0.05 Bq (Dean and Chiu, 1984).

Th-232, Th-230, Th-228

Summary: HRAS (Th-234 Tracer)

Method: A tracer solution of Th-234 was added prior to digestion. Thorium was coprecipitated with $PbSO_4$, isolated by solvent extraction, and then

coprecipitated with cerous hydroxide. The thorium precipitate was then beta-counted for Th-234 to measure the overall yield, and then Th-230, Th-232 and Th-228 were determined by alpha spectroscopy. The detection limit for Th-230, Th-232 and Th-228 was 0.01 Bq (Dean and Chiu, 1984).

Uranium - Total

Summary: Fluorimetry (liquids) delayed neutron activation (solids)

Method: In liquid samples, natural uranium was determined fluorimetrically as its fluoride complex following fusion with sodium fluoride-lithium fluoride. In solid samples, U was determined by DNA. The detection limit for uranium was 0.1 ug (Dean and Chiu, 1984).

Detection Limits

Detection limits for various radionuclides are given in Table A3. The mass of each isotope meaured is so small that one does not have a "normal operating range" or a "bias" (versus true value), such as one would encounter for chemical methods of analysis for cations and anions. Accordingly, the routine analytical operating range is not given because it is not meaningful.

Quality Assurance and Quality Control Program (Monenco)

Quality Assurance Program

The quality assurance program for radiochemistry of solids involved the analysis of one or two CANMET reference materials (UTS-1 to UTS-5) or reference ore (e.g., DL-1, DL-2, etc.) for every 15 to 20 field samples analyzed. For liquids, one reference solution is used for up to ten samples in a batch for Ra-226, Th isotopes and Po-210. Two reference solutions are used for up to ten samples for Ra-228 and Po-210 determinations. In addition, the alpha spectrometers, gamma spectrometers and beta spectrometers were calibrated daily.

One replicate analysis per batch of 15 to 20 samples was made. A tracer was added to every sample, reference solution or certified reference to check recovery.

Laboratory Quality Control Program

The quality control program, which attempts to assure the scientific reliability of the laboratory data, used management, administrative, statistical, investigative, preventive and corrective techniques to maximize reliability of the data.

It involved:

- the publication and distribution of current and complete analytical methods and procedures and analytical instrument operating instructions;
- the distribution and retention of laboratory reports with provision for administrative technical review; and
- other provisions detailed in Dean and Chiu (1984).

TABLE A3a: OPERATING CHARACTERISTICS OF RADIONUCLIDE ANALYSIS FOR WATER (Routine Procedure)

Parameter	Unit of Measurement	Best Method Lowest Reported Value*
Total U	ug/L (ppb)	0.5
Th-230	Bq/L	0.005
Ra-226	Bq/L	0.005
Pb-210	Bq/L	0.1
Po-210	Bq/L	0.005
Th-232	Bq/L	0.005
Ra-228	Bq/L	0.1
Th-228	Bq/L	0.005

* Assuming 1 litre sample size.

TABLE A3b: OPERATING CHARACTERISTICS OF RADIONUCLIDE ANALYSIS FOR SOLIDS (Routine Procedure)

Parameter	Unit of Measurement	Best Method Lowest Reported Value*
Total U	ug/g	0.5
Th-230	Bq/g	0.005
Ra-226	Bq/g	0.005
Pb-210	Bq/g	0.1
Po-210	Bq/g	0.005
Th-232	Bq/g	0.005
Ra-228	Bq/g	0.1
Th-228	Bq/g	0.005

* Assuming 1 gm sample size.

APPENDIX A.4

Chemical Methods of Analysis by Becquerel Laboratories

Chemical Methods of Analysis for Liquid Samples by Becquerel Laboratories

The following samples and analytical procedures were applied to either solid phases or to solution phases in which extraction and concentration steps were required. For the measurement of radiosotopes in the settling particles, the particles were freeze-dried, and then counted directly by gamma counting.

For the measurement of lead-210, the sample was acidified with two normal hydrochloric acid for 48 hours. The lead was chloride complex evaporated to dryness, and then taken back into solution with dilute (0.05) nitric acid. When sulphide was added and the lead that had been added as a tracer and lead-210 were precipitated as a lead sulphide precipitate, the precipitate was filtered, redissolved with HCl and then evaporated to dryness. It was brought back into solution into 1.5 N HCl and then passed over an ion exchange column. The lead chloride anionic complex ($PbCl_4^{-2}$) sticks to the column whereas other cations such as iron, barium, etc. pass on through. The lead was elutriated from the column with water and dilute nitric acid and then reprecipitated as a lead sulfide complex. The lead sulphide solid was removed from solution using a glass fibre filter and then the Bi daughter gama counted. Because the gamma counting was below the detection limit of a solid, the solid was then forward to Monenco for analysis by their normal procedures for beta counting the Bi daughter.

For the Ra-224, 226 and 228 analysis, Ra-224 had been added as a yield tracer for the sample to which it is desired to measure Ra-226 and Ra-228. The Ra-226 and 228 had been coprecipitated from dilution by addition of barium sulphate, and coagulation of the precipitate with an iron hydroxide. This iron hydroxide barium sulphate solid was not cleaned up; rather, the Ra-226 and Ra-228 were direct counted by gamma spectroscopy using the 214, daughters of Ra-226, and the ??? 228 daughter of Ra-228 for counting purposes, after the yield tracer of Ra-224 had been counted. For certain samples, because of the low detection limit, substantive periods of time (up to 20 hrs.) were required for counting the associated radionuclides.

For measurement of uranium, a aluminum tracer was added to an acidified sample and aluminum 8 hydroquinolate was used to precipitate the uranium. As well, thorium would be precipitated by this solid. The solution pH was adjusted to a pH of 6 to 7, and the precipitate filtered. Then, uranium and thorium were determined by neutron activation

analysis of the sample collected on the filtered disk and compared with standards composed of spike solutions of uranium and thorium.

For analysis of Th-232, 230 and 228, the yield tracer Th-234 had been added originally to the 50-100 L alliquot of water and the thorium isotopes precipitated with an hydroxide precipitate. This precipitate was dissolved in the normal nitric acid which would dissolve all of the residue and any filtered material. This solution will then pass through an ion exchange column after additional nitrate. The thorium nitrate negative complex stays on the column whereas other isotopes pass on through. The solution passed through the column contained mainly iron which washed clear through the column. To further clean up the thorium containing solution, additional steps were carried out. The column was elutriated using 10-20 mL of 3% sulphuric acid and then the thorium separated by use of 50 ug of lanthanium added to 1 ml of -N hydrochloric acid. The lanthanium fluoride (LaF_3) precipitate which carries the thorium fluoride (ThF_4) precipitate was then filtered through 0.22 micron filters and used for alpha counting, after counting the precipitate content of Th-234 to give an overall estimate of yield all the way from the initial addition of Th-234 to the 50-100 L alliquot to the amount of Th contained (Th-234) in the precipitate.

For Po-210 analysis, Po-208 had been added as a yield tracer. Polonium isotopes were coprecipitated with iron hydroxide solution in one case, and brought down with the barium sulphate (iron hydroxide precipitate) in the second set of the samples. A portion of the precipitate which was basically used for either radium analysis (the barium sulphate solid), or for Th analysis (iron hydroxide solid) was pinched off the precipitate, and extracted and dissolved with 6 N hydrochloric acid and filtered. The hydrochloric acid dissolved all of the iron hydroxide, the barium sulphate and the isotopes contained in the solid. The solution was filtered, hydrochloric acid added in order to complex iron and to prevent it from interfering with Po chemistry, (by the formation of a soluble FeF_6^{-3}) complex, the solution was diluted into 6 N hydrochloric acid, and then Po was plated out onto a silver disk. The n Po-210 was counted by alpha spectroscopy and the yield tracer (Po-208) by gamma spectroscopy. The yield tracer gave a low overall recapturate in the plated Po. Analysis of the steps in the laboratory procedure compared to the amount of yield tracer added to the large vats indicated that most of the losses of the yield tracer occurred in the initial precipitation step (with the iron hydroxide and/or barium sulphate in the large 50-100 L vats). Accordingly, in the future it is recommended that additional attention be paid to these aspects to improve their recoveries of the Po-208 and Po-210.